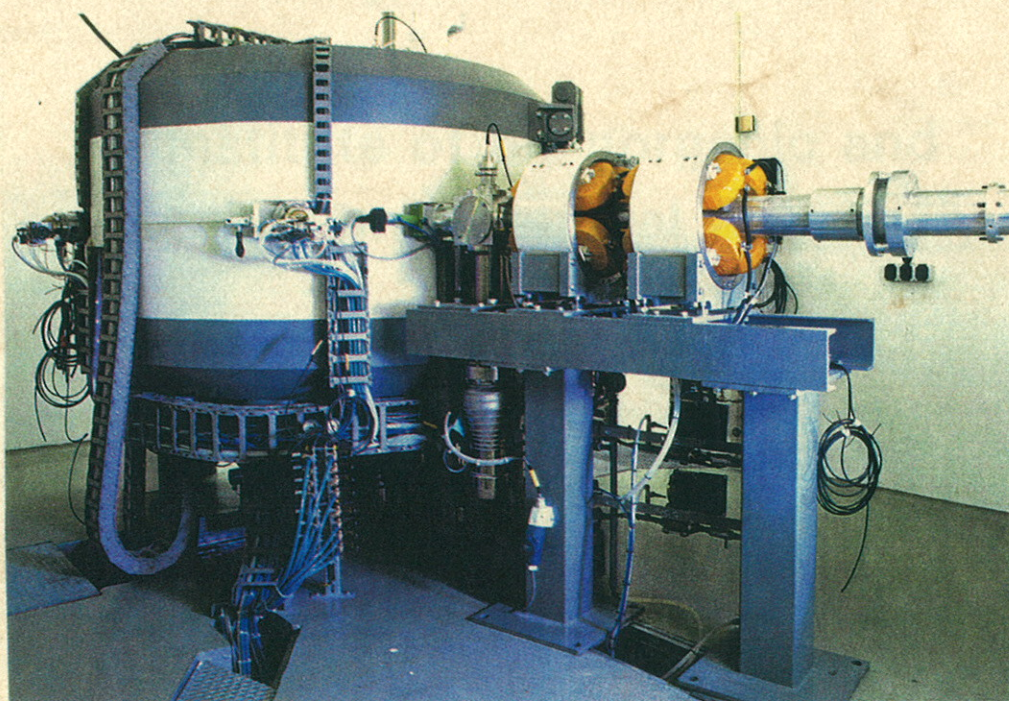


FORSCHUNGSZENTRUM
ROSSENDORF e.V.

FZR -
122

INSTITUTE OF BIOINORGANIC AND
RADIOPHARMACEUTICAL
CHEMISTRY



Annual Report 1995



BRD

Cover picture:

The Institute's cyclotron CYCLONE 18/9 for production of the radionuclides ^{18}F , ^{11}C , ^{15}O and ^{13}N for the Rossendorf PET Center. The cyclotron also includes an external beam line.

Forschungszentrum Rossendorf e.V.
Postfach 51 01 19 ; D-01314 Dresden
Bundesrepublik Deutschland
Telefon (0351) 260 3170
Telefax (0351) 260 3232
E-Mail johannsen@fz-rossendorf.de

FZR - 122
February 1996

Annual Report 1995

**Institute of Bioinorganic and
Radiopharmaceutical Chemistry**

Editor: B. Johannsen

Editorial staff: S. Seifert

FOREWORD

Research at the Institute of Bioinorganic and Radiopharmaceutical Chemistry of the Research Center Rossendorf Inc. is focused on radiotracers as molecular probes for diagnosis of disease. Derived from an awareness of the very important role modern nuclear medicine is playing, as expressed explicitly in the synonym *in vivo* biochemistry, this research effort has two main components:

- positron emission tomography (PET)
- technetium chemistry and radiopharmacology.

To make positron emission tomography available also in the eastern part of Germany, a PET center was established at Rossendorf. As envisaged in a contract signed in February 1995 between the Research Center Rossendorf and the Dresden University of Technology, the Institute is closely linked to the University Hospital in this PET center. A joint team of staff members from both the Institute and the Department of Nuclear Medicine with the University Hospital has been working at the Rossendorf PET Center. The first patient investigations commenced on the 7th of June 1995. A brochure (in German) issued on the 1st of February 1995 provides information on the layout, equipment and programme of the PET center.

To contribute to further exploitation of technetium-99m with its ideal nuclear properties for single photon emission tomography (SPECT), great commitment to interdisciplinary research into technetium tracers is required. The Institute's projects therefore address new approaches to tracer design. Although radioactive work on ^{99m}Tc was still affected by a pending licence, we were able to compensate for this by extensive studies with rhenium as a surrogate for technetium as well as investigations at a very low radioactivity level.

The research activities of our Institute have been performed in three administratively classified groups. A PET tracer group is engaged in the chemistry and radiopharmacy of ^{11}C and ^{18}F compounds and in the setup of the PET center, which is jointly run by the Institute and the Clinic and Polyclinic of Nuclear Medicine at the University Hospital. A SPECT tracer group deals with the design, synthesis and chemical characterization of metal coordination compounds, primarily rhenium and technetium complexes. A biochemical group is working on SPECT and PET-relevant biochemical and biological projects. This includes the characterization and assessment of new compounds developed in the two synthetically oriented groups.

The annual report presented here covers the research activities of the Institute of Bioinorganic and Radiopharmaceutical Chemistry in 1995.

The achievements attained so far have only been possible because of the dedication and commitment of the permanent and temporary staff, the Ph.D. students and collaborators inside and outside the Rossendorf Research Center Inc. I would like to extend my thanks to all of them.

Bernd Johannsen

CONTENTS

I. RESEARCH REPORTS

1. The Rossendorf PET Cyclotron Facility - A Status Report 1
St. Preusche, J. Steinbach, F. Füchtner, H. Krug, W. Neumann
2. Substances Labelled in Metabolically Stable Positions: 3
10. Precursors for the Synthesis of 3-Nitro-[3-¹¹C]toluene and
4-Nitro-[4-¹¹C]toluene
P. Mäding, J. Steinbach, H. Kasper
3. Substances Labelled in Metabolically Stable Positions: 6
11. The Synthesis of 3-Nitro-[3-¹¹C]toluene and 4-Nitro-[4-¹¹C]toluene
P. Mäding, J. Steinbach, H. Kasper
4. Substances Labelled in Metabolically Stable Positions: 8
12. The Synthesis of 3-Methyl-[1-¹¹C]aniline and 4-Methyl-[1-¹¹C]aniline
P. Mäding, J. Steinbach, H. Kasper
5. Substances Labelled in Metabolically Stable Positions: 10
13. The Synthesis of [1-¹¹C] Phenole
P. Mäding, J. Steinbach, H. Kasper
6. Substances Labelled in Metabolically Stable Positions: 12
14. Synthesis of ¹¹C-Labelled Pyridine and Derivatives by Pyrolysis
K. Chebani, J. Zessin, J. Steinbach
7. Substances Labelled in Metabolically Stable Positions: 16
15. Synthesis of Cyano-[¹¹C]Pyridines and ¹¹C-Labelled Pyridine Carboxy-Amides
by Pyrolysis
K. Chebani, J. Zessin, J. Steinbach
8. Synthesis of 3-O-Methoxymethyl-16 β ,17 β -O-sulfuryl-estra-1,3,5(10)-triene-
3,16 β ,17 β -triol 19
J. Römer, J. Steinbach, H. Kasch
9. Synthesis of 16 -[¹⁸F]Fluoroestradiol 21
J. Römer, J. Steinbach, H. Kasch
10. ¹³C NMR Spectroscopic Characterization of Estra-1,3,5(10)-triene-3,17 β -diol and
3,16,17-triols, and some of their 3-O-Methoxymethyl and 16 -Fluor Derivatives 27
J. Römer, D. Scheller
11. Serotonin Receptor-Binding Technetium and Rhenium Tracers 31
1. Design Concept and Synthesis Strategy
H.-J. Pietzsch, M. Scheunemann, H. Spies, P. Brust, B. Johannsen
12. Serotonin Receptor-Binding Technetium and Rhenium Tracers 34
2. Synthesis, Chemical Characterization and Biochemical Evaluation of Partial
Structures of Ketanserin
M. Scheunemann, H.-J. Pietzsch, P. Brust, J. Wober, H. Spies, B. Johannsen
13. Serotonin Receptor-Binding Technetium and Rhenium Tracers 39
3. Synthesis, Characterization and Biochemical Evaluation of Oxorhenium(v)
Complexes Bearing the Quinazolinedione Portion of Ketanserin
H.-J. Pietzsch, M. Scheunemann, T. Fietz, H. Spies, P. Brust, J. Wober,
B. Johannsen

14. Serotonin Receptor-Binding Technetium and Rhenium Tracers 4. Synthesis and Characterization of Ligands Derived from the 4-[<i>p</i> -Fluorobenzoyl]-Piperidine Pharmacophore of Ketanserin M. Scheunemann, H.-J. Pietzsch, H. Spies, P. Brust, B. Johannsen	44
15. Serotonin Receptor-Binding Technetium and Rhenium Complexes 5. Synthesis, Characterization and Biochemical Evaluation of Technetium and Rhenium Complexes Derived from the 4-[<i>p</i> -Fluorobenzoyl]-Piperidine Pharmacophore of Ketanserin H.-J. Pietzsch, M. Scheunemann, T. Fietz, P. Brust, H. Spies, B. Johannsen	48
16. Serotonin Receptor-Binding Technetium and Rhenium Complexes 6. Distribution and Brain Uptake in the Rat of ^{99m/99} Tc Oxotechnetium(V) Complexes with Affinity to the 5-HT ₂ Receptor R. Syhre, R. Berger, H.-J. Pietzsch, M. Scheunemann, H. Spies, B. Johannsen	51
17. Serotonin Receptor-Binding Technetium and Rhenium Complexes 7. Binding of ^{99m/99} Tc Oxotechnetium(V) Complexes to Erythrocytes of Rats and Humans R. Syhre, H.-J. Pietzsch, M. Scheunemann, H. Spies, B. Johannsen	58
18. Serotonin-Receptor-Binding Technetium and Rhenium Complexes 8. Quantitative Autoradiographic Studies (Radioluminography) Using Rat Brain Sections M. Kretzschmar, P. Brust, H.-J. Pietzsch, M. Scheunemann, B. Noll, B. Johannsen	63
19. Determination of Partition Coefficients for Coordination Compounds by Using HPLC R. Berger, T. Fietz, M. Glaser, H. Spies, B. Johannsen	69
20. pK _a Value Determinations by HPLC of Some Tc and Re Complexes Containing an Ionizable Group R. Berger, M. Scheunemann, H.-J. Pietzsch, B. Noll, St. Noll, A. Hoeping, M. Glaser, T. Fietz, H. Spies, B. Johannsen	73
21. Rhenium and Technetium Mixed-Ligand Chelates Functionalized by Amine Groups. 1. Rhenium Complexes with <i>p</i> -Substituted Benzenethiols as Monodentate Ligands M. Papadopoulos, S. Chiotellis, H. Spies, M. Friebe, R. Berger, B. Johannsen	80
22. Technetium and Rhenium Complexes Derived from 6-Methyl-8 α -Amino Ergoline 1. Synthesis and Molecular Structure of [ReO(SSS)(MAerg)] P.E. Schulze, St. Noll, B. Noll, H. Spies, P. Leibnitz, W. Semmler, B. Johannsen	82
23. Technetium and Rhenium Complexes Derived from 6-Methyl-8 α -Amino Ergoline 2. Preparation and Biodistribution of Mixed Ligand Tc Complexes B. Noll, R. Syhre, St. Noll, H. Spies, P. Brust, B. Johannsen, P. E. Schulze, W. Semmler	85
24. Preparation of 2,3-Dimercaptopropionic Acid Ethyl Ester A. Hoeping, H. Spies	89
25. Preparation, Characterization and Enzymatic Hydrolysis of Re/Tc Complexes with Dimercaptocarboxylic Acids and Ethyl Esters S. Seifert, R. Syhre, A. Hoeping, K. Klostermann, H. Spies, B. Johannsen	91
26. Preparation, Characterization and Enzymatic Hydrolysis of Re/Tc Complexes with Mercaptocarboxylic Acids and their Ethyl Esters S. Seifert, R. Syhre, M. Friebe, K. Klostermann	98

27. Enzymatic Hydrolysis of Mixed Ligand Complexes of Rhenium and Technetium with DMS Ethyl Esters and Mercaptocarboxylic Acid Ethyl Esters and their Acids S. Seifert, R. Syhre, K. Klostermann	102
28. Technetium and Rhenium Complexes of Mercaptoacetyl Glycine Ligands. 6. Preparation and X-ray Structure of $\text{Ph}_4\text{As}[\text{ReO}(\text{MAG}_1)\text{Cl}]$ B. Noll, St. Noll, P. Leibnitz, H. Spies, B. Johannsen	105
29. Technetium and Rhenium Complexes of Mercaptoacetyl Glycine Ligands. 7. Formation and Molecular Structure of a Re(V) Complex of Mercaptoacetyl Glycine Ethyl Ester with N,S,S,O-Coordination B. Noll, St. Noll, P. Leibnitz, H. Spies, B. Johannsen, P. E. Schulze, W. Semmler,	108
30. Preparation and Characterization of Rhenium (V) Complexes with Cysteine and its Derivatives Penicillamine and Cysteamine S. Kirsch, B. Noll, D. Scheller, K. Klostermann, P. Leibnitz, H. Spies, B. Johannsen	110
31. Rhenium and Technetium Carbonyl Complexes for the Labelling of Bioactive Molecules or Small Peptides 1. Preliminary Investigations on the Complex Formation of the Tetradentate Thioether $\text{HOOC-CH}_2\text{-S-CH}_2\text{CH}_2\text{-S-CH}_2\text{-COOH}$ with $[\text{ReBr}_3(\text{CO})_3]^+$ H.-J. Pietzsch, R. Alberto, R. Schibli, M. Reisgys, H. Spies, P.A. Schubiger	114
32. Technetium and Rhenium Complexes with Thioether Ligands 7. Mononuclear Trichlorooxorhenium(V) Complexes with Bi- and Tetradentate Thioethers M. Reisgys, H.-J. Pietzsch, H. Spies, P. Leibnitz	116
33. Substitution Reaction on Trigonal Bipyramidal Coordinated Rhenium(III) Tripod Complexes. A Study of the Kinetics M. Glaser, H. Spies	120
34. Formation of $\{\text{Re}(\text{O})[(\text{SCH}_2\text{CH}_2)_2\text{NH}](\text{SPh})\}$ by Reaction of $\text{N}(\text{CH}_2\text{CH}_2\text{SH})_3$ with $[\text{Re}(\text{O})(\text{SPh})_4]^-$. A new Example of Metal Core Induced Transformation of a Ligand M. Glaser, H. Spies, K. Neubert, K. Klostermann	123
35. Preparation of a Spiperone-like Isocyanide Ligand and its Complexation with Rhenium(III) coordinated with 2,2',2''-Nitrilotris(ethanethiol) Using a New Access M. Glaser, H. Spies	126
36. Molecular Modelling on Technetium and Rhenium Complexes: Possibilities and Limitations M. Glaser, H. Spies, B. Johannsen	130
37. Cyclovoltammetric Investigations into Oxorhenium(V) Complexes of the "3+1" Type T. Knieß, B. Noll, H. Spies	136
38. Rhenium(V) Gluconate, a Suitable Precursor for the Preparation of Rhenium(V) Complexes B. Noll, T. Knieß, M. Friebe, H. Spies, B. Johannsen	139
39. Structural Investigations of Technetium and Rhenium Complexes by EXAFS. 1. Studies on "n+1" Mixed-Ligand Rhenium Complexes T. Reich, G. Bernhard, H. Nitsche, H. Spies B. Johannsen	141

40. The Permeability of Several Lipophilic ^{99/99m} Tc Complexes through Cerebral Endothelial Cell Monolayers of Low Electrical Resistance B. Ahlemeyer, P. Brust, S. Matys, J. Wober, H.J. Pietzsch, M. Scheunemann, B. Johannsen	146
41. Conditioned Media of Astrocytes and Other Proliferating Cells Increase the Activity of Alkaline Phosphatase and g-Glutamyltranspeptidase in Cultured Cerebral Endothelial Cells B. Ahlemeyer, S. Matys, and P. Brust	151
42. Chronic Fluoxetine Treatment did not Change Monoamine Oxidase Activity in Cerebral Endothelial Cells B. Ahlemeyer, P. Brust, A. Friedrich, J. Wober, S. Matys	158
43. PCR Analysis of Blood-Brain Barrier Specific Transporters in RBE4 Cells R. Bergmann, F. Roux, L.R. Drewes, P. Brust	161
44. Is the Serotonin Transporter on the Blood-Brain Barrier involved in the Regulation of Cerebral Blood Volume and Cerebral Blood Flow in the Rat? Ch. Schenker, P. Brust	164
45. Tumour Cell-Targeting with the Radiometals Yb-169 and In-111 G. Kampf, G. Knop, W.-G. Franke, G. Wunderlich, P. Brust, B. Johannsen	167
II. PUBLICATIONS, LECTURES, POSTERS AND PATENTS	173
III. TEACHING AND TRAINING ACTIVITIES	180
IV. SCIENTIFIC COOPERATION	181
V. SEMINARS	182
VI. ACKNOWLEDGEMENTS	183

I. RESEARCH REPORTS

1. The Rossendorf PET Cyclotron Facility - A Status Report

St. Preusche, J. Steinbach, F. Füchtner, H. Krug¹, W. Neumann¹

¹Scientific Dept. Experimental Facilities and Information Technology

Introduction

A first report concerning the layout of the Rossendorf PET cyclotron facility with its main part, the IBA cyclotron "CYCLONE 18/9", was given in a previous paper (Preusche and Steinbach, 1994). By now all installations and the functional and acceptance tests of the cyclotron have been completed. Details of the final layout of the Rossendorf PET cyclotron facility and the results of the tests are summarized in the present paper.

PET cyclotron with external beam line

Radiation protection, safety, security

The final layout of the PET cyclotron rooms is given in Fig. 1.

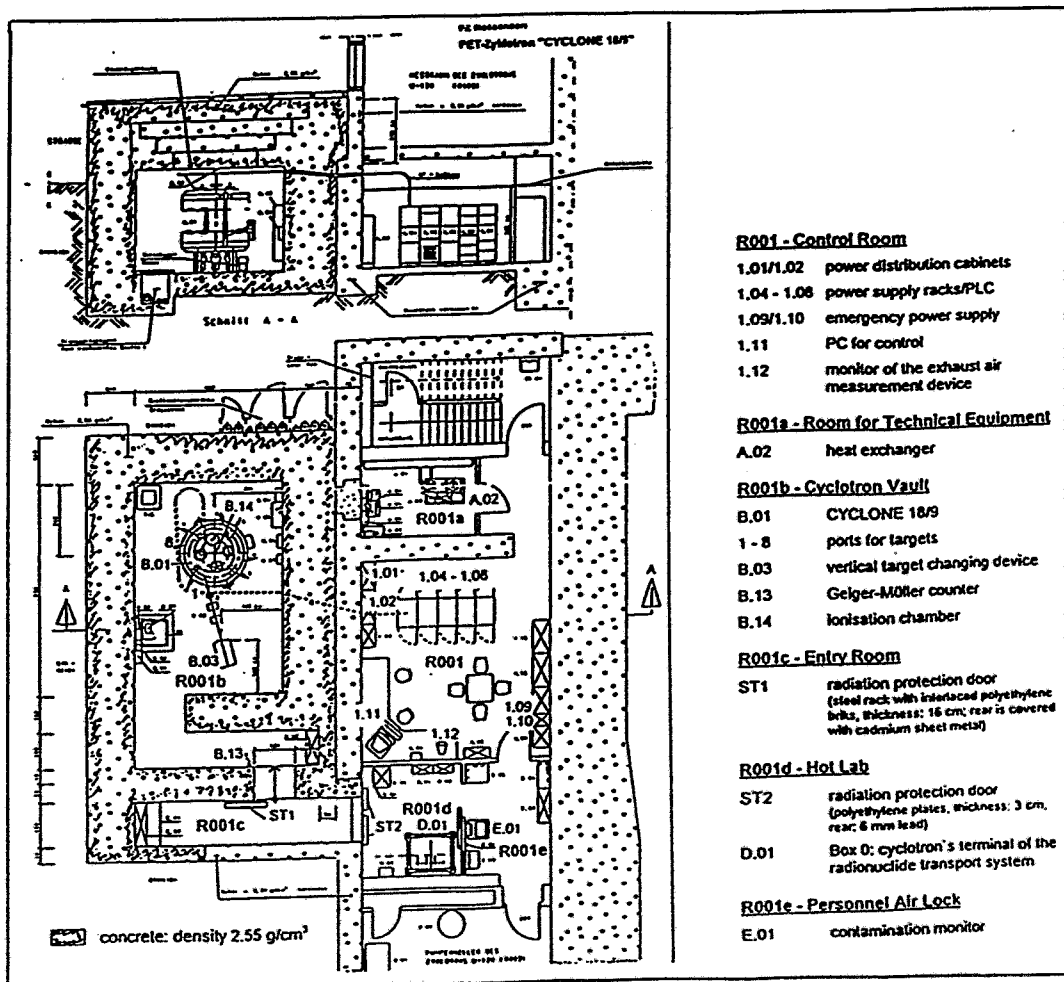


Fig 1: Final layout of the PET cyclotron rooms

The radiation protection areas are:

	without beam	with beam
controlled area:	R001b, R001c, R001d	R001d
prohibited area:	none	R001b, R001c.

For personnel security we installed an **external interlock system** which works with four independent components:

- emergency stop buttons in all rooms
- sensors of the fire-alarm system in all rooms
- ST1/ST2 door security circuit (comp. Fig. 1)
- pressure conditions in the vault: 50 Pa \pm 20 Pa.

The interlock system switches off or disables the beam, if one of these conditions is not in OK status.

The **control system** of the PET cyclotron is based on PLC SIMATIC. It is possible to control the cyclotron and the chemistry modules with both terminal 1 (cyclotron building) and terminal 2 (radiochemistry building). Each of the terminals can be either the master or the slave. Only the master terminal has control of the cyclotron but all information is given on both screens. There is a special procedure for handling the control to the other terminal.

Beam and chemistry tests

Comprehensive tests were carried out to accept the predicted parameters of the PET cyclotron. The so-called beam tests included all work to form and transport the 2 different ion beams (protons and deuterons) from the center of the cyclotron to the targets located at the circumference of the yoke. For these tests we used dummy targets made of aluminium. For the so-called chemistry tests the IBA targets were used to produce the predicted amount of activity in the targets in the desired chemical form. The results of the tests are summarized in Table 1.

The external beam line (BL) at exit 2 (comp. Fig. 1) is a special IBA development for Rossendorf to use our own targets and the vertical target changing device used until now at the U-120 cyclotron. To accept the BL parameters only beam tests were carried out but with both particle types.

Table 1: Results of beam and chemistry tests

Exit	1	2		3	4	5	7
Target for	^{11}C	FZR targets		$^{18}\text{F}]\text{F}_2$	$^{13}\text{N}]\text{NH}_3$	$^{18}\text{F}]\text{F}^-$	^{15}O
Particle	H ⁺	H ⁺	D ⁺	D ⁺	H ⁺	H ⁺	D ⁺
<i>Beam test</i>							
Beam current at							
- Stripper / μA	80	37	29	40	83	81	42
- Collimator / μA	25	12	13	13	63	35	20
- Target / μA	55	25	15	27	20	46	23
<i>Chemistry test</i>							
Activity / GBq	> 74	—	—	> 11	> 15	> 74	> 9

The measured instabilities of all beam currents on targets during irradiation times were less than $\pm 5\%$ and fulfilled our requirements of beam stability on target for production of radionuclides. The diameters of the beam spot on a quartz at the end of BTL both for protons and deuterons were approximately 15 mm and confirmed the IBA calculations. If required, it is possible to reach higher beam currents at exit 2. Dual beams were tested at the exits 1/5 and 3/7. The results are given in Table 2.

Table 2: Results of dual beams

Particle	H ⁻		D ⁻	
	1	5	3	7
Dual beam at exit				
Beam current at				
- Stripper / μ A	32.8	39.2	10.8	22.3
- Collimator / μ A	14.5	21.0	1.0	11.7
- Target / μ A	18.3	18.2	9.8	10.6

Radionuclide transport system (RATS)

The 500 m long RATS was designed to transport small volumes of the irradiated liquids [¹⁸O]H₂O/[¹⁸F]F⁻ and H₂O/[¹³N]NH₃ with a pneumatic post system and the radioactive gases within capillaries from the cyclotron to the radiochemistry laboratories. In more than 300 runs with pneumatic post boxes the reliability of RATS was demonstrated.

RATS is also controlled by 2 terminals using the same master-slave principle as in the control of the cyclotron. Both control systems are now coupled. Several interlock signals prevent the unloading process of a target if RATS is not ready for unloading (Preusche *et al.*, 1995). The whole transfer time (unloading the target into the pneumatic post box, transfer of this box, distribution of the activated liquid to the chemistry modules) is approximately 8 minutes.

Conclusions

The technical equipment is ready for use now. After the final check of the cyclotron facility by the TÜV organization (TÜV = Association for Technical Inspection) we anticipate the granting of a licence for routine operation of our PET cyclotron "CYCLONE 18/9".

References

- Preusche St. and Steinbach J., The Rossendorf PET cyclotron "Cyclone 18/9" - a status report. (1993) *Annual Report 1993*, Institute of Bioinorganic and Radiopharmaceutical Chemistry, FZR-32, pp. 28-32.
- Preusche St., Steinbach J., Füchtner F., Krug H., DeLeenheer M. and Ghyoot M. (1995) The new cyclotron of the Rossendorf PET Center, Poster at the 14. Int. Conf. On Cyclotrons And Their Applications, Cape Town, South Africa, 08.-13.10.1995.

2. Substances Labelled in Metabolically Stable Positions:

10. Precursors for the Synthesis of 3-Nitro-[3-¹¹C]toluene and 4-Nitro-[4-¹¹C]toluene

P. Mäding, J. Steinbach, H. Kasper

Introduction

The ¹¹C-ring labelling of benzenoid compounds using the principle of the synchronous six-electron cyclization of hexatriene systems into aromatics was recently described (Steinbach *et al.*, 1995). In this way unsubstituted and 3-methoxy substituted nitro-[1-¹¹C]benzene (Mäding *et al.*, 1994a) could be synthesized on the n.c.a. level. By reducing these nitro compounds, the appropriate [1-¹¹C]anilines (Steinbach *et al.*, 1995, Mäding *et al.*, 1994b) were obtained. Our efforts to apply the basic principle to methyl-substituted ¹¹C-ring labelled benzenoid compounds required the synthesis of the appropriate methyl-substituted pentamethinium salts as nonradioactive precursors. These syntheses are described here.

Experimental

(Di)methyl-substituted N-(2,4-dinitrophenyl)pyridinium chlorides

A mixture of 1-chloro-2,4-dinitrobenzene (20.2 g; 0.1 mol) and the appropriate picoline or lutidine (0.1 mol) was refluxed in ethanol (50 ml) for 3 h. The pyridinium salts crystallized by cooling the solutions

to room temperature. The salts were filtered through a frit glass filter, washed with diethyl ether and dried.

5-Dimethylamino-2 (or 3)-methyl-penta-2,4-dien-1-al

N-(2,4-Dinitrophenyl)-3 (or 4)-methyl-pyridinium chloride (15 g; 0.05 mol) in ethanol (150 ml) was treated with 60 % aqueous dimethylamine (9.5 ml; 0.1 mol). The mixture was heated to 70 °C for 30 min, evaporated under reduced pressure, and treated with cold water (100 ml). The precipitated 2,4-dinitroaniline was separated by filtration and the filtrate made alkaline with sodium hydroxide (3 g; 0.075 mol) in water (15 ml). This mixture was extracted with methylene chloride (4 x 40 ml), the combined extracts were dried with Na₂SO₄. Evaporation of the filtered extract left a brownish solid (2-methyl compound) or a brownish liquid (3-methyl compound). These products were used for the following synthetic step without further purification.

5-Dimethylamino-2-methyl-penta-2,4-dienylidene-1-dimethylammonium tetrafluoroborate

5-Dimethylamino-2-methyl-penta-2,4-dien-1-al (2 g; 0.014 mol), dimethylamine tetrafluoroborate (1.91 g; 0.014 mol), and ethanol (8 ml) were refluxed for 2 h. The mixture was evaporated under reduced pressure, and the oily residue treated with ether. The salt separated was filtered through a frit glass filter and recrystallized from n-propanol. The orange crystals (0.72 g; 19.7 %) had m.p. 117-123 °C.

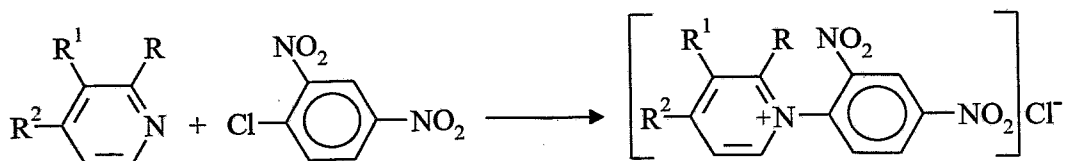
5-Dimethylamino-3-methyl-penta-2,4-dienylidene-1-dimethylammonium tetrafluoroborate

5-Dimethylamino-3-methyl-penta-2,4-dien-1-al (3.8 g; 0.027 mol), dimethylamine tetrafluoroborate (3.6 g; 0.027 mol), and ethanol (12 ml) were refluxed for 6.5 h. The salt separated after cooling was recrystallized from ethanol. The brownish orange crystals (4.1 g, 59.1 %) had m.p. 183-188 °C.

Results and Discussion

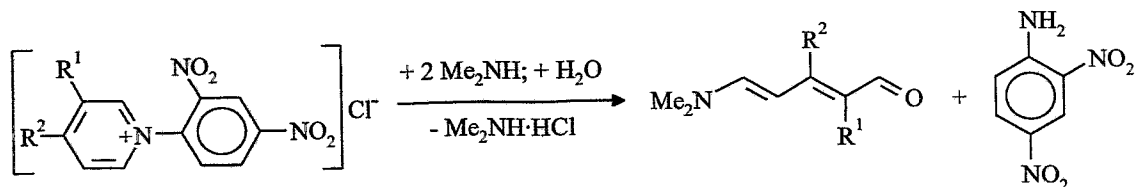
For our purposes the method for the synthesis of the unsubstituted pentamethinium salt, 5-dimethylaminopenta-2,4-dienylidene-dimethylammonium perchlorate (Zinke, 1904; Malhotra and Whiting, 1960), was modified. The methyl-substituted pentamethinium salts were prepared according to the following three synthesis steps:

1. Arylation of picoline or lutidine with 1-chloro-2,4-dinitrobenzene to a (di)methyl-substituted N-(2,4-dinitrophenyl)pyridinium chloride:



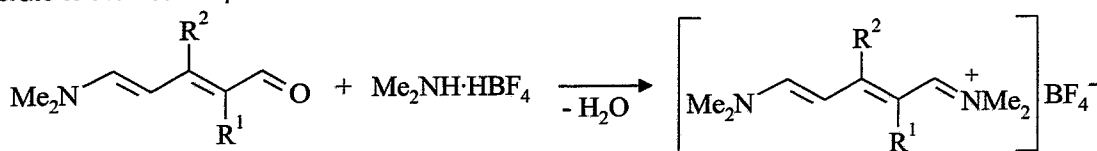
The yields of the synthesized pyridinium salts are listed in Table 1. Starting from α -picoline (R = Me; R¹, R² = H), this reaction is not possible probably due to the shielding effect of the α -methyl group on the pyridine nitrogen.

2. Cleavage of the pyridine ring of the pyridinium salt with dimethylamine to form 5-dimethylamino-2(or 3)-methyl-penta-2,4-dien-1-al:



The yields of the pentadienals prepared are listed in Table 1. In the case of $R^1, R^2 = \text{Me}$ (i.e. starting from the 3,4-lutidinium salt) the desired reaction does not take place.

3. Conversion of 5-dimethylamino-2(or 3)-methyl-penta-2,4-dien-1-al with dimethylamine tetrafluoroborate to the desired pentamethinium salt:



The yields of the synthesized pentamethinium tetrafluoroborates are listed in Table 1.

Table 1: Yields of the synthesized compounds

Synthesized compounds	Yields of compounds [%]		
	$R^1=\text{Me}; R, R^2=\text{H}$	$R^2=\text{Me}; R, R^1=\text{H}$	$R^1, R^2=\text{Me}; R=\text{H}$
pyridinium salt	67.9	87.1	68.9
5-dimethylamino-methyl-penta-2,4-dien-1-al	81.6	53.9	-
pentamethinium tetrafluoroborate	19.7	59.1	-

The 5-dimethylamino-2(and 3)-methyl-penta-2,4-dienylidene-1-dimethylammonium tetrafluoroborates proved to be suitable for synthesizing 3-nitro-[3- ^{11}C]toluene and 4-nitro-[4- ^{11}C]toluene.

The structures of the 5-dimethylamino-2(and 3)-methyl-penta-2,4-dien-1-al and the 5-dimethylamino-2(and 3)-methyl-penta-2,4-dienylidene-1-dimethylammonium tetrafluoroborate were confirmed by ^{13}C NMR data.

References

- Mäding P., Steinbach J. and Kasper H. (1994a) Substances labelled in metabolically stable positions: 6. The synthesis of 3-nitro-[3- ^{11}C]anisole. *Annual Report 1994*, Institute of Bioinorganic and Radiopharmaceutical Chemistry, FZR-73, pp. 100-104.
- Mäding P., Steinbach J. and Kasper H. (1994b) Substances labelled in metabolically stable positions: 7. The synthesis of 3-amino-[3- ^{11}C]anisole - a ^{11}C -ring-labelled synthone. *Annual Report 1994*, Institute of Bioinorganic and Radiopharmaceutical Chemistry, FZR-73, pp. 105-108.
- Malhotra S.S. and Whiting M.C. (1960) Researches on polyenes. Part VII. The preparation and electronic absorption spectra of homologous series of simple cyanines, merocyanines, and oxonols. *J. Chem. Soc.* **1960**, 3812-3822.
- Steinbach J., Mäding P., Füchtner F. and Johannsen B. (1995) N.c.a. ^{11}C -labelling of benzenoid compounds in ring positions: synthesis of nitro-[1- ^{11}C]benzene and [1- ^{11}C]aniline. *J. Labelled Compd. Radiopharm.* **36**, 33-41.
- Zincke Th. (1904) Über Dinitrophenylpyridiniumchlorid und dessen Umwandlungsprodukte. *Liebigs Ann. Chem.* **333**, 296-345.

3. Substances Labelled in Metabolically Stable Positions: 11. The Synthesis of 3-Nitro-[3-¹¹C]toluene and 4-Nitro-[4-¹¹C]toluene

P. Mäding, J. Steinbach, H. Kasper

Introduction

The applicability of the principle of synchronous six-electron cyclization of hexatriene systems into aromatics for ¹¹C-ring labelling of benzenoid compounds was recently described (Steinbach *et al.*, 1995). Based on this method, the syntheses of 3-nitro-[3-¹¹C]toluene and 4-nitro-[4-¹¹C]toluene as further new ¹¹C-ring-labelled benzenoid compounds were worked out, using the appropriate precursors (Mäding *et al.*, 1995).

Experimental

Analysis

To determine the extent of conversion and the radiochemical purity as well as to identify the products, an HPLC system (Merck-Hitachi) was used, including a pump, a Rheodyne injector with a 20 µl loop, a LiChrospher 100 RP-18 endcapped column (5 µm, 150 mm x 3.3 mm, Merck) and a UV detector coupled in series with a radioactivity detector FLO-ONE/Beta A500 (Canberra Packard). The HPLC analyses were carried out at a flow rate of 0.5 ml/min and the following linear gradient of the eluents: 0 min - 70 % buffer/ 30 % MeCN; 10 min - 0 % buffer/ 100 % MeCN; 20 min - 0 % buffer/ 100 % MeCN; buffer = phosphate buffer pH 7 (c[NaH₂PO₄] = 0.26 mM; c[Na₂HPO₄] = 0.51 mM).

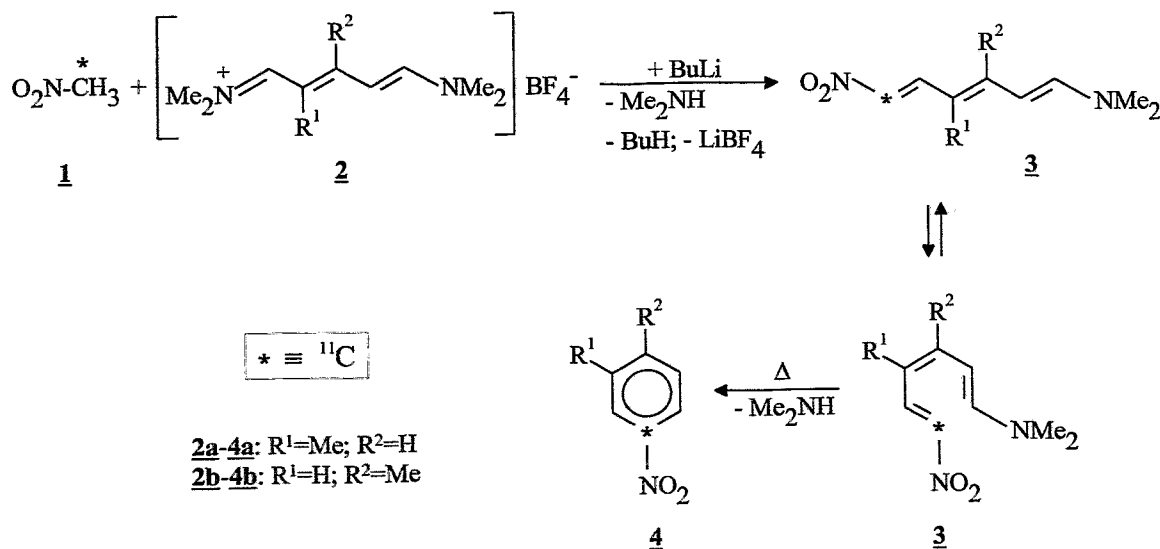
For identification of the labelled compounds by HPLC the following reference substances from Aldrich, Germany, were used: nitromethane 99 %, 3-nitrotoluene 99 % and 4-nitrotoluene 99 %.

Synthesis

The gaseous nitro-[¹¹C]methane produced according to Steinbach *et al.*, (1995) was introduced into a cooled mixture of 250 µl HMPT, 8 mg (30 µmol) precursor **2** (as tetrafluoroborate) and 25 µl 1.6 M BuLi in hexane (40 µmol), followed by heating the well sealed vessel at 170 °C for 10 min.

Results and Discussion

Nitro-[¹¹C]methane (**1**) reacts in the presence of BuLi with the homemade precursor 5-dimethylamino-2(or 3)-methyl-penta-2,4-dienylidene-1-dimethylammonium tetrafluoroborate (**2a** or **2b**) (Mäding *et al.*, 1995) to form 1-dimethyl-amino-4(or 3)-methyl-6-nitro-[6-¹¹C]hexatriene (**3a** or **3b**) followed by cyclization/ aromatisation into 3-nitro-[3-¹¹C]toluene (**4a**) or 4-nitro-[4-¹¹C]toluene (**4b**) at increased temperatures according to the following equation:



Lithium butyl (1.6 M solution in hexane) proved to be a suitable base for the desired ring closure reaction analogously to the synthesis of 3-nitro-[3-¹¹C]anisole (Mäding *et al.*, 1994).

The optimized conditions for the synthesis of **4a** and **4b** are:

Solvent: 250 µl HMPT
Precursor: 8 mg (30 µmol) 5-dimethylamino-2(or 3)-methyl-penta-2,4-dienylidene-1-dimethylammonium tetrafluoroborate (**2a** or **2b**)
Base: 25 µl 1.6 M BuLi in hexane (40 µmol)
Reaction temperature: 170 °C
Reaction time: 10 min

In this way 3-nitro-[3-¹¹C]toluene was prepared with a radiochemical purity of about 87 %. The reproducible radiochemical yields of **4a** are in the range of 85±5 % (decay-corrected), within a synthesis time from [¹¹C]CH₃NO₂ of 10 min. An HPLC radiogram of unpurified 3-nitro-[3-¹¹C]toluene is shown in Fig. 1.

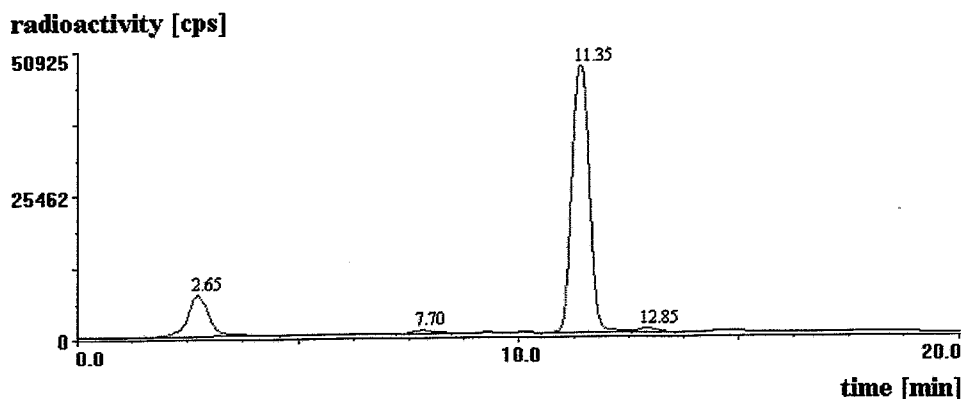


Fig. 1: HPLC radiogram obtained from the reaction mixture of the 3-nitro-[3-¹¹C]toluene synthesis
2.65 min:[¹¹C]CH₃ONO; 11.1 %; 11.35 min:3-nitro-[3-¹¹C]toluene; 87.3 %

4-Nitro-[4-¹¹C]toluene was prepared with a radiochemical purity of about 78 %. The reproducible radiochemical yields of **4b** are in the range of 75±5 % (decay-corrected). The synthesis time of **4b**, starting from [¹¹C]CH₃NO₂, was 10 min. A typical HPLC radiogram of unpurified 4-nitro-[4-¹¹C]toluene is demonstrated in Fig. 2.

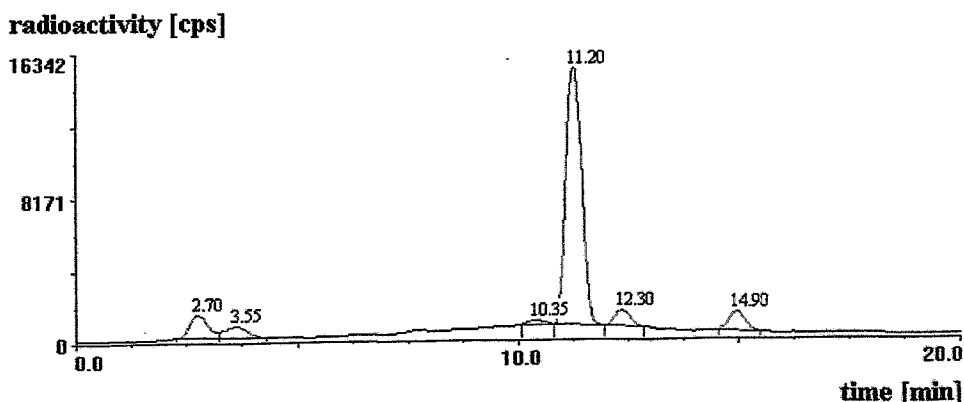


Fig. 2: HPLC radiogram obtained from the reaction mixture of the 4-nitro-[4-¹¹C]toluene synthesis
2.70 min:[¹¹C]CH₃ONO; 6.0 %; 3.55 min:[¹¹C]CH₃NO₂; 3.6 %; 11.20 min:4-nitro-[4-¹¹C]toluene; 77.9 %; 12.30 min:unidentified product; 5.0 %; 14.90 min:unidentified product; 6.2 %

Under the same reaction conditions mentioned above but using solid potassium tert.butylate (3.5 mg; 30 μ mol) instead of BuLi, only 59 % of 4-nitro-[4- 11 C]toluene was obtained in this ring closure reaction. However, 26 % [11 C]methylnitrite and 10 % nitro-[11 C]methane were found, i.e. t-BuOK was not a suitable base for the synthesis of 4-nitro-[4- 11 C]toluene.

References

- Mäding P., Steinbach J. and Kasper H. (1994) Substances labelled in metabolically stable positions: 6. The synthesis of 3-nitro-[3- 11 C]anisole. *Annual Report 1994*, Institute of Bioinorganic and Radio-pharmaceutical Chemistry FZR-73, pp. 100-104.
- Mäding P., Steinbach J. and Kasper H. (1995) Substances labelled in metabolically stable positions: 10. Precursors for the synthesis of 3-nitro-[3- 11 C]toluene and 4-nitro-[4- 11 C]toluene. *This report*, pp.3-5.
- Steinbach J., Mäding P., Füchtner F. and Johannsen B. (1995) N.c.a. 11 C-labelling of benzenoid compounds in ring positions: synthesis of nitro-[1- 11 C]benzene and [1- 11 C]aniline. *J. Labelled Compd. Radiopharm.* **36**, 33-41.

4. Substances Labelled in Metabolically Stable Positions:

12. The Synthesis of 3-Methyl-[1- 11 C]aniline and 4-Methyl-[1- 11 C]aniline

P. Mäding, J. Steinbach, H. Kasper

Introduction

The synthesis of 3-nitro-[3- 11 C]toluene (**4a**) and 4-nitro-[4- 11 C]toluene (**4b**) was described by Mäding et al. (1995). In continuation of this work these methyl-substituted nitro-[1- 11 C]benzenes were converted into the appropriate methyl-substituted [1- 11 C]anilines **5a** and **5b**, another two 11 C-ring-labelled benzenoid syntheses.

Experimental

Analysis

To determine the extent of conversion and the radiochemical purity as well as to identify the products, an HPLC system (Merck-Hitachi) was used, including a pump, a Rheodyne injector with a 20 μ l loop, a LiChrospher 100 RP-18 endcapped column (5 μ m, 150 mm x 3.3 mm, Merck) and a UV detector coupled in series with a radioactivity detector FLO-ONE\Beta A500 (Canberra Packard). The HPLC analyses were carried out at a flow rate of 0.5 ml/min and the following linear gradient of the eluents: 0 min - 70 % buffer/ 30 % MeCN; 10 min - 0 % buffer/ 100 % MeCN; 20 min - 0 % buffer/ 100 % MeCN; buffer = phosphate buffer pH 7 (c[NaH₂PO₄] = 0.26 mM; c[Na₂HPO₄] = 0.51 mM).

For identification of the labelled compounds by HPLC the following reference substances from Aldrich, Germany, were used: nitromethane 99 %, 3-nitrotoluene 99 %, 4-nitrotoluene 99 %, m-toluidine 99 % and p-toluidine 99.7 %.

Synthesis

The methyl-substituted [1- 11 C]aniline **5a** (**5b**) was prepared by reduction of the reaction mixture of **4a** (**4b**) as a one-pot process. The methyl-substituted nitro-[1- 11 C]benzenes **4a** and **4b** synthesized from **1**, 8 mg (30 μ mol) precursor **2a** or **2b**, and 40 μ mol BuLi (25 μ l 1.6 M BuLi in hexane) in 250 μ l HMPT at 170 °C within 10 min (Mäding et al., 1995) were reduced by adding a solution of the optimized amount of Na₂S·9H₂O in 100 μ l H₂O (79 μ mol (19 mg) for **5a** and 50 μ mol (12 mg) for **5b**) and heating at 170 °C for 10 min (**5a**) or 5 min (**5b**).

Results and Discussion

The required methyl-substituted nitro-[1- 11 C]benzenes **4a** and **4b** were prepared in a special cyclization/aromatization reaction by conversion of [11 C]CH₃NO₂ with 5-dimethylamino-2(or 3)-methyl-penta-2,4-dienylidene-1-dimethylammonium tetrafluoroborate in the presence of BuLi in HMPT (Mäding et al., 1995).

Starting from such a reaction mixture, the following reduction was carried out by addition of an aqueous solution of sodium sulphide and subsequent heating:

Using the reaction mixture of **4a** (radiochemical purity 87 % (Mäding *et al.*, 1995)), we elaborated the optimum reduction conditions. It was found that the radiochemical yield of 3-methyl-[1-¹¹C]aniline (**5a**) increased as a function of the amount of sodium sulphide added. Using 79 μmol Na₂S·9H₂O in 100 μl H₂O and heating the reaction mixture at 170 °C within 10 min, 3-methyl-[1-¹¹C]aniline (**5a**) could be obtained with a radiochemical purity of about 82 %. The reproducible radiochemical yields of **5a** (decay-corrected) are in the range of 80±5 %, within a synthesis time from [¹¹C]CH₃NO₂ of 21 min. An HPLC radiogram of unpurified **5a** is shown in Fig. 1.

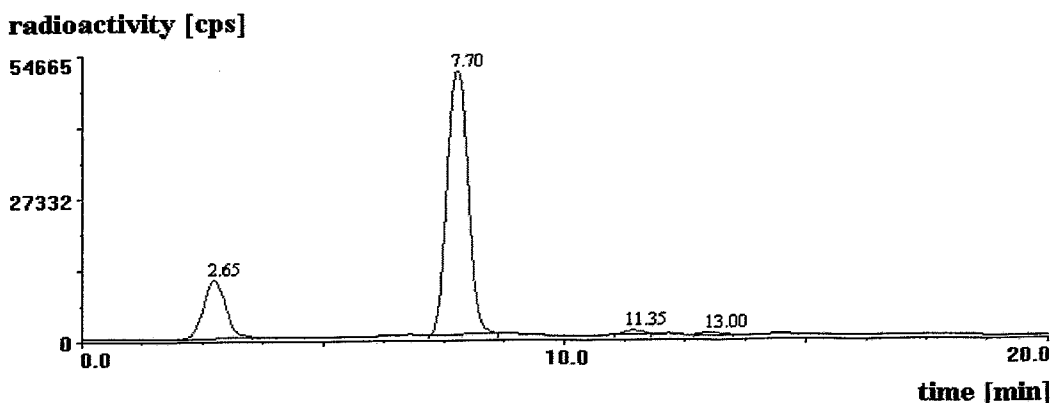


Fig. 1: HPLC radiogram obtained from the reaction mixture of the 3-methyl-[1-¹¹C]aniline synthesis
 2.65 min: [¹¹C]CH₃ONO and probably ionic compounds¹⁾; 15.5 %;
 7.70 min: 3-methyl-[1-¹¹C]aniline (**5a**); 82.5 %

When 50 μmol Na₂S·9H₂O in 100 μl H₂O were used and the reaction mixture was heated at 170 °C within 5 min, only 20 % 3-methyl-[1-¹¹C]aniline (**5a**) as well as 62 % unconverted **4a** were obtained. Additional heating for 10 min gave 37 % of 3-methyl-[1-¹¹C]aniline (**5a**) and 41 % of unconverted **4a**.

Using the reaction mixture of **4b** (radiochemical purity 78 % (Mäding *et al.*, 1995)) and 50 μmol Na₂S·9H₂O in 100 μl H₂O, 4-methyl-[1-¹¹C]aniline (**5b**) with a radiochemical purity of about 68 % was produced at 170 °C within 5 min. The reproducible radiochemical yields of **5b** (decay-corrected) are in the range of 70±5 %, within a synthesis time from [¹¹C]CH₃NO₂ of 16 min. An HPLC radiogram of unpurified **5b** is shown in Fig. 2.

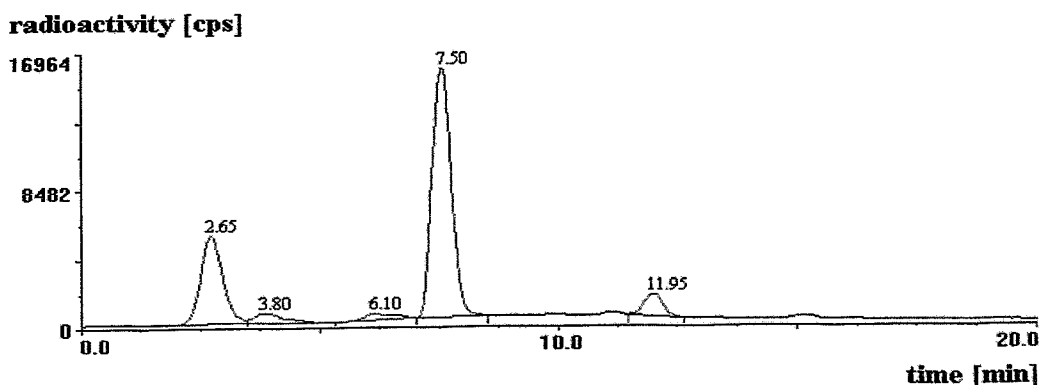


Fig. 2: HPLC radiogram obtained from the reaction mixture of the 4-methyl-[1-¹¹C]aniline synthesis
 2.65 min: [¹¹C]CH₃ONO and probably ionic compounds¹⁾; 22.9 %; 3.80 min: [¹¹C]CH₃NO₂; 1.7 %
 7.50 min: 4-methyl-[1-¹¹C]aniline (**5b**); 68.4%; 11.95 min: unidentified product; 6.2 %

¹)In addition to [¹¹C]methylnitrite (as a by-product of the nitro-[¹¹C]methane synthesis) the peak at 2.65 min probably includes N-[¹¹C]phenylsulphamic and amino-[¹¹C]benzenesulphonic acids (as possible by-products of the reduction reaction caused by SO₃²⁻ impurities in the Na₂S).

References

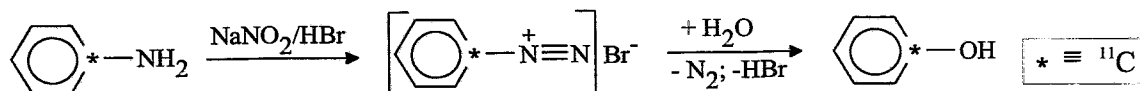
Mäding P., Steinbach J. and Kasper H. (1995) Substances labelled in metabolically stable positions: 11. The synthesis of 3-nitro-[3-¹¹C]toluene and 4-nitro-[4-¹¹C]toluene. *This report*, pp. 6-8.

5. Substances Labelled in Metabolically Stable Positions: 13. The Synthesis of [1-¹¹C] Phenole

P. Mäding, J. Steinbach, H. Kasper

Introduction

The successful synthesis of [1-¹¹C]aniline was described by Steinbach et al. (1995). Within the scope of our investigations to develop methods for ¹¹C-ring labelling of aromatic compounds we dealt with the preparation of [1-¹¹C]phenol as another important aromatic ¹¹C-synthone. It was our intention to synthesize [1-¹¹C]phenol from [1-¹¹C]aniline via diazotization and the following boildown of the diazonium salt formed:



Experimental

Analysis

To determine the extent of conversion and the radiochemical purity as well as to identify the products, an HPLC system (Merck-Hitachi) was used, including a pump, a Rheodyne injector with a 20 µl loop, a LiChrospher 100 RP-18 endcapped column (5µm, 150 mm x 3.3 mm, Merck) and a UV detector coupled in series with a radioactivity detector FLO-ONE\Beta A500 (Canberra Packard). The mobile phase was optimized as regards the composition of the eluents (MeCN and phosphate buffer pH 7 (c[NaH₂PO₄] = 0.26 mM; c[Na₂HPO₄] = 0.51 mM)) and their linear gradient at a flow rate of 0.5 ml/min. For identification of the labelled compounds by HPLC the following reference substances were used: aniline p.a. (Laborchemie Apolda, Germany) and phenol p.a. (Berlin Chemie, Germany).

Purification of the prepared [1-¹¹C]aniline and synthesis of [1-¹¹C]phenol

The synthesis of [1-¹¹C]aniline was carried out according to the one-pot procedure recently described (Steinbach et al., 1995). The reaction mixture containing the [1-¹¹C]aniline was diluted with 1 ml water and given on a LiChrolut EN cartridge (adsorber resin from Merck). After washing the cartridge with 10 ml water, [1-¹¹C]aniline was eluted with 2 ml ethanol.

The ethanolic [1-¹¹C]aniline solution was diluted with 8 ml aqueous HBr (about 1 %) and passed through a cartridge filled with cation exchange resin DOWEX 50 WX 8 (SERVA, 100-200 mesh, H⁺, neutral). The resin was washed with water to make it neutral. Radiochemically pure [1-¹¹C]aniline could be eluted with 2 M ammonia.

2 ml of the ammoniacal solution was acidified with 0.5 ml HBr (40 %) and cooled to 0 °C. The diazotization of the [1-¹¹C]aniline was carried out by adding 10 mg NaNO₂ in 100 µl water to the cooled solution. After 5 min at 0 °C the reaction mixture was heated at 100 °C for 5 min. In this way the diazonium salt formed was boiled down and [1-¹¹C]phenol was obtained.

Results and Discussion

The diazotization of the unpurified [$1\text{-}^{11}\text{C}$]aniline was not possible, because the nonradioactive substances in the reaction mixture (dimethylamine, potassium perchlorate, by-products from the excess precursor, sodium sulphide, hexamethylphosphoric triamide) interfered with the desired reaction. It was proved that the following two purification steps had to be carried out by all means:

1. Adsorption of the [$1\text{-}^{11}\text{C}$]aniline out of the water-diluted reaction mixture by using an adsorber resin from Merck (LiChrolut EN), which is able to adsorb nonpolar and weakly polar substances, such as aniline. With organic solvents, e.g. ethanol, the adsorbed compounds can be eluted from the neutrally washed resin.
2. The second purification step consisted in a cation exchange process in which the water-diluted acidified ethanolic solution containing the [$1\text{-}^{11}\text{C}$]aniline was given on cation exchange resin DOWEX 50 WX 8 (SERVA). Radiochemically pure [$1\text{-}^{11}\text{C}$]aniline could be eluted with 2 M ammonia from the neutralized resin.

The HPLC radiogram of the [$1\text{-}^{11}\text{C}$]aniline purified by these 2 steps is shown in Fig. 1.

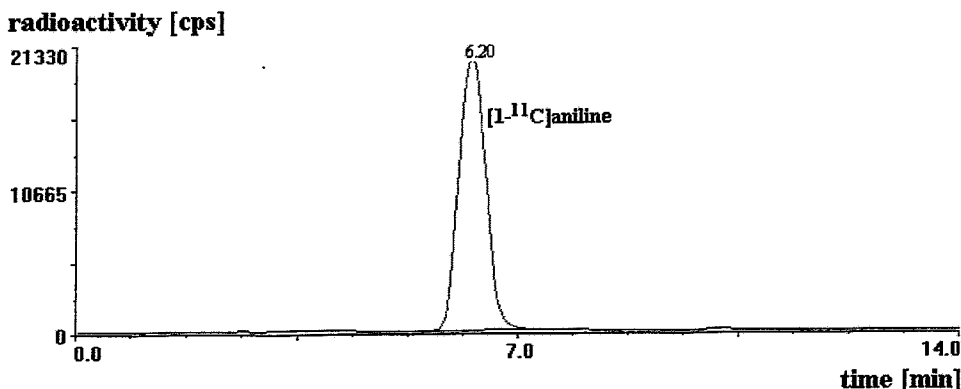


Fig. 1: HPLC radiogram of radiochemically pure [$1\text{-}^{11}\text{C}$]aniline after 2 steps of purification
1st step: LiChrolut EN cartridge (adsorber resin from Merck); 2nd step: cation exchange resin DOWEX 50 WX 8 (SERVA, 100-200 mesh, H^+ , neutral) gradient: 0 min - 70 % buffer/ 30 % MeCN; 10 min - 0 % buffer/ 100 % MeCN; 20 min - 0 % buffer/ 100 % MeCN

The used linear gradient of the eluents of Fig. 1 was not able to differentiate aniline and phenol. Using a gradient with a slower slope (0 min - 100 % buffer/ 0 % MeCN; 20 min - 0 % buffer/ 100 % MeCN), the separation of aniline and phenol was possible. This gradient was applied for the detection of [$1\text{-}^{11}\text{C}$]aniline (13.0 min) and [$1\text{-}^{11}\text{C}$]-phenol (13.85 min).

The radiochemically pure [$1\text{-}^{11}\text{C}$]aniline was diazotized with NaNO_2/HBr at $0\text{ }^\circ\text{C}$ for 5 min. The buildown of the diazonium salt at $100\text{ }^\circ\text{C}$ for 5 min gave 79.1 % of [$1\text{-}^{11}\text{C}$]phenol and 18.2 % of an unidentified product (radiochemical yields are decay-corrected). [$1\text{-}^{11}\text{C}$]Aniline could not be found, i.e. it was completely converted. The HPLC radiogram of the [$1\text{-}^{11}\text{C}$]phenol is shown in Fig. 2.

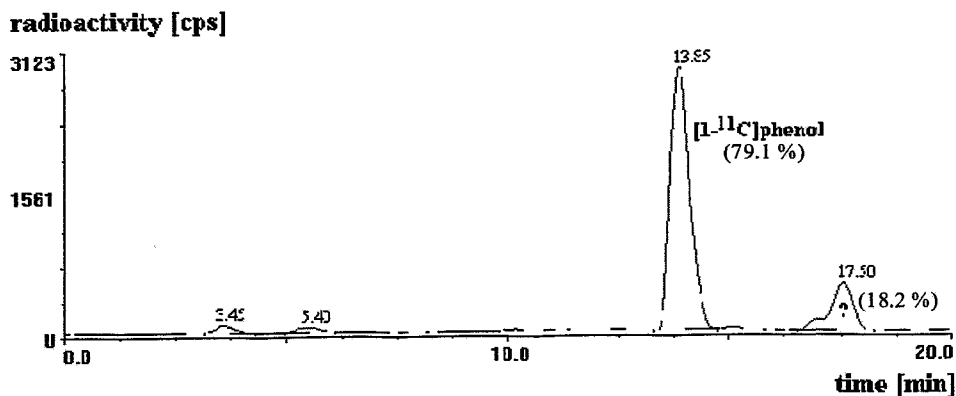


Fig. 2: HPLC radiogram of $[1-^{11}\text{C}]$ phenol after diazotization of the purified $[1-^{11}\text{C}]$ aniline with 5 mg NaNO_2 (72 μmol) in diluted HBr (5 min at 0 °C) and the following boildown of the diazonium salt formed (5 min at 100 °C); gradient: 0 min - 100 % buffer/ 0 % MeCN; 20 min - 0 % buffer/ 100 % MeCN.

References

Steinbach J., Mäding P., Füchtner F. and Johannsen B. (1995) N.c.a. ^{11}C -labelling of benzenoid compounds in ring positions: synthesis of nitro- $[1-^{11}\text{C}]$ benzene and $[1-^{11}\text{C}]$ aniline. *J. Labelled Compd. Radiopharm.* **36**, 33-41.

6. Substances Labelled in Metabolically Stable Positions:

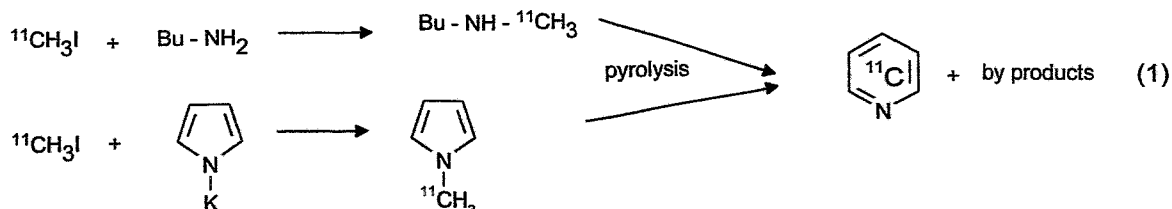
14. Synthesis of $[^{11}\text{C}]$ -labelled Pyridine and Derivates by Pyrolysis

K. Chebani, J. Zessin, J. Steinbach

Introduction

In accordance with indications in the literature (Bell *et al.*, 1969, Patterson *et al.*, 1962) pyrolysis has proved to be a useful tool to prepare pyridine and pyridine derivatives. This method exploits the stabilizing energy of aromatics.

In order to apply these results to the synthesis of $[^{11}\text{C}]$ pyridine and its derivatives we carried out nonradioactive initial pyrolysis experiments (Chebani *et al.*, 1994). Pyrrole potassium and butylamine were selected to be the most suitable candidates for future ^{11}C labelling. The essential step of this method of preparing $[^{11}\text{C}]$ pyridine is the preparation of an ^{11}C -labelled compound containing the C_5N structure and its pyrolysis (see equation (1)). The experiments with ^{11}C were started under comparable conditions as the nonradioactive experiments on a carrier added (c.a.) scale and continued in the non carrier added (n.c.a.) scale.



Experimental

The general procedure utilized is as follows: A C₄N-amine is methylated with [¹⁴C]CH₃I and subsequently pyrolysed. Products generated are collected and analysed.

Synthesis of [¹⁴C]methyl iodide

[¹⁴C]Methyl iodide was prepared by the classic one-pot method involving the reduction of [¹⁴C]carbon dioxide with LiAlH₄, hydrolysis of the intermediate organometallic complex and the subsequent iodization of the [¹⁴C]methanol formed with HI (Crouzel *et al.*, 1987).

Formation of butyl-[¹⁴C]methylamine and N-[¹⁴C]-methylpyrrole

Butyl-[¹⁴C]methylamine was synthesized in a similar manner as described by (Chebani *et al.*, 1994). The [¹⁴C]methyl iodide in a nitrogen carrier gas stream was introduced into a cooled mixture of 5 µl butyl amine and 0.5 ml acetone. After reaching a constant level of radioactivity the reaction vial was closed and heated to 100 °C for 2 minutes. At this time a nitrogen gas stream passed through the vial forcing the solvent to evaporate. The residue was mixed with 0.2 ml nonradioactive butylmethylamine and this solution was used directly for the pyrolysis experiments.

N-[¹⁴C]Methylpyrrole was formed by the same procedure as described above. Pyrrole sodium or pyrrole potassium was suspended in tetrahydrofuran (THF). After introducing the [¹⁴C]methyl iodide the reaction vial was warmed to 100 °C for 1 minute. This solution was used directly or after adding 0.2 ml nonradioactive N-methylpyrrole for further experiments.

Pyrolysis experiments - general rules:

The pyrolyses of butyl-[¹⁴C]methylamine and N-[¹⁴C]methylpyrrole were carried out in two horizontally arranged quartz glass tubular reactors (reactor (I) for c.a. scale: 400 mm x 12 mm; reactor (II) for n.c.a. scale: 380 mm x 3 mm). Argon was used as an inert carrier gas. The substances were injected either by a syringe, an HPLC pump or via a gas chromatograph directly at the beginning of the hot zone of the oven. The residence time was in the order of 5 to 15 seconds (reactor (I)) and 2 to 4 seconds in the case of reactor (II). The pyrolysis products were collected in a cooled trap filled with 1 ml absolute ethanol. The overall time necessary for the whole procedure starting from [¹⁴C]CO₂ is about 20 minutes.

The analysis of the pyrolysis products was performed by an HPLC system (from Merck/Hitachi consisting of a pump, a Rheodyne injector with 20 µl loop, a LiChrospher 100 column (5 µm, 150 mm x 3.3 mm) and a UV/VIS detector coupled in series with the radioactivity detector FLO-ONE/Beta A500 from Canberra Packard). The eluent started with 100 % phosphate buffer according to Sørensen (0.26 mM NaH₂PO₄ and 0.51 mM Na₂HPO₄, pH 7) and changed to acetonitrile with the following linear gradient: 0 min: 100 % buffer, 0 % acetonitrile; 10 min: 0 % buffer, 100 % acetonitrile; 20 min: 0 % buffer, 100 % acetonitrile. The flow rate was 0.5 ml/min.

In the case of c.a. experiments the products were analysed by a gas chromatograph with a mass selective detector (GC system HP 5890 with MSD HP 5972; column: Chrompack HP-5, 30 m, 0.25 mm; helium flow: 65 ml/min, temperature programme: 45 °C (2 min) to 150 °C at 8 K/min).

Pyrolysis of c.a. butyl-[¹⁴C]methylamine

A solution of c. a. butyl-[¹⁴C]methylamine in benzene was injected with an HPLC pump over a sample loop into the reactor (I) filled with palladium on charcoal as dehydrogenation catalyst. The optimized oven temperature was 500 °C.

Pyrolysis of c.a. N-[¹⁴C]methylpyrrole

The pyrolysis of N-[¹⁴C]methylpyrrole with the addition of nonradioactive N-methylpyrrole was carried out in the same way as outlined above. The reaction temperature was 600 °C. THF was used as a solvent for the injection by means of an HPLC pump.

Pyrolysis of n.c.a. N-[¹⁴C]methylpyrrole

The pyrolysis of N-[¹⁴C]methylpyrrole on the n.c.a. level was performed in reactor (II) with a quartz glass packing at an oven temperature of 750 °C. Before injecting the labelled compound, the THF was removed by a gas chromatograph. A Perkin-Elmer F22 chromatograph with a thermal conductivity detector (column: glass, 2 m, 5 % Carbowax 20M on Porolith, 0.2 - 0.25 mesh; helium with 20 ml/min, temperature: 80 °C to 120 °C at 4K/min, injector temperature: 230 °C, detector temperature: 250 °C) was

used. 10 - 50 μ l of the reaction mixture were injected. If the solvent passed the GC, it was discarded. The pure N- ^{11}C methylpyrrole was introduced by the carrier gas of the chromatograph directly into the pyrolysis tube.

Results and Discussion

Pyrolysis of c.a. butyl- ^{11}C methylamine

The best pyrolysis conditions (see experimental part) were found by experiments with nonradioactive butylmethylamine. The highest yields of pyridine were obtained using a reactor filled with palladium on charcoal as dehydrogenation catalyst at 500 °C (Chebani *et al.*, 1994). Analogously to these investigations, the pyrolysis of c.a. butyl- ^{11}C methylamine produces a mixture of various nitrogen containing heterocycles (see Fig. 1). In addition to ^{11}C pyridine (20 %), also N- ^{11}C methylpyrrole (15 %) and other products were obtained. The share of the substances was determined by HPLC, the values are decay corrected. The absolute radiochemical yield of ^{11}C pyridine was not determined.

The formation of ^{11}C pyrrole (16 %) is very remarkable. That means, that pyrrole was not only formed by cleavage of the $\text{CH}_3\text{-N}$ bond followed by cyclization of the resulting butylamine. Obviously, the $\text{CH}_3\text{-CH}_2$ bond also cleaves and the ^{11}C methylpropylidene amine fragment forms the pyrrole ring.

The fourth product identified was ^{11}C toluene (3 %), resulting from benzene used as a solvent.

In addition to the identification of compounds by reference substances, the compounds could also be identified by GC-MS.

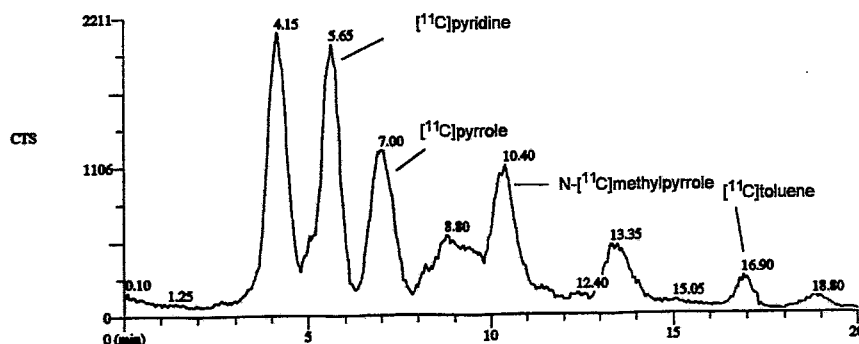


Fig. 1: HPLC radiogram obtained from pyrolysis of c.a. butyl- ^{11}C methylamine (palladium on charcoal filled reactor (I) at 500 °C)

Pyrolysis of c.a. N- ^{11}C methylpyrrole

In comparison with butylmethylamine, pyrolysis of N-methylpyrrole yields smaller amounts of by-products (Chebani *et al.*, 1994). This could also be confirmed by pyrolysis of N- ^{11}C methylpyrrole on the c.a. level at 600 °C. The reactor (I) was filled with palladium on charcoal. The product mixture contains above all ^{11}C pyridine (57 %), unreacted N- ^{11}C methylpyrrole (19 %) and ^{11}C toluene (8 %). The last-named results from the injection mode (see experimental part). The absolute decay-corrected radiochemical of ^{11}C pyridine varied from 3 % to 8 % because of losses in the reactor.

In comparison with the pyrolysis of butyl- ^{11}C methylamine, the share of ^{11}C pyridine in the product mixture increased in these experiments. But the absolute yield of ^{11}C pyridine was nearly unchanged. The analysis by GC-MS showed that tetrahydrofuran (THF) is rather stable under pyrolysis conditions.

Pyrolysis of n.c.a. N- ^{11}C methylpyrrole

Because of the more successful results with c.a. N- ^{11}C methylpyrrole, n.c.a. experiments were only performed with n. c.a. N- ^{11}C methylpyrrole.

The pyrolysis of the N- ^{11}C methylated pyrrole on the n.c.a. level was carried out in the small reactor (II) with a quartz glass packing at 750 °C. The N- ^{11}C methylpyrrole solution from the reaction vial was purified by semipreparative gas chromatography to remove the solvent THF. The pure substance was introduced into the oven by the carrier gas of the GC system (helium).

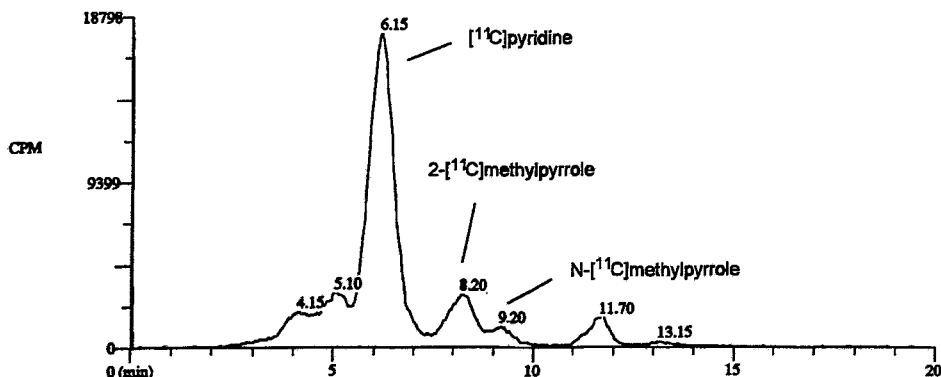


Fig. 2: HPLC radiogram obtained from the pyrolysis of n.c.a. N-[^{11}C]methylpyrrole (reactor (II) with quartz glass packing at 750 °C)

The product composition changed considerably under these conditions in comparison with the c.a. experiments (Fig. 2). The main product was [^{11}C]pyridine. The percentage is in the order of 83 %. The absolute decay corrected radiochemical yield of [^{11}C]pyridine was in the order of 9 % \pm 7 %. The use of quartz glass packings instead of the dehydrogenation catalyst palladium on charcoal leads to an increase in this quantity. Other products were unreacted N-[^{11}C]methylpyrrole (1 %) and the intermediate 2-[^{11}C]methylpyrrole (11 %). These compounds indicate an incomplete conversion of the N-[^{11}C]methylpyrrole.

Why is this result so different from that of c.a. conditions? Because of the n.c.a. state and the injection of only the GC-separated N-[^{11}C]methylpyrrole, the pure compound is passed through the reactor in a very low concentration. The number of other reaction molecules is very low. The open number of reaction channels are therefore directed to intramolecular ones. The formation of unsubstituted [^{11}C]pyridine is favoured.

Pyrolysis of N-[^{11}C]methylated pyrrole and the special concentration conditions in the n.c.a. state lead to the highest share of [^{11}C]pyridine. Further work has to be done to optimize the absolute yield.

References

- Bell W.H., Carter G.B. and Dewing J.J. (1969) Heterocycles synthesis by high temperature dehydrocyclization of amines and imes with iodine. *J. Chem. Soc. (C)* **1969**, 352.
- Chebani K., Zessin J. and Steinbach J. (1994) Substances labelled in metabolically stable positions: 9. Synthesis of pyridine by thermal rearrangement of amines containing the C_5N structure. *Annual Report 1994*, Institute of Bioinorganic and Radiopharmaceutical Chemistry, FZR-73, pp. 113-117.
- Crouzel C., Langström B., Pike V.W. and Coenen H.H. (1987) Recommendations for a practical production of [^{11}C]methyl iodide. *Appl. Radiat. Isot.* **38**, 601-603.
- Patterson J.M. and Drenchko P.J. (1962) Pyrolysis of N-methylpyrrole and 2-methylpyrrole. *J. Org. Chem.* **27**, 1650.

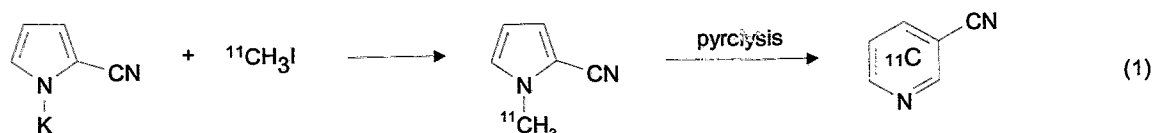
7. Substances Labelled in Metabolically Stable Positions:

15. Synthesis of Cyano-[¹¹C]pyridines and [¹¹C]labelled Pyridine Carboxyamides by Pyrolysis

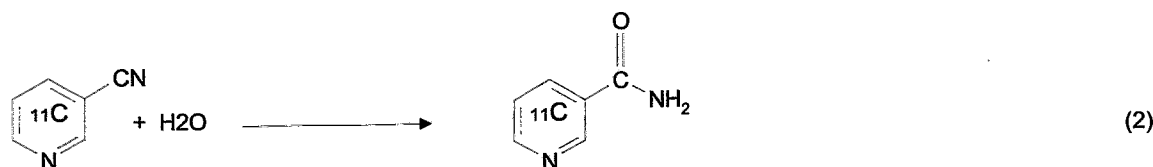
K. Chebani, J. Zessin, J. Steinbach

Introduction

Pyrolysis of various ¹¹C-labelled C₅N amines is a suitable method for the synthesis of ring-labelled pyridine. The best results were achieved by pyrolysis of N-[¹¹C]methylpyrrole (Chebani *et al.*, 1995). In continuation of this work, the synthesis of substituted [¹¹C]pyridines based on this method was investigated. The aim is the synthesis of 3-cyano-[¹¹C]pyridine (equation (1)).



This compound can be easily converted to nicotinamide by hydrolysis (equation (2)).



Experimental

2-Cyanopyrrole potassium

2-Cyanopyrrole potassium was synthesized from 2-cyanopyrrole. Potassium was suspended in a solution of 2-cyanopyrrole in toluene. The 2-cyanopyrrole was synthesized according to Barnett *et al.*, 1980). This reaction mixture was refluxed until all potassium was dissolved. After complete reaction, the suspension was filtered and the moist crude product was stored without drying because of the instability of the dry substance.

Synthesis of non carrier added (n.c.a.) 2-cyano-N-[¹¹C]methylpyrrole

Approximately 30 mg of the crude precursor were washed several times with dry tetrahydrofuran (THF) and resuspended in 200 μ l THF. [¹¹C]Methyl iodide was introduced into this reaction mixture at -78 °C.

After finishing the adsorption, the reaction mixture was heated to 100 °C for one minute. The resulting solution was directly used for the pyrolysis experiments.

Pyrolysis of n.c.a. 2-cyano-N-[¹¹C]methylpyrrole

A horizontally arranged quartz glass tubular reactor (380 x 3 mm) was used for the pyrolysis experiments. This reactor was filled with quartz glass packings. We tested the reaction temperatures 700 °C, 750 °C, 850 °C or 900 °C during various experiments. Argon was used as an inert carrier gas with a flow of 5 ml per minute.

A gas chromatograph F22 from Perkin Elmer (glass column, 2600 mm x 5 mm, 5 % Carbowax 20M on Porolith, 0.2 - 0.25 mesh; helium with 20 ml/min, temperature: 180 °C to 200 °C at 4 K/min, injector temperature: 230 °C, detector temperature: 200 °C, injection volume: 10 to 50 μ l) was used to remove the THF and for separating 2-cyano-N-[¹¹C]methylpyrrole. The pure 2-cyano-N-[¹¹C]methylpyrrole was introduced into the reactor by the carrier gas of the GC. The pyrolysis products were collected in a dry ice cooled trap filled with 1 ml of absolute ethanol.

Hydrolysis of the cyano-[¹¹C]pyridines

The cyano-[¹¹C]pyridines were converted into the corresponding pyridine carboxyamides by an anion exchange resin (Wofatit SBW column, OH⁻ form) (Galat, 1948). A water-ethanol mixture was used as eluent. It takes 5 to 10 minutes to complete the hydrolysis.

Determination of the cyanopyridines and their derivatives

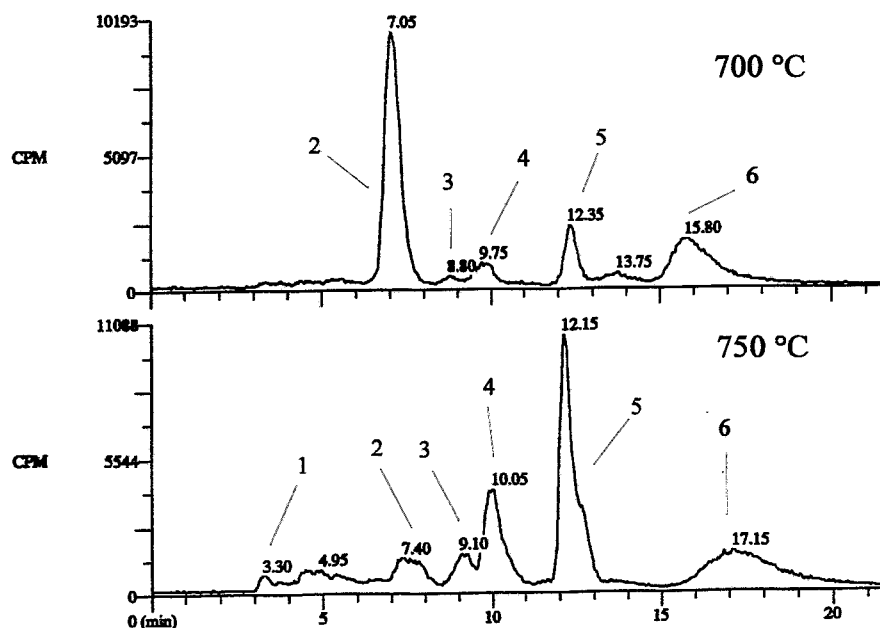
The analysis of the pyrolysis products and the corresponding hydrolysed compounds was performed by means of a Merck/Hitachi HPLC system. It consists of a pump with a low pressure gradient system, a Rheodyne injector with a 20 µl loop, a UV/VIS detector (215 nm) and a radioactivity detector FLO-ONE\Beta A500 (Canberra Packard) coupled in series.

The cyano-[¹¹C]pyridine isomers as pyrolysis products were separated using an NH₂-modified column (Separon SGX-NH₂ (7 µm), 250 mm x 4mm). The eluent consists of a mixture of 100 volume parts n-heptane and 2.4 volume parts isopropanol. The HPLC was run in an isocratic mode with a flow of 1 ml/min.

The pyridine carboxyamides were separated by means of an RP18-column (150 mm x 3.3 mm, LiChrospher, 5 µm). The mobile phase - a mixture of 95 % phosphate buffer according to Sørensen (0.26 mM NaH₂PO₄ and 0.51 mM Na₂HPO₄, pH 7) and 5 % acetonitrile - was applied in an isocratic mode (flow 0.8 ml/min). This method does not allow the separation of nicotinamide and isonicotinamide. The problem was solved by HPLC with a CN-modified material (250 mm x 4 mm, LiChrosorb CN, 5 µm). The eluent contains 90 volume percent n-heptane and 14 volume percent isopropanol. The flow rate was 2 ml/min (isocratic mode).

Results and Discussion

The pyrolysis of 2-cyano-N-[¹¹C]methylpyrrole yields a product mixture containing the cyano-[¹¹C]pyridine isomers, unsubstituted [¹¹C]pyridine, N-[¹¹C]methylpyrrole and the unreacted parent compound. The composition of these products was influenced above all by the reaction temperature. This fact is illustrated by the radiograms in Fig. 1. The upper radiogram indicates a lower conversion of the 2-cyano-N-[¹¹C]methylpyrrole at 700 °C in comparison with that at 750 °C. Only 42 % were reacted to the monocyano-[¹¹C]pyridine isomers. The product composition changed considerably when the pyrolysis was performed at 750 °C (Fig. 1, lower radiogram). Now only 1 % of the parent substance was detected. The percentage of the cyano-[¹¹C]pyridine isomers was 87 %. Another product is the unsubstituted [¹¹C]pyridine with a remarkable share of 6 %. That means that a cleavage of the bond between the cyano group and the heterocyclic ring occurs at this temperature. At temperatures above 750 °C the cleavage of this bond became more evident.



Compound	Percentage at 700 °C	Percentage at 750 °C
1) N-[¹¹ C]methylpyrrole	-	1 %
2) 2-cyano-N-[¹¹ C]methylpyrrole	54 %	6 %
3) [¹¹ C]pyridine	2 %	5 %
4) 4-cyano-[¹¹ C]pyridine	5 %	18 %
5) 3-cyano-[¹¹ C]pyridine	12 %	41 %
6) 2-cyano-[¹¹ C]pyridine	25 %	28 %

The other substances could not be identified

Fig. 1: HPLC radiograms of the products after pyrolysis of 2-cyano-N-[¹¹C]methylpyrrole at 700 °C and 750 °C

The ratio of the monocyano[¹¹C]pyridines also depended on the pyrolysis temperature. The percentage of 2-cyano-[¹¹C]pyridine was higher than at of the 3-cyano compound at 700 °C. The latter was the main product at 750 °C and higher temperatures. The amount of 4-cyano-[¹¹C]pyridine was nearly constant in all cases. The reaction mechanism is not well understood. It is not possible to decide whether the cyano group moved at the pyrrole or at the pyridine ring. The 3-cyano pyridine seems to be the most stable isomer, because it was the main product at higher pyrolysis temperatures.

The absolute overall radiochemical yields of the three cyano-[¹¹C]pyridines related to 2-cyano-N-[¹¹C]methylpyrrole was 24 % ± 10 % (decay corrected). A lot of substance was lost by carbonization of the substances. All percentages of the compounds were determined by means of HPLC and the values are decay-corrected.

The cyano-[¹¹C]pyridines obtained could be hydrolysed with various acids or bases as catalysts. If dissolved sulfuric acid was used, the cyanopyridines were converted into the corresponding carboxylic

acids. The use of an anionic exchange resin leads very selectively and fast to the intermediate carboxyamides. This is illustrated by the HPLC radiogram in Fig. 2.

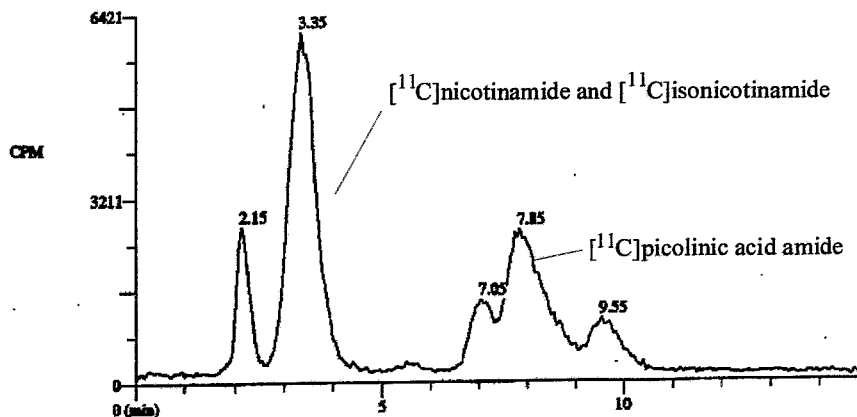


Fig. 2: HPLC radiogram after the hydrolysis of pyrolysis products from 2-cyano-N-[¹¹C]methylpyrrole at 750 °C (RP-18 column, phosphate buffer - acetonitrile eluent (see experimental part)).

These investigations demonstrate that also selected ring-labelled substituted pyridines can be synthesized by pyrolysis of the corresponding N-[¹¹C]methylpyrrole derivatives, e.g. 2-, 3- and 4-cyano-[¹¹C]pyridine was obtained, starting from 2-cyano-N-[¹¹C]methylpyrrole.

The obtained overall yields of the desired 3-cyano-[¹¹C]pyridine and 3-[¹¹C]nicotinoamide are expected to increase by optimizing the reaction conditions. In view of the short reaction times the pyrolysis method presented here provides a valuable access to ring-labelled pyridine derivatives.

References

- Barnett G.H., Anderson H.J. and Loader L.E. (1980) Pyrrole chemistry XXI. Synthetic approaches to cyanopyrrole. *Can. J. Chem.* **58**, 409-411.
- Chebani K., Zessin J. and Steinbach J. (1995) Substances labelled in metabolically stable positions: 14. synthesis of ¹¹C-labelled pyridines and derivatives by pyrolysis. *This report*, pp. 12-15.
- Galat A. (1948) Nicotinamide from nicotinonitrile by catalytic hydration. *J. Am. Chem. Soc.* **70**, 3945.

8. Synthesis of 3-O-Methoxymethyl-16 β ,17 β -O-sulfuryl-estra-1,3,5(10)-triene-3,16 β ,17 β -triol

J. Römer, J. Steinbach, H. Kasch¹
¹Hans-Knöll-Institut Jena

Introduction

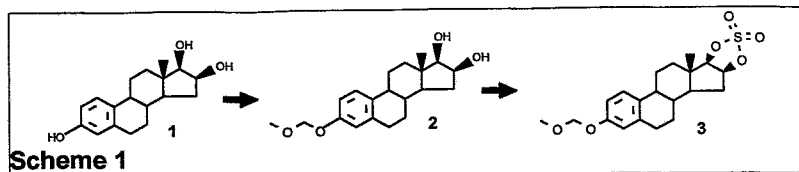
The title compound representing a cyclic sulfate was used as a suitable precursor in a new procedure for preparing 16 α -[¹⁸F]fluoroestradiol (Lim *et al.*, 1994).

According to recent literature (Berridge *et al.*, 1990) cyclic sulfates are considered useful substrates for selective nucleophilic substitution. The cyclic sulfate group appears to be a generally useful means for simultaneously facilitating nucleophilic reactions and protecting nearby hydroxyl functions.

There were stereochemical and steric arguments which favoured the title steroid as a precursor. The nucleophilic fluoride attacking from the less hindered α -side reacts preferentially with the carbon atom C(16). C(17) is not attractive because its C - α H bond is arranged in three 1,3-diaxial H-H interactions (Beierbeck and Saunders, 1976). In this way mainly 16 α -F is formed.

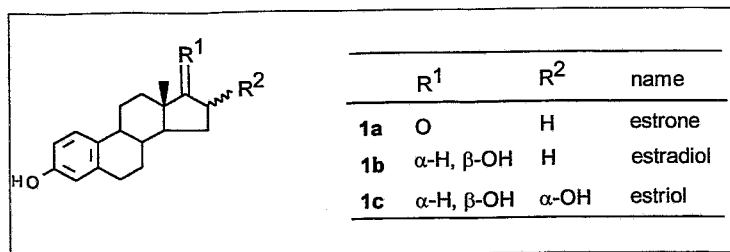
This precursor could not be acquired by purchase. It had to be prepared from 16-epiestriol (**1**), a commercially available steroid. The synthesis seemed to be simple. First the 3-hydroxy group of **1** had to be protected by the methoxymethyl group. Then the 3-O-methoxymethyl-estra-1,3,5(10)-triene-3,16 β ,17 β -triol (**2**) obtained had to be converted into 3-O-methoxymethyl-16 β ,17 β -O-sulfuryl-estra-1,3,5(10)-triene-3,16 β ,17 β -triol (**3**) using sulfuryl chloride or sulfuryldiimidazol.

In the following the synthesis of the new precursor **3** is described. The two reactions are shown in Scheme 1.



Results and Discussion

Before converting the expensive 16-epiestriol **1**, we studied the etherification of the 3-hydroxyl group with methoxymethyl chloride (MOMCl) at three commercially available, cheaper 3-hydroxy-estra-1,3,5(10)-trienes, namely estrone (**1a**), estradiol (**1b**), and estriol (**1c**). The reaction medium was anhydrous tetrahydrofuran (THF) in which estrone and estradiol were readily dissoluble. The double molar amount of NaH was used as the base. The etherification reagent MOMCl was applied in one and a half molar amounts. The etherification was carried out at room temperature and controlled by HPLC. One hour was sufficient for nearly full conversion.



Estriol was not readily soluble in THF. Using a suspension of estriol in THF, the etherification reaction did not start. This inhibition could be overcome by adding ethanol. Using THF/EtOH mixtures, the reaction of 16-epiestriol (**1**) with MOMCl was also successful. 3-O-Methoxymethyl-estra-1,3,5(10)-triene-3,16 β ,17 β -triol (**2**) was obtained in a 97 % yield. According to HPLC an unknown by-product was contained in a negligible amount.

Sulfonyldiimidazol was used for esterifying **2**. A solution of **2** in dry THF was treated with a fourfold molar amount of NaH. After stirring the suspension for some minutes, a solution of the molar amount of sulfonyldiimidazol in dry THF was added. Esterification yielded 3-O-methoxymethyl-16 β ,17 β -O-sulfuryl-estra-1,3,5(10)-triene-3,16 β ,17 β -triol (**3**) within a few minutes. According to HPLC this cyclic sulfate represented the expected unpolar steroid.

Experimental

1. General

Solvents and reagents were purchased from the following commercial sources: Aldrich, Fluka, and Sigma. They were used as received.

Melting points were determined on a Thermogalen melting point apparatus (Leica) and are uncorrected. ¹³C NMR spectra were recorded on an FT-NMR spectrometer MSL 300 (Bruker spectrospin) at 75 MHz, using tetramethylsilane as an internal standard. Mass spectra were obtained on a Finigan MAT 95 spectrometer and on a VG Quattropol spectrometer (Fisons Instruments). For the chromatographic experiments HPLC equipment from Merck-Hitachi was used, including a gradient pump (L-6200A), a Rheodyne injector with a 20 μ l loop, a Macherey & Nagel column ET 125/8/4 Nucleosil 120-5C₁₈, and a diode array detector (L-4500 DAD) coupled in series with a radioactivity detector. MeCN-water mixtures were the mobile phase at a flow rate of 0.5 ml/min with a linear gradient (0 min - 20 % MeCN, 10 min - 90 % MeCN) and isocratic elution for a further 5 min with 90 % MeCN.

2. Syntheses

3-O-Methoxymethyl-estra-1,3,5(10)-triene-3,16 β ,17 β -triol (2):

16-epiestriol (1) (SIGMA, 875 mg = 3 mmol), tetrahydrofuran (dry, 40 ml) and a magnetic stirrer were placed in a bulb. After adding NaH (60 % suspension in mineral oil, 200 mg = 5 mmol), the suspension was stirred and a solution of methoxymethyl chloride (0.35 ml = 4.4 mmol) in THF (about 2 ml) was dropped in. Then EtOH (abs., 10 ml) was added. After the suspension had been stirred for 1 h, the solvent was evaporated in vacuo and the residue extracted with ether. The ether extract was washed with water, dried (Na₂SO₄) and evaporated. Yield: (980 mg, 97 %) as white crystals; melting point: 145 °C (from EtOH). ¹³C NMR data : δ_{C-13} (22.63 MHz, solvent CDCl₃, standard SiMe₄). In comparison with the spectrum of 1, there were two additional signals for the two carbon atoms of the methoxymethyl group: methylene-C (δ = 94.4 ppm), methoxy-C (δ = 55.8 ppm). Mass spectrum: m/z 332.1986 (M⁺) for C₂₀H₂₈O₄.

3-O-Methoxymethyl-16 β ,17 β -O-sulfuryl-estra-1,3,5(10)-triene-3,16 β ,17 β -triol (3):

In a bulb with a magnetic stirrer, 3-O-methoxymethyl-estra-1,3,5(10)-triene-3,16 β ,17 β -triol (2) (980 mg = 2.95 mmol) was dissolved in anhydrous THF (30 ml). NaH (500 mg = 12.5 mmol) was added while stirring. Ten minutes later, a solution of sulfonyldiimidazol (600 mg = 3 mmol) in anhydrous THF (12 ml) was dropped in and stirring continued. After 1 h the solution was filtered and evaporated. The residue was extracted with ether, the extract was washed with water and dried (Na₂SO₄). By vaporizing the ether, fine crystals were obtained. Yield: (1010 mg, 85 %). Melting point 139-145 °C (from Me₂CO/H₂O). ¹³C-NMR data: δ_{C-13} (22.63 MHz, solvent CDCl₃, standard SiMe₄). In comparison with 2, the cyclic sulfate 3 showed significant shifts of the signals of the carbon atoms C(13) 1.00 ppm, C(14) 1.28 ppm, C(15) - 3.69 ppm, C(16) 11.94 ppm, C(17) 9.84 ppm. Mass spectrum: m/z 394.1460 (M⁺) for C₂₀H₂₆O₆S.

Acknowledgements

We wish to express our gratitude to the Deutsche Forschungsgemeinschaft for its grant in support of this work. The authors also thank Dr. Scheller and Dr. Klostermann of the Dresden University of Technology for recording the ¹³C NMR and the mass spectra, and Dr. Saldarreaga (Comision Ecuatoriana de Energia Atomica Quito) for his kind assistance and helpful discussions.

References

- Beierbeck, H. and Saunders, J.K. (1976) A new interpretation of the α -, β -, and γ -substituent effects on the ¹³C chemical shift. *Can. J. Chem.* **54**, 2985.
- Berridge, M.S., Franceschini, M.P., Rosenfeld, E., and Tewson, T.J. (1990) Cyclic sulfates: useful substrates for selective nucleophilic substitution. *J. Org. Chem.* **55**, 1211.
- Lim J.L., Berridge M.S. and Tewson T.J. (1994) Preparation of [¹⁸F]16 α -fluoro-17 β -estradiol by selective nucleophilic substitution. *J. Labelled Compd. Radiopharm.* **35**, 176 (Abstract).

9. Synthesis of 16 α -[¹⁸F]Fluoroestradiol

J. Römer, J. Steinbach, H. Kasch¹

¹Hans-Knöll-Institut Jena

Introduction

The imaging of estrogen receptor sites is of growing interest in the search for estrogen receptor positive tumours. In order to exploit the opportunities of PET, a suitable radiotracer was required. In the eighties it was demonstrated that 16 α -[¹⁸F]fluoroestradiol has a similarly high binding affinity to the estrogen receptor as estradiol and should consequently be a suitable imaging agent. Therefore, a first synthetic route was developed (Kiesewetter *et al.*, 1984 a). In this synthesis the bis-triflate of 16 β -hydroxyestrone was used as a precursor. Treatment with tetrabutylammonium fluoride followed by LiAlH₄ reduction in ether produced mainly 16 α -fluoroestradiol. In the radioactive synthesis the overall time from EOB to the purified tracer was 70 - 110 min, the overall yields were 30 - 60 % (Kiesewetter *et al.*, 1984 b).

Using PET, the n.c.a. 16 α -[¹⁸F]fluoroestradiol has already been successfully applied for imaging human breast carcinomas (Mintun *et al.*, 1988) and their metastases (McGuire *et al.*, 1991). This PET tracer can become a valuable tool and its widespread clinical application will depend on its ready availability. This explains the producer's general wish for an even more rapid, convenient, and efficient synthesis of this radiotracer.

Recently a new one-pot procedure was proposed (Lim *et al.*, 1994). This procedure seemed to meet all the above-mentioned demands. The overall radiochemical yield was reported to be 50 - 60 %, the total time requirement 60 min.

As precursor in his new procedure Lim used 3-O-methoxymethyl-16 β ,17 β -O-sulfuryl-estra-1,3,5(10)-triene-3,16 β ,17 β -triol (**1**) which was converted in a 3-step synthesis into 16 α -fluoroestradiol (**4**). Lim's procedure is shown in Fig. 1.

Unfortunately, full details of the reaction sequence were not published in Lim's abstract. Concerning the synthesis of 16 α -fluoroestradiol (**4**), it was only reported that **1** is treated with stoichiometric anhydrous tetramethylammonium fluoride (Me₄NF) and then hydrolysed with 2 M HCl. Comments about the intermediates of the 3-step reaction sequence were not made. Moreover, Tewson (1995) mentions that there were difficulties in hydrolysis.

In our investigations we were able to duplicate the nucleophilic substitution reaction of **1** with fluoride. However, the hydrolysis caused unexpected difficulties with regard to achieving a rapid reaction and a high radiochemical yield of 16 α -fluoroestradiol. As furthermore the knowledge of the reaction sequence **1** \rightarrow **4** is deficient, we decided to investigate these reaction steps thoroughly and to transfer the results to an improved radiosynthesis.

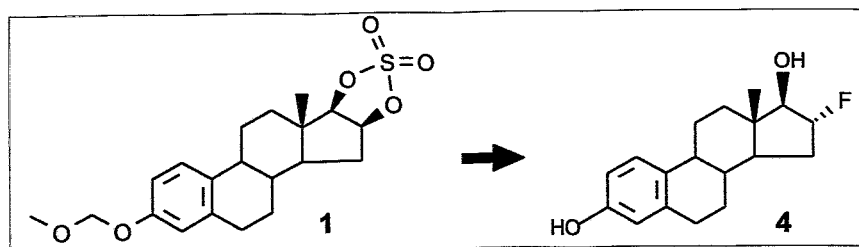


Fig. 1: Conversion of 3-O-methoxymethyl-16 β ,17 β -O-sulfuryl-estra-1,3,5(10)-triene-3,16 β ,17 β -triol (**1**) into 16 α -fluoroestradiol (**4**) according to Lim *et al.* (1994)

Results and Discussion

1. Elaboration of the method

3-O-methoxymethyl-16 β ,17 β -O-sulfuryl-estra-1,3,5(10)-triene-3,16 β ,17 β -triol (**1**) was prepared as previously described (Römer *et al.*, 1995). Then we investigated the exact course of the 3-step reaction **1** \rightarrow **4**. This 3-step reaction consists of a nucleophilic substitution step and two subsequent hydrolysis steps. We found that the sulfuryl ring of **3** was opened by tetramethylammonium fluoride (Me₄NF, carefully dried) in refluxing absolute acetonitrile for a few minutes. The resulting fluorosteroid after work-up was shown to be stable 3-O-methoxymethyl-16 α -fluoro-estra-1,3,5(10)-triene-3,17 β -diol-17 β -sulfate (**2**), which was characterized by MS and ¹³C NMR spectroscopy .

After refluxing **2** with HCl, the methoxymethyl group and the sulfate group were split. 16 α -fluoro-estra-1,3,5(10)-triene-3,17 β -diol-17 β -sulfate (**3**) was formed first, then 16 α -fluoro-estra-1,3,5(10)-triene-3,17 β -diol (= 16 α -fluoroestradiol)(**4**).

In order to characterize 16 α -fluoro-estra-1,3,5(10)-triene-3,17 β -diol-17 β -sulfate (**3**) by ¹³C NMR spectroscopy it was necessary to prepare the pure compound. The simplest way consisted in passing the raw material **2** through a column filled with cation exchange resin in the H⁺ form, followed by refluxing the eluted acid solution. The small H⁺ concentration was enough for quantitative conversion **2** \rightarrow **3** and did not attack the 17 β -sulfate group. After refluxing, the H⁺ ions were removed using the same column in the Na⁺ form. Finally the eluted neutral solution was lyophilized.

For preparing pure 16 α -fluoro-estra-1,3,5(10)-triene-3,17 β -diol (**4**), a hydrolysed batch containing mainly **4** was extracted by ether. After ether evaporation the residue was dissolved in acetonitrile and purified by reversed phase HPLC. The final product **4** was also characterized by MS and ¹³C NMR spectroscopy.

The characterization of all the compounds allowed the unequivocal presentation of the reaction course **1** \rightarrow **4** which is shown in Fig. 2.

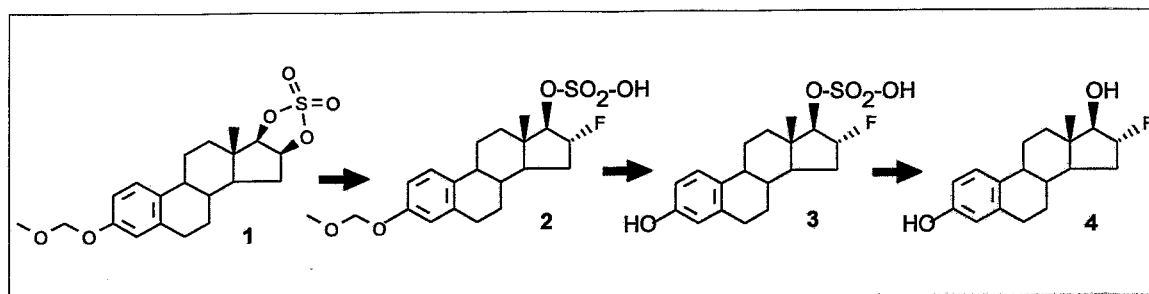


Fig. 2: The exact reaction sequence of the nucleophilic fluorination **1** \rightarrow **2** and the hydrolysis steps **2** \rightarrow **3** \rightarrow **4** of the new procedure to prepare 16 α -fluoroestradiol (**4**)

The steroids studied here differ widely in their chromatographic behaviour. The cyclic sulfate **1** is a non-polar steroid whereas the opened sulfates **2** and **3** are very polar ones. However, using an HPLC gradient method with the portion of MeCN growing from 20 to 90 % , we were able to separate all the steroids. The following retention times were found: **1** - 18.7 min, **2** - 12.5 min, **3** - 6.5 min, and **4** - 15.4 min.

Studying the hydrolysis time of the reflux process **2** \rightarrow **3** \rightarrow **4** using 2 M HCl, the required time for quantitative hydrolysis was found to be 1.5 - 2 h. 2 M HBr or hydrochloric acid in higher concentrations shortened this time a little, but by-products were formed and blue steroidal condensation products were finally precipitated. Nor did the use of mixed reflux solvents (MeCN/HCl or HCl/EtOH) result in drastically shortened hydrolysis times.

As all our reflux attempts had failed, we investigated the hydrolysis of a hydrochloric acid solution of **2** in a closed bulb at temperatures > 100 °C. We found that the hydrolysis time could be significantly reduced

with increasing temperature. But temperatures $> 150\text{ }^{\circ}\text{C}$ caused condensation products to be precipitated. If the bath temperature was $135\text{ }^{\circ}\text{C}$, the time requirement for the steps $2 \rightarrow 3 \rightarrow 4$ was about 15 min.

Using this method, a hydrochloric acid solution of **4** had to be processed. It may be desirable to remove the acid. A small volume of dilute HCl can be readily removed by adding MeCN and evaporating. In this connection the idea was conceived of hydrolysing **2** in an azeotropically evaporable MeCN/HCl solution in a closed bulb. The results of such experiments indicated, surprisingly, that rapid hydrolysis also took place by evaporating the MeCN/HCl solution in an unclosed bulb. This was the basis of a second hydrolysis procedure, which followed directly on the fluorination step without evaporating MeCN. Some drops of 1 M HCl were simply added to the MeCN solution of **2** and the MeCN/HCl mixture was removed in a hot bath. In order to obtain a high yield of **4**, the evaporation process had to be carried out four times. But since a volume of 1 ml MeCN/HCl solution can be removed in 1 - 2 min, the hydrolysis time did not exceed 10 min. Moreover, the procedure was gentle, by-products did not occur.

Two examples are shown in Fig. 3. The fluorination of 1 mg **3** was carried out in 1 ml absolute MeCN. Then two drops of HCl (1 M or 3 M) were added, the MeCN/HCl solution was evaporated and the residue dissolved in 1 ml MeCN. After HPLC control the procedure was repeated three times. As can be seen, the yields of 16 α -fluor-estradiol were high after four evaporation processes.

2. Radioactive experiments

In the radioactive synthesis the presence of kryptofix 2.2.2 was necessary in order to introduce the n.c.a. ^{18}F fluoride. Before preparing the dried reagent, small amounts of kryptofix and K_2CO_3 were placed in the reaction vessel. K_2CO_3 was necessary for binding the radioactivity, which is delivered from the cyclotron as H^{18}F .

In numerous tests we worked out the optimum conditions for a rapid radioactive synthesis. In order to obtain a high yield of 3-O-methoxymethyl-16 α - ^{18}F fluoro-estra-1,3,5(10)-triene-3,17 β -diol-17 β -sulfate (^{18}F **2**), it was sufficient to reflux the reaction mixture consisting of **1**, $^{18}\text{F}\text{F}^-$, kryptofix, CO_3^- , and 1 ml MeCN for 15 min at $100\text{ }^{\circ}\text{C}$. This reaction was carried out in a thick-walled bulb.

Concerning rapid hydrolysis, both methods mentioned above were tested and found to be useful. Using the first method, MeCN of the radio-fluorination reaction was evaporated, 1 ml 1 M HCl was added to the residue, the bulb was closed and heated in a bath at $135\text{ }^{\circ}\text{C}$ for 15 min. During this time 16 α - ^{18}F fluoroestradiol (^{18}F **4**) was formed in a high yield. In Fig. 4 some results are shown at various temperatures. The findings of the nonradioactive experiments were confirmed. Rapid hydrolysis required a bath temperature of $135\text{ }^{\circ}\text{C}$. At $110\text{ }^{\circ}\text{C}$ the results did not differ from the simple reflux process of ^{18}F **2**.

Using the second method, two drops of 1 M HCl were immediately added to the refluxed solution of ^{18}F **2**. Azeotropic evaporation of the solvent followed by three repetitions caused quantitative conversion of ^{18}F **2** providing ^{18}F **4** in a 70 % overall yield related to the radioactivity at the start.

Based on the present results, the time requirement for a rapid synthesis of ^{18}F **4** could therefore consist of 15 min for preparing the dry radiofluorination reagent, 15 min for the fluorination reaction, 10 min for hydrolysis according to method 2, and 16 min for the HPLC purification. As some minutes will be necessary for evaporating MeCN and dis-solving ^{18}F **4** in a suitable solvent, the full time could be about 60 min.

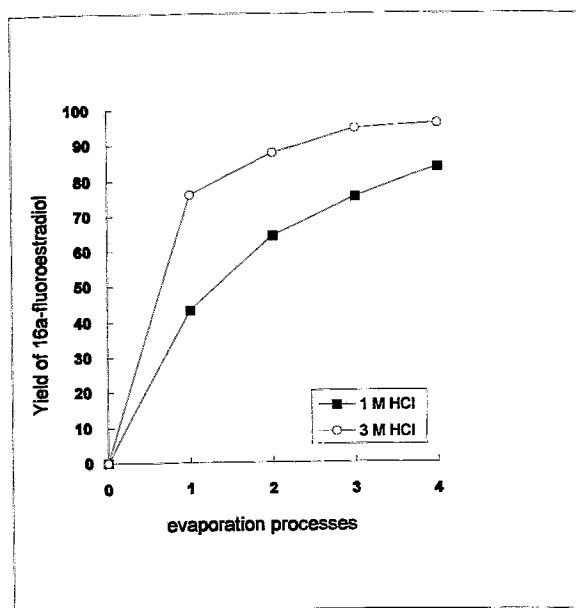


Fig.3 : Yield of 16 α -fluoroestradiol in dependence on the number of evaporation processes

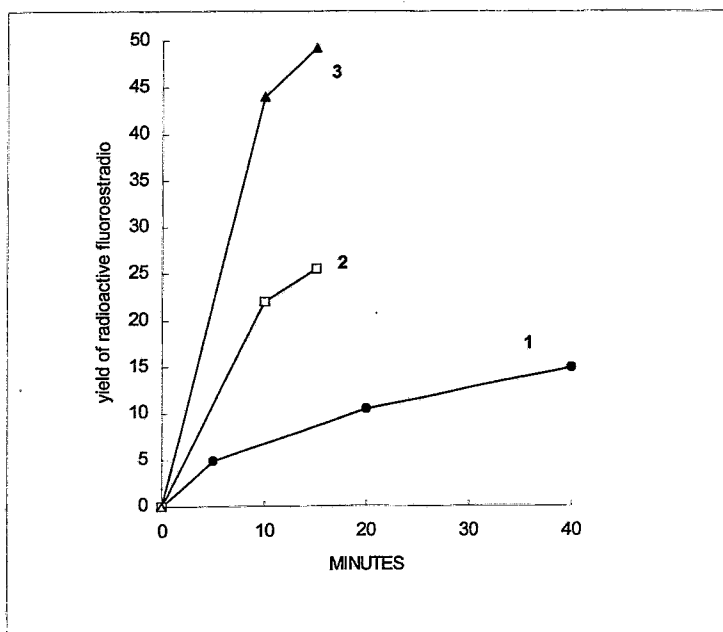


Fig.4: Yield of 16α - $[^{18}\text{F}]$ fluoroestradiol in dependence on hydrolysis time and hydrolysis temperature by using 1 M HCl
 1 - 110 °C 2 - 123 °C 3 - 135 °C

Experimental

1. General

Solvents and reagents were purchased from the following commercial sources: Aldrich, Fluka, and Sigma. They were used as received.

Melting points were determined on a Thermogalen melting point apparatus (Leica) and are uncorrected. ^{13}C NMR spectra were recorded on an FT-NMR spectrometer MSL 300 (Bruker spectrosin) at 75 MHz, using tetramethylsilane as an internal standard. Mass spectra were obtained on a Finigan MAT 95 spectrometer and on a VG Quattropol spectrometer (Fisons Instruments). For the chromatographic experiments HPLC equipment from Merck-Hitachi was used, including a gradient pump (L-6200A), a Rheodyne injector with a 20 μl loop, a Macherey & Nagel column ET 125/8/4 Nucleosil 120-5C₁₈, and a diode array detector (L-4500 DAD) coupled in series with a radioactivity detector. MeCN-water mixtures were the mobile phase at a flow rate of 0.5 ml/min with a linear gradient (0 min - 20% MeCN, 10 min - 90% MeCN) and isocratic elution for a further 5 min with 90% MeCN. For preparative HPLC, a Macherey & Nagel column SP 250/10 Nucleosil 120-7 C₁₈ was used. The UV absorption was detected at $\lambda = 280$ nm.

2. Syntheses

3-O-Methoxymethyl-16 α -fluoro-estra-1,3,5(10)-triene-3,17 β -diol-17 β -sulfate (2):

In a bulb with a magnetic stirrer, 200 μmol Me₄NF was carefully dried. A solution of **1** (60 mg, 150 μmol) in absolute MeCN (6 ml) was added followed by refluxing for 20 min at 100 °C. HPLC purification with a preparative column gave **2** (25 mg) as a fine, white product. The yield was 40.2%. ^{13}C NMR data: As a result of coupling with the fluorine atom, the α carbon atom C(16) as well as the β carbon atoms C(15) and C(17) and the γ carbon atom C(13) have double signals, with the greatest coupling constant being 180.66 Hz for C(16). In comparison with **1** all the ring C and ring D carbon atoms were deshielded due to, first, the effect of 16 α -F on C(15), C(16), C(17) and, second, the interaction between the oxygenium atoms of 17 β sulfate and the C(18) protons. The deshielding values for the carbon atoms C(8), C(9), C(11) - C(13), and C(15) - C(18) are: 1.81, 1.41, 1.16, 1.02, 1.81, 2.23, 18.55, 3.24, and 0.47 ppm. Mass spectrum: m/z 413.2 (M-H) for C₂₀H₂₆O₆SF as anion of **2**.

16 α -Fluoro-estra-1,3,5(10)-triene-3,17 β -diol-17 β -sulfate (3):

The solvent of a refluxed MeCN solution of raw **2** (starting materials: 190 μ mol **1** and 250 μ mol Me₄NF) was removed under reduced pressure. After adding water (25 ml), the aqueous solution was extracted with ether (15 ml) and then passed over a cation exchange column which contained 2 ml resin in the H⁺ form. The acid eluate was refluxed for 45 min. After refluxing, the solution was passed over the cation exchange column in the Na⁺ form. The neutral solution was concentrated to 5 ml under reduced pressure. After lyophilizing, 62 mg **3** was obtained as a fine, pale product. ¹³C NMR data: The effect of 16 α -F was the same as in compound **2**. Double signals were found for C(13), C(15), C(16), and C(17) with the greatest coupling constant also being 180.66 Hz for C(16). In comparison with **1** the deshielding values for the ring C and ring D carbon atoms are similar to those of **2**.

16 α -Fluoro-estra-1,3,5(10)-triene-3,17 β -diol (4):

To a refluxed batch as above (starting materials: 150 μ mol **1** and 200 μ mol Me₄NF) 2 M HCl (6 ml) was added and reflux continued for 90 min. Ether extraction of **4**, ether evaporation, adding MeCN (10 ml) and HPLC purification with a preparative column produced **4** (10.5 mg, 24 %) as a fine, white product. ¹³C NMR data: Double signals for C(13), C(14), C(15), C(16), and C(17); the coupling constant for C(16) was 178.48 Hz. The chemical shift of the signal of C(16) was 101.10 ppm. Compared with the data of estradiol, the chemical shifts of estriol (= 16 α -hydroxy-estradiol) and the present 16 α -fluoroestradiol have the same tendency.

16 α -[¹⁸F]Fluoro-estra-1,3,5(10)-triene-3,17 β -diol ([¹⁸F]4**):**

K₂CO₃ (5 μ mol) and kryptofix 2.2.2 (10 μ mol) were placed in a thick-walled bulb. Irradiated [¹⁸O]H₂O and dry MeCN (3 ml) were added. After evaporating most of the solvent, dry MeCN (1 ml) was added and evaporated. This process was repeated three times. A solution of cyclic sulfate **1** (2 mg) in dry MeCN (1 ml) was added to the dry reagent and the mixture was refluxed for 15 min. Using hydrolysis method 1, the solvent was evaporated and 1 M HCl (1 ml) was added. After closing, the bulb was heated in a bath of 130 °C for 15 min. Then the bulb was cooled. A sample of the solution was injected into the HPLC system. 16 α -[¹⁸F]fluoroestradiol was eluted for between 15.3 and 16.0 min. Using hydrolysis method 2, two drops of 1M HCl were added to the MeCN solution of [¹⁸F]**2** and the MeCN/HCl mixture was removed in a hot bath. After adding 1 ml MeCN and two drops of 1 M HCl, the evaporation process was repeated three times. Then MeCN (a few drops) was added and a sample of the solution was analysed using HPLC.

Acknowledgements: We wish to express our gratitude to the Deutsche Forschungsgemeinschaft for its grant in support of this work. The authors also thank Dr. Scheller and Dr. Klostermann of the Dresden University of Technology for recording the ¹³C-NMR and the mass spectra.

References

- Kiesewetter D.O., Katzenellenbogen J.A., Kilbourn M.R., and Welch M.J. (1984 a) Synthesis of 16-fluoroestrogens by unusually facile fluoride ion displacement reactions: prospects for the preparation of fluorine-18 labelled estrogens. *J. Org. Chem.* **49**, 4900.
- Kiesewetter D.O., Kilbourn M.R., Landvatter S.W., Heiman D.F., Katzenellenbogen J.A., and Welch M.J. (1984 b) Preparation of four fluorine-18-labelled estrogens and their selective uptakes in target tissues of immature rats. *J. Nucl. Med.* **25**, 1212.
- Lim J.L., Berridge M.S. and Tewson T.J. (1994) Preparation of [¹⁸F]16 α -fluoro-17 β -estradiol by selective nucleophilic substitution. *J. Labelled Compd. Radiopharm.* **35**, 176 (Abstract).
- McGuire A.H., Dehtashti F., Siegel B.A., Lyss A.P., Brodack J.W., Mathias C.J., Mintun M.A., Katzenellenbogen J.A., and Welch M.J. (1991) Positron tomographic assessment of 16 α -[¹⁸F]fluoro-17 β -estradiol uptake in metastatic breast carcinoma. *J. Nucl. Med.* **32**, 1526.
- Mintun M.A., Welch M.J., Siegel B.A., Mathias C.J., Brodack J.W., McGuire A.H., and Katzenellenbogen J.A. (1988) Breast cancer: PET imaging of estrogen receptors. *Radiology* **169**, 45.
- Römer J., Steinbach J. and Kasch H. (1995) Synthesis of 3-O-methoxymethyl-16 β , 17 β -O-sulfuryl-estra-1,3,5(10)-triene-3,16 β ,17 β -triol. *This report*, pp. 19-21.
- Tewson T.J. (1995) The routine synthesis of fluorine-18 16 α -fluoroestradiol. *Abstracts of the 11th International Symposium on Radiopharmaceutical Chemistry, Vancouver (Canada), August 1995*, 589.

10. ^{13}C NMR Spectroscopic Characterization of Estra-1,3,5(10)-triene-3,17 β -diol and 3,16,17-triols, and some of their 3-O-Methoxymethyl and 16 α -Fluor Derivatives

J. Römer, D. Scheller ¹

¹Dresden University of Technology

Introduction

^{13}C NMR spectroscopy has proved to be a suitable tool for characterizing organic compounds such as steroids. Chemical shifts of numerous steroids were reported in a review (Blunt *et al.*, 1977). At the same time the additional behaviour of dihydrosteroids was investigated (van Antwerp *et al.*, 1977). Chemists researching contraceptive steroids dealt with the substituent effects of 16,17-disubstituted 3-methoxy-estra-1,3,5(10)-trienes and reported chemical shifts of estra-1,3,5(10)-triene-3,16 α ,17 β -triol (= estriol) and estra-1,3,5(10)-triene-3,16 β ,17 β -triol (= 16-epiestriol) (Engelhardt *et al.*, 1979).

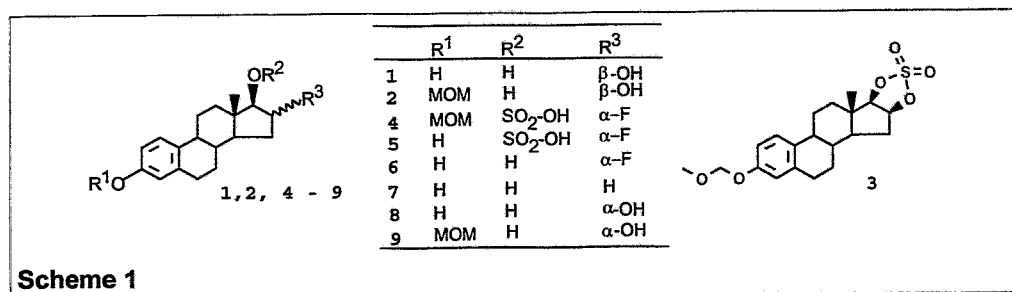
Monohalogenating with fluorine, chlorine, or bromine causes a deshielding effect on α and β carbons with the substituent effect of fluorine being the greatest. It was reported to be 70 ppm on an α carbon, 7.8 ppm on a β carbon, and - 6.8 ppm on a γ carbon (Kalinowski *et al.*, 1984a). The ^{13}C - ^{19}F coupling constants are also great.

Some years ago we dealt with the substituent effects of bromine in cholestanes and cholestenes. Applying these effects, we were able to characterize some new bromosteroids without resorting to other spectroscopic methods (Römer *et al.*, 1987).

Now we report on ^{13}C NMR studies exploiting the great substituent effects of fluorine for characterizing the fluorinated steroids which occur in Lim's new synthesis of 16 α -fluoroestradiol (Lim *et al.*, 1994). The preparation of these fluorinated steroids was described in the preceding paper (Römer *et al.*, 1995a).

Results and Discussion

All the discussed steroids are represented in Scheme 1. 16-Epiestriol (1) was used as starting material for synthesizing 3-O-methoxymethyl-estra-1,3,5(10)-triene-3,16 β ,17 β -triol (2) and 3-O-methoxymethyl-16 β ,17 β -O-sulfuryl-estra-1,3,5(10)-triene-3,16 β ,17 β -triol (3) (Römer *et al.*, 1995b). In Lim's new synthesis (1994) the fluorinated steroids 3-O-methoxymethyl-16 α -fluoro-estra-1,3,5(10)-triene-3,17 β -diol-17 β -sulfate (4), 16 α -fluoro-estra-1,3,5(10)-triene-3,17 β -diol-17 β -sulfate (5), and 16 α -fluoro-estradiol (6) occurred. Three steroids, estradiol (7), estriol (8), and 3-O-methoxymethyl-estriol (9), were recorded for comparison. The latter had been prepared from 8 in connection with the necessary etherification of 16-epiestriol (1) with methoxymethyl chloride.



Scheme 1

The chemical shifts of all the steroids 1 - 9 are listed in Table 1. We will discuss these values in three respects. We are interested in the influence of the methoxymethyl group, the effects of sulfate and cyclic sulfate, and, above all, the effect of 16 α -F as a substituent.

The influence of a substituent is designated as SCS (Substituent effect on Chemical Shift) or, mathematically, as $\Delta\delta$. Generally, it is $\Delta\delta_i = \delta_i(B) - \delta_i(A)$ for each carbon atom i when a substituent is introduced in compound A with compound B resulting.

Table 1: Chemical shifts (in ppm) of the carbon atoms of all the recorded steroids

Carbon-atom	1	2	3	4	5	6	7	8	9
1	125.43	126.19	126.24	127.16	127.14	125.98	126.07	125.70	126.07
2	112.05	113.65	114.12	115.09	113.80	112.61	112.47	112.34	113.57
3	153.91	154.90	155.48	156.66	155.95	154.27	154.04	154.06	154.80
4	114.46	116.16	116.40	117.50	116.05	115.08	115.00	114.81	116.11
5	137.09	137.87	137.43	138.97	138.64	137.67	137.79	137.48	137.87
6	28.86	29.56	29.36	30.54	30.53	29.38	29.41	29.12	29.48
7	26.84	27.28	27.50	28.39	28.44	27.10	27.05	26.87	26.99
8	37.84	37.95	37.86	39.67	39.67	38.09	38.71	38.10	38.02
9	43.58	44.04	43.62	45.10	45.01	43.65	43.74	43.57	43.74
10	130.96	133.82	132.54	135.03	132.25	131.22	131.56	131.22	133.74
11	25.50	25.90	25.89	27.05	27.03	25.68	26.13	25.55	25.64
12	36.84	37.26	37.11	38.13	37.97	36.35	36.48	36.30	36.40
13	42.14	42.64	43.64	45.45	45.37	43.79	42.98	43.42	43.58
14	46.03	46.43	47.71	n.d.	n.d.	47.73	49.83	47.50	47.63
15	33.89	34.46	30.77	33.00	32.95	31.46	22.83	33.08	33.15
16	68.98	69.54	81.48	100.03	100.04	101.10	29.72	77.60	77.74
17	80.06	80.49	90.33	93.57	93.57	87.01	81.30	89.05	89.20
18	10.99	11.73	12.70	13.17	13.19	12.00	10.78	11.67	12.01
O-CH ₂ -O	-	94.39	94.58	95.91	-	-	-	-	94.30
CH ₃ O	-	55.76	55.88	56.08	-	-	-	-	55.70

Estra-1,3,5(10)-trienes represent C₁₈ steroids and thus cause 18 signals in the ¹³C NMR spectrum. 3-O-Methoxymethyl-estra-1,3,5(10)-trienes (**2**, **4**, **9**) have two additional signals due to the methoxymethyl carbon atoms (Table 1). Comparing the chemical shift of their carbon atoms with the corresponding values of the 3-hydroxy-estra-1,3,5(10)-trienes (**1**, **5**, **8**), we find that the selective etherification of the 3-hydroxy group by methoxymethyl chloride influences primarily the chemical shifts of the olefinic carbon atoms C(1) - C(5) and C(10) with the deshielding effect on C(10) being the greatest.

Ring D substituents mainly influence ring D carbons and C(18). We have therefore summarized the SCS of cyclic sulfate, opened 17 β -sulfate, 16 α -fluorine, and 16 α -OH on these carbon atoms in Table 2. $\Delta\delta(\text{cyclic sulfate})$ was calculated from $\delta_i(\mathbf{3}) - \delta_i(\mathbf{2})$, $\Delta\delta(17\beta\text{-sulfate})$ from $\delta_i(\mathbf{5}) - \delta_i(\mathbf{6})$, $\Delta\delta(16\alpha\text{-F})$ from $\delta_i(\mathbf{6}) - \delta_i(\mathbf{7})$, and $\Delta\delta(16\alpha\text{-OH})$ from $\delta_i(\mathbf{8}) - \delta_i(\mathbf{7})$.

First, we shall look at the SCS of cyclic sulfate. The effects on C(15), C(16), and C(17) are remarkably great here. The shielding effect on C(15) is connected with interaction between the H atoms of the 13 methyl group and an oxygen atom of the cyclic sulfate group which is β -orientated. The deshielding effects on C(16) and C(17) are greater than those of the methoxymethyl group and an opened sulfate. Similar to methoxymethyl or opened sulfate, they do not represent real α -effects. The real α -effects of a cyclic sulfate group on C(16) and C(17) can only be calculated from chemical shifts of C(16) and C(17) of **3** and *estra-1,3,5(10)-triene* (Blunt et al., 1977). The chemical shifts (in ppm) for *estra-1,3,5(10)-triene*: C(13) 41.4, C(14) 54.2, C(15) 25.5, C(16) 20.9, C(17) 40.9, and C(18) 17.6. From the corresponding values the following α -effects were found: α -C(16) 60.6 ppm, α -C(17) 49.4 ppm.

Table 2: Substituent effects (in ppm) of 16-O,17-O cyclic sulfate, 17 β sulfate, 16 α -F, and 16 α -OH on the ring D carbon atoms and C(18)

Ring D carbon atom	$\Delta\delta$ (cyclic sulfate)	$\Delta\delta$ (17 β sulfate)	$\Delta\delta$ (16 α -F)	$\Delta\delta$ (16 α -OH)
13	1.00	1.58	0.81	0.44
14	1.28	n.d.	- 2.10	- 2.33
15	- 3.69	1.49	8.63	10.25
16	11.94	- 1.06	71.38	47.88
17	9.84	6.56	5.71	7.75
18	0.97	1.19	1.22	0.89

We now take a look at the SCS of 17 β -sulfate. We see that the signals of C(15), C(16), and C(17) were influenced in another way than by cyclic sulfate. The SCS on C(13) and C(18) do not differ from cyclic sulfate. Up to now we have not been able to clearly determine the chemical shift of C(14).

In the ^{13}C NMR spectra of the fluorosteroids **4**, **5**, **6** it was to be expected that the signal of the α carbon atom C(16) was split into a doublet. The $^1\text{J}(\text{C},\text{F})$ coupling constant was found to be - 178.5 Hz and agrees with literature data, e. g. - 173.5 Hz for fluorocyclopentane (Kalinowski *et al.*, 1984b). Doublets were also found for the β and γ carbon atoms with the $^2\text{J}(\text{C},\text{F})$ coupling constants being 21.7 Hz for C(17) and 23.1 Hz for C(15).

The substituent effect of 16 α -F on C(16) is 71.38 ppm and also agrees with literature data (Kalinowski *et al.* 1984a). If one compares $\Delta\delta$ (16 α -F) and $\Delta\delta$ (16 α -OH), the same tendency of the substituent effects is found. 16 α -F and 16 α -OH show deshielding effects on the β carbon atoms C(15) and C(17), and weak ones on the γ carbon atom C(13), but shielding effects on the γ carbon atom C(14). We concluded from this same tendency that the fluorine atom is α -orientated in the fluorosteroids investigated.

References

- Antwerp van C.L., Eggert H., Meakins G.D., Miners J.O. and Djerassi C. (1977) ^{13}C NMR additional behaviour of dihydroxy steroids. *J. Org. Chem.* **42**, 789.
- Blunt, J.W. and Stothers J.B. (1977) ^{13}C NMR spectra of steroids - a survey and commentary. *Org. Magn. Reson.* **9**, 439.
- Engelhardt, G., Zeigan D. and Schönecker B. (1979) ^{13}C NMR-Untersuchungen an Steroiden. Substituenteneffekte an 16-mono- und 16,17-disubstituierten 3-Methoxyöstra-1,3,5(10)-trienen. *Org. Magn. Reson.* **12**, 628.
- Kalinowski H.-O., Berger S. and Braun S. (1984a) ^{13}C -NMR-Spektroskopie, Georg-Thieme-Verlag Stuttgart, S. 95.
- Kalinowski H.-O., Berger S. and Braun S. (1984b) ^{13}C -NMR-Spektroskopie, Georg-Thieme-Verlag Stuttgart, S. 522.
- Lim J.L., Berridge M.S. and Tewson T.J. (1994) Preparation of [^{18}F]16 α -fluoro-17 β -estradiol by selective nucleophilic substitution. *J. Labelled Compd. Radiopharm.* **35**, 176 (Abstract).

- Römer J., Scheller D. and Großmann G. (1987) Carbon-13 nuclear magnetic resonance study of the bromo derivatives of 5α -cholestan-3-one and cholest-4-en-3-one. *Magn. Reson. Chem.* **25**, 135.
- Römer J., Steinbach J. and Kasch H. (1995a) Synthesis of 16α - ^{18}F fluoroestradiol. *This report*, pp.21-26.
- Römer J., Steinbach J. and Kasch H. (1995b) Synthesis of 3-O-methoxymethyl- 16β , 17β -O-sulfuryl-estra-1,3,5(10)-triene-3, 16β , 17β -triol. *This report*, pp. 19-21.

11. Serotonin Receptor-Binding Technetium and Rhenium Complexes

1. Design Concept and Synthesis Strategy

H.-J. Pietzsch, M. Scheunemann, H. Spies, P. Brust, B. Johannsen

Investigations dealt with in a series of articles in this annual report are part of our programme to design technetium and rhenium coordination compounds as potentially receptor binding tracers.

After some first studies on rhenium complexes derived from spiperone (Spies *et al.*, 1993), the following articles refer to the preparation and evaluation of new technetium and rhenium complexes that are able to bind at the serotonin receptor binding sites.

The design of receptor binding metal complexes advantageously starts from known receptor binding pharmaceuticals. Formally two principal approaches can be differentiated, the well-known *Bifunctional Concept* and the *Partial Structure Concept*.

1. Bifunctional Concept

A known receptor binding substance is used as a biological "anchor molecule", and a suitable metal/ligand unit is coupled to it. The coupling of the complex unit should take place at an insensitive position of the molecule to retain the receptor binding capability. The complex unit itself should not - or only minimally - affect the "anchor group", that means it must not cause strong steric and electronic changes in the receptor binding agent.

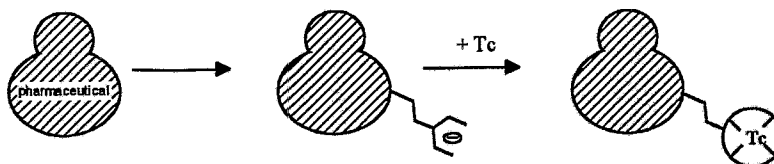
The Johns Hopkins group in Baltimore started this concept with Tc-DADT-QN as a mimic of QNB for muscarinic acetylcholine receptors (Lever *et al.*, 1994). Very recently, Chi *et al.* reported on a similar approach to bis-bidentate Tc complexes in order to mimic steroid hormones (Chi *et al.*, 1994).

2. Partial Structure Concept

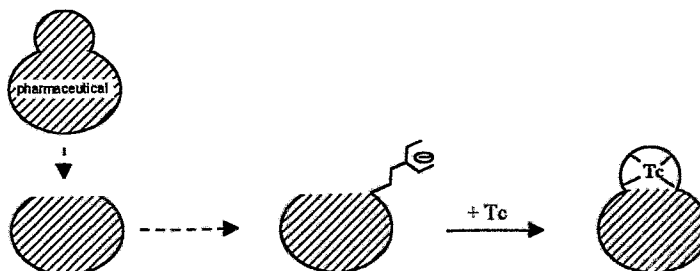
Using a partial structure only of a receptor binding ligand instead of the entire lead molecule one can try to "restore" the binding molecule by introducing a metal/ligand unit that formally imitates a nonessential moiety which is present in the lead structure. In this case it is important to know which structure subunit of the lead structure is essential for binding to the receptor.

This concept assigned as *Partial Structure Concept* appears to be much more suitable for our objectives. Its use requires, however, large molecules of a higher degree of complexity and versatility to replace part of it by a technetium/ligand unit. For example, the molecule should contain lipophilic ring systems which are expected to be replaceable by a neutral metal/ligand unit.

1. Bifunctional Concept

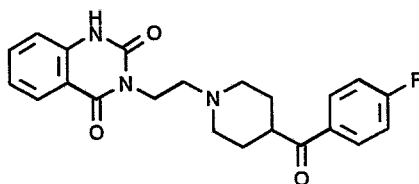


2. Partial Structure



Thus, we will focus our attention on the *Partial Structure Concept*.

It was applied to the known serotonin receptor antagonist ketanserin, which provides a good starting point for the development of a radiotracer, although it also displays affinity for adrenergic α_1 and histaminergic H_1 or $5-HT_{2C}$ receptors.



ketanserin

Studying serotonin receptors in the brain, particularly the $5-HT_2$ receptors, is of great interest because of the importance of altered serotonergic neurotransmission in many neurological and psychological diseases, such as Alzheimer's disease, schizophrenia, anxiety and depression.

Aiming at SPECT tracers, ketanserin (Mertens *et al.* 1989), aminoketanserin (Schotte and Leysen, 1989) and the agonist DOI (α -methyl-2,5-dimethoxy-4-iodo-phenylethylamine) (McKenna *et al.*, 1989) were labelled with ^{123}I or ^{125}I .

Other groups have reported attempts to synthesize ^{99m}Tc labelled ligands for various targets, e.g. for the dopamine receptor (Lever *et al.*, 1989, Samnick *et al.*, 1995), $5-HT_{1A}$ receptor (Baidoo *et al.*, 1995, Kung *et al.*, 1995), cholinergic neurons (Del Rosario *et al.*, 1994).

The purpose of the present studies is to determine which specific structural features have to be chosen to make a technetium and rhenium compound acceptable by the $5-HT_2$ brain receptor, and to obtain structure-affinity relationships within a series of systematically altered substances.

Strategy in designing "ketanserin-like" coordination compounds

At the initial stage of our studies, rhenium was mainly used as the convenient model nuclide for technetium, followed by the long-lived ^{99}Tc and then ^{99m}Tc .

The key compounds in our design concept of $5-HT_{2A}$ receptor-binding agents are small-sized neutral Re and Tc complexes having the potential for convenient derivatization in order to easily provide a range of mimics of organic receptor-binding ligands, such as ketanserin.

With the "3+1" type of mixed-ligand complexes, combining the tridentate $HS-CH_2-CH_2-S-CH_2-CH_2-SH$ and a monodentate mercapto compound (R-SH), a versatile chelate system is available (Pietzsch *et al.*, 1989; Spies *et al.*, 1995).

The synthesis principle consists in saturating three of the four coordination sites of the oxometal(V) core with a small tridentate ligand and filling the fourth position with an appropriate co-ligand that permits the desired functionalization of the chelate. The tridentate ligand can be viewed as a small cap for the metal core. Almost any compound can be fitted as the co-ligand with the rhenium or technetium unit, provided that a mercapto group can be introduced into the molecule. The monodentate thiol ligand, bearing a ketanserin fragment, is very flexible and does not generate additional stereoisomers.

Our strategy of designing "ketanserin-like" coordination compounds consists of four general synthesis principles as illustrated in Fig. 1.

- Imitation of the whole ketanserin molecule (A).
- Coupling of the "left" partial structure of ketanserin with a chelate unit (B).
- Coupling of the "right" partial structure of ketanserin with a chelate unit (C).
The fluorobutyrophenone substituted oxorhenium chelate was originally synthesized and evaluated as a "spiperone-like" complex for the D_2 receptor (Spies *et al.*, 1993). It is practically identical with the "right" partial structure of ketanserin.
- In order to gain an insight into the pharmacophore groups of ketanserin, the molecule will be successively cut back to simple structure moieties such as ethyl or phenethyl groups. These subunits will also be coupled with the chelate unit (D).

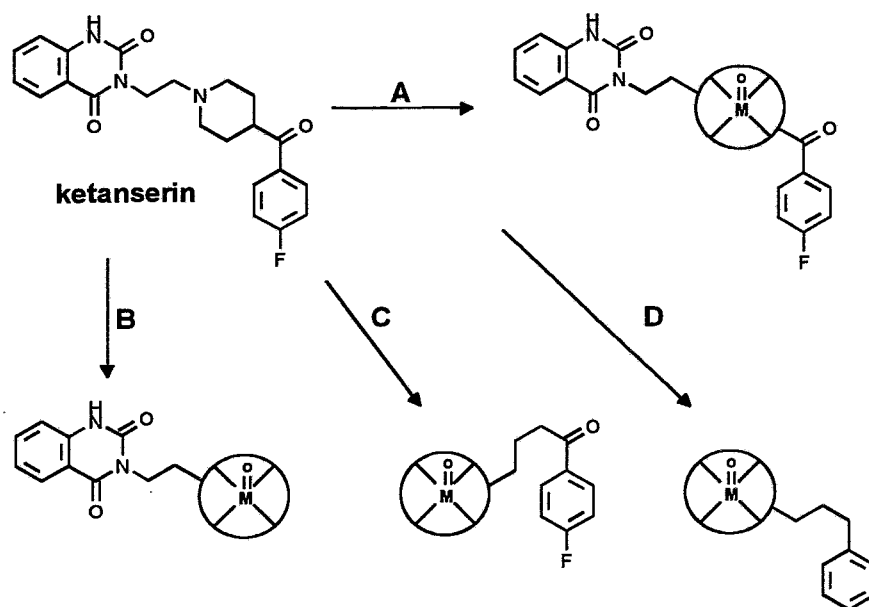


Fig. 1: Strategy in designing "ketanserin-like" coordination compounds

The following papers describe the synthesis of partial structures of ketanserin, the coupling of these moieties with technetium (rhenium) containing chelate units and their biochemical evaluation with respect to the affinity to the 5-HT₂ receptor.

References

- Baidoo K.E., Scheffel U., Lever S.Z., Stathis M. and Wagner H.N. (1995) Serotonin-1A receptor binding technetium-99m-labelled complexes *J. Nucl. Med.* **36**, 28P (abstr.).
- Chi D.Y., Neil J.P.O., Anderson C.J., Welch M.J. and Katzenellenbogen J.A. (1994) Homodimeric and heterodimeric bis(aminothiol) oxometal complexes with rhenium(V) and technetium (V). Control of heterodimeric complex formation and an approach to metal complexes that mimic steroid hormones. *J. Med. Chem.* **37**, 928-937.
- Del Rosario R.B., Jung Y.-W., Baidoo K.E., Lever S.Z. and Wieland, D.M. (1994) Synthesis and *in vivo* evaluation of a ^{99m/99}Tc-DADT-benzovesamicol: A potential marker for cholinergic neurons. *Nucl. Med. Biol.* **21**, 197-203.
- Kung H.F., Bradshaw J.E., Chumpradit S., Zhuang Z.-P., Kung M.-P., Mu M. and Frederick D. (1995) New TcO(III) and ReO(III) N₂S₂ complexes as potential CNS 5-HT_{1A} receptor imaging agents. In: *Technetium and Rhenium in Chemistry and Nuclear Medicine* (Edited by Nicolini M., Bandoli G., Mazzi U.), SGEDITORIALI, Padova, pp. 293-298.
- Lever S.Z. and Wagner Jr. H.N. (1989) The status and future of technetium-99m radiopharmaceuticals. In: *Technetium and Rhenium in Chemistry and Nuclear Medicine* (Edited by Nicolini M., Bandoli G., Mazzi U.), Cortina Intern. Verona, pp. 649-659.
- Lever S.Z., Baidoo K.E., Mohamood A., Matsumura K., Scheffel U. and Wagner H.N. (1994) Novel technetium ligands with affinity for the muscarinic cholinergic receptor. *Nucl. Med. Biol.* **21**, 157-164.
- McKenna D. J., Nazarali A.J., Hoffman A.J., Nichols D.E., Mathis C.A. and Saavedra J.M. (1989) Common receptors for hallucinogens in rat brain: a comparative autoradiographic study using [¹²⁵I]LSD and [¹²⁵I]DOI, a new psychomimetic radioligand. *Brain Res.* **476**, 45-56.
- Pietzsch H.-J., Spies H. and Hoffmann S. (1989) Lipophilic technetium complexes VI. Neutral oxotechnetium(V) complexes with monothiole/tridentate dithiole coordination. *Inorg. Chim. Acta* **165**, 163-166.
- Sarnick S., Brandau W. and Schober O. (1995) Synthesis, characterization and biodistribution of neutral and lipid-soluble ^{99m}Tc-BP-BAT and ^{99m}Tc-BUP-BAT: Possible ligands for dopamine

- receptor imaging with SPECT. In: *Technetium and Rhenium in Chemistry and Nuclear Medicine* (Edited by Nicolini M., Bandoli G., Mazzi U.), SGEDITORIALI, Padova, pp. 293-298.
- Schotte A. and Leysen J.E. (1989) Identification of 5-HT₂ receptors, α -adrenoreceptors and amine release sites in rat brain by autoradiography with [¹²⁵I]7-amino-8-iodo-ketanserin. *Eur. J. Pharmacol. [Mol. Sect.]* **172**, 99-106.
- Spies H., Noll St., Noll B., Leibnitz P. and Klostermann, K. (1993) Technetium and rhenium complexes derived from spiperone. *Annual Report 1993*, Institute of Bioinorganic and Radiopharmaceutical Chemistry, FZR-32, pp. 37, 40, 43.
- Spies H., Fietz Th., Pietzsch H.-J., Johannsen B., Leibnitz P., Reck, G., Scheller D. and Klostermann K. (1995b) Alkyl and aryl substituted oxorhenium(V) complexes with tridentate/monodentate coordination. *J. Chem. Soc., Dalton Trans.* **2277-2280**.

12. Serotonin Receptor-Binding Technetium and Rhenium Complexes

2. Synthesis, Chemical Characterization and Biochemical Evaluation of Partial Structures of Ketanserin

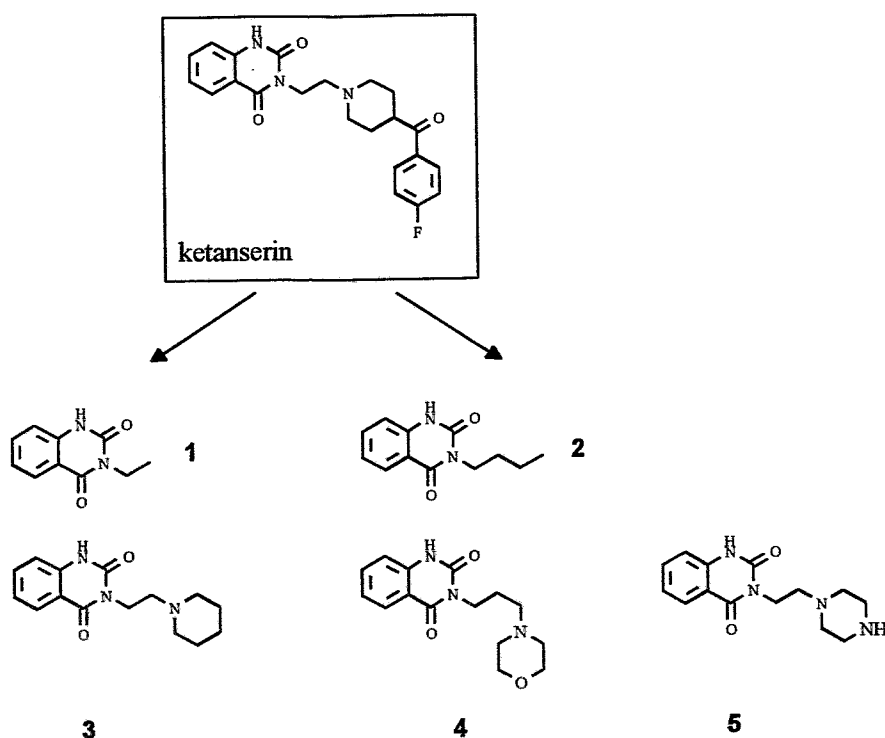
M. Scheunemann, H.-J. Pietzsch, P. Brust, J. Wober, H. Spies, B. Johannsen

Introduction

Pursuing the *Partial Structure Concept* as outlined in part 1 of our report the lead structure of ketanserin was gradually cut back to the benzopyrimidone subunits **1** and **3**.

Each of these subunits also forms the starting point for homologous series of derivatives in order to gain an insight into the influence of minor structural alterations on the receptor binding behaviour and later proceed to functionalized compounds capable of binding technetium.

The derivatives **2**, **4** and **5** were synthesized and checked for receptor binding.



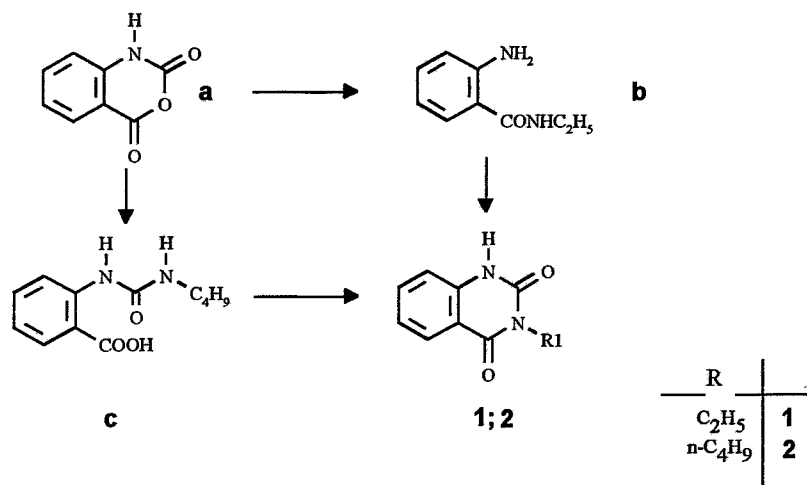
Results and Discussion

Synthesis of partial structures of ketanserin

3-alkyl-substituted 2,4-(1*H*,3*H*)-quinazolidiones **1** and **2**

The usual method for the preparation of simple 3-alkyl-substituted 2,4-(1*H*,3*H*)-quinazolidiones consists of the reaction of isatoic anhydride with a primary amine followed by cyclocondensation of the resultant anthranile amide.

Scheme 1:



Scheme 1 illustrates the synthetic route chosen for the preparation of two 3-alkyl-substituted 2,4-(1*H*,3*H*)-quinazolidiones **1** and **2**.

Starting from isatoic anhydride **a**, both **1** and **2** were prepared by reaction of **a** with a 5 to 7.5 molar excess of the corresponding amine in aqueous solution (Staiger *et al.*, 1953).

In the first case the anthranile amide **b** was isolated as a product (51 %), which after ethoxy-carbonylation (ethyl chloroformate/dioxane; 100 °C) and subsequent ring closure (Gadekar *et al.*, 1964) (KOH - ethanol; 78 °C) was converted to **1** in a 75 % yield.

In the other case the product from the nucleophilic attack by the amine nitrogen on the carbamate-C atom, an *o*-uramido benzoic acid **c**, was isolated. This compound cyclized under acidic conditions (Staiger *et al.*, 1953) (5 N HCl; 115 °C) to give **2** in a 36 % overall yield.

Structures **1** and **2** are consistent with the IR and NMR spectra of the products and are supported by the published melting points.

3-amino-substituted 2,4-(1*H*,3*H*)-quinazolidiones **3**, **4** and **5**

Similar to the synthesis of the 3-alkyl-substituted derivatives **1** and **2**, the mixed anhydride **a** was treated with 3-(4-morpholino)-propylamine (Scheme 2). In contrast to the reaction described above, the cleavage was carried out in an aprotic solvent (DMF/DMAP (catalyst); ambient temperature; 54 % yield). After conversion of the resulting anthranile amide **d** into the corresponding carbamate and successive treatment with ethanolic KOH, the 3-substituted 2,4-(1*H*,3*H*)-quinazolidione **4** (Hayao *et al.*, 1965) was obtained in a 40 % yield.

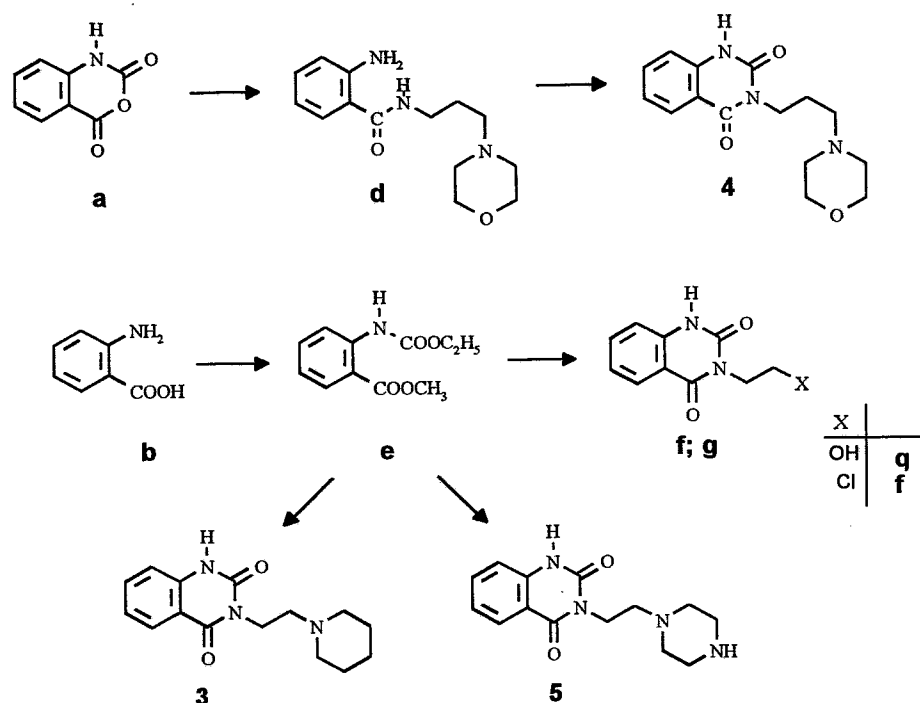
Due to the particular interest of 3-(2-chloroethyl)-2,4-(1*H*,3*H*)-quinazolidione as a synthetic intermediate for the preparation of ketanserin (Janssen *et al.*, 1988), this compound was prepared following a literature procedure (Grout *et al.*, 1960) (Scheme 2).

Starting from **b** the chloro derivative **f** was obtained via esterification and subsequent acylation with ethyl chloroformate, followed by cyclocondensation of the carbamate with ethanolamine to yield **g** in a 48 % overall yield. Finally the alcohol can be almost quantitatively converted to the chloride **f** by treatment with thionyl chloride.

However, the most direct approach to 2,4-(1*H*,3*H*)-quinazolidiones, bearing amino groups in the side chain, namely reaction of **e** with an appropriate diamine, has not been reported. As compound **e** was readily available, it was chosen as an intermediate to prepare additional analogues.

In the same manner as described for the synthesis of **g** the piperidine derivative **3** (Herndon *et al.*, 1992) and the new piperazine derivative **5** can be obtained via reaction of **e** with the corresponding diamine.

Scheme 2:



Biochemical evaluation of the partial structures of ketanserin

Method:

The cortex of rat brain was homogenized in 10 volumes of ice-cold buffer (50 mM tris-HCl, pH 7.6) with an Ultra-Turrax T25. The homogenate was centrifuged at 20,000 g for 10 min. The resulting pellet was resuspended with the Ultra-Turrax and centrifuged again at 20,000 g for 10 min. After repeating the same procedure the pellet was resuspended in 10 volumes of buffer and stored at -20 °C until used in the binding studies.

The time dependency of ketanserin binding was studied on these membrane preparations (0.013 mg/ml protein). The samples were incubated with ketanserin hydrochloride[ethylene-³H] (2356.9 GBq/mmol, Amersham) at 23 °C for various length of time in the presence and absence of 1 μM unlabelled mianserin. For inhibition studies the samples were incubated at 23 °C for 60 min. The binding assays were terminated by rapid filtration through GF/B glass fibre filters (Whatman). The filters were rapidly washed with four 4 ml portions of ice-cold buffer, transferred to 10 ml of scintillation fluid (Ultima-Gold, Packard) and analysed for radioactivity. Aliquots of the incubation fluid were measured as well. Corrections were made for binding ³H-ketanserin to the filters. The protein content of the membrane suspensions was estimated according to the method of (Lowry *et al.*, 1951).

The time dependency of ³H-ketanserin binding to membranes from the rat cortex is shown in Fig. 1. Equilibrium is reached after about 30 minutes. In accordance with other studies (Hrdina *et al.*, 1993) an incubation time of 60 min was therefore chosen for the inhibition studies.

Different concentrations of unlabelled ketanserin were used to inhibit the binding of ³H-ketanserin (Fig. 2). The IC₅₀ value obtained is 50 nM.

Ketanserin-binding could be inhibited by mianserin (IC₅₀ = 0.4 nM), a drug which specifically binds to 5-HT₂ receptors (Hrdina *et al.*, 1993) (Fig. 3). We conclude that ³H-ketanserin labels 5-HT₂ receptors in our preparation.

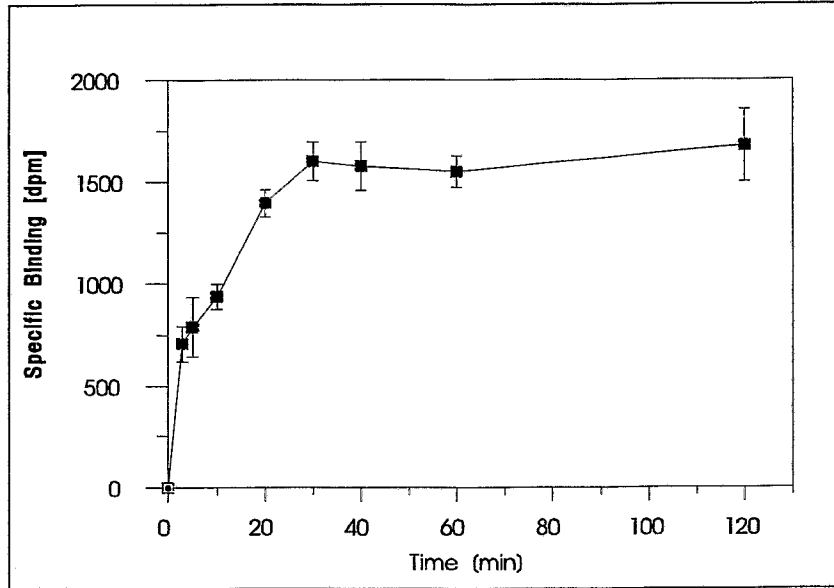


Fig. 1: Time dependency of [³H]ketanserin binding in rat frontal cortical tissue homogenates

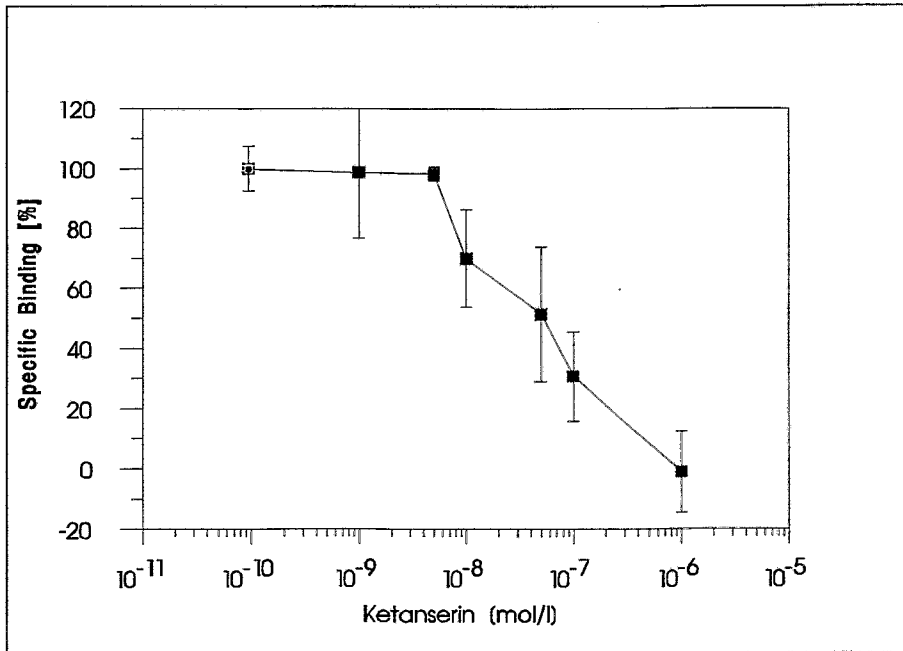


Fig. 2: Inhibition of [³H]ketanserin binding by unlabelled ketanserin

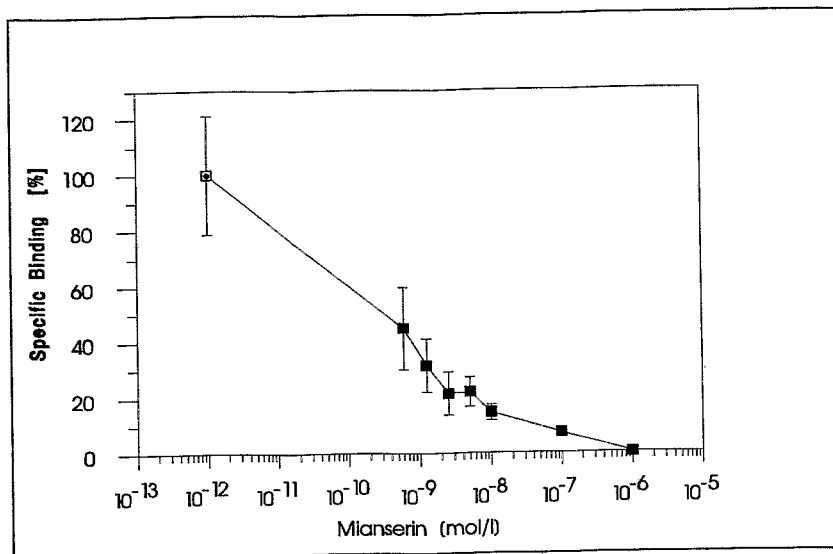


Fig. 3: Inhibition of [³H]ketanserin binding by different concentrations of unlabelled mianserin

Fig. 4 shows the inhibition of ³H-ketanserin binding by the derivatives 1, 2, 3 and 4 (see above). No inhibition was observed for 1 and 2. However, the presence of 3 or 4 in the incubation medium inhibited ³H-ketanserin binding significantly. Compared with ketanserin the 100 fold amount of these substances is necessary to obtain similar effects. At the highest concentration (10⁻⁵ mol/l) the incubation medium contained 2 % ethanol. This concentration of ethanol reduced the specific binding by almost 50 % (Fig. 4). Related to this there was a further reduction by 3 and 4.

All the derivatives studied so far lack the benzoyl moiety of the ketanserin molecule. As shown by others, this is followed by a drastic reduction of the affinity to 5-HT₂ receptors (Herndon *et al.*, 1992).

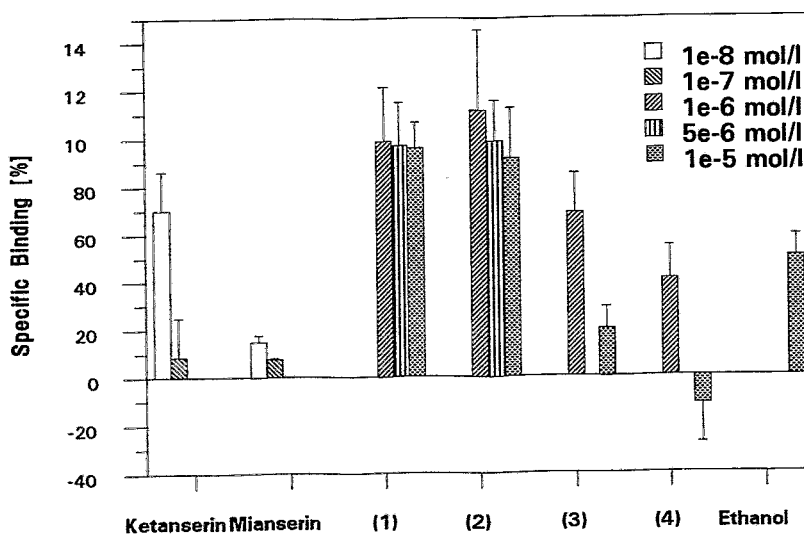


Fig. 4: Inhibition of [³H]ketanserin binding by the derivatives of ketanserin 1 - 4 at different concentrations

References

- Gadekar S.M., Kotsen A.M. and Cohen E. (1964) Anthranilamides as intermediates for 3-substituted quinazolinodiones *J. Chem. Soc.* 4666-4668.
- Grout, R.J. and Partridge M.W. (1960) Cyclic amidines. Part XI, Rearrangements of quinazoline ethers *J. Chem. Soc.* 3546-3550.
- Hayao S., Havera H. J., Strycker W.G., Leipzig T.J., Kulp R.A. and Hartzler H.E. (1965) New sedative and hypotensive 3-substituted quinazolinodiones. *J. Med. Chem.* **8**, 807-811.
- Herndon J.L., Ismaiel A., Ingher S.P., Teitler M. and Glennon R.A. (1992) Ketanserin analogues: structure-affinity relationships for 5-HT₂ and 5-HT_{1C} serotonin receptor binding *J. Med. Chem.* **35**, 4903-4910.
- Hrdina, P.D. and Vu T.B. (1993) Chronic fluoxetine treatment upregulates 5-HT uptake sites and 5-HT₂ receptors in rat brain - an autoradiographic study *Synapse* **14**, 324-331.
- Janssen C.G.M., Lenoir H.A.C., Thijssen J.B.A., Knaeps A.G., Verluyten W.Lm.M. and Heykants J.J.P. (1988) Synthesis of ³H and ¹⁴C-ketanserin *J. Labelled Compd. Radiopharm.* **25**, 783-792.
- Lowry O.H., Rosebrough N.J., Farr A.L. and Randall R.J. (1951) Protein measurement with the Folin phenol reagent. *J. Biol. Chem.* **193**, 265-275.
- Staiger, R.P. and Wagner E.C. (1953) Isatoic anhydride III. Reactions with primary and secondary amines *J. Org. Chem.* **18**, 1427-1439.

13. Serotonin Receptor-Binding Technetium and Rhenium Complexes

3. Synthesis, Characterization and Biochemical Evaluation of Oxorhenium(V) Complexes Bearing the Quinazolinodione Portion of Ketanserin

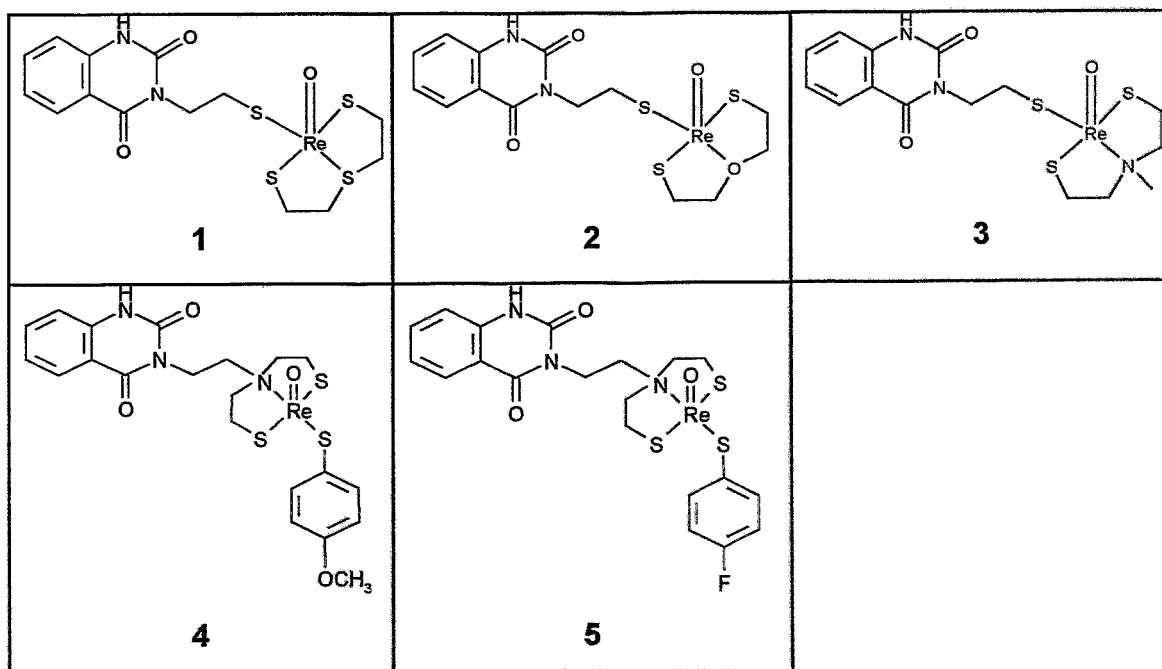
H.-J. Pietzsch, M. Scheunemann, T. Fietz, H. Spies, P. Brust, J. Wober, B. Johannsen

Introduction

The topography of the 5-HT₂ receptor appears to accept a wide array of structural types. According to our design concept (Pietzsch *et al.*, 1995), a hybrid molecule is to be developed from the quinazolinodione portion of the lead molecule ketanserin and a neutral chelate moiety connected by an ethylene spacer.

The mixed-ligand complexes are listed in Table 1.

Table 1: Oxorhenium(V) complexes bearing the quinazoline part of ketanserin



Experimental

(3-thiapentane-1.5-dithiolato)[2-(2.4-dioxo-1H.3H-quinazoline-3-yl)ethanethiolato]-oxorhenium(V) 1: 50.4 mg (129 μmol) $[\text{ReO}(\text{SSS})\text{Cl}]$ are dissolved in 5 ml refluxing acetonitrile. 49.8 mg (224 μmol) of 2-(2.4-dioxo-1H.3H-quinazoline-3-yl)-ethanethiol **HL**¹ are added. The colour changes to violet and a brown powder precipitates. The solid is separated after refluxing for further 15 minutes.

The reddish-brown compound is dissolved in hot dimethylformamide. After addition of 1 ml methanol the complex crystallizes as small needles.

Yield: 66 %

(3-oxapentane-1.5-dithiolato)[2-(2.4-dioxo-1H.3H-quinazoline-3-yl)ethanethiolato]-oxorhenium(V) 2: 45 mg (200 μmol) **HL**¹ and 30.3 mg (219 μmol) 3-oxapentane-1.5-dithiol are dissolved in a 1:1 mixture of methanol/dmf. This solution is added to a methanolic solution of 117 mg (219 μmol) $[\text{NBzEt}_3][\text{ReOCl}_4]$ at 0 °C. The colour changes from orange to violet and brown, and a light brown solid precipitates. After stirring for 1 hour, the complex is separated and dissolved in hot acetonitrile. In the refrigerator the product crystallizes as reddish-brown needles.

Yield: 55 %

[3-(methylaza)pentane-1.5-dithiolato][2-(2.4-dioxo-1H.3H-quinazoline-3-yl)ethane-thiolato]oxorhenium(V) 3:

118 mg (532 μmol) **HL**¹ are suspended in 2 ml hot acetonitrile. 25 mg (167 μmol) 3-N-methyl-azapentane-1.5-dithiol are added. This mixture is dropped to a methanolic solution of 90 mg (167 μmol) $[\text{NBzEt}_3][\text{ReOCl}_4]$ (1 ml). After refluxing for 15 minutes the colour changes to green.

The product is isolated by preparative TLC on silica gel (mobile phase: n-butanol/acetic acid/water 4:1:1 v/v). The complex migrates with the front and a brown by-product remains at the starting point. **3** is extracted from the silica gel with acetonitrile. After evaporation of the organic phase a green residue remains, which is dissolved in dmf. After addition of methanol the product can be isolated as a green powder.

Yield: 17 %.

[3-{2-(2.4-(1H,3H)-quinazolinedionyl)ethyl}aza-pentane-1.5-dithiolato](4-methoxy-benzenethiolato)-oxorhenium(V) 4 and **[3-{2-(2.4-(1H,3H)-quinazolinedionyl)ethyl}aza-pentane-1.5-dithiolato](4-fluoro-benzenethiolato)-oxorhenium(V) 5:**

A mixture of 45 mg (137 μmol) of 3-(2-[[N,N-bis(2-mercapto-S-ethyl)-amino]ethyl)-2,4-(1H,3H)-quinazolindione **H₂L²** and 20 mg (137 μmol) of 2-methoxybenzenethiol (for **4**) {18 mg (137 μmol) 2-fluorobenzenethiol (for **5**)} in 2 ml chloroform is added to an acetonic solution of 100 mg $\text{AsPh}_4[\text{ReOCl}_4]$ (1 ml). A grey solid precipitates immediately. After addition of 1 ml methanol the reaction mixture is refluxed for 2 hours. During this time the colour changes to dark green. The grey insoluble precipitate is filtered off and 2 ml methanol is added to the filtrate. The complexes crystallize as greenish-brown plates by slow evaporation of the mother liquor.

Yields: 65 % (**4**), 70 % (**5**).

Table 2: Analytical data of the complexes 1 - 5

Complex	calc./found (%)			
	C	H	N	S
1	29.2	3.0	4.9	22.3
	29.1	2.9	4.9	21.0
2	30.0	3.0	5.0	17.2
	30.0	3.0	5.0	17.1
3	31.5	3.5	7.3	16.8
	31.1	3.3	7.3	15.8
4	38.0	3.6	6.3	14.4
	38.3	3.9	5.8	13.8
5	36.8	3.2	6.4	14.7
	36.4	3.1	6.3	14.4

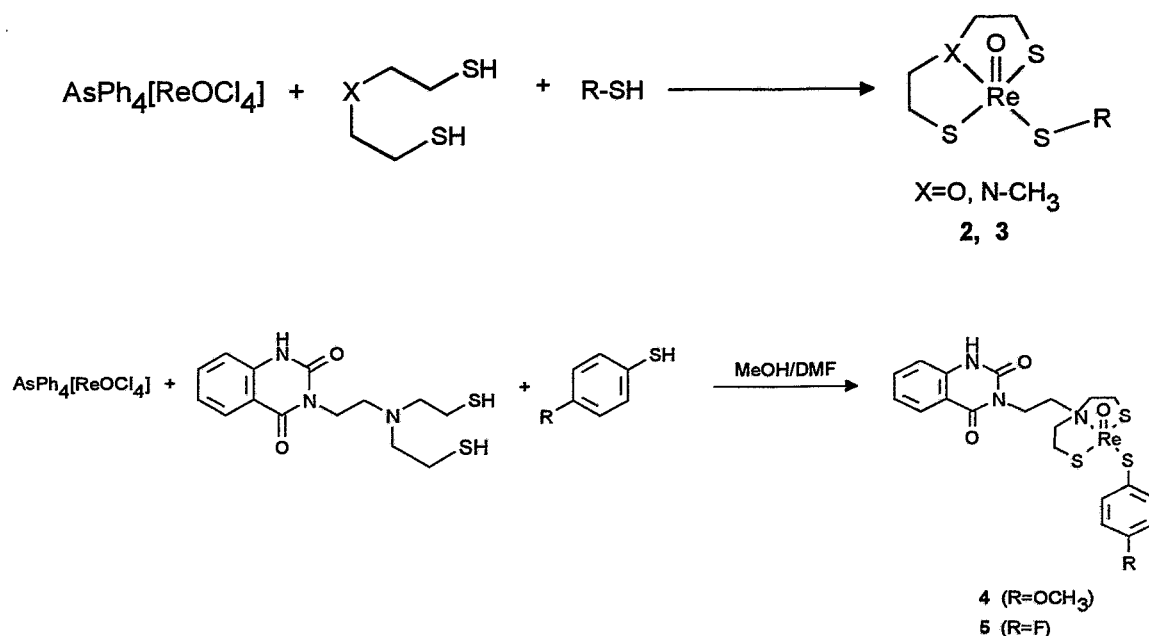
Results and Discussion

Preparation of the complexes

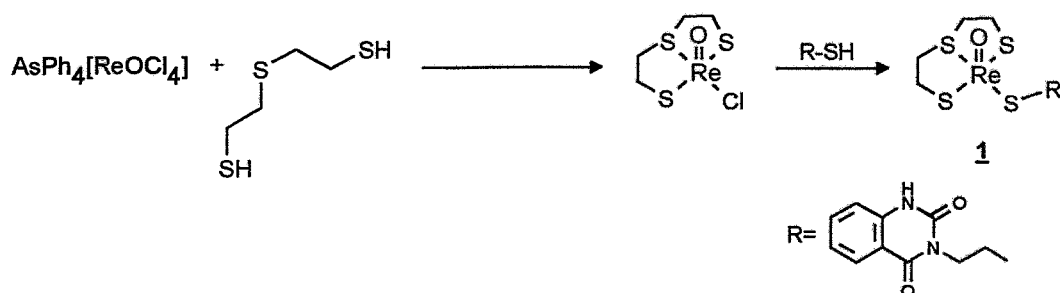
Two general synthesis procedures are available:

1. Common action of a mixture of equimolar amounts of the tridentate ligand and the monodentate thiol on $[\text{ReOCl}_4]^-$ in acetonitrile/methanol gives the neutral oxorhenium(V) complexes, which are purified by column chromatography.

Compounds **4** and **5** precipitate from the reaction mixtures as dark green powders. Due to their slight solubility in all common organic solvents they were used without further purification.



2. In special cases the ligand exchange procedure can take place as a two-pot reaction. The precursor $[\text{ReO}(\text{SSS})\text{Cl}]$ is isolated in pure form and reacts with the monothiol in a subsequent step. This may become important if the reactivities of the tridentate and monodentate ligands differ too much to guarantee a simultaneous attack of the ligands on the precursor (Fietz *et al.*, 1995).



All products were characterized by elemental analysis, infrared and proton NMR spectroscopy. The data of the elemental analyses are listed in Table 2.

In the infrared spectra all the complexes show an intense and characteristic stretching vibration band between 900 and 1000 cm^{-1} indicating the $\text{Re}=\text{O}^{3+}$ core.

Although very complex due to the multiplicity of the methylene protons, the ^1H NMR spectra clearly indicate the presence of both the tridentate and the monodentate ligand.

Preparation of the ligands

3-(2-mercaptoethyl)-2,4-(1H,3H)-quinazolinedione **HL**¹:

3-(2-chloroethyl)-1H,3H-quinazoline-2,4-dione **a** was obtained as described in our previous report, starting from methyl anthranilate (Scheunemann *et al.*, 1995).

For the preparation of the isothiuronium salt **b**, the starting material was heated with a twofold excess of thiourea in 2-methoxyethanol for 2 hours (Fig. 1). Isolation of the product was supported by its low solubility in the reaction medium.

HL¹ was prepared by stirring a mixture of the isothiuronium salt and an aqueous solution of NaOH in the absence of oxygen at 80 - 90 °C for several hours.

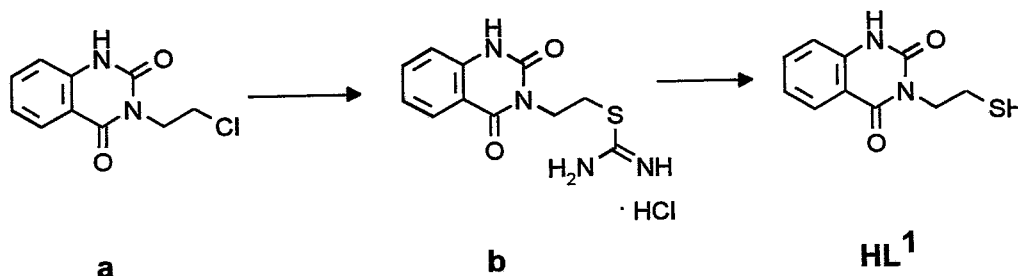


Fig. 1: Synthesis of the monodentate ligand **HL**¹

3-(2-[[N,N-bis(2-mercapto-S-ethyl)-amino]ethyl)-2,4-(1H,3H)-quinazolindione **H**₂**L**²:

Preliminary attempts to directly alkylate diethanolamine with the chlorinated compound **a** always led to the expected *N*-substituted 3-aza-1,5-pentanediol **d** and a water-insoluble product that was shown by its NMR spectrum and melting point to be 2,3-dihydro-5*H*-oxazolo[2,3-*b*]quinazolin-5-one **c**. The concurrent formation of **c** and **d** under basic conditions apparently occurred after a partial deprotonation of the ring amide and thus a negatively charged oxygen atom, which forced the ring closure by elimination of the terminal chlorine.

c itself was found to be a more convenient starting material for the preparation of the diol **d**. This tricyclic compound was prepared in a virtually quantitative yield by treatment of **a** with potassium carbonate in acetone at reflux temperature for 4 hours.

The synthesis of the tridentate ligand **H**₂**L**² is convergent to the preparation of the monodentate ligand **HL**¹ presented in Fig. 2. Nucleophilic ring opening of **c** was performed by autoclaving a mixture of diethanolamine and 2,3-dihydro-5*H*-oxazolo[2,3-*b*]quinazolin-5-one in toluene at 135 °C for 6 hours. The adduct, a water-soluble solid, was formed in a satisfying yield and identified by its NMR spectrum and elemental analysis.

The formation of *N*-substituted 3-aza-1,5-pentanedithiol **H**₂**L**² was achieved by conversion of **d** into the dichloro compound (SOCl₂, reflux), which was directly converted into the bis-isothiuronium derivative **e**. Subsequent treatment with an aqueous solution of NaOH (50 °C, 4 h) removed the S-protecting groups to give **H**₂**L**² in a moderate yield. The structures of intermediate **e** and **H**₂**L**² are consistent with their C and H NMR spectrum and elemental analysis.

In vitro receptor binding

Materials and methods were described in part 2 of our report (Scheunemann *et al.*, 1995).

The compounds compiled in Table 1 were tested for their ability to compete in [³H]ketanserin binding to rat cortical tissue homogenate.

The IC₅₀ values of **1-5**, indicating the concentration of the compound which inhibits 50 % of the specific [³H]ketanserin binding, are in the range > 10000 nM.

Insufficient ability of all four rhenium complexes to displace [³H]ketanserin in the binding assay suggests that combining the quinazoline portion of ketanserin with the chelate unit (Pietzsch *et al.*, 1995) is not successful. They all compete with the radiotracer at unacceptably high concentrations, if at all. No attempts were made to improve the affinity by further modification of the structure in this route.

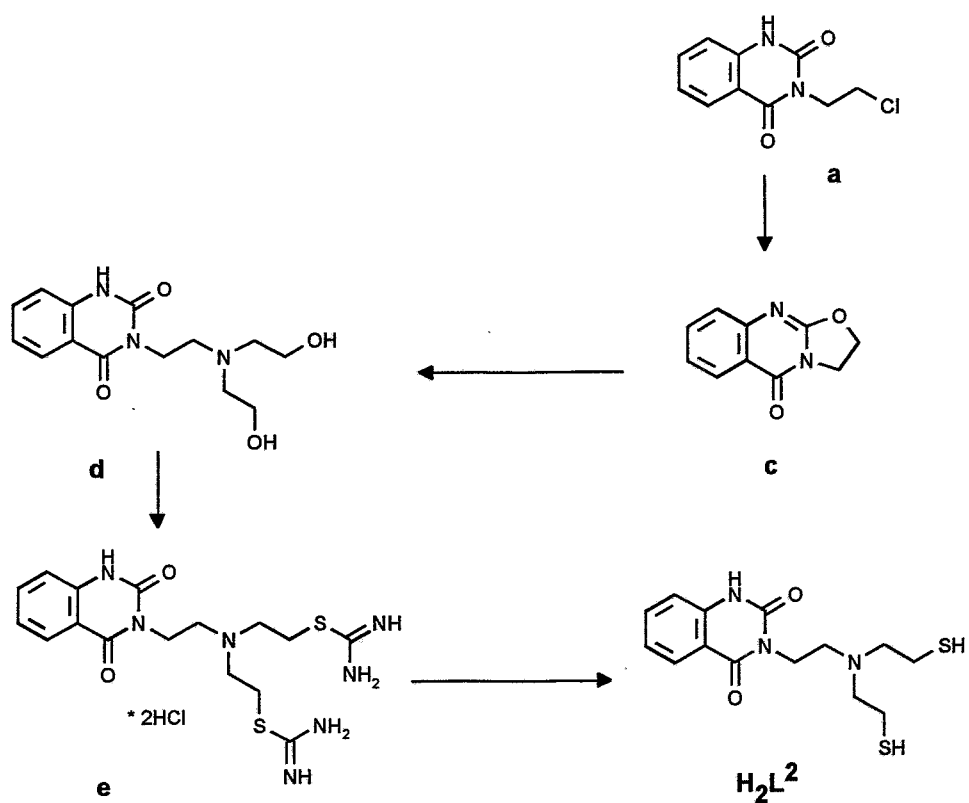


Fig. 2: Synthesis of the tridentate ligand H_2L^2

References

- Fietz T., Spies H., Pietzsch H.-J. and Leibnitz P. (1995) Synthesis and crystal structure of (3-thiapentane-1.5-dithiolato)chlorooxorhenium(V). *Inorg. Chim. Acta* 231 (1,2), 233-236.
- Scheunemann M., Pietzsch H.-J., Brust P., Wober J., Spies H. and Johannsen B. (1995) Serotonin receptor-binding technetium and rhenium complexes. 2. Synthesis, chemical characterization and biochemical evaluation of partial structures of ketanserin. *This report*, pp. 34-39.
- Pietzsch H.-J., Scheunemann M., Spies H., Brust P. and Johannsen B. (1995) Serotonin receptor-binding technetium and rhenium complexes. 1. Design concept and synthesis strategy. *This report*, pp. 31-34.

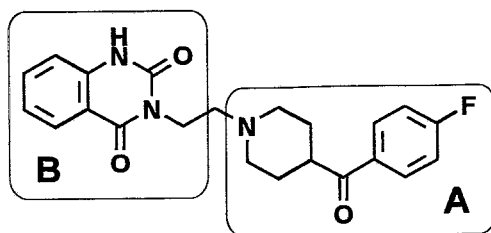
14. Serotonin Receptor-Binding Technetium and Rhenium Complexes

4. Synthesis and Characterization of Ligands Derived from the 4-[*p*-Fluorobenzoyl]-Piperidine Pharmacophore of Ketanserin

M. Scheunemann, H.-J. Pietzsch, H. Spies, P. Brust, B. Johannsen

Introduction

After having studied rhenium complexes bearing the quinazolinone portion of ketanserin (Pietzsch *et al.*, 1995a) we now investigate mixed-ligand complexes derived from the *p*-fluorobenzoylpiperidine portion (fragment A of the lead molecule).



ketanserin

In order to be used as a monodentate ligand in the [3+1] concept, new or improved procedures have to be developed for the preparation of ligands derived from fragment A of ketanserin.

For this purpose we prepared at first quite simple terminal aralkyl mercaptans **6** (Braun, 1912) and **7**, following procedures already described in the literature.

In the next step we sought to further improve HT_{2A} receptor affinity via additional modifications, especially involving the incorporation of a protonable nitrogen located in the spacer between the aromatic system and the donating mercapto group.

Another paper of this report contains the evaluation of a series of terminal aromatic substituted alkylmercaptans in the form of their oxorhenium(V) complexes for binding to 5-HT₂ receptors (Pietzsch *et al.*, 1995b). In this respect we also prepared a derivative **20** with a quinazolinone substituent at the central tertiary amino group.

Experimental (selected examples)

1-(2-hydroxyethyl)-4-benzylpiperidine **15**

14 (7.01 g, 0.04 mol) and 2-bromoethanol (5.0 g, 0.04 mol) together with a catalytic amount of NaJ (75 mg) were added to a suspension of potassium carbonate (13.8 g, 0.1 mol) in dry dioxane (30 ml). The resultant mixture was refluxed for 9 h. After cooling to ambient temperature, the solid was removed by filtration and the filtrate was evaporated to give an oil which was fractionally distilled to yield 7.01 g (80 %) **15** as a low melting solid; b.p. 108 - 115 °C (15 Pa).

General procedure for synthesis of mercaptans **11**, **12**, **13** and **16**

An ethereal solution of hydrogenchloride (26.5 %, 5.8 g, 42 mmol) was added to a solution of *N*-substituted aminoalcohol (30 mmol) in chloroform (50 ml). The resultant homogeneous mixture was cooled to -20 °C and thionyl chloride (5 g, 42 mmol) was added in one portion. The mixture was allowed to warm to room temperature and then refluxed for 3 - 5 h. The solvent was removed *in vacuo* to give a solid or a viscous oil which was used without further purification.

Thiourea (2.44 g, 32 mmol) was added to a stirred mixture of crude hydrochloride in ethanol (30 ml). The reaction mixture was refluxed for 8 - 12 h until the starting material disappeared on TLC. After cooling to room temperature the solvent was evaporated and the viscous residue was dissolved in water (40 ml). While a slow current of nitrogen was passed through the stirred solution, the mixture was heated to 80 °C and aqueous NaOH (8 N, 14 ml) was added in one portion. The resultant two-phase system was refluxed for 1 - 3 h and after the mixture had been cooled to room temperature, it was neutralized by addition of solid KH₂PO₄ to pH 8 - 9. Extracting with ether (3 × 25 ml) followed by washing (sat. NaCl, 20 ml) and drying (MgSO₄) afforded a coloured solution which was concentrated

in vacuo. The oily residue was finally purified by short-path distillation (Kugelrohr) at 40 Pa to yield the desired mercaptan as a colourless liquid.

3-[2-(*N*-benzyl-*N*-hydroxyethyl)-aminoethyl]-2,4-(1*H*,3*H*)-quinazolidione **19**

A mixture of **17** (8.4 g, 44.6 mmol) (Scheunemann *et al.*, 1995) and **18** (7.8 g, 51.6 mmol) in toluene (10 ml) was stirred and heated at 155 - 160 °C in an autoclave for 6 h and allowed to stand overnight at room temperature. The precipitated solid was filtered and washed with ethyl acetate (2 × 10 ml) to yield 13.7 g (90 %) of **19** as colourless crystals; m.p.: 144 °C.

3-[2-(*N*-benzyl-*N*-2-mercaptoethyl)-aminoethyl]-2,4-(1*H*,3*H*)-quinazolidione **20**

An ethereal solution of hydrogen chloride (26.5 %, 2.8 g, 20 mmol) was added to a solution of **19** (5.1 g, 15 mmol) in chloroform (35 ml). The resultant homogeneous mixture was cooled to - 20 °C and thionyl chloride (2.62 g, 22 mmol) was added in one portion. The mixture was allowed to warm to room temperature and then refluxed for 5 h. The solvent and the excess of thionyl chloride were removed *in vacuo* to give a yellowish solid (quant.). A colourless product (chloro derivative) can be obtained by recrystallization from ethanol.

Elemental analysis: (Found C, 57.31; H, 5.31; N, 10.67; C₁₉H₂₀ClN₃O₂•HCl (394.09) requires C, 57.91; H, 5.12; N, 10.66 %).

The crude material (15 mmol) was suspended in a mixture of ethanol (30 ml) and methoxyethanol (30 ml). Thiourea (1.7 g, 22.3 mmol) was added and the whole was heated at 90 - 95 °C for 2 h. After cooling to ambient temperature the precipitated product was filtered and washed with ethanol-ethyl acetate (1:1, 2 × 15 ml). After drying in a desiccator it yielded of 5.6 g (79 %) isothiuronium salt as a colourless solid.

Elemental analysis: (Found C, 50.36; H, 4.52; N, 14.66; S, 6.72; C₂₀H₂₃N₅O₂S•2HCl (470.42) requires C, 51.07; H, 5.36; N, 14.89; S, 6.82 %).

While a slow current of nitrogen was passed through the stirred solution of NaOH (1 g, 25 mmol) in aqueous ethanol (8 %, 14 ml), it was heated to 60 °C. The crude isothiuronium salt (2.35 g, 5 mmol) was added and the resultant clear solution heated at 95 - 105 °C for 3h. After cooling to room temperature, the reaction mixture was neutralized by addition of H₃PO₄ (85 %, 1 ml → pH 8 - 9). The oily product which was formed was extracted (methylene chloride, 2 × 20 ml) and dried (MgSO₄). After evaporation the solid residue (1.7 g) was recrystallized from methanol to give 1.41 g (79 %) of **20** as colourless crystals.

¹H NMR data: δ_H (90 MHz; solvent CDCl₃) 1.56 (1H, -SH), 2.6- 3.0 (m, 6H, N-CH₂-CH₂-SH, NCH₂-CH₂N-CH₂Ph), 3.70 (s, 2H, -NCH₂Ph), 4.23 [A-part of AA'MM'-system, 2H, NCH₂-CH₂N-CH₂Ph]; 7.12, 7.20, 7.59, 8.08 [4m, 9H, 2 × Ar-H]; 10.50 [br, 1H, quinazolidione: NH].

¹³C NMR data: δ (75.475 Hz; solvent CDCl₃) 22.68, 38.70, 50.88, 57.31, 58.90, 114.68, 115.02, 123.28, 126.88, 128.08, 128.30, 128.69, 134.91, 138.62, 139.11, 152.24, 162.25.

Elemental analysis: Found C, 64.59; H, 5.94; N, 11.96; S, 8.99; C₁₉H₂₁N₃O₂S (355.46) requires C, 64.20; H, 5.95; N, 11.82; S, 9.02 %).

Results and Discussion

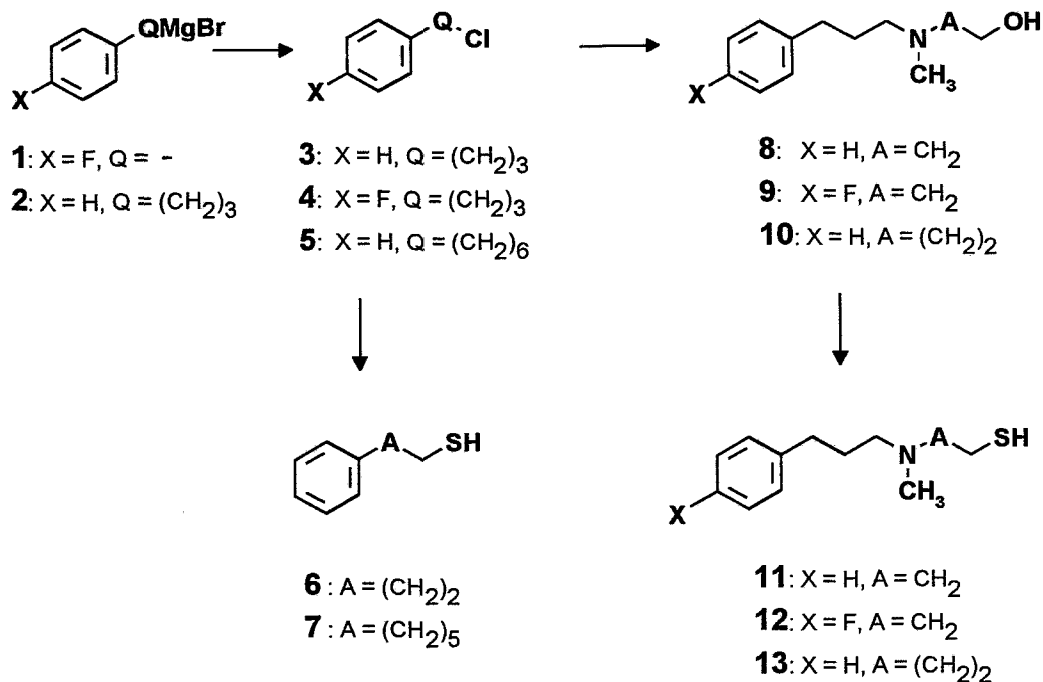
Cross coupling of *p*-fluorophenyl magnesium bromide (**1**) and 3-phenylpropyl magnesium chloride (**2**) with 1-bromo-3-chloropropane gives **4** and **5** (Scheme 1).

3-Phenylpropyl chloride (**3**) and 6-phenylhexyl chloride (**5**) were converted to **6** and **7** by reaction with thiourea, followed by saponification of the isothiuronium intermediate.

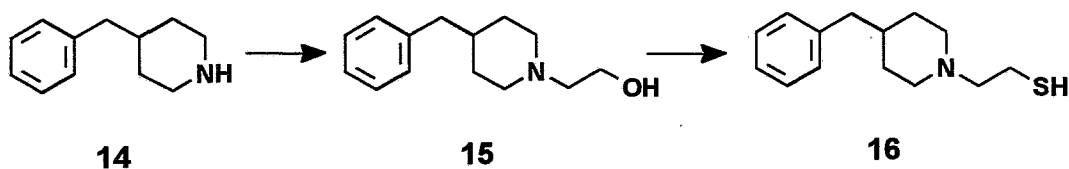
Synthesis of *N*-methylated aminoalcohols **8** - **10** is accomplished through one common methodology. Alkylation of *N*-methylaminoethanol and 3-aminopropanol with **3** or **4** at elevated temperatures (100 - 130 °C), usually in *n*-butanol as a solvent and with potassium carbonate as a basic agent, yields the corresponding amino alcohols **8** and **9** directly. The *N*-methyl derivative **10** was obtained after treatment of the secondary amino alcohol intermediate with a mixture of formic acid and aqueous formaldehyde following the *Eschweiler-Clark Procedure*.

On the other hand, 1-(2-hydroxyethyl)-4-benzylpiperidine (**15**) was prepared by reaction of 4-benzylpiperidine (**14**) with 2-bromoethanol (dioxane/ K_2CO_3 , reflux) in an about 80 % yield or with less expensive 2-chloroethanol (toluene/ K_2CO_3 , reflux) in 69 % yield.

Scheme 1:



Scheme 2:



The synthesis of N-alkyl substituted aminoalkyl mercaptans was achieved by the reaction described in Scheme 1 and 2. Chlorination of the amino alcohols **8** - **10** and **15** to generate the corresponding chloro derivatives is conveniently done with thionyl chloride in chloroform. For preparing the desired thiols these intermediates were prepared by heating an ethanolic solution of the aminoalkyl chlorides in the form of their hydrochlorides with a small excess of thiourea to give the appropriate isothiuronium salt.

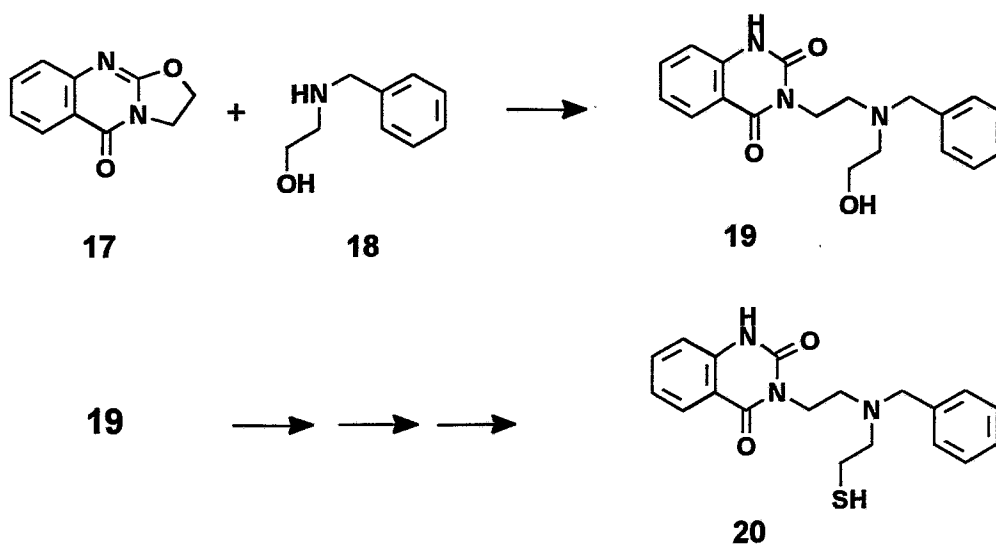
Finally, the crude isothiuronium salts were saponified (2 N NaOH, 110 °C) to give the corresponding aminoalkyl mercaptans **11** - **13** and **16**. The free bases were easily purified by distillation (Kugelrohr, 40 Pa) to give the desired compounds in reasonably good yields. The products, which were prepared for the first time, are homogeneous on TLC and show satisfying elemental analyses.

The synthesis of compound **20** was accomplished by incorporating this heterocyclic substituent in commercially available *N*-benzylaminoethanol (**18**) by means of 2,3-dihydro-5H-oxazolo[2,3-b]quinazolin-5-one (**17**) (Scheme 3).

17 was autoclaved with **18** in toluene at 155 - 160 °C for 6 h to give the amino alcohol **19** in 90 % yield. Conversion into the chloro derivative, reaction with thiourea to yield the corresponding isothi-

uronium salt and subsequent saponification (1.8 N NaOH, 100 °C) give **20** in a 62 % yield (overall yield starting from **17**).

Scheme 3:



References

- Braun J.v. (1912) Synthesen in der fettaromatischen Reihe (IV Mercaptane)
Ber. Dtsch. Chem. Ges. **45**, 1563-1567.
- Pietzsch H.-J., Scheunemann M., Fietz T., Spies H., Brust P., Wober J. and Johannsen B. (1995a) Serotonin receptor-binding technetium and rhenium complexes. 3. Synthesis, characterization and biochemical evaluation of oxorhenium(V) complexes bearing the quinazolidinedione portion of ketanserin. *This report*, pp. 39-43.
- Pietzsch H.-J., Scheunemann M., Fietz T., Spies H., Brust P., Wober J. and Johannsen B. (1995b). Serotonin receptor-binding technetium and rhenium complexes. 5. Synthesis, characterization and biochemical evaluation of oxorhenium(V) and oxotechnetium(V) complexes derived from the 4-[p-fluorobenzoyl]-piperidine pharmacophore of ketanserin. *This report*, pp. 48-50.
- Scheunemann M., Pietzsch H.-J., Brust P., Wober J., Spies H. and Johannsen B. (1995) Serotonin receptor-binding technetium and rhenium complexes. 2. Synthesis, chemical characterization and biochemical evaluation of partial structures of ketanserin. *This report*, pp. 34-39.

15. Serotonin Receptor-Binding Technetium and Rhenium Complexes

5. Synthesis, Characterization and Biochemical Evaluation of Technetium and Rhenium Complexes Derived from the 4-[*p*-Fluorobenzoyl]-Piperidine Pharmacophore of Ketanserin

H.-J. Pietzsch, M. Scheunemann, T. Fietz, P. Brust, H. Spies, B. Johannsen

Introduction

Rhenium complexes bearing the quinazolinodione portion of ketanserin show no affinity to the 5-HT₂ receptor. In *in-vitro* binding assays they compete with the radiotracer only at unacceptably high concentrations (Pietzsch *et al.*, 1995).

To determine what structural aspects of the protonable nitrogen are to be considered and how it influences the binding to the receptor, three representatives **9** -**11** with simple terminal aryl mercaptans of various chain lengths were examined (Fig. 1).

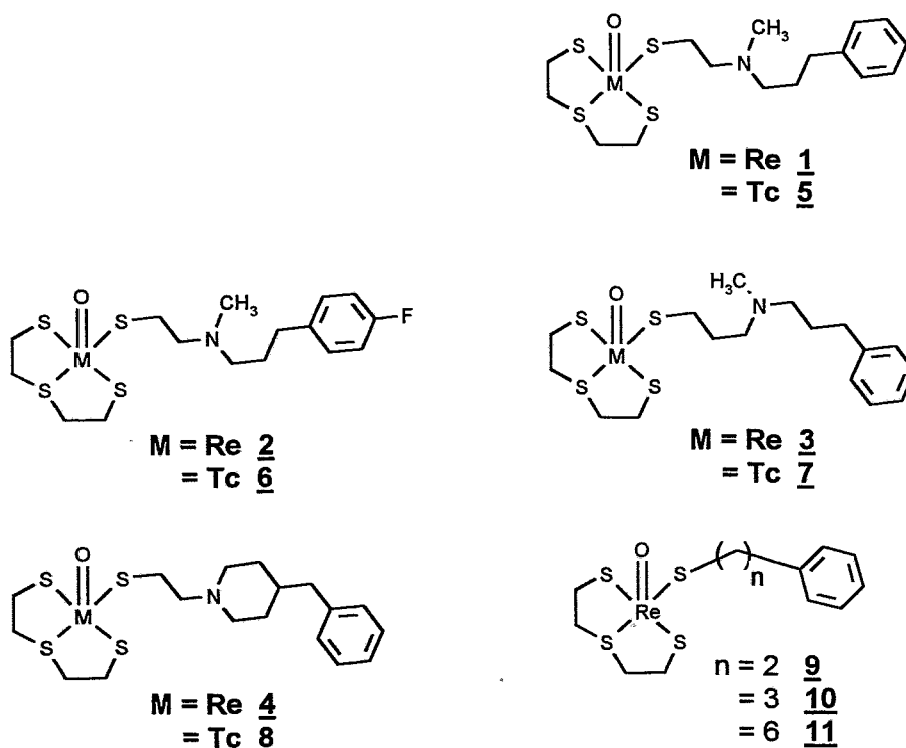


Fig. 1: Neutral oxotechnetium(V)/oxorhenium(V) complexes having integrated the (4-fluorobenzoyl)-piperidine portion of ketanserin in drastically reduced versions; in **9** - **11** alternative spacers are chosen.

Experimental

Preparation of oxorhenium(V) complexes

Mixed-ligand oxorhenium(V) complexes were synthesized either by common action of the tridentate ligand and the monodentate thiol on [ReOCl₄]⁻ or, for the thioether dithiol (HSSSH), in a two-step procedure based on the reaction of HSSSH with [ReOCl₄]⁻ and subsequent exchange of the chlorine in the resulting complex [ReO(SSS)Cl] by the monothiolate ligand (Fietz *et al.* 1995, Spies *et al.* 1995). All complexes were characterized by correct elemental analyses, ¹H NMR spectroscopy and, in some cases, by X-ray structural analysis.

Preparation of the ^{99/99m}Tc complexes

Complexes were prepared with "carrier" ⁹⁹Tc in order to facilitate their complete analytical characterization, which is a prerequisite for studies of structure-activity relationships.

$^{99/99m}\text{Tc(V)}$ gluconate was prepared by gradual addition of stannous chloride to an aqueous solution of $^{99}\text{TcO}_4^-/^{99m}\text{TcO}_4^-$ (2 $\mu\text{mol}/\text{ca. 5 MBq}$) in an excess of sodium gluconate. 1 ml of the Tc gluconate solution was diluted with 1 ml of ethanol. A solution of 2 μmol of 3-thiapentane-1,5-dithiol ("HSSSH") and 2 μmol of the appropriate thiol in 0.2 ml ethanol was added. The colour of the mixture turned to reddish-brown. After stirring for 30 min and adding 2 ml of water, the Tc compound was isolated by selective extraction of the reaction mixture with 2 ml of chloroform. The organic phase was washed twice with 1 ml of water and dried over Na_2SO_4 . The yields are in the range from 75 to 80 percent (related to technetium gluconate). For receptor binding and biodistribution studies a stock solution of the appropriate complex was prepared by evaporating the organic solvent under nitrogen and redissolving the residue in 1 ml of DMSO.

5-HT₂ receptor binding assay

The cortex of rat brain was homogenized in 10 volumes of ice-cold buffer (50 mM tris-HCl, pH 7.6) with an Ultra-Turrax T 25. The homogenate was centrifuged at 20,000 g for 10 min. The resulting pellet was resuspended with the Ultra-Turrax and centrifuged again at 20,000 g for 10 min. After repeating the same procedure the pellet was resuspended in 10 volumes of buffer and stored at -20 °C until used in binding studies.

[³H]ketanserin (3148.7 GBq/mmol from Du Pont) was used as a radioligand for 5-HT₂ receptor binding. The binding assay was carried out in a final volume of 5 ml tris-HCl buffer, pH 7.6, containing 0.12 nM [³H]ketanserin, membrane homogenate (about 20 $\mu\text{g}/\text{ml}$ protein), and various concentrations of the Re or ⁹⁹Tc complexes. The complexes were dissolved in DMSO up to 1 mM, then diluted with buffer.

Nonspecific binding was defined as the amount of [³H]ketanserin bound in the presence of 1 μM mianserin (Sigma), and ranged from 17 percent to 24 percent of the total binding. The samples were incubated in triplicates at 20 °C for 60 min. The incubation was terminated by rapid filtration through GF/B glass fibre filters (Whatman) using a 30-port Brandel Cell Harvester. The filters were rapidly washed with four 4 ml portions of ice-cold buffer, transferred into 10 ml scintillation fluid (Ultima-Gold, Packard) and analyzed for radioactivity. In case of ⁹⁹Tc complexes, interference by ⁹⁹Tc radioactivity in ³H counting was eliminated by appropriate adjustment of the energy channel, except at the highest ⁹⁹Tc concentration used, which required correction. The protein content of the membrane suspensions was determined according to the literature (Lowry *et al.* 1951).

Results and Discussion

Novel technetium and rhenium mixed ligand complexes 1 - 8 (Fig. 1) containing quite simple terminal aralkyl mercaptans (Scheunemann *et al.*, 1995) are stronger in the binding assay than the endogenous substrate serotonin (Johannsen *et al.*, 1995, 1996).

Table 1 summarizes the IC₅₀ values of the tested compounds, indicating the concentration of the compound which inhibits 50 % of the specific [³H]ketanserin binding.

Table 1: Comparison of the IC₅₀ values of Re/Tc complexes 1 - 11, as obtained in competition of [³H]ketanserin binding in rat frontal cortical tissue homogenates

Complex	IC ₅₀ (nM)
1	29
2	19
3	14
4	23
5	64
6	67
7	7
8	24
9	1250
10	845
11	1000
serotonin	638

The data are consistent with the realization that a protonable nitrogen is a standard feature among many ketanserin-related analogues. It has been assumed that electrostatic interactions between negatively charged domains of the G-protein-coupled receptor and the positively charged ketanserin may be a part of the ligand binding mechanism (Kristiansen *et al.*, 1993).

Consistent with the assumption that replacement of the carbonyl oxygen atom by hydrogens in the 4-fluorobenzoyl portion of ketanserin decreases the receptor affinity only slightly and that the fluoro group also plays a minor role in binding, the 4-fluorobenzoyl group is reduced to a benzyl structure in the candidates **4** and **8**.

The positive results allow us to evaluate the elongation of the central nitrogen-containing unit between the chelate and the benzyl moiety. The distance between nitrogen atom and chelate seems to influence binding. The ethyl chain can be advantageously extended to propyl.

Because of the high flexibility with several accessible conformations, the distance between amine and the centre of the benzoyl ring is reported to vary in ketanserin between 6.7 Å and 5.7 Å (Herndon *et al.*, 1992). Therefore, the piperidine ring can be abbreviated to a structurally simple amine.

In summary, one can say that structural elements for the design of rhenium and technetium complexes capable of strong 5-HT₂ serotonin receptor-binding *in vitro* have been successfully derived from systematic structure-affinity studies. Our new lead structure with complexes **3** and **7** presented here is considered to be the leads for the development of corresponding imaging agents.

References

- Fietz T., Spies H., Pietzsch H.-J. and Leibnitz P. (1995) Synthesis and crystal structure of (3-thiapentane-1,5-dithiolato)chlorooxorhenium(V). *Inorg. Chim. Acta* **231**, 233-236.
- Herndon J.L., Ismaiel A., Ingher S.P., Teitler M. and Glennon R.A. (1992) Ketanserin analogues: structure-affinity relationships for 5-HT₂ and 5-HT_{1C} serotonin receptor binding. *J. Med. Chem.* **35**, 4903-4910.
- Johannsen B., Pietzsch H.-J., Scheunemann M., Spies H. and Brust P. (1995) Oxotechnetium(V) and oxorhenium(V) complexes as potential imaging agents for the serotonin receptor. *J. Nucl. Med.* **36**, 27P (abstr.).
- Johannsen B., Scheunemann M., Spies H., Brust P., Wober J., Syhre R. and Pietzsch H.-J. (1996) Technetium(V) and rhenium(V) complexes for 5-HT_{2A} serotonin receptor-binding: structure-affinity considerations. *Nucl. Med. Biol.*, in press.
- Kristiansen K., Edvardsen O. and Dahl S.G. (1993) Molecular modelling of ketanserin and its interactions with the 5-HT₂ receptor. *Med. Chem. Res.* **3**, 370-385.
- Lowry O.H., Rosebrough N.J., Farr A.L. and Randall R.J. (1951) Protein measurement with the Folin phenol reagent. *J. Biol. Chem.* **193**, 265-275.
- Pietzsch H.-J., Scheunemann M., Fietz T., Spies H., Brust P., Wober J. and Johannsen B. (1995a) Serotonin receptor-binding technetium and rhenium complexes. 3. Synthesis, characterization and biochemical evaluation of oxorhenium(v) complexes bearing the quinazolinedione portion of ketanserin. *This report*, pp. 39-43.
- Spies H., Fietz Th., Pietzsch H.-J., Johannsen B., Leibnitz P., Reck, G., Scheller D. and Klostermann K. (1995b) Alkyl and aryl substituted oxorhenium(V) complexes with tridentate/monodentate coordination. *J. Chem. Soc., Dalton Trans.* 2277-2280.
- Scheunemann M., Pietzsch H.-J., Spies H., Brust P. and Johannsen B. (1995) Serotonin receptor-binding technetium and rhenium complexes. 4. Synthesis and characterization of ligands derived from the 4-[*p*-fluorobenzoyl]-piperidine pharmacophore of ketanserin. *This report*, pp. 44-47.

16. Serotonin Receptor-Binding Technetium and Rhenium Complexes

6. Distribution and Brain Uptake in the Rat of [^{99m/99}Tc]Oxotechnetium(V) Complexes with Affinity to the 5-HT₂ Receptor

R. Syhre, R. Berger, H.-J. Pietzsch, M. Scheunemann, H. Spies, B. Johannsen

Introduction

Neutral ^{99m/99}Tc complexes with an (S_S_S) chelate unit and a thiol ligand of various chains (Table 1) show affinity to 5-HT₂ receptors, as determined by *in vitro* studies of the binding on rat cortex. Nanomolar IC₅₀ values have been obtained for derivatives containing protonable nitrogen in the molecule (complexes 5 - 8). The IC₅₀ values of the nitrogen-free derivatives 1a and 2a were significantly higher (Johannsen *et al.*, 1995). All complexes are lipophilic with logP_{HPLC} in the range from 3.39 - 3.85 (Table 1).

In order to test and to address the following issues, biodistribution studies in rats were performed:

- ability to cross the intact blood-brain barrier,
- retention of radioactivity in selected rat brain regions,
- influence of nitrogen in the molecule on brain uptake,
- influence of association with circulating blood components and affinity to excretory organs on the initial distribution and retention *in vivo*.

Experimental

^{99m/99}Tc complexes

The preparation of the ^{99m/99}Tc complexes (Table 1) was previously described (Johannsen *et al.*, 1995, Pietzsch *et al.*, 1995). For the biological studies the solutions of the complexes were diluted with polypropylene glycol and sodium chloride for injection to adjust the desired radioactive concentration.

In vivo experiments

Animal experiments were carried out according to the relevant national regulations.

The studies were performed on male Wistar rats (5 - 6 weeks old). 0.5 ml complex solution was injected into the tail vein. 1 - 120 min. p.i. the rats were sacrificed by heart puncture under ether anaesthesia. The selected organs were isolated for weighing and counting. For displacing experiments 2 mg/kg BW ketanserin was injected 10 minutes before the radiotracer application.

Determination of in vivo binding on erythrocytes

After *in vivo* incubation heparinized whole blood was taken by heart puncture. Red blood cells and plasma were separated by centrifugation. The cells were washed plasma-free wae (sodium chloride for injection) and the radioactivity of the red cell fraction was counted and calculated.

Results and Discussion

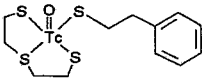
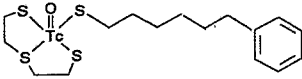
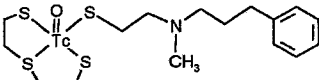
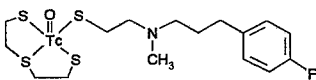
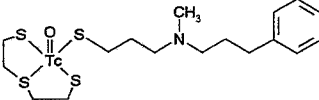
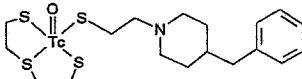
Table 2 displays the distribution of complexes after i.v. injection in rats.

All complexes containing protonable nitrogen (5 - 8) show similar distribution patterns, independent of the length and nature of the side chain that bears the nitrogen functionality. High activity in the blood pool, slow blood clearance as well as increased retention in the kidney and prolonged retention in the liver were found. The complexes displayed a low initial brain uptake of 0.2 - 0.5 % of the injected dose. The pK_{HPLC} values ranging from 8.3 to 8.6 (Table 1) are apparently unsuitable for a good brain uptake.

Compared with the nitrogen-containing complexes, the nitrogen-free complexes 1a and 2a showed a higher brain activity and a lower blood pool activity. However, more than 50 % of the injected dose was extracted by the liver during the firstly minutes after injection. The complexes were eliminated via the bile.

Fig. 1 illustrates the brain clearance curves of both series of complexes. The initial brain uptake of the nitrogen-free complexes was higher and the brain washout more rapid compared with the nitrogen-containing complexes.

Table 1: Structure, log P_{HPLC}, and pK_{HPLC} values of [^{99m/99}Tc]oxotechnetium(V) complexes

Complex	Structures of Tc complexes	pK _{HPLC}	log P _{HPLC}
1a		-	3.63
2a		-	n.d.
5		8.2	3.34
6		8.1	3.29
7		8.6	3.65
8		8.3	3.82

The distribution of brain radioactivity in the cortex (frontal), the caudate putamen, the hippocampus and in the cerebellum is shown in Fig. 2 for the complexes 1a and 5. The nitrogen-containing complex 5 was retained in the brain regions rich in receptors at a nearly constant level within 10 - 120 minutes p.i.. The data were corrected for the radioactive part of the regional blood volume (Cremer *et al.*, 1983, Del Rosario *et al.*, 1994). In contrast to the nitrogen-containing complex 5, a constant value of the brain activity was not yet attained 120 minutes after injection of the nitrogen-free complex 1a, possibly on account of the moderate affinity to the receptors found for this complex (Johannsen *et al.*, 1995).

As expected, during the investigation the radioactivity in the cerebellum slowly decreased for all complexes. These results and the results of preliminary displacement experiments with ketanserin (Fig. 3) suggest a higher affinity to receptor rich regions for nitrogen-containing complexes. An overview of the interesting regions/cerebellum ratios in rat brain is given in Table 3.

Table 2: Biodistribution of [^{99m}Tc]oxotechnetium(V) complexes in rats (mean % dose, n = 3)

Complex	Time	Brain		Blood	Heart	Lung	Kidney	Liver	
		min.p.i.	%dose/organ	%dose/g	%dose/g	%dose/organ	%dose/organ	%dose/organ	%dose/organ
1a	5		0.99	0.62	0,5	0.3	4.6	2.9	55.2
	10		0.74	0.47	0.4	0.3	5.7	3.3	49.0
	60		0.40	0.30	0.3	0.2	1.8	4.5	20.0
	120		0.38	0.25	0.2	0.2	1.8	4.6	14.4
2a	5		1.33	0.87	0.3	1.8	2.7	3.1	34.8
	10		0.92	0.62	0.2	1,2	2.1	2.5	39.2
	60		0.64	0.45	0.2	0.2	1.2	3.2	46.7
	120		0.51	0.32	0.1	0.2	1.2	3.7	45.6
5	5		0.44	0.28	5.0	0.9	10.7	5.7	11.0
	10		0.36	0.26	4.1	0.9	7.3	4.1	12.0
	60		0.27	0.16	2.8	0.6	7.1	17.5	16.8
	120		0.26	0.10	2.3	0.6	6.9	19.5	17.1
6	5		0.25	0.14	3.5	0.7	7.5	5.8	15.2
	10		0.22	0.15	3.4	0.6	5.6	6.5	17.5
	60		0.11	0.10	1.9	0.5	5.3	14.4	17.4
7	120		0.10	<0.10	1.4	0,4	4.9	17.5	17.5
	5		0.36	0.22	4.4	0.7	8.1	4.1	14.0
	10		0.33	0.17	4.2	1.1	5.2	6.9	11.3
8	60		0.22	0.16	2.7	0.5	5.9	12.7	18.9
	120		0.22	0.15	1.8	0.4	4.7	16.1	18.0
	5		0.28	0.18	4.2	1.0	6.8	4.9	13.5
8	10		0.27	0.19	3.8	1.2	6.9	6.4	14.9
	60		0.17	0.14	2.5	0.5	4.1	13.6	16.9
	120		0.17	0.12	1.8	0.2	4.7	16.1	16.8

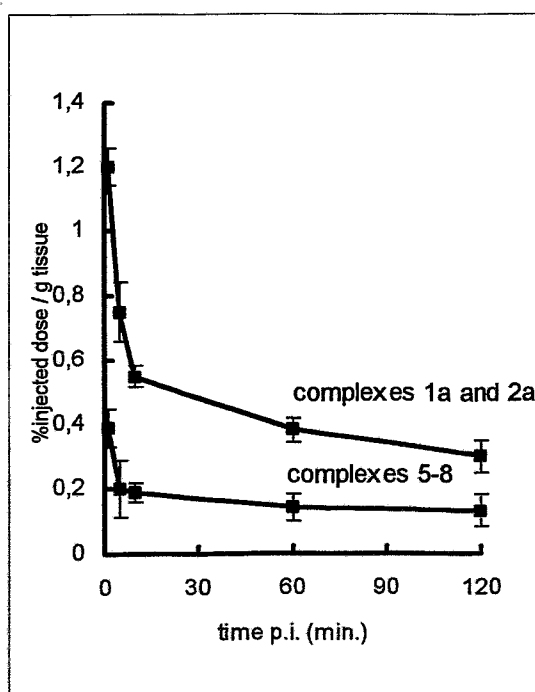


Fig. 1: Brain washout of [^{99m}Tc]oxotechnetium(V) complexes in rats (mean values ± SD, n = 6)

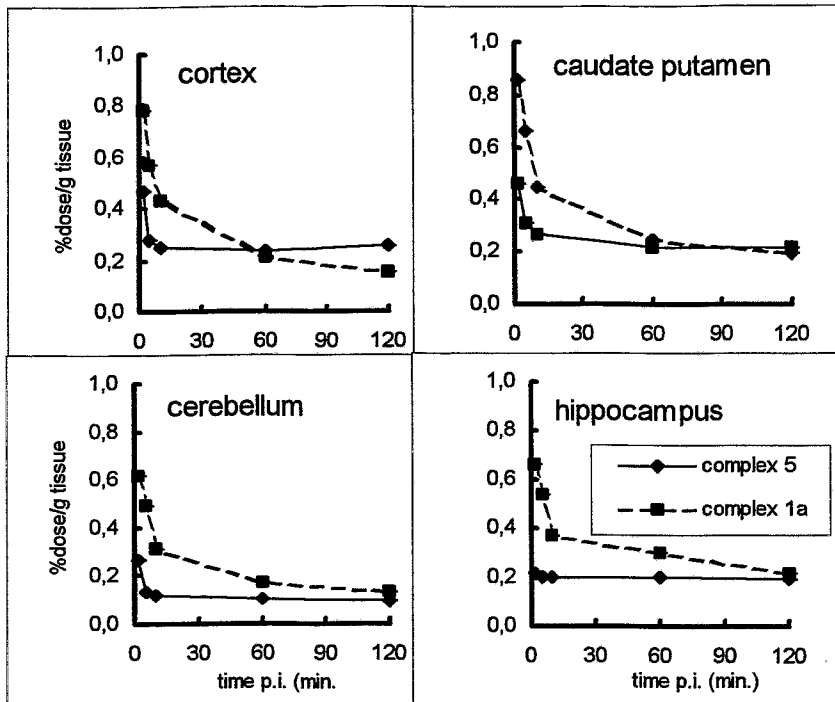


Fig. 2: Comparison of the time radioactivity course of brain regions after injection of nitrogen-free complex 1a and nitrogen-containing complex 5 in rats (mean %dose, n = 3)

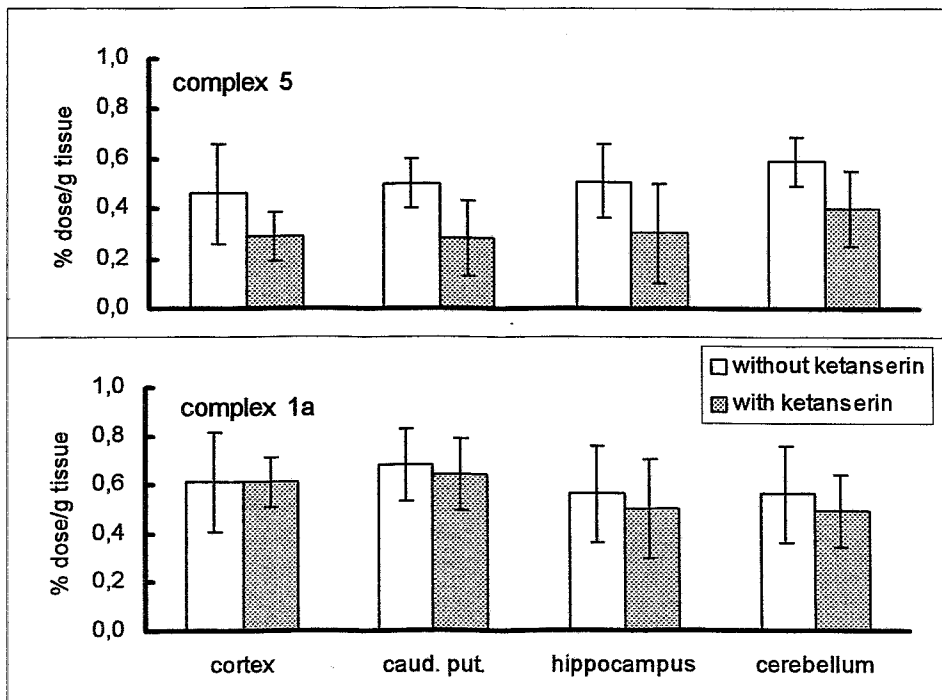


Fig. 3: Radioactive concentration in brain regions 5 minutes after injection of nitrogen-free complex 1a and nitrogen-containing complex 5 in rats with and without ketanserin pretreatment (mean values \pm SD; n = 6).

Table 3: Calculated ratios of receptor-rich rat brain regions and the cerebellum 5 min. after injection of [^{99m}Tc]oxotechnetium(V) complexes % dose/g ± SD, corrected by the blood activity part in the regions; n = 6)

Complex	Cortex/ cerebellum	Caudate putamen/ cerebellum	Hippocampus/ cerebellum
1a	1.2 ± 0.1	1.3 ± 0,2	1.2 ± 0,3
5	1.9 ± 0.8	2.5 ± 0,3	1.9 ± 0.3
6	1.5 ± 0.7	2.3 ± 0.9	1.2 ± 0.4

The blood clearance and the RBC/plasma ratio of the radioactivity after i.v. injection of the complexes was a further point of interest. Table 2 as well as Fig. 4 demonstrate significant differences in blood elimination between the two types of complexes.

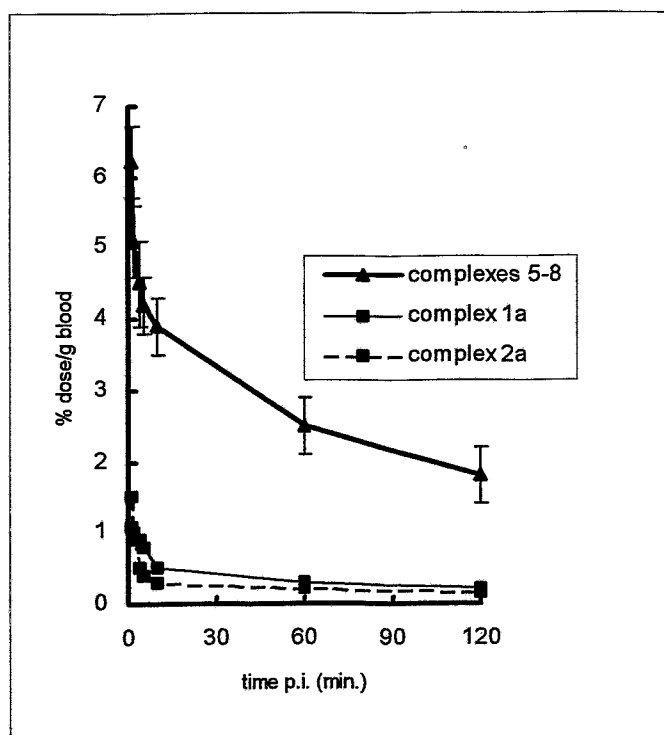


Fig. 4: Blood clearance curves of [^{99m}Tc]oxotechnetium(V) complexes in rats (mean values ± SD, n = 6)

Approximately 70 % of the injected dose of radioactivity was obtained in the blood pool after injection of nitrogen-containing complexes 5 - 8. Their elimination is slow. A fast erythrocyte uptake of these complexes in the firstly minutes after injection was found (Table 4), with about 60 % of the activity inside of the erythrocytes (Syhre *et al.*, 1995). A constant RBC/plasma ratio was found for complex 6 from 30 to 120 minutes p.i. (Fig. 5).

The percentage of radioactivity not bound to erythrocytes is mainly extracted by and retained in the liver and kidney. The initial liver uptake and the retention characteristic of the liver for the lipophilic complexes also demonstrated a high affinity and a strong nonspecific binding possibly to tissue proteins (Fig. 6).

Table 4: Erythrocyte uptake *in vivo* 5 minutes after injection of [^{99m}Tc]oxotechnetium(V) complexes in rats, (mean % uptake ± SD ; n = 6)

Complex	% Radioactivity of erythrocytes
1a	48 ± 2
2a	36 ± 2
5	68 ± 3
6	63 ± 2
7	67 ± 2
8	63 ± 2

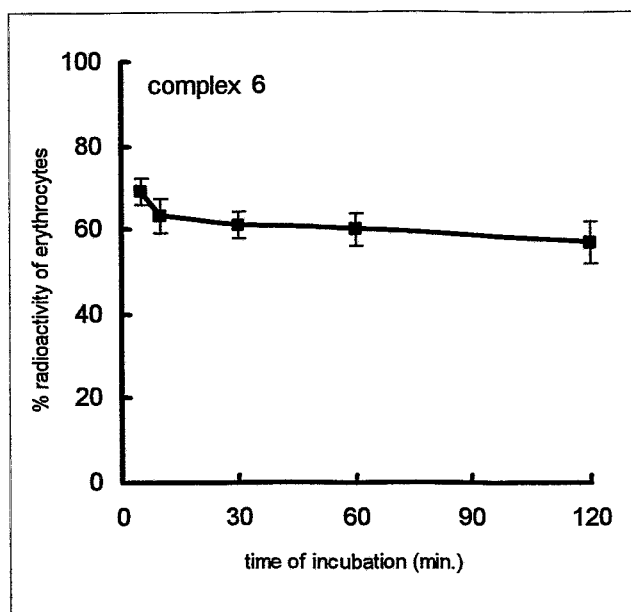


Fig. 5: Time course of erythrocyte binding in rats after injection of the nitrogen- containing complex 6 (mean values ± SD ; n = 6).

In the case of the nitrogen-free complexes 1a and 2a, the activity of the blood compartment is not important. The blood elimination proceeds quickly. The radioactivity available for the brain uptake is not expected to be reduced by the binding on erythrocytes as shown for complexes 5 - 8. It is likely that the lower radioactivity in the brain results from a high extraction in the liver during the first few minutes after the injection. The results of the erythrocyte binding studies in plasma and in plasma-free medium indicate, that the interactions between the nitrogen-free complexes and rat plasma are slightly stronger or more restrictive, than the interactions of the protonable nitrogen-containing complexes (Syhre *et. al.*, 1995). It is possible that the protein bound part can be rapidly extracted by the liver.

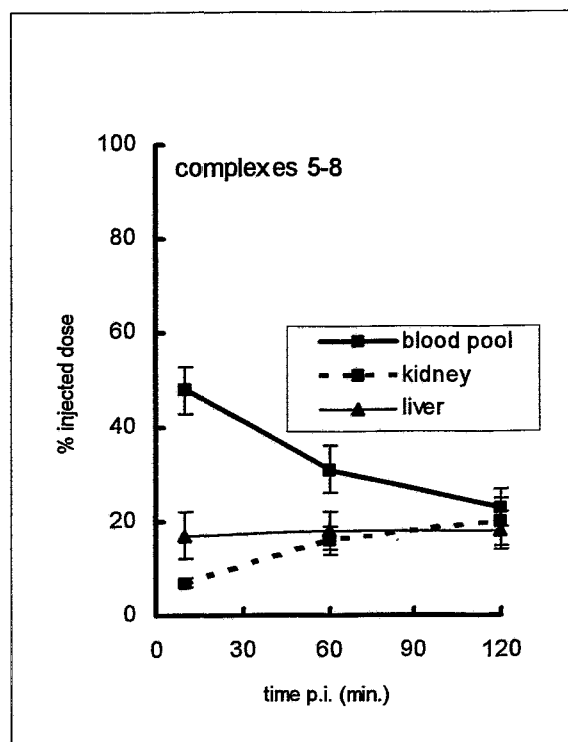


Fig. 6: Comparison of blood pool clearance and accumulation in the liver and kidney after injection of nitrogen-containing complexes in rats (mean % dose of complexes \pm SD, n = 3 / complex)

Summary

- All examined complexes are able to cross the blood-brain barrier.
- A retention in selected regions in the rat brain after i.v. injection was observed.
- As expected the nitrogen-containing, protonable complexes show a lower brain uptake than the nitrogen-free, uncharged complexes.
- In case of a rapid extraction by other organs, the brain uptake was reduced (nitrogen-free complexes).
- In case of association with circulating blood components and a protonation of complexes a low level of brain extraction was resulted (nitrogen-bearing complexes).

A relationship between the initial radioactivity taken up from the rat brain and the freely available neutral complex in the plasma during the first pass was demonstrated.

References

- Cremer J.E. and Malcom P.S. (1983) Regional brain flow, blood volume, and haematocrit values in the adult rat. *J. Cerebr. Blood Flow Metab.* **3**, 254-256.
- del Rosario R.B., Jung Y.-W., Baidoo K.E., Lever S.Z. and Wieland D.M. (1994) Synthesis and *In vivo* evaluation of a $^{99m/99}\text{Tc}$ -DADT-benzovesamicol: a potential marker for cholinerg neurons. *Nucl. Med. Biol.* **21**, 197-203.
- Johannsen B., Pietzsch H.-J., Scheunemann M., Spies H. and Brust P. (1995) Oxotechnetium(V) and oxorhenium(V) complexes as potential imaging agents for the serotonin receptor. *J. Nucl. Med.* **36**, 27P (abstr.)
- Johannsen B., Scheunemann M., Spies H., Brust P., Wober J., Syhre R. and Pietzsch H.-J. (1995) Technetium(V) and rhenium(V) complexes for 5-HT_{2A} serotonin receptor binding: structure-affinity considerations. *Nucl. Med. Biol.*, in press.
- Pietzsch H.-J., Scheunemann M., Fietz T., Brust P., Spies H. and Johannsen B. (1995) Serotonin receptor-binding technetium and rhenium complexes. 5. Synthesis, characterization and biochemical evaluation of technetium and rhenium complexes derived from the 4-[*p*-fluorobenzoyl]-piperidine pharmacophore of ketanserin. *This report*, pp. 48-50.

Syhre R., Pietzsch H.-J., Scheunemann M., Spies H. and Johannsen B. (1995) Serotonin receptor-binding technetium and rhenium complexes. 7. Binding of [$^{99m/99}\text{Tc}$] oxotechnetium(V) complexes to erythrocytes of rats and humans. *This report*, pp. 58-62.

17. Serotonin Receptor-Binding Technetium and Rhenium Complexes

7. Binding of [$^{99m/99}\text{Tc}$]Oxotechnetium(V) Complexes to Erythrocytes of Rats and Humans

R. Syhre, H.-J. Pietzsch, M. Scheunemann, H. Spies, B. Johannsen

Introduction

It is well known that only the uncharged, freely diffusible fraction of a drug or a tracer is available to enter the brain (Greig, 1990, Novotnik, 1992, Eckelmann *et al.*, 1995). Protein or cell binding of the tracers in the blood is considered to affect this transport.

Especially lipophilic tracers are able to rapidly cross the diffusion barrier of red cell membranes and can be trapped in the cells. It is therefore important to know the interaction of potential brain tracers with plasma proteins and blood cells. The binding characteristics especially of the tracers should be involved in the interpretation of animal experiments.

These studies were performed to evaluate the *in vitro* and *in vivo* binding of [$^{99m/99}\text{Tc}$]oxotechnetium(V) complexes in whole blood and in isolated erythrocytes (RBCs) of rats. Human whole blood and isolated erythrocytes were included in the *in vitro* experiments as a bridge between laboratory animals and humans.

Experimental

$^{99m/99}\text{Tc}$ complexes

Neutral and lipophilic $^{99m/99}\text{Tc}$ complexes are listed in Table 1. The preparation and the chemical, biochemical and biological characterization of these complexes have been published before (Johannsen *et al.*, 1995, Pietzsch *et al.*, 1995, Syhre *et al.*, 1995).

1. Whole blood binding *in vitro*

The time course uptake of tracers in erythrocytes was determined in 0.5 ml heparinized whole blood incubated at 37 °C with 0.05 ml (0.3 MBq) $^{99m/99}\text{Tc}$ complexes in a thermoshaker for 5 - 120 minutes. After the incubation, erythrocytes and plasma were rapidly separated by centrifugation and the erythrocytes were washed 5 times with sodium chloride for injection. The radioactivity was measured by an γ -counter.

2. *In vitro* binding in the presence of plasma-free medium

Plasma-free washed erythrocytes were reconstituted with a plasma equivalent volume of sodium chloride for injection. The cell-associated radioactivity was determined after incubation with the complexes as described in 1.

3. *In vitro* haemolysis of radioactive erythrocytes

6 tubes of heparinized whole blood were incubated with the complexes at 37 °C for 5 minutes. The red blood cells and plasma were separated by centrifugation. The cell fraction was washed with sodium chloride for injection and the radioactivity of 3 tubes was measured (100 %). The erythrocytes of the other 3 tubes were haemolysed with distilled water and the membrane fragments were separated and washed. The distribution of radioactivity between the red cell membrane and plasma was measured and calculated.

4. *In vitro* exchange experiments

To test whether the complexes are exchangeable between erythrocytes and plasma or plasma-free medium, 6 tubes of heparinized whole blood were initially incubated at 37 °C for 5 minutes. Erythrocytes and plasma were separated by centrifugation and the cell fractions were washed five times with sodium chloride for injection. The RBC radioactivity of 3 tubes was measured (100 %). The erythrocytes of the other 3 tubes were immediately reconstituted with fresh nonradioactive plasma or sodium chloride for injection and reincubated at 37 °C for 120 minutes. The radioactivity of the erythrocytes and of the plasma or plasma-free medium was also separated, measured and calculated.

5. *In vitro* binding in the presence of species different plasma

In order to check the influence of heterologous plasma proteins, human plasma was used for the reconstitution of plasma-free erythrocytes of rats, and rat plasma was used for the reconstitution of human erythrocytes.

Results and Discussion

In vivo studies of our new series of Tc complexes described elsewhere in this report have shown a fundamental difference between complexes with and without a protonable nitrogen functionality in the molecule. Nitrogen-containing complexes (complexes 5 - 8) have a slow blood clearance in rats, whereas nitrogen-free complexes (complexes 1a and 2a) are cleared rapidly (Syhre *et al.*, 1995).

Table 1: Structure of [^{99m}Tc]oxotechnetium(V) complexes

	Nitrogen-free complexes	Nitrogen-containing complexes	Nitrogen-containing complexes
1a		5	
2a		6	
		7	
		8	

A rapid uptake of the nitrogen-containing complexes in red cells was found *in vitro* in rats. Up to 70 % of the blood radioactivity was concentrated in the erythrocytes within the first 5 minutes of incubation. The RBC activity after the incubation of the nitrogen-free complexes was significantly lower. Approximately 45 % of blood activity was the maximum erythrocyte uptake of the tracers 1a and 2a (Fig. 1A).

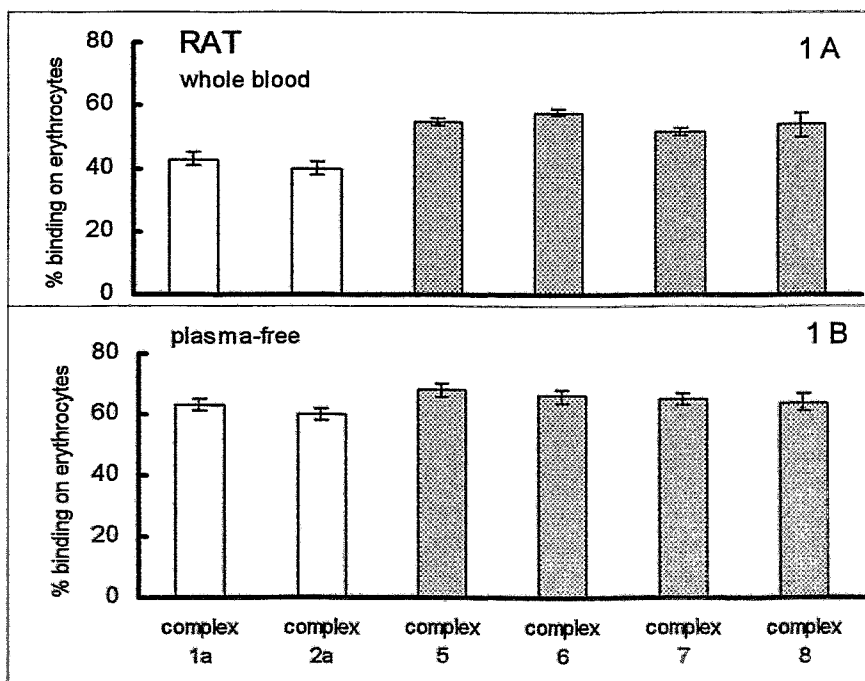


Fig. 1: *In vitro* binding to rat erythrocytes 10 minutes after incubation of nitrogen-free complexes (1a and 2a) and nitrogen-containing complexes (5 - 8) in whole blood (1A) and in plasma-free medium (1B) (mean values \pm SD; n = 6).

The data of haemolysis studies show for all complexes that about 60 % of the RBC activity were trapped in the cells.

Fig. 3A demonstrates a constant erythrocyte/plasma ratio for *in vivo* incubation of complex 6 in the period from 30 to 120 minutes p.i. (Syhre *et al.*, 1995). For this complex (Fig. 3A) as well as for other derivatives of this group constant ratios were not reached in this incubation period *in vitro*.

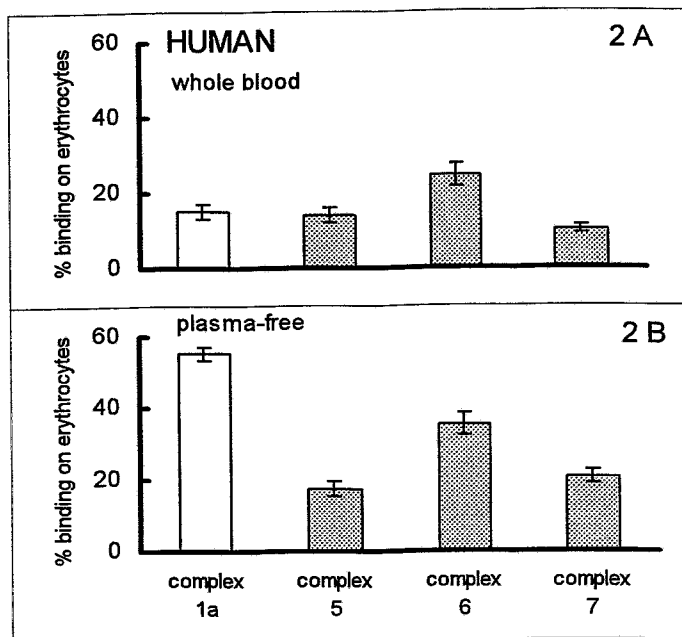


Fig. 2: *In vitro* binding to human erythrocytes 10 minutes after incubation of nitrogen-free complexes (1a and 2a) and nitrogen-containing complexes (5 - 8) in whole blood (2A) and in plasma-free medium (2B), (mean values \pm SD; n = 6).

Results from the exchange ability experiments of all complexes indicate that the uptake of erythrocytes is partially reversible under *in vitro* conditions. After 120 minutes about 60 % of the initial RBC activity was extracted by reincubation with fresh nonradioactive plasma.

These results in the whole blood of rats differ from those in plasma-free medium.

After incubation of the nitrogen-containing complexes with erythrocytes in the absence of plasma the radioactivity associated with the erythrocyte fraction was found to be up to 10 % higher than in the presence of blood plasma. This increase was higher after the plasma-free incubation of the nitrogen-free complexes 1a and 2a (Fig. 1B).

Within 30 to 120 minutes of incubation the erythrocyte/plasma ratio of radioactivity was constant as were the results of the *in vivo* experiments (Fig. 3A).

Not more than 20 % of the RBC activity is exchangeable in the plasma-free medium.

It is possibly the different degree of reversibility of the erythrocyte binding in plasma vs plasma-free medium that influences the time course of the erythrocyte/plasma ratios *in vitro* (Fig. 3A).

The results of these series of experiments suggest an interaction between the complexes and the plasma proteins of rats.

Contrary to the rat erythrocyte uptake, the binding of all complexes to human erythrocytes was low. An initial RBC uptake of 10 to 20 % of the radioactivity in human whole blood was measured (Fig. 2A). The time course in Fig. 3B is comparable to those of rat erythrocytes *in vitro* (Fig. 3A). The low RBC uptake could be a result of a different affinity of the complexes to rat and human erythrocytes.

Incubation of human erythrocytes in plasma-free medium increases the binding. This increase was considerably higher for the complexes 1a and 2a than for others. These results indicate that the interaction between the nitrogen-free complexes and human or rat plasma proteins is stronger than the interaction between the nitrogen-containing complexes and plasma proteins (Fig. 2B).

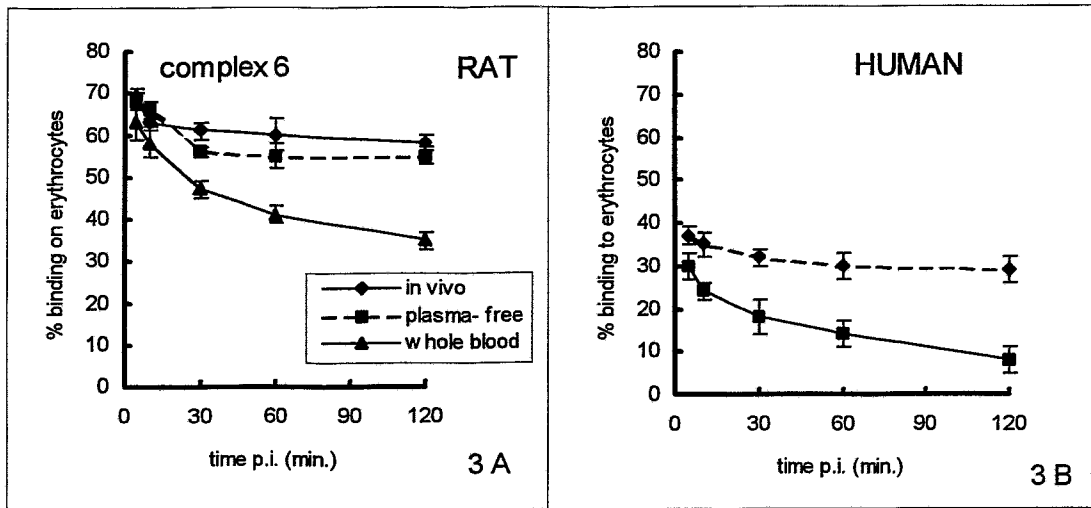


Fig. 3: Time course of erythrocyte binding of the nitrogen-containing complex 6 in rats (*in vivo* and *in vitro*) compared with the human erythrocyte binding *in vitro* (mean values \pm SD; n = 6).

Results obtained with plasma of different species confirm this assumption. The highest increase in RBC uptake was found for complex 1a and human erythrocytes in the presence of rat plasma. The rat erythrocyte uptake of complex 1a was significantly reduced in the presence of human plasma in comparison to the uptake in rat whole blood (Fig. 4).

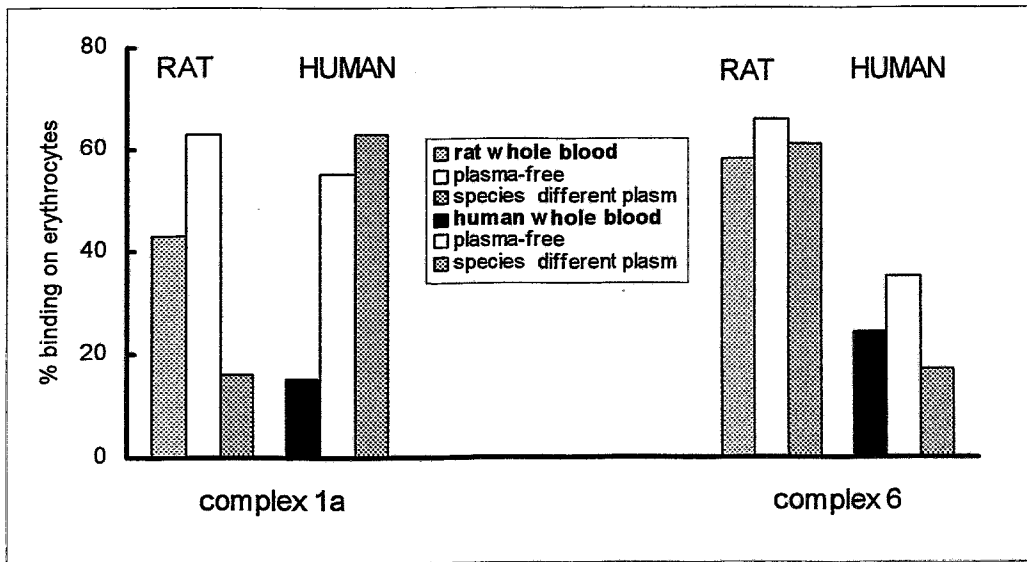


Fig. 4: *In vitro* binding to erythrocytes 10 minutes after incubation of nitrogen-free complexes 1a and nitrogen-containing complexes 6 in whole blood, in plasma-free medium and in heterologous plasma (mean values; n = 3).

Summary

The results of the binding experiments indicate that:

- the level of radioactivity associated with erythrocytes within the first few minutes of *in vivo* incubation of rats (which means the time before the influence of the blood clearance becomes significant) is comparable to that obtained by *in vitro* incubation with rat whole blood;
- all complexes are able to cross the red cell membranes;
- they are trapped in the red cells;
- the *in vitro* binding on erythrocytes is partially reversible in the presence of plasma;
- the complexes are not freely diffusible between erythrocytes and plasma;
- the affinity of all complexes to *erythrocytes* is considerably species dependent, with significant differences between rats and humans;
- the different level of RBC uptake of complex 1a in the presence of species different plasma can be assumed to be an effect of a different affinity to the human and rat *plasma proteins*.

As a consequence of our studies, the biodistribution of the complexes under investigation obtained in the rat model does not reflect the biological behaviour of these complexes in humans. This is partly due to species different affinity to erythrocytes and plasma proteins and therefore to different amounts of the freely diffusible portion of the tracer entering the brain.

References

- Greig N.H. (1990) Drug entry into the brain and its pharmacologic manipulation, in: *Physiology and Pharmacology of the Blood-Brain Barrier* (M.W.B. Brandbury), chapter 20, pp. 287-523.
- Eckelmann W.C. (1995) Radiolabeling with technetium-99m to study high-capacity and low-capacity biochemical systems. *Eur. J. Nucl. Med.* **22**, 249-263.
- Novotnik D.P. (1992) Technetium-based brain perfusion agents, in: *Radiopharmaceuticals Chemistry and Pharmacology* (A.D. Nunn) pp. 38-95.
- Johannsen B., Pietzsch H.-J., Scheunemann M., Spies H. and Brust P. (1995) Oxotechnetium(V) and oxorhenium(V) complexes as potential imaging agents for the serotonin receptor. *J. Nucl. Med.* **36**, 27P (abstr.).
- Johannsen B., Scheunemann M., Spies H., Brust P., Wober J., Syhre R. and Pietzsch H.-J. (1995) Technetium(V) and rhenium(V) complexes for 5-HT_{2A} serotonin receptor-binding: structure-affinity considerations. *Nucl. Med. Biol.*, in press.
- Pietzsch H.-J., Scheunemann M., Fietz T., Brust P., Spies H. and Johannsen B. (1995) Serotonin receptor-binding technetium and rhenium complexes. 5. Synthesis, characterization and biochemical evaluation of technetium and rhenium complexes derived from the 4-[*p*-fluorobenzoyl]-piperidine pharmacophore of ketanserin. *This report*, p. 48-50.
- Syhre R., Berger R., Pietzsch H.-J., Scheunemann M., Spies H. and Johannsen B. (1995) Serotonin receptor-binding technetium and rhenium complexes. 6. Distribution and brain uptake in the rat of ^{99m/99}Tc oxotechnetium(V) complexes with affinity to the 5-HT₂ receptor. *This report*, pp. 51-58.

18. Serotonin Receptor-Binding Technetium and Rhenium Complexes

8. Quantitative Autoradiographic Studies (Radioluminography) Using Rat Brain Sections

M. Kretzschmar, P. Brust, H.-J. Pietzsch, M. Scheunemann, B. Noll, B. Johannsen

Introduction

The design of 5-HT_{2A} receptor-binding Re and Tc complexes resulted in series of compounds with IC₅₀ values in the nanomolar range in *in vitro* binding assays (Johannsen *et al.*, 1995a,b).

The aim of this study was to determine the relative binding affinities and distribution of the Re and Tc compounds compiled in Table 1 in different rat brain regions by quantitative autoradiography of brain sections.

Experimental

Animals, tissue preparation, and labelling of 5-HT_{2A} binding sites

The preparation of the rat brain sections and labelling of HT_{2A} binding sites were carried out as described earlier (Kretzschmar *et al.*, 1994). Briefly, the frozen sections (20 µm) were warmed up to room temperature and preincubated for 15 min in 50 ml Coplin jars containing 50 mM tris-HCl buffer (pH 7.6) to remove endogenous ligands. The total 5-HT_{2A} binding was determined by incubation of these brain sections in a solution of 50mM tris-HCl buffer (pH 7.6), 1 nM [³H]ketanserin (3.15 TBq/mmol) and 2 µM tetrabenazine to mask the vesicular amine uptake sites. The nonspecific binding was obtained by incubating adjacent sections of the same brain areas in the presence of 1 nM

Table 1: Re and Tc complexes used for investigation

Complex M = Re	Configuration	Complex M = Tc
9		1a
1		5
3		7
12		
13		
14		

[³H]ketanserin, 2 μM tetrabenazine and 1 μM mianserin. The time of incubation was 40 min at room temperature. After incubation the sections were washed for 2 x 10 min in ice-cold buffer, rinsed in distilled water, and dried by cold air. The specific [³H]ketanserin binding was obtained by subtracting the nonspecific binding from the total binding.

In vitro inhibition by oxorhenium complexes

To examine the inhibition of [³H]ketanserin binding by Re complexes (Table 1), adjacent sections of the brain areas showing specific [³H]ketanserin binding were incubated and washed under the same conditions as described above. The Re complexes to be tested were dissolved in DMSO up to 1 mM and then diluted with tris-buffer to 1 μM in the incubation medium.

In vitro and in vivo 5-HT₂ receptor binding of oxotechnetium complexes

The Tc compounds 1a, 5 and 7 (Table 1), analogues of the Re complexes 9, 1 and 3, were prepared as 0.4 - 1.0 mM ^{99/99m}Tc complexes in DMSO with a specific ⁹⁹Tc activity of 62.2 MBq/mmol.

The *in vitro* incubation was carried out as described above. The brain sections were preincubated and then incubated in 50 mM tris-HCl buffer (p_H 7.6) containing 2 μM tetrabenazine and one of the ^{99/99m}Tc compounds in the range from 4 - 40 nM (= 0.9 - 9.5 MBq ^{99m}Tc) at room temperature for 40 min. The inhibition of the total binding was determined by incubating adjacent tissue sections under the same conditions, but in the presence of 10 μM 5-HT₂ antagonist ketanserin.

The *in vivo* distribution of the oxotechnetium compound 1a in the rat brain regions was established 10 and 60 min p.i. after i.v. application of 100 μg (= 20 - 35 MBq ^{99m}Tc ; 15 kBq ⁹⁹Tc) compound diluted in propylene glycol solution. Rats weighing 180 - 240 g were used. The rats were sacrificed by CO₂ inhalation and their brains rapidly removed, frozen quickly in an isopentane/dry ice solution at -70 °C. To prepare sections, the brains were mounted on cryostat chucks and 20 μm horizontal sections were cut at -20 °C, thaw-mounted onto gelatin-coated microscope slides, collected in the cryostat and dried at room temperature for 30 min.

Data acquisition

Data acquisition was performed by autoradiography and by measuring the radioactivity of the tissue sections in an LS counter 6000 (Beckman Instruments, Fullerton) for β-emitters and in a Cobra II Auto Gamma counter (Packard Instruments Company, IL) for ^{99m}Tc.

For autoradiography the method of radioluminography was used. Tritium-containing sections and tritium standards (Amersham, Braunschweig), calibrated for intact brain grey matter, were apposed to tritium-sensitive imaging plates for one week. In the case of ^{99m}Tc and ⁹⁹Tc the sections were exposed to standard imaging plates for 4 - 18 hours (^{99m}Tc) and 10 days (⁹⁹Tc). The exposed imaging plates were scanned in the Fuji BAS 2000 device. The image data were recorded as PSL (= photostimulated luminescence). The PSL values are proportional to the radioactivity of the measuring sample. The evaluation was carried out with the TINA 2.07 c program (Raytest, Straubenhardt).

Results and Discussion

Re complexes as displacers

The reference compound mianserin displaced 35 % of the total 5-HT₂ binding of the whole brain sections under the conditions used. The Re complexes tested inhibited 10 to 26 % of the [³H]ketanserin binding as obtained by LSC measurements and radioluminography of the whole brain sections. However, the various Re complexes differ in the degree of inhibition of [³H]ketanserin binding in individual brain areas (Fig. 1). Compound 1 exerts the strongest inhibition (40 % of the total [3H]ketanserin binding) in areas with high receptor density, for example in the cortical laminae. This compound also showed high receptor affinity in rat brain cortical homogenates with an IC₅₀ value of 29 nM (Johannsen *et al.*, 1995b). The other compounds displaced [³H]ketanserin only marginally between 0 and 28 % of the total binding in areas with high receptor density. However, a higher inhibition of [³H]ketanserin binding was also found with some Re complexes compared with mianserin in the hippocampal region and the cerebellar cortex, see Fig. 2 (Kretzschmar *et al.*, 1994).

Fig. 2 shows the remaining specific [³H]ketanserin binding (measured with mianserin) which is not inhibited by the Re complexes. It is about 24 - 32 % for compounds 1, 13 and 14 and 73 % for compound 12 in the whole brain sections. The remaining specific [³H]ketanserin binding was very low (30-40%) in the cortical areas with reference to compound 1, but high (50 - 100 %) in the case of the other compounds.

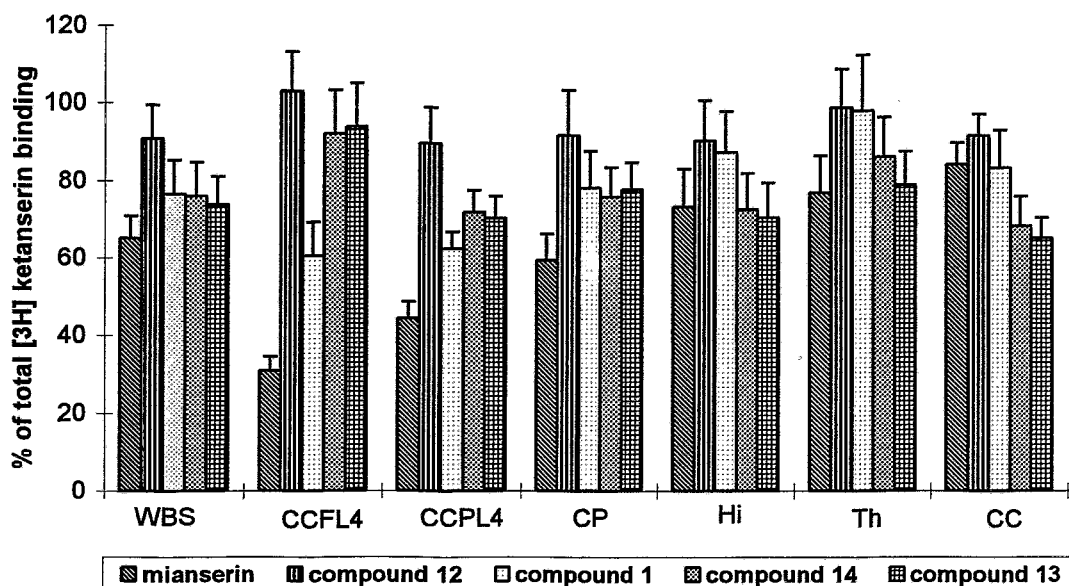


Fig.1. Inhibition of [³H]ketanserin binding (percentage of the total binding) by various Re compounds, n = 6. WBS, whole brain section; CCFL4, cerebral cortex frontal lamina 4; CCPL4, cerebral cortex parietal lamina 4; CP, caudate putamen; Hi, hippocampus; Th, thalamus; CC, cerebellar cortex.

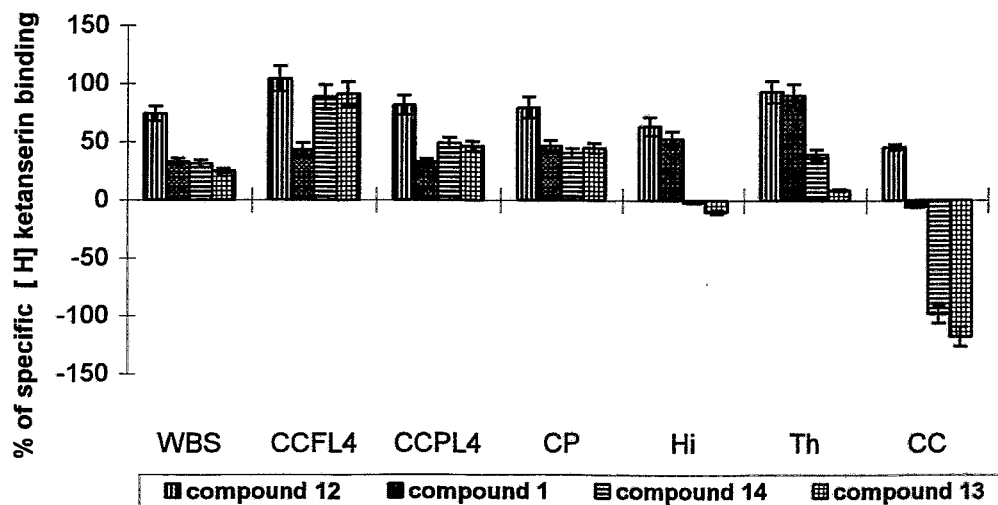


Fig. 2. Percentage of the specific [³H]ketanserin binding which remained after addition of the Re compounds to the incubation medium, n = 6, WBS, whole brain section; CCFL4, cerebral cortex frontal lamina 4; CCPL4, cerebral cortex parietal lamina 4; CP, caudate putamen; Hi, hippocampus; Th, thalamus; CC, cerebellar cortex.

The displacement of the ^{99/99m}Tc complexes by the 5-HT₂ antagonist ketanserin *in vitro* is shown in Fig. 3 .

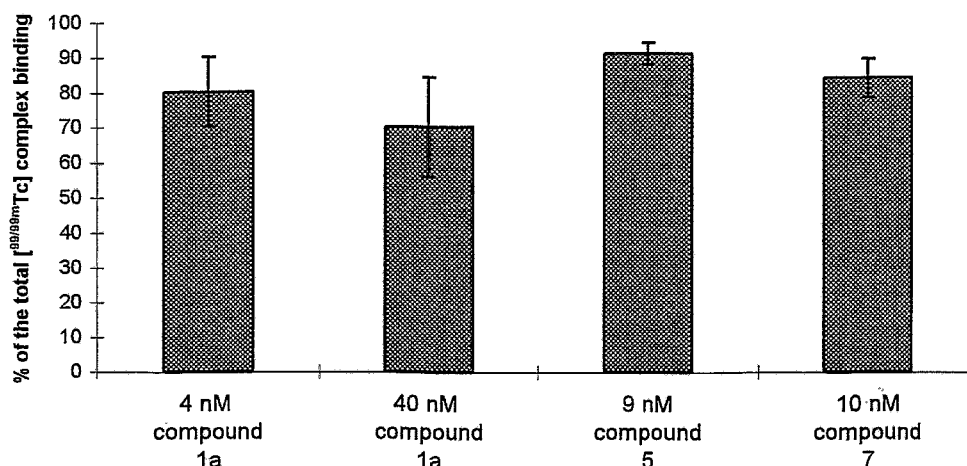


Fig. 3. Displacement of several ^{99/99m}Tc complexes (percentage of total binding) in whole brain sections obtained by adding 10 μ M ketanserin to the incubation medium.

The ^{99/99m}Tc complexes were displaced between 9 and 30 %, complex 1a shows the highest degree of displacement. However, a selective accumulation did not occur in brain regions rich in 5-HT₂ receptors (Kretzschmar *et al.*, 1994). The ^{99/99m}Tc complexes were distributed evenly in several brain regions with the exception of the cerebral white matter. The ^{99/99m}Tc complex 5 binds 24 % more in white matter than in grey matter, especially in the corpus callosum and in the external and internal capsules (Fig.4). The contrast with the other ^{99/99m}Tc compounds was not so marked, only an about 9 % higher uptake in the cerebral white matter was noticed. However, the percentage displacement by ketanserin was the same in white matter and in the whole brain.

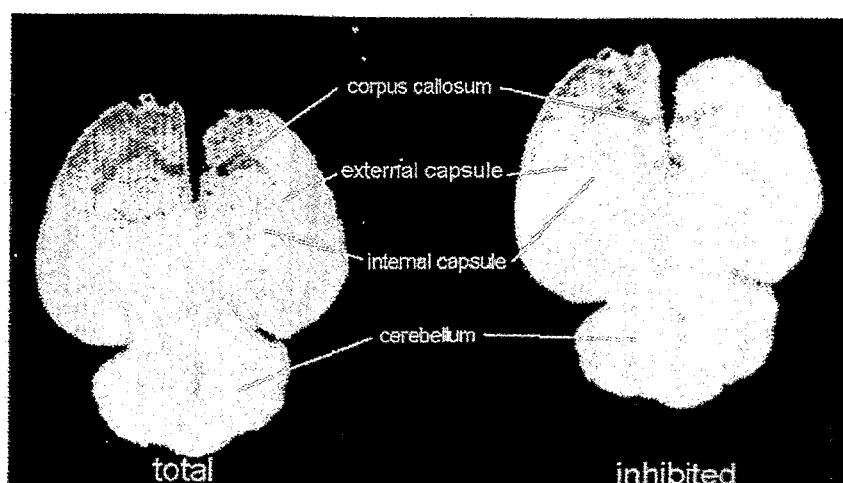


Fig.4: Distribution of ^{99/99m}Tc complex 5 in horizontal rat brain sections, left total binding, right binding after displacement with 10 μ M ketanserin (magnification 2.6fold). The radioactive concentration decreases from red to orange and yellow.

Compound 1a shows a moderate accumulation *in vivo* in the whole rat brain at a faster blood clearance 10 and 60 min p.i. (0.47 ± 0.03 % D/g brain and 0.30 ± 0.04 % D/g brain), see Syhre *et al.*, 1995. The *in vivo* distribution of this compound was thus measured autoradiographically in several regions of the brain.

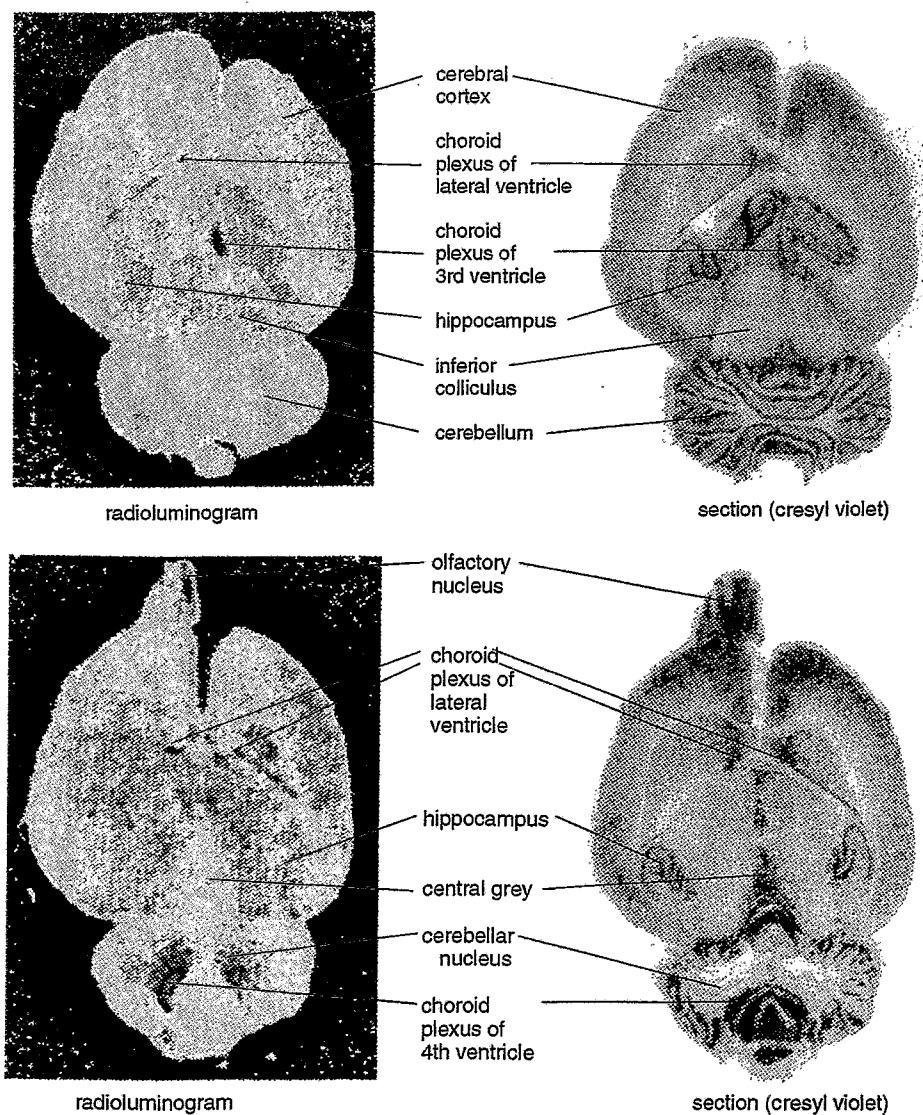


Fig.5: Autoradiograms illustrating the distribution of ^{99m}Tc complex 1a in two horizontal rat brain sections 10 min after i.v. application (left autoradiogram, right histological cresyl violet stained section, magnification 3.1fold). The radioactive concentration decreases from black to red, orange and yellow.

Fig. 5 shows a high accumulation of radioactivity in the choroid plexus. The uptake was up to 4 times higher than in the surrounding cerebral tissue, followed by the olfactory nucleus and the cerebellar nuclei with a moderate uptake of radioactivity. The retention of radioactivity in the choroid plexus remained nearly constant throughout the period of investigation (Fig. 6).

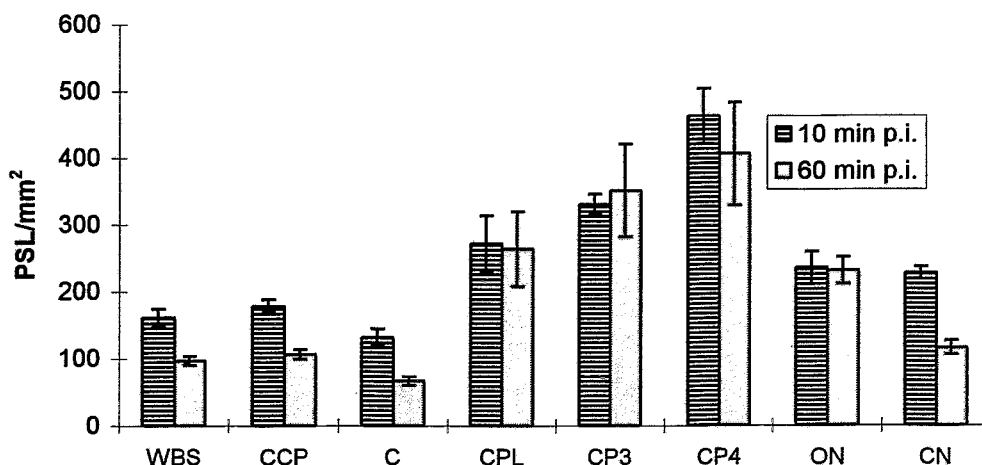


Fig. 6: Distribution of the $^{99/99m}\text{Tc}$ complex 1a in several brain regions 10 and 60 min after i.v. application. WBS, whole brain section; CCP, cerebral cortex parietal; C, cerebellum; CPL, choroid plexus lateral ventricle; CP3, choroid plexus 3rd ventricle; CP4, choroid plexus 4th ventricle; ON, olfactory nucleus; CN, cerebellar nucleus.

Further studies with appropriate displacer compounds have to specify these binding sites.

In summary, the Re compounds tested inhibit the specific binding of [^3H]ketanserin between 0 and 40 % in areas rich in 5-HT₂ receptors. The total *in vitro* binding of Tc analogues of favourable Re compounds was inhibited by ketanserin by about 9 - 30 %. *In vivo* the $^{99/99m}\text{Tc}$ compound 1a showed a high uptake in those structures of the brain which are not specific for 5-HT_{2A} binding sites but possibly for other serotonergic receptor subtypes.

References

- Johannsen B., Pietzsch H.-J., Scheunemann M., Spies H. and Brust P. (1995a) Oxotechnetium(V) and oxorhenium(V) complexes as potential imaging agents for the serotonin receptor. *J. Nucl. Med.* **36**, 27P (abstr.).
- Johannsen B., Scheunemann M., Spies H., Brust P., Wober J., Syhre R. and Pietzsch H.-J. (1995b) Technetium(V) and rhenium(V) complexes for 5-HT_{2A} serotonin receptor-binding: structure-affinity considerations. *Nucl. Med. Biol.*, in press.
- Kretzschmar M. and Brust P. (1994) Quantitative autoradiographic studies of the distribution of [^3H]ketanserin in horizontal rat brain sections after influence of several displacing compounds including Re complexes. *Annual Report 1994*, Institute of Bioinorganic and Radiopharmaceutical Chemistry, FZR-73, pp. 121-127.
- Syhre R., Berger R., Pietzsch H.-J., Scheunemann M., Spies H. and Johannsen B. (1995) Serotonin receptor-binding technetium and rhenium complexes 6. Distribution and brain uptake in the rat of [$^{99m/99}\text{Tc}$]oxotechnetium(V) complexes with affinity to the 5-HT₂ receptor. *This report*, pp. 51-58.

19. Determination of Partition Coefficients for Coordination Compounds by Using HPLC

R. Berger, T. Fietz, M. Glaser, H. Spies, B. Johannsen

Introduction

The lipophilicity of drugs plays a central role in their biological action. It is mainly this property which determines the fate of a drug in the body, governing the absorption, distribution, storage and elimination processes as well as its bioavailability to the receptor microenvironment in special circumstances after passing membranes.

Hence, lipophilic properties are also of crucial importance for the design of radiotracers intended to be used as brain agents, penetrating through the blood-brain barrier.

A usual quantitative measure of the lipophilicity of a solute in unionized, monomer form is its partition ratio between a water immiscible solvent (e.g. octanol) and an aqueous phase, expressed according to the Nernst law by the true partition coefficient (P or $\log P$) (Berger *et al.*, 1995). For ionizable molecules the partition coefficient experimentally measured at a certain pH is an apparent value (P_{app} , $\log P_{app}$ or $\log D$). The octanol/water partition coefficient is a generally accepted physico-chemical parameter for characterization of lipophilicity. As demonstrated by Hansch *et al.* (1987), $\log P$ is the single most important factor for determining the solubility properties of a drug.

However, the measurement of P by the conventional "shake flask" method is tedious, troublesome, often complicated by instability in aqueous media, impurities and the tendency of the compound to dissociate. Furthermore, it is difficult to determine P of very hydrophobic compounds.

In the past attempts have been undertaken to introduce chromatographic techniques, particularly reversed-phase high performance liquid chromatography (RP-HPLC), for the determination of lipophilicity of various interesting substances. As is known from the literature (Braumann and Grimme, 1981; Valkó, 1984; El Tayar *et al.*, 1985; Minick *et al.*, 1987; Kaune *et al.*, 1995), this method represents a very convenient technique with respect to accuracy, sensitivity and application range. The retention of any solute can be used as a measure for the partition behaviour between the non-polar bonded stationary phase and the more polar eluent. For example correlations between $\log P$ and the logarithm of the capacity factor, k' , mainly obtained with octadecyl silica or poly(styrene-divinylbenzene) copolymer as the bonded stationary phase (e.g. in RP 18 or PRP-1 columns) have been published (D'Amboise and Hanai, 1982; Hammers *et al.*, 1982; Lambert *et al.*, 1990).

The objectives of this study were to gain insights into structure-lipophilicity relationships of Re coordination compounds. In this article lipophilicity parameters of several recently synthesized rhenium complexes from two series with the different structures **1** and **2** (Fig. 1) are presented (Fietz, 1995; Glaser, 1995). It is supposed that these RP-HPLC partition coefficients will facilitate a better assessment and prediction of the lipophilicity of further similar compounds (Braumann, 1986; Kaliszan, 1993).

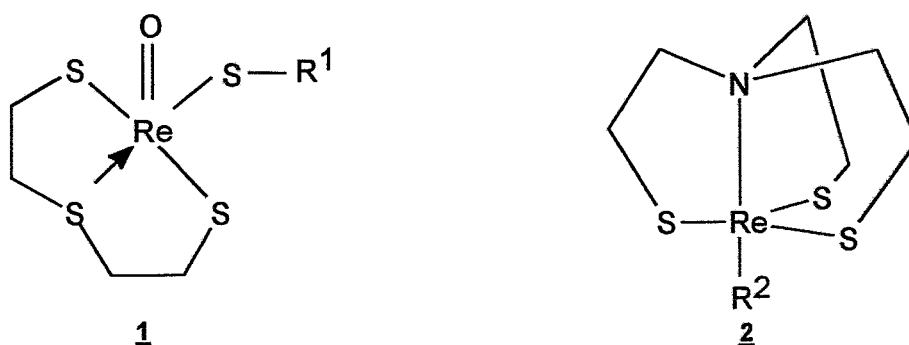


Fig. 1: General structure of rhenium complexes **1** and **2**

Experimental

Before starting an HPLC run a small quantity of the compounds selected was dissolved in a mixture of methanol and acetonitrile or dimethyl sulphoxide (about 2 mg/ml). All reference chemicals were commercial products, and they were used without further purification. Sample volumes of 5 - 10 μ l were injected into the Rheodyne valve 7125 connected with the Perkin Elmer Model 1020. A Perkin Elmer UV/VIS spectrophotometric detector LC 290 with an operating wavelength mostly at 254 nm

and the recorder Kodak Diconix 150 Plus were used throughout the study. All experiments were carried out with the columns RP 18 (120 x 4 mm; Hypersil ODS, 5 μ m; Knauer) or PRP-1 (250 x 4.1 mm; 10 μ m; Hamilton) under isocratic elution conditions at room temperature and with a flow rate of 1.5 ml/min. Reagent-grade chemicals were used for the buffer preparation. Water was prepared with an ion exchange unit. Methanol and acetonitrile from Roth and Merck were purchased as eluents. For the RP 18 and PRP-1 columns mobile phases consisting of methanol/water or 0.03 M $\text{KH}_2\text{PO}_4/\text{Na}_2\text{HPO}_4$ buffer (usually 3:2, v/v); pH 7.4 and acetonitrile/0.01 M $\text{KH}_2\text{PO}_4/\text{Na}_2\text{HPO}_4$ buffer (between 3:2 and 3:1, v/v); pH 7.4, were applied.

The capacity factors (k') were evaluated from the chromatograms by $k' = (t_R - t_0)/t_0$, where t_R and t_0 are the retention times of a retained and an unretained solute. Methanol was applied as the nonretained reference compound.

The capacity factors of the complexes of interest were changed to the corresponding log P values with the aid of the equation $\log P = a \log k' + b$. For a suitable computer trend program the substances aniline (0.9), benzene (2.13), bromobenzene (2.99) and in some cases diphenyl (4.09) served as the log P reference. Because these log P values depend on various unknown factors caused and influenced by the RP-HPLC system, the designation P_{HPLC} for an apparent constant was employed throughout this work.

Results and Discussion

By means of two different reversed-phase columns the P_{HPLC} values of Re complexes containing the structure form **1** are compared with some P_{OW} values of the shake flask method (Berger *et al.*, 1995) in Table 1.

Table 1: Partition coefficients (P_{HPLC} , P_{OW}) of various rhenium complexes **1** obtained by using different determination methods [PRP-1 and RP 18 with acetonitrile and methanol, solvent:buffer (pH 7.4) = 3:2 (v/v)]

R^1	RP 18		PRP-1		Shake flask	
	P_{HPLC}	$\log P_{\text{HPLC}}$	P_{HPLC}	$\log P_{\text{HPLC}}$	P_{OW}	$\log P_{\text{OW}}$
$-\text{CH}_2-\text{CH}_2-\text{N}(\text{CH}_3)_2$	15	1.18	0,7	-0.15	6 \pm 3	0.78 \pm 0.5
$-\text{CH}_2-\text{CH}_2-\text{N}(\text{C}_2\text{H}_5)_2$	18	1.26	1,4	0.15	-	-
$-\text{CH}_2-\text{COOH}$	4	0.60	-	-	-	-
$-\text{CH}_2-\text{CO}-\text{OCH}_3$	16	1.20	32	1.51	21 \pm 5	1.32 \pm 0.7
$-\text{CH}_2-\text{CO}-\text{OC}_2\text{H}_5$	39	1.59	74	1.87	25 \pm 8	1.40 \pm 0.9
$-\text{CH}_2-\text{CO}-\text{O}-n\text{-C}_3\text{H}_7$	132	2.12	173	2.24	-	-
$-\text{CH}_2-\text{CO}-\text{O}-n\text{-C}_4\text{H}_9$	455	2.66	398	2.60	-	-
$-\text{CH}_3$	25	1.40	146	2.16	28 \pm 4	1.45 \pm 0.6
$-\text{C}_2\text{H}_5$	62	1.79	244	2.39	52 \pm 7	1.72 \pm 0.8
$-n\text{-C}_3\text{H}_7$	222	2.35	598	2.78	247 \pm 90	2.39 \pm 1.9
$-n\text{-C}_4\text{H}_9$	763	2.88	1452	3.16	312 \pm 200	2.49 \pm 2.3
$-n\text{-C}_8\text{H}_{17}$	4754	3.68	4535	3.66	-	-
$-\text{C}_6\text{H}_5$	224	2.35	993	3.00	-	-
$-\text{CH}_2-\text{C}_6\text{H}_5$	610	2.79	1898	3.28	-	-
$-\text{CH}_2-\text{CH}_2-\text{C}_6\text{H}_5$	1784	3.25	4260	3.63	-	-

Preliminary P_{HPLC} values of Re complexes with the structure **2** were obtained by using an RP 18 column and are summarized in Table 2.

For verification, the determined $\log P_{\text{HPLC}}$ values of some standard compounds were compared with data from the literature (Table 3).

Despite the fact that all the compounds listed in Tables 1 and 2 are metal complexes, they are lipophilic. The lipophilic character arises from the fact that even in the case of complexes with the general structure **1** the very polar metal-oxo bond is wrapped in organic ligand molecules, resulting in stable neutral compounds.

Relative partition coefficients were obtained by using the two HPLC columns as can be seen in Table 1. They are not expected to closely correlate with the octanol/water partition coefficients. As the carbon chain is lengthened, the partition coefficients grow. This also holds true for the series of simple alkanes and for appropriate esters. Introduction of an aryl part into the molecule is also reflected by an increase in P_{HPLC} values.

Table 2: Partition coefficients (P_{HPLC}) of various rhenium complexes **2**
[PRP-1, acetonitrile:buffer(pH 7.4) = 3:1 (v/v)]

R^2	P_{HPLC}	$\log P_{\text{HPLC}}$
-CN-CH ₂ -COOH	0.02	-1.70
-CN-CH ₂ -CO-OCH ₃	74	1.87
-CN-CH ₂ -CO-OC ₂ H ₅	148	2.17
-CN-(CH ₂) ₁₀ -COOH	105; 12 *)	2.02; 1.08 *)
-CN-(CH ₂) ₁₀ -CO-OC ₂ H ₅	177000	5.25
-CN-C ₆ H ₅	4340	3.64
-CN-(CH ₂) ₂ -N[CH ₃](CH ₂) ₂ -C ₆ H ₅	2830; 8400 *)	3.45; 3.92 *)
-CN-(CH ₂) ₃ -CO-[<i>p</i> -F-C ₆ H ₄]	3340	3.52
-CN-(CH ₂) ₃ -C[O-(CH ₂) ₂ -O]-[<i>p</i> -F-C ₆ H ₄]	5700	3.76
-CN-(CH ₂) ₂ -N[(CH ₂) ₂ -O-(CH ₂) ₂]	115	2.06
-P[(CH ₃) ₂]-C ₆ H ₅	12000	4.08

*) acetonitrile:water = 3:1 (v/v)

Table 3: Comparison of the partition coefficients ($\log P_{\text{HPLC}}$) of some organic bases and acids determined in their unionized forms by using the respective buffers [PRP-1, acetonitrile:buffer = 3:1 (v/v)] with $\log P$ values from the literature

Compound	$\log P_{\text{HPLC}}$ (determined)	$\log P$ (Leo <i>et al.</i> , 1971)
B Pyridine	0.23	0.65 ¹ , 0.42 ² , 0.16 ³ , 0.31 ⁴
A Benzylamine	0.33	1.09 ¹ , 0.61 ² , 0.30 ³ , 0.32 ⁵
S Aniline	0.88	0.94 ¹ , 1.00 ² , 0.89 ³ , 0.85 ⁵
E <i>p</i> -Toluidine	1.00	1.40 ¹ , 1.43 ² , 1.11 ⁶
<i>N</i> -Ethylaniline	2.20	2.26 ¹
<i>N,N</i> -Dimethylaniline	2.61	2.31 ¹ , 2.47 ⁷
<i>N,N</i> -Diethylaniline	3.26	3.58 ¹ *)
A Benzoic acid	0.11	1.87 ¹ , 0.12 ² , 0.36 ³ , 0.44 ⁴
C <i>o</i> -Chlorobenzoic acid	0.30	1.98 ¹ , 0.27 ³ , 0.01 ⁴
I <i>trans</i> -Cinnamic acid	0.65	2.13 ¹ , 1.60 ³ , 0.15 ⁴
D Diphenylacetic acid	0.85	2.06 ¹
Thiophenol	2.59	2.52 ¹

*) *N*-butylaniline; ¹octanol; ²benzene; ³toluene; ⁴xylene; ⁵diethyl ether; ⁶carbon tetrachloride; ⁷cyclohexane

For ligands with carbon chains containing more than eight C-atoms an elution by using the former solvent to water ratio of three to two was too time-consuming or simply futile because of the strong interaction with the stationary phase. The solvent part was therefore increased in the eluent. As a consequence and in contrast to their former behaviour, the P_{HPLC} values were either distinctly higher or a little smaller, depending on whether an RP 18 or PRP-1 column was used.

In the case of the RP 18 column, monodentate ligands such as -C₁₂H₂₅ and -C₁₆H₃₃ result in $\log P_{\text{HPLC}}$ values of 7.4 and 12.4. For these apparent $\log P$ values, which are presumably too high, a valid explanation cannot be given. Depending on the lengthening of the carbon chain and the reduction of the amount of water, both growing (non-specific) interactions and surface effects between solutes and the stationary as well as mobile phases should be taken into consideration (Rudzinski *et al.*, 1982).

The same order of lipophilicity but two to three times higher absolute values were obtained with the PRP-1 instead of the RP 18 column. Because of the aromatic support of the PRP-1 column, the presence of solutes with aryl residues may give rise to π - π interactions. These rather specific interactions are expected to influence the retention behaviour (Rudzinski *et al.*, 1982; Thévenon-Emeric *et al.*, 1991).

The determination of the true octanol/water partition coefficients of the above compounds may be affected by some sources of error (Minick *et al.*, 1987). Only the P_{OW} values of ligands having relative low lipophilic properties agree more or less with the values obtained by using the HPLC. For rather lipophilic ligands, the values resulting from the shake flask method exhibit particularly a growing deviation (Berger *et al.*, 1995).

In principle the P_{HPLC} values of the Re complexes with isocyanide ligands listed in Table 2 show a similar dependence on the underlying structures as shown in Table 1. Only the log P values of the long-chained ethyl ester and the substituted dimethyl-phenylphosphane seem to be relatively high.

In Table 3 the log P_{HPLC} values of the unionized forms of some organic bases and acids show an approximate correspondence with some published solvent/water partition coefficients. A relatively good agreement was reached between some log P_{HPLC} values and the values obtained with solvents such as benzene, toluene and xylene. Thus, similar partition values could find an explanation in the analogous aromatic properties of the polymeric stationary phase of the PRP-1 column.

References

- Berger R., Fietz T., Glaser M., Noll B. and Spies H. (1994) Octanol/water partition coefficients of some rhenium complexes. *Annual Report 1994*, Institute of Bioinorganic and Radiopharmaceutical Chemistry, FZR-73, pp. 52-55.
- Braumann T. and Grimme I.H. (1981) Determination of hydrophobic parameters for pyridazinone herbicides by liquid-liquid partition and reversed-phase high-performance liquid chromatography. *J. Chromatogr.* **206**, 7-15.
- Braumann T. (1986) Determination of hydrophobic parameters by reversed-phase liquid chromatography: Theory, experimental techniques, and application in studies on quantitative structure-activity relationships. *J. Chromatogr.* **373**, 191-225.
- D'Amboise M. and Hanai T. (1982) Hydrophobicity and retention in reversed phase liquid chromatography. *J. Liq. Chromatogr.* **5**, 229-244.
- El Tayar N., Van de Waterbeemd H. and Testa B. (1985) The prediction of substituent interactions in the lipophilicity of disubstituted benzenes using RP-HPLC. *Quant. Struct.-Act. Relat.* **4**, 69-77.
- Fietz T. (1996) Rhenium-Komplexe mit 3+1-Koordination, *Thesis*, TU Dresden.
- Glaser M. (1996) Tripodal-tetradentat/monodentat koordinierte Rheniumkomplexe mit Tris(2-thiolatoethyl)amin, *Thesis*, TU Dresden.
- Hammers W.E., Meurs G.J. and De Ligny C.L. (1982) Correlations between liquid chromatographic capacity ratio data on Lichrosorb RP-18 and partition coefficients in the octanol-water system. *J. Chromatogr.* **247**, 1-13.
- Hansch C., Björkroth J.P. and Leo A. (1987) Hydrophobicity and central nervous system agents: on the principle of minimal hydrophobicity in drug design. *J. Pharm. Sci.* **76**, 663-686.
- Kaliszan R. (1993) Quantitative structure-retention relationships applied to reversed-phase high-performance liquid chromatography. *J. Chromatogr. A* **656**, 417-435.
- Kaune A., Knorrenschild M., Kettrup A. (1995) Predicting 1-octanol-water partition coefficient by high-performance liquid chromatography gradient elution. *Fresenius J. Anal. Chem.* **352**, 303-312.
- Lambert W.J., Wright L.A. and Stevens J.K. (1990) Development of a preformulation lipophilicity screen utilizing a C-18-derivatized polystyrene-divinylbenzene high-performance liquid chromatographic (HPLC) column. *Pharm. Res.* **7**, 577-586.
- Leo A.J., Hansch C. and Elkins D. (1971) Partition coefficients and their uses. *Chem. Rev.* **71**, 525-616.
- Minick D.J., Sabatka J.J. and Brent D.A. (1987) Quantitative structure-activity relationships using hydrophobicity constants measured by high-pressure liquid chromatography: a comparison with octanol-water partition coefficients. *J. Liq. Chromatogr.* **10**, 2565-2589.
- Rudzinski W.E., Bennett D. and Garica V. (1982) Retention of ionized solutes in reversed-phase high performance liquid chromatography. *J. Liq. Chromatogr.* **5**, 1295-1312.
- Thévenon-Emeric G., Tchaplal A. and Martin M. (1991) Role of π - π interactions in reversed-phase liquid chromatography. *J. Chromatogr.* **550**, 267-283.
- Valkó, K. (1984) General approach for the estimation of octanol/water partition coefficient reversed-phase high-performance liquid chromatography. *J. Liq. Chromatogr.* **7**, 1405-1424.

20. pK_a Value Determinations by HPLC of Some Tc and Re Complexes Containing an Ionizable Group

R. Berger, M. Scheunemann, H.-J. Pietzsch, B. Noll, St. Noll, A. Hoeping, M. Glaser, T. Fietz, H. Spies, B. Johannsen

Introduction

Knowledge of the aqueous ionization constant, pK_a , of a pharmacologically effective substance is very advantageous. The ionization constant is as important a physicochemical parameter as the partition coefficient $\log P$. Several experimental methods such as potentiometry, spectrophotometry, conductometry and proton magnetic resonance spectrometry are available for the determination of the ionization constant of a compound.

The potentiometric titration method is very commonly used, but good water solubility and an adequate quantity of the compound is needed. The spectrophotometric method requires chromophores which absorb ultraviolet or visible light. Also, the ionic and molecular species need different spectra. The conductometric method is quite tedious and more time-consuming. The proton magnetic resonance method may be useful for substances whose ultraviolet spectra do not change upon ionization. All of these four methods require a very pure compound (Palalikit and Block, 1980; Avdeef *et al.*, 1993).

An alternative approach is to use chromatography, especially high performance liquid chromatography (HPLC), including a reversed phase (RP).

Advantages of this method are that (1) only small quantities of compounds are required, (2) poor water solubility need not be a serious drawback and (3) the sample has not to be pure.

Over the past few years, reversed-phase chromatography on silica gel with covalently bonded alkyl chains has proved to be a valuable alternative for separating polar ionogenic compounds. Nevertheless, columns prepared in such a manner suffer from two shortcomings. First, they cannot be operated above pH 8, when deteriorations of the silica support become significant, and second, these columns have active silanol sites where no bonding of the hydrocarbon to the silica has occurred (Van de Venne and Hendrikx, 1978; Vigh *et al.*, 1982).

These disadvantages can be removed by using PRP-1 columns, in which the stationary phase consists of a poly(styrene-divinylbenzene) material. The polymeric reversed phase support possesses a relatively high pH stability within the range from 1 to 13 without the possibility of matrix degradation or loss of efficiency. Besides, the column life time is longer for PRP-1 than for silica-based columns (Lee, 1982; Rudzinski *et al.*, 1982; Terada, 1986; Miyake *et al.*, 1987; Stylli and Theobald, 1987; Pagliara *et al.*, 1995).

Use of a PRP-1 column requires the application of a suitable solvent interacting with the stationary phase in order to remove the interesting compound which is bound there more or less strongly. Acetonitrile seems to have proved its worth as an effective solvent. Due to the presence of a π -electron system forming π - π interactions with the aromatic rings of the poly(styrene-divinylbenzene) support, the addition of this solvent also favours interaction between the solute and stationary phase (Thevenon-Emeric, 1991).

Concerning an ionizable solute, similar conditions exist both on a reversed phase column, which is in an equilibrium with the mobile phase and between two non-miscible solvents, e.g. octanol/water. In such systems the equations

$$\log P = \log D + \log(1 + 10^{pH - pK_a}) \quad (1)$$

$$\log P = \log D + \log(1 + 10^{pK_a - pH}) \quad (2)$$

reflect the relation between the partition coefficients P and D for acids and bases (Takács-Novák, 1995).

Our studies refer to relations between pK_a values (pK_a values determined by HPLC are notated as pK_{HPLC} in this work) as well as partition coefficients (P , $\log P$ and D , $\log D$) on the one hand and to the nature of substituents in series of systematically varied ionizable coordination compounds on the other. Neutral technetium and rhenium chelates bearing a tertiary amine group of a weak basic character are of particular interest. However, complexes of a similar general structure which have a functional group with acid properties in the side chain are also the object of these experiments.

Experimental

Experiments were performed and evaluated under almost the same conditions as described elsewhere in this annual report (Berger *et al.*, 1995) for the determination of partition coefficients, i.e. with identical materials, reagent-grade chemicals, and methods. The determination of pK_{HPLC} involves the use of mobile phases of different pH values.

Only a PRP-1 column was used, and the elutions were carried out with a mixture of acetonitrile and buffers of definite pH values (volume ratio 3:1, if not otherwise reported). For a test series, buffers

(frequently about ten or more) to cover the pH range of about 2 to 10 were employed. The buffer components KH_2PO_4 and Na_2HPO_4 were completed by citric acid and a certain expansion of the pH range was achieved by adding either 0.1 M HCl or 0.1 M NaOH. Before each application the pH values of the eluents were measured after preparing the appropriate mixture of buffer and acetonitrile by using a glass electrode. At such a well defined pH value several samples with various chelates and the solution of reference substances were sequentially injected. Before injecting the first sample of a new eluent series with changed pH value, the time for equilibration of the column was at least 10 min at a flow rate of 2.5 ml/min.

Results and Discussion

Typical sigmoidal curves of both an acid Re and a basic Tc mixed-ligand complex are exhibited in Fig. 1. They reflect the pH-dependent distribution coefficient ratio of the ionized to unionized form in the aqueous mobile phase. At sufficiently high or low pH values, the pH-dependent distribution coefficients D approach the partition coefficients P .

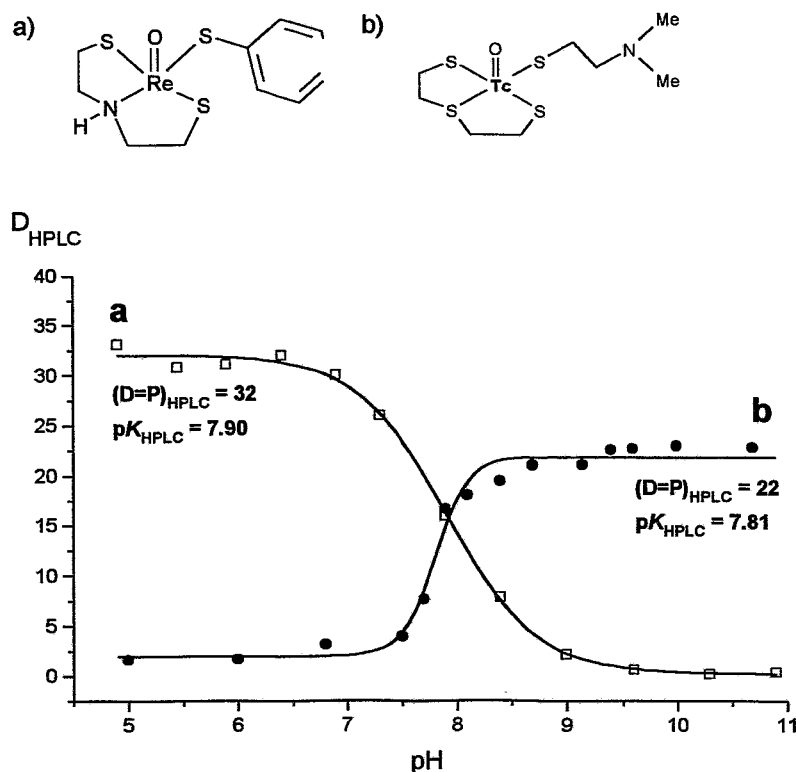
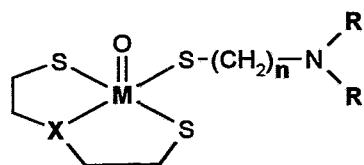


Fig. 1: Typical sigmoidal distribution curves of an acid (a) and basic (b) coordination compound determined by HPLC

Table 1 summarizes the $\text{p}K_{\text{HPLC}}$ and P_{HPLC} values of several neutral Tc and two Re complexes which differ with regard to the length of the N-alkyl side chains in their amine group and the type of the tridentate ligand. As can be seen, the parameters determined are influenced above all by two variables in the structure of the Tc chelates. First, lengthening of the N-alkyl side chains increases both the $\text{p}K_{\text{HPLC}}$ and the P_{HPLC} values. Interestingly, a lengthening of the carbon chain of the monodentate ligands between the sulphur and nitrogen atom does not affect the parameters. Second, replacement of the central heteroatom in the tridentate ligand in the rank order $\text{N-Me} < \text{S} < \text{O}$ increases P_{HPLC} . For the $\text{p}K_{\text{HPLC}}$ values a similar dependence is not evident. Only a growth of $\text{p}K_{\text{HPLC}}$ can be noted if the central oxygen is exchanged by either sulphur or nitrogen.

Table 1: pK_{HPLC} and P_{HPLC} values of some mixed-ligand complexes of the general structure



with varying M (Tc, Re), X (N-Me, S, O),
n (2, 8), and R (Me, Et, Bu)

Complex structure				pK_{HPLC}	P_{HPLC}	$\log P_{\text{HPLC}}$
M	X	n	R			
Tc	N-Me	2	Me	7.75	11	1.04
		2	Et	8.31	47	1.67
		8	Et	8.37	48	1.68
		2	Bu	8.54	3210	3.51
Tc	S	2	Me	7.81	22	1.34
		2	Et	8.43	97	1.99
		8	Et	8.37	106	2.03
		2	Bu	8.52	7540	3.88
Re	S	2	Me	8.57	13	1.11
		2	Et	9.00	62	1.79
Tc	O	2	Me	7.64	21	1.32
		2	Et	8.19	120	2.08
		8	Et	8.25	118	2.07
		2	Bu	8.40	10400	4.02

For the two Re complexes similar relations between the structure and the parameters are deducible. Table 2 shows further pK_{HPLC} and P_{HPLC} values of some basic Tc and Re coordination compounds. Tc and Re complexes prepared from the same ligands have identical pK_{HPLC} values.

From this table it is possible to identify modifications through which pK_{HPLC} can be diminished by about one to two units. The P_{HPLC} values of the unionized chelates show a similar relation to the corresponding structures as above described, i.e. the longer a carbon chain and/or the more benzene rings are in a chelate molecule, the higher are the appropriate $\log P$ values.

In addition, an almost identical ratio of the P_{HPLC} values of approximately 1.5 can be taken from Tables 1 and 2 for all pairs of Tc and Re chelates with the same mixed-ligand structure.

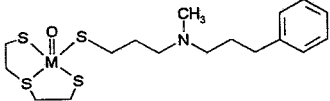
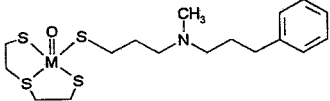
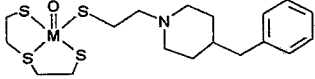
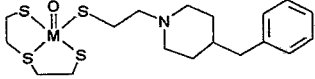
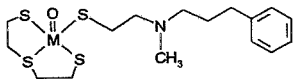
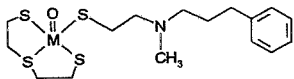
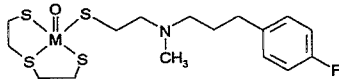
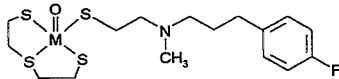
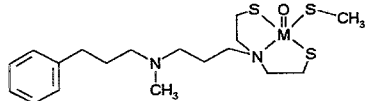
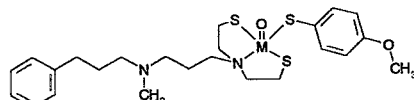
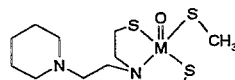
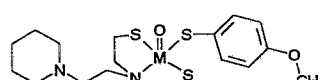
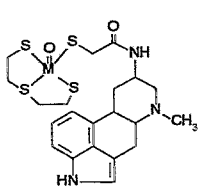
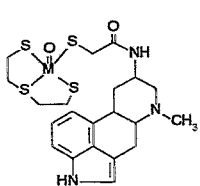
Table 3 lists the pK_{HPLC} and P_{HPLC} values of some compounds having structures like the partial structures of the Tc/Re complexes in Tables 1 and 2.

As can be seen, the dialkylated amines linked with a benzyl residue are more lipophilic than the mixed-ligand Tc complexes (cp. Table 1). As expected, the P value of the amine containing two ethyl groups is higher than that of the dimethylated amine. The pK_{HPLC} values of the pure ergoline and its derivatives are of the same order as the coordination compounds.

In Table 4 the pK_{HPLC} and P_{HPLC} values of some acid mixed-ligand Re complexes are summarized. Both carboxyl groups and a dissociable proton of a nitrogen atom cause the acid behaviour of the chelate compound.

The partition coefficients of the two complexes with isocyanide ligands differ significantly (by about two orders of magnitude) due to lengthening of the monodentate ligand by a decyl carbon chain. Besides, the pK_{HPLC} values of these related coordination compounds display a decrease in acidity by a sufficiently long carbon chain to the neighbouring carboxyl group in the monodentate ligand. The complex containing a $\text{Re}=\text{O}^{3+}$ core has a remarkably low P_{HPLC} value. (In comparison, a $\log P_{\text{HPLC}}$ of 3.00 was measured for the similar complex with three sulphur atoms in the tridentate ligand (Berger *et al.*, 1995).) This may have been caused by an additional protonation of the nitrogen atom, which is not strongly linked with the metal core.

Table 2: pK_{HPLC} and P_{HPLC} values of some basic N-containing Re and Tc chelates determined by using HPLC

Complex structure	Metal [M]	pK_{HPLC}	P_{HPLC}	$\log P_{\text{HPLC}}$
	Re	8.6	3000	3.48
	Tc	8.6	4450	3.65
	Re	8.3	4150	3.62
	Tc	8.3	6600	3.82
	Re	8.2	1460	3.16
	Tc	8.2	2200	3.34
	Re	8.1	1300	3.11
	Tc	8.1	1950	3.29
	Re	7.6	3500	3.54
	Re	7.6	11900	4.08
	Re	6.75	850	2.93
	Re	6.7	3350	3.53
	Re	6.0	33	1.52
	Tc	6.2	45	1.65

All pK_{HPLC} values presented above seem to be relative. As shown in Table 5 with basic compounds of known pK_a values, all the pK_{HPLC} determined by HPLC differ from the corresponding values in the literature (Lide, 1992-1993) by a more or less constant amount of 1.3. For organic acids this amount was found to be about -1.7. The reason for this is not yet clear.

Table 3: pK_{HPLC} - and P_{HPLC} values of dialkylated amines, ergoline, and some of its derivatives as determined by HPLC

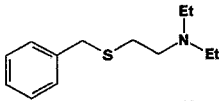
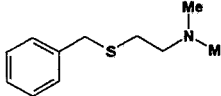
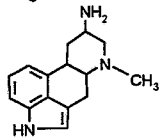
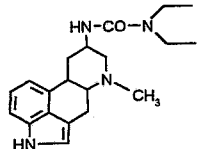
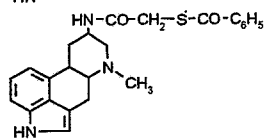
Monodentate ligand structure-like compound	pK_{HPLC}	P_{HPLC}	$\log P_{\text{HPLC}}$
	8.43	460	2.66
	8.15	65	1.81
	6.4	2.5	0.40
	6.2	5	0.70
	6.0	80	1.90

Table 4: pK_{HPLC} and P_{HPLC} values of some acid mixed-ligand Re complexes determined by HPLC

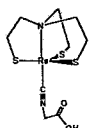
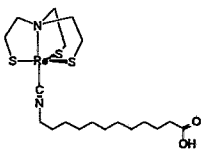
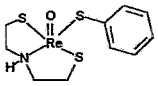
Complex structure	pK_{HPLC}	P_{HPLC}	$\log P_{\text{HPLC}}$
	4.6	3.8	0.58
	6.7	950	2.98
	7.9	32	1.51

Table 5: Comparison of pK_{HPLC} values of some organic bases and acids with the corresponding pK_a values taken from the literature (Lide, 1992-1993)

	Compound	pK_{HPLC}	pK_a^x	$\Delta (pK_a - pK_{\text{HPLC}})$	Mean values
B	Pyridine	3.83	5.25	1.42	
A	Benzylamine	7.98	9.33	1.35	
S	Aniline	3.43	4.63	1.20	
E	<i>p</i> -Toluidine	3.78	5.08	1.30	
	<i>N</i> -Ethylaniline	3.81	5.12	1.31	
	<i>N,N</i> -Dimethylaniline	3.81	5.15	1.34	
	<i>N,N</i> -Diethylaniline	5.26	6.61	1.35	1.32
A	Benzoic acid	5.85	4.19	- 1.66	
C	<i>o</i> -Chlorobenzoic acid	4.56	2.92	- 1.64	
I	<i>trans</i> -Cinnamic acid	6.24	4.44	- 1.80	
D	Diphenylacetic acid	5.51	3.94	- 1.57	
	Thiophenol	8.44	6.52	- 1.92	- 1.72

The influence of the volume ratio of acetonitrile to buffer in the eluent on the determination of pK_{HPLC} is shown in Fig. 2. There the pK_{HPLC} values and the corresponding true values of three compounds studied are plotted versus the percental content of acetonitrile in the eluent.

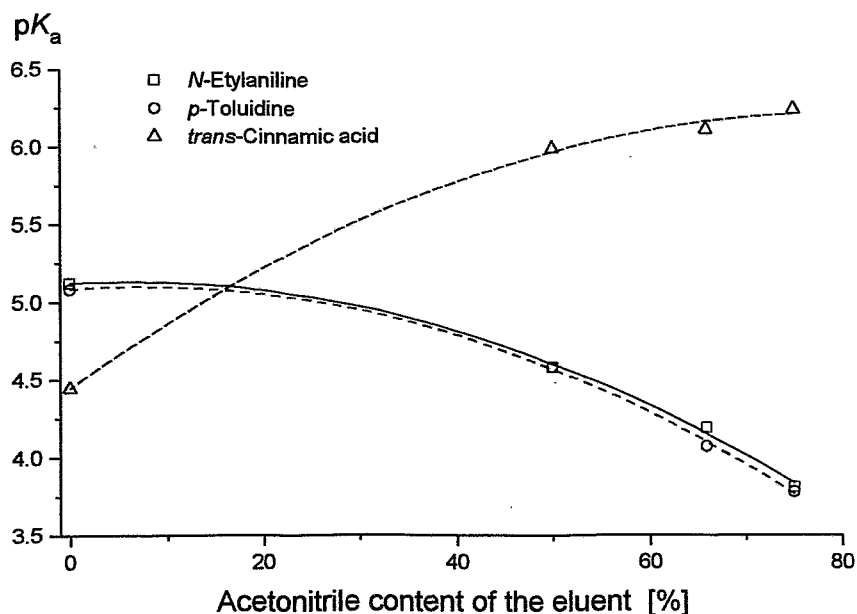


Fig. 2: pK_{HPLC} values determined by HPLC as a function of the percental content of acetonitrile in the aqueous eluent

Generally, if true pK_a or also $\log P$ values of lipophilic compounds are determined, organic solvents in the eluents should be as small as possible (Miyake *et al.*, 1987; Yamagami *et al.*, 1994). In order to extrapolate to solvent-free eluent, the sums of apparent pK_a values measured at different weight percentages of solvent and $\log [H_2O]$ are plotted versus reciprocal values of dielectric constants of the corresponding solvent/water mixture. The so-called Yasuda-Shedlovsky plot produces a straight line, allowing an extrapolation to zero solvent content (Yasuda, 1959; Shedlovsky, 1962; Avdeef *et al.*, 1993; Slater *et al.*, 1994). Presumably, because the pK_{HPLC} values measured in our system (cp. Fig. 2) were derived from relatively high acetonitrile portions, the results obtained by using the Yasuda-

Shedlovsky plot were not satisfactory. The values found by extrapolation were too high in case of both weak bases and the acid (error of 10 % and even more!).

In conclusion, it cannot be said at present if the results concerning the deviation of pK_{HPLC} values from true values in case of reference compounds may be used to correct values obtained by measuring compounds with basically other structures, i.e. also coordination compounds. In fact, the values presented may help to gain a certain feeling for discrete structural changes in a coordination compound of interest.

References

- Avdeef A., Comer J.E.A. and Thomson S.J. (1993) pH-Metric log *P*. 3. Glass electrode calibration in methanol-water, applied to pK_a determination of water-insoluble substances. *Anal. Chem.* **65**, 42-29.
- Berger R., Fietz T., Glaser M., Spies H. and Johannsen B. (1995) Determination of partition coefficients for coordination compounds by using HPLC. *This report*, pp. 69-72.
- Lee D.P. (1982) Reversed-phase HPLC from pH 1 to 13. *J. Chromatogr. Sci.* **20**, 203-208.
- Lide D.R. (ed.). (1992-1993) *CRC Handbook of Chemistry and Physics*, pp. 8-37. CRC Press, Tokyo.
- Miyake K., Kitaura F., Mizuno N. and Terada H. (1987) Determination of partition coefficient and acid dissociation constant by high-performance liquid chromatography on porous polymer gel as a stationary phase. *Chem. Pharm. Bull.* **35**, 377-388.
- Pagliara A., Khamis E., Trinh A., Carrupt P.-A., Tsai R.-S. and Testa, B. (1995) Structural properties governing retention mechanisms on RP-HPLC stationary phases used for lipophilicity measurements. *J. Liq. Chromatogr.* **18**, 1721-1745.
- Palalikit D. and Block J.H. (1980) Determination of ionization constants by chromatography. *Anal. Chem.* **52**, 624-630.
- Rudzinski W.E., Bennett D. and Garica V. (1982) Retention of ionized solutes in reversed-phase high performance liquid chromatography. *J. Liq. Chromatogr.* **5**, 1295-1312.
- Shedlovsky T. (1962) The behaviour of carboxylic acids in mixed solvents. In *Electrolytes* (Edited by Pesce B.), Pergamon Press, New York, pp. 146-151.
- Slater B., McCormack A., Avdeef A. and Comer J.E.A. (1994) pH-Metric log *P*. 4. Comparison of partition coefficients determined by HPLC and potentiometric methods to literature values. *J. Pharm. Sci.* **83**, 1280-1283.
- Stylli C. and Theobald A.E. (1987) Determination of ionisation constants of radiopharmaceuticals in mixed solvents. *Appl. Radiat. Isot.* **38**, 701-708.
- Takács-Novák K., Józsan M. and Szász G. (1995) Lipophilicity of amphoteric molecules expressed by the true partition coefficient. *Int. J. Pharm.* **113**, 47-55.
- Terada H. (1986) Determination of log P_{oct} by high-performance liquid chromatography, and its application in the study of quantitative structure-activity relationships. *Quant. Struct.-Act. Relat.* **5**, 81-88.
- Thévenon-Emeric G., Tchaplá A. and Martin M. (1991) Role of π - π interactions in reversed-phase liquid chromatography. *J. Chromatogr.* **550**, 267-283.
- Van de Venne J.L., Hendrikx J.L. and Deelder R.S. (1978) Retention behaviour of carboxylic acids in reversed-phase column liquid chromatography. *J. Chromatogr.* **167**, 1-16.
- Vigh G., Varga-Puchony Z. and Bartha A. (1982) Retention behaviour of acetyl-indandiones in reversed-phase high-performance liquid chromatography. *J. Chromatogr.* **241**, 169-176.
- Yamagami C., Yokota M. and Takao N. (1994) Hydrophobicity parameters determined by reversed-phase liquid chromatography. VIII. Hydrogen-bond effects of ester and amide groups in hetero-aromatic compounds on the relationship between the capacity factor and the octanol-water partition coefficient. *J. Chromatogr.* **662**, 49-60.
- Yasuda M. (1959) Dissociation constants of some carboxylic acids in mixed aqueous solvents. *Bull. Chem. Soc. Japan* **32**, 429-432.

21. Rhenium and Technetium Mixed-Ligand Chelates Functionalized by Amine Groups

1. Rhenium Complexes with *p*-Substituted Benzenethiols as Monodentate Ligands

M. Papadopoulos¹, S. Chiotellis¹, H. Spies, M. Friebe, R. Berger, B. Johannsen

¹Institute of Radioisotopes and Radiodiagnostic Products of the National Center for Scientific Research "Demokritos", Athens

Introduction

Radiotracers for the CNS, either for perfusion or for more specific binding tracers, have to pass the intact blood-brain barrier (BBB). Whether and in which way the physicochemical and structural properties of a Tc tracer enhance or limit the transport of these foreign molecules through the BBB have not been understood so far, however. In this context, a project for cooperation between the Institute of Radioisotopes and Radiodiagnostic Products of the National Center for Scientific Research "Demokritos", Athens, and the Institute of Bioinorganic and Radiopharmaceutical Chemistry of the Research Center Rossendorf within the COST B3 programme is concerned with the passage or lack of passage of Tc/Re complexes across barrier sites. As the lipophilicity and ionization state under physiological conditions belong to dominant factors influencing blood-brain barrier passage of radio tracers, studies involve relations between structural parameters of the complexes, their lipophilicity as well as basicity (expressed in terms of log P and p*K*) and brain uptake.

Working program includes the preparation of neutral amine-bearing Tc and Re complexes and variable substituents, structural characterization (elemental analysis, IR, ¹H NMR, mass spectrometry, X-ray structure determination), characterization of lipophilicity parameters and p*K* values as well as biodistribution studies.

First part of cooperation refers to amine-bearing "3+1" mixed-ligand complexes of the type 1 (shown in reaction scheme 1), which are able to pass the BBB and are accumulated in the brain (Mastro-stamatis *et al.*, 1994; Pirmettis *et al.*, 1995a,b). The present report informs on preparation and characterization of rhenium complexes where the tridentate SNS ligand contains a pendant diethylaminoethyl group and the monodentate benzenethiol is varied in the *p*-position by substituents covering the range from -OCH₃ to -NO₂.

Experimental

Synthesis of complexes **1** - **9** (general procedure)

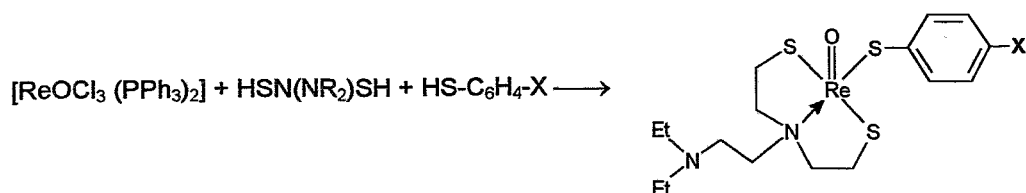
To a stirred suspension of [ReOCl₃(PPh₃)₂] (250 mg; 0.3 mmol) in 0.15 N sodium acetate in methanol (20 ml) were added 0.3 mmol of the tridentate ligand and 0.3 mmol of *p*-substituted benzenethiols. The reaction mixture was heated to 70 °C for 30 minutes at which time the green-yellowish colour of the starting material had been changed to green-brown. After cooling to room temperature, the reaction mixture was diluted with dichloromethane (50 ml), and washed with water. The organic phase was separated from the mixture and dried over sodium sulphate. The volume of the solution was reduced to 5 ml and 5 ml of methanol were added. Slow evaporation of the solvent at room temperature afforded the products as green or brown crystals.

The log P and D/pH profiles were determined as described (Berger *et al.*, 1995) by HPLC at a PRP-1 column, acetonitrile : buffer = 3 : 1 (v/v).

Results and Discussion

The complexes [ReO(SN(NR₂)S)(SC₆H₄-X)] were prepared according to reaction scheme 1.

Reaction scheme 1: Synthesis of complexes [ReO(SN(NR₂)S)(SC₆H₄-X)]



HSN(NR₂)SH = HS-CH₂CH₂-N(CH₂CH₂-NEt₂)-CH₂CH₂-SH;

X = NH₂ (**1**), OMe (**2**), Me (**3**), *t*-Bu (**4**), H (**5**), Cl (**6**), Br (**7**), I (**8**), NO₂ (**9**)

The rhenium compounds **1** – **9** are representatives of mixed-ligand "3+1" complexes, where the coordination sphere is built up by a *p*-substituted benzenethiol as monodentate ligand and a chelate ligand having a SNS donor sequence and bearing a pendant diethylaminoethyl group moiety. The analogous Tc complexes are known (Pirmettis, 1995a,b) as compounds showing high brain uptake. Variation of the substituent in para position of the aromatic ring were done in order to see whether and how the nature of the substituent influences *D*/*pK* and whether an correlation to the penetration properties of the corresponding technetium species exists.

D/*pH* profiles were determined by the shake flask method as well as by HPLC. Typical profiles obtained by HPLC are shown for two representatives in Fig. 1. Log *P* values are derived from right part of the curve, which reflects the lipophilicity of the free amine. The pK_{HPLC} values derive from the turning point of the curve. However, since measurements are done in organic/aqueous solutions, values were corrected by comparing the experimental values with those obtained for amines (benzylamine, N,N-diethyl-, N,N-dimethyl-, N-ethylaniline, aniline, *p*-toluidine, pyridine) for which the pK_a values are known from literature (Lide, 1992).

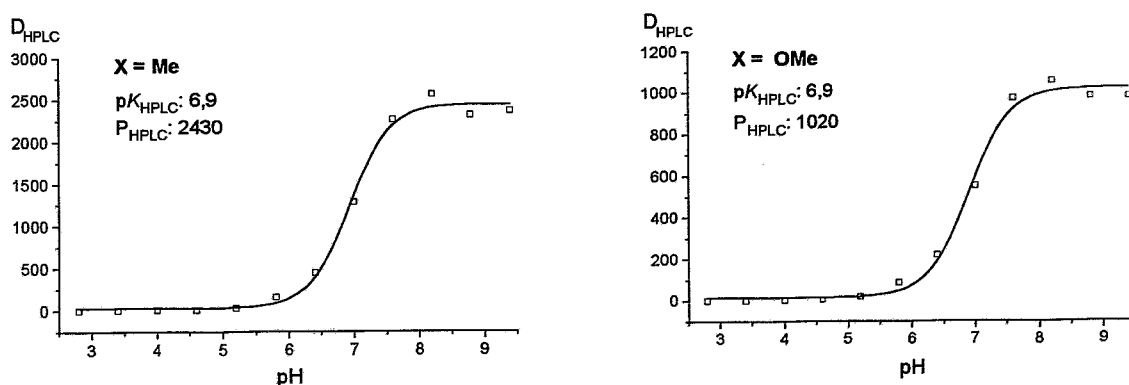


Fig. 1: *D*/*pH* profiles for complexes **2** and **3** obtained by HPLC

Table 1: Lipophilicity/*pK* data of complexes **1** – **9**

No.	X	log <i>P</i>	log <i>D</i> ^{†)}	pK_{Korr}
1	NH ₂	1.64	0.85	8.2
2	OMe	3.02	1.98	8.2
3	Me	3.40	2.22	8.2
4	<i>t</i> -Bu	4.05	2.74	8.3
5	H	3.23	2.23	8.1
6	Cl	4.09	3.14	8.1
7	Br	4.33	3.24	8.1
8	I	4.59	3.49	8.2
9	NO ₂	3.68	2.76	8.0

^{†)} at pH 7.4

Lipophilicity data log *P* and log *D* as well as corrected *pK* values of all complexes are listed in Table 1. Apart from compound **1**, where a free amine group makes the complex less lipophilic, the values of log *P* are in the range of about 3.0 to 4.6. The corresponding log *D* values, considering the co-existence of both charged and uncharged forms at pH 7.4, are one logarithmic unit lower.

It is noticed that within this series the log *P* values of halogen-substituted complexes (**6** – **8**) exceed that of e. g. the *t*-butyl-substituted derivative. It cannot be ruled out that the influence of halogen substitution is overestimated by the special column used.

The *pK* values, varying in a very limited region of 8.3 to 8.0, reveal that the fraction of free amine present in the reaction mixture at pH 7.4 is in the order of 10 %. Regardless the relatively slow variation of *pK* values with X, the effect of electron-donating/withdrawing properties of the substituent X follows in general the anticipation. While apparent discrepancies occur with complexes where either X

is protonable itself (1) or X is a relatively large unit (4, 7, 8), the values of complexes 2, 3, 5, 6, 9 having typical Hammett-substituents go well with normal σ_p -values.

References

- Berger R., Fietz T., Glaser M., Spies H. and Johannsen B. (1995) Determination of partition coefficients for coordination compounds by using HPLC. *This report*, pp. 69-72.
- Lide D.R. (ed.) (1992) *CRC Handbook of Chemistry and Physics*, CRC Press, Tokyo, pp. 8-37.
- Mastrostamatis S.G., Papadopoulos M.S., Pirmettis I.C., Paschali E., Varvarigou A.D., Stassinopoulou C.I., Raptopoulou C.P., Terzis A. and Chiotellis E. (1994) Tridentate ligands containing the SNS donor atom set as a novel backbone for the development of technetium brain-imaging agents. *J. Med. Chem.* **37**, 3212-3218.
- Pirmettis I.C. (1995a) Mixed-ligand complexes of oxotechnetium(V): synthesis, characterization and biological evaluation as possible brain imaging agents. *Doctoral Thesis*.
- Pirmettis I.C. *et al.* (1995b) unpublished data.

22. Technetium and Rhenium Complexes Derived from 6-Methyl-8 α -Amino Ergoline 1. Synthesis and Molecular Structure of [ReO(SSS)(MAerg)]

P.E. Schulze¹, St. Noll, B. Noll, H. Spies, P. Leibnitz², W. Semmler¹, B. Johannsen
¹Institut für Diagnostikforschung Berlin, ²Bundesanstalt für Materialforschung Berlin

Introduction

The ergot alkaloids (Berde and Schild; 1978, Hansch *et al.*, 1990), derivatives of lysergic acid or ergoline structures, exhibit a broad range of pharmacological activities. Many of them are DA₂ or D₂ receptor agonists, but some ergoline derivatives also interact with serotonin and noradrenaline receptors with very high affinities.

Many compounds, among them terguride (Fig. 1) having high dopaminergic activity, are used as potent drugs. [¹²³I]2-iodolisuride has been successfully applied as a SPECT imaging agent in the study of healthy subjects and patients (Maziere *et al.*, 1992; Chabriat *et al.*, 1992).

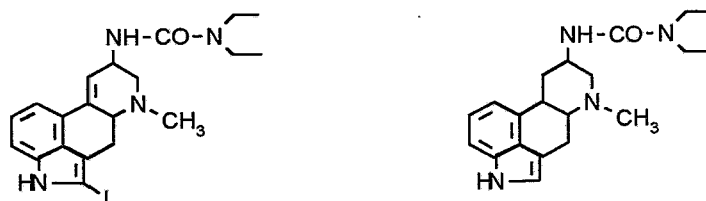


Fig. 1: 2-iodolisuride and terguride

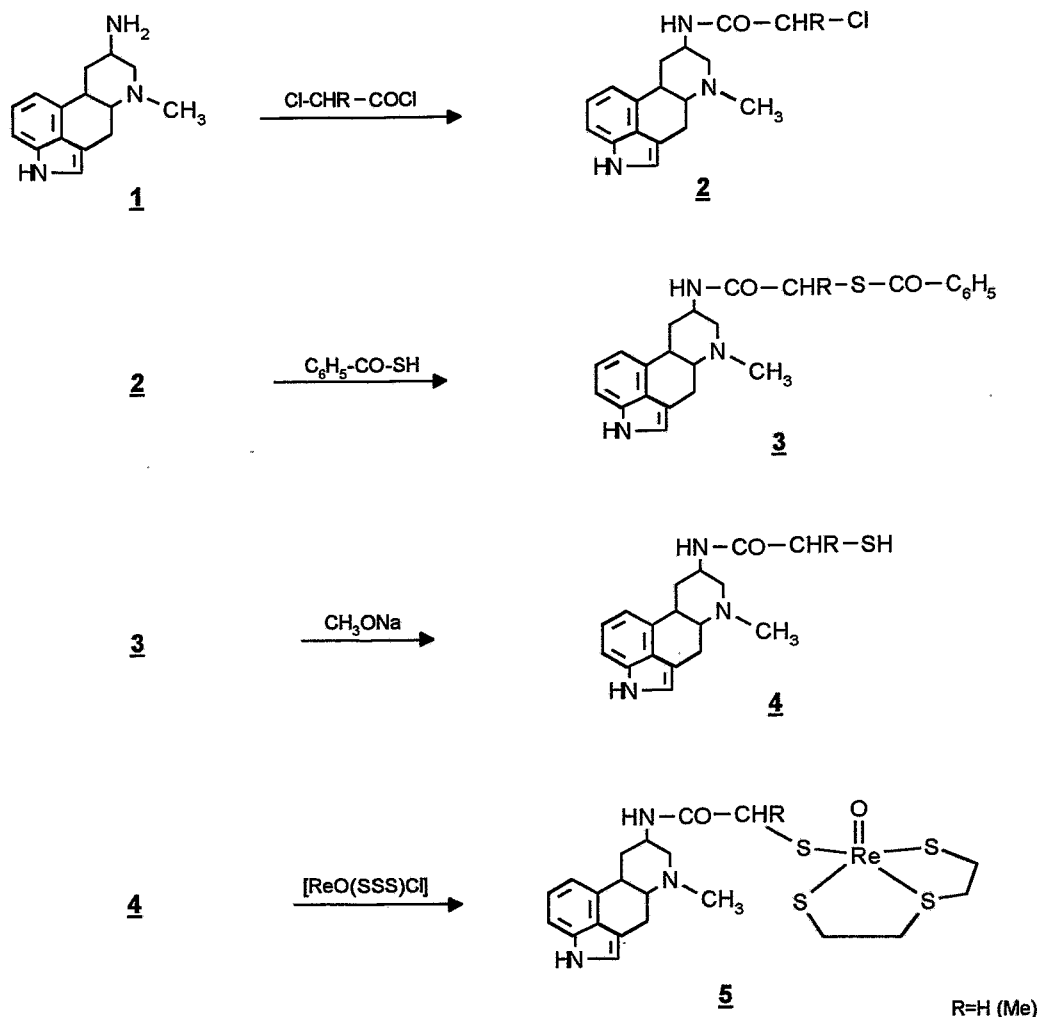
Our efforts are aimed at the design of receptor-binding radiotracers on the basis of technetium because of the excellent nuclide properties and wide availability of the isotope ^{99m}Tc. However, technetium as a metal, when combined with a structure having the required receptor affinity, drastically alters its molecular and biological properties. The question as to whether coordination compounds, preferably those of technetium, are able to imitate organic receptor-binding compounds is therefore of basic interest. In this respect, ergoline derivatives have been included in our ongoing studies of the potential receptor binding of Tc and Re complexes.

The present report deals with the functionalization of 6-methyl-8 α -aminoergoline with a 2-mercaptoacetyl group and the subsequent synthesis of the first rhenium complex [Re(SSS)(MAerg)] (MAerg = 6-methyl-N-(2-mercaptoacetyl)-8 α -amino-ergoline and HSSSH = HSCH₂CH₂-S-CH₂CH₂SH), containing a pendant ergoline moiety as well as its molecular structure. Part 2 will describe the preparation and biodistribution characteristics of the corresponding Tc complexes. In both parts, special attention is devoted to studying the effect caused by introducing the chelate unit into the parent 8 α -amino-6-methylergoline on changes of the size and lipophilicity of the resulting species.

Results and Discussion

To enable the ergoline functionality to act as a monodentate ligand in the intended mixed-ligand "3+1" complex, a mercapto group has to be introduced. S-functionalization was accomplished by mercaptoacetylation of the amino group in the parent 6-methyl-8 α -aminoergoline. 3-thiapentane-1,5-dithiol HS-CH₂CH₂-S-CH₂CH₂-SH was utilized as a tridentate ligand to provide a neutral rhenium(V) complex of the "3+1" type (Spies *et al.*, 1995) according to the reaction scheme.

Scheme 1: Synthesis of mercaptoacetyl 6-methyl-8 α -aminoergoline MAErg and the "3+1" complex **5**



6-methyl-8 α -aminoergoline (**1**) was converted into 6-methyl-8 α -chloroacetylaminoergoline (**2**) by chloroacetyl chloride. Reaction of **2** with thiobenzoic acid yields 6-methyl-N-(2-benzoylmercapto)acetyl-8 α -aminoergoline **3**. Immediately before complexation, the benzoyl group was removed by sodium methylate to give, after neutralization with dil. HCl, N-(2-mercapto)acetyl-8 α -amino-6-methyl-ergoline **4**. (The methyl derivatives of **2** to **4** were obtained using 2-chloropropionyl chloride instead of chloroacetyl chloride).

For preparation of the rhenium complex $[\text{ReO}(\text{SSS})(\text{MAErg})]$ **5**, the mercaptane **4** was allowed to react with $[\text{ReO}(\text{SSS})\text{Cl}]$ (Fietz *et al.*, 1995a) as a precursor with a preformed metal/tridentate unit, yielding brown crystals [m.p. 247.-.250 °C, $\text{C}_{21}\text{H}_{28}\text{N}_3\text{O}_2\text{S}_4\text{Re}$, IR 968 cm^{-1} (Re=O)] suitable for X-ray crystal structure determination.

The structure of compound **5** shows the square-pyramidal geometry as typical of sulphur-coordinated "3+1" oxorhenium(V) complexes (Spies *et al.*, 1993; Fietz *et al.*, 1994, 1995b). The bond lengths and angles are in the region normally found. Fig. 2 impressively illustrates the increase in size as a con-

sequence of introducing the chelate moiety according to an increase in molecular weight from 241 for 1 to 578 for 5.

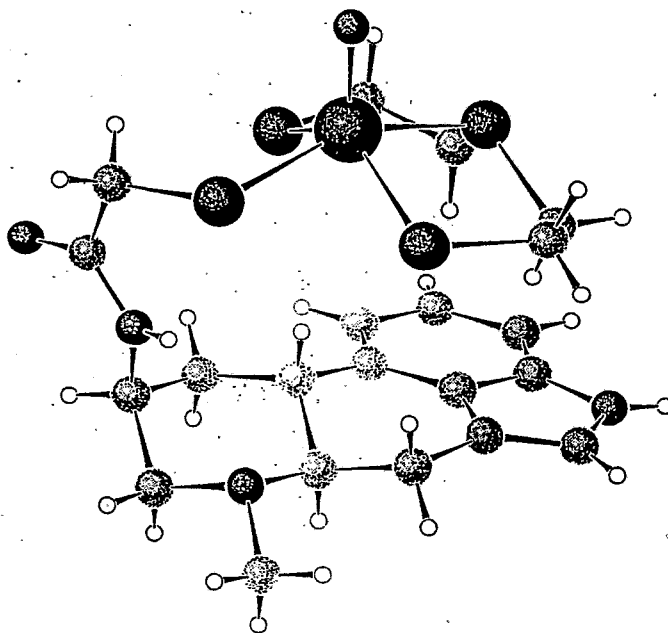


Fig. 2: Molecular structure of 5

As far as we know, 5 is the first compound where an ergoline as the parent molecule is combined with a chelate of a group VII metal. The second part of this report will refer to the preparation and evaluation of analogous technetium complexes.

References

- Berde B. and Schild H.O. (Ed.) (1978) *Ergot alkaloids and related compounds* (Springer Berlin, Heidelberg, New York), pp. 1-140.
- Chabriat H., Levasseur M., Vidailhet M., Loch C., Maziere B., Bourguignon M.H., Bonnet A.M., Zilbovicius M., Raynaud C. and Agid Y.J. (1992) *In vivo* SPECT imaging of D₂ receptor with iodine-iodolisuride: results in supranuclear palsy. *J. Nucl. Med.* **33**, 1481-1485.
- Fietz T., Spies H., Pietzsch H.-J. and Leibnitz P. (1995) Synthesis and molecular structure of chloro-(3-thiapentane-1.5-dithiolato)oxorhenium(V). *Inorg. Chim. Acta* **231**, 233-236.
- Fietz T. (1995) Rhenium-Komplexe mit 3+1-Koordination. *Thesis*, TU Dresden.
- Hansch C., Sammes P.G. and Taylor J.B. (Ed.) (1990) Ergot derivatives. *Comprehensive Medicinal Chemistry* (Pergamon Press) Vol 3, 250-309.
- Maziere B., Coenen H.H., Haldin C., Nagren K. and Pike V.W. (1992) PET radioligands for dopamine receptors and Re uptake sites: chemistry and biochemistry. *Nucl. Med. Biol.* **19**, 479-512.
- Spies H., Fietz T., Pietzsch H.-J., Johannsen B., Leibnitz P., Reck G. and Klostermann K. (1995) Alkyl- and aryl substituted oxorhenium(V) complexes with tridentate/monodentate coordination. *J. Chem. Soc., Dalton Trans.* 2277-2280.

23. Technetium and Rhenium Complexes Derived from 6-Methyl-8 α -Amino Ergoline

2. Preparation and Biodistribution of Mixed-Ligand Tc Complexes

B. Noll, R. Syhre, St. Noll, H. Spies, P. Brust, B. Johannsen, P.E. Schulze¹, W. Semmler¹
¹IDF Berlin

We report on preparation and biological evaluation of mixed ligand ^{99/99m}Tc complexes containing the ergoline moieties 6-methyl-N-(2-mercaptoacetyl)-8 α -aminoergoline (MAerg) and 6-methyl-N-(2-mercaptoacetyl)-8 α -aminoergoline (MPerg) as monodentate ligands and HS-CH₂CH₂-S-CH₂CH₂-SH (HSSH) or mercaptoacetyl-N-methylglycine (NMe-MAG₁) as tridentate ligands.

Experimental

Preparation of MAerg and MPerg are described in the preceding report (Schulze *et al.*, 1995)

Technetium complexes

Complexes **3a-d** were prepared by the reaction of both the monodentate and the tridentate ligand with ^{99/99m}Tc gluconate. 1 ml acetonitrile is given to 1 ml Tc gluconate (1 mmol) solution before addition of the ligands to prevent a precipitation of the lipophilic mercaptoacylated ergoline ligands.

Tc-complexes with SSS **3a,b**:

4 μ mol S-benzoylic MAerg resp. MPerg solved in 200 μ l MeOH are saponificated by adding 50 μ l 1.1 M NaOCH₃. After 20 min the alkaline solution is given to Tc gluconate. After another 20 min 2 μ mol SSS-solution (50 μ l stock solution + 50 μ l acetone) are added. Before HPLC-separation the solution is neutralized by adding 1 M HCl.

Tc-complexes with NMe-MAG₁ **3c,d**:

4 μ mol S-benzoylic MAerg resp. MPerg solved in 200 μ l MeOH are saponificated by adding 50 μ l 1.1 M NaOCH₃. After 20 min the alkaline solution is given to Tc gluconate. After another 20 min the solution is neutralized with 40 μ l 1 N HCl and 2 μ mol MMAG₁ is added.

HPLC-separations

All preparations were purified by semipreparative HPLC on RP 18 column (Eurosphere, 250 x 4 mm) and 0.01 M phosphate buffer pH 5.8 (A) and acetonitrile (B) as eluents.

Method 1: 5 min 75 % A, 25 % B; 15 min from 75 % A / 25 % B to 10 % A / 90 % B; 5 min 10 % A / 90 % B; Flow rate: 1 ml / min

Method 2: 3 min 100 % A; 15 min from 100 % A to 10 % A / 90 % B; 5 min 10 % A / 90 % B; Flow rate: 2 ml / min

Lipophilicity data

Octanol-buffer (pH 7.4) partition coefficients log P were determined by the shake flask method.

In vivo experiments

The biodistribution and elimination were investigated in rats as previously described (Syhre *et al.*, 1995). Animal experiments were carried out according to the relevant national regulations.

Results and Discussion

^{99/99m}Tc complexes **3a-d** were obtained by a two-step procedure starting with the reaction of the mercaptoacylated ergoline as the monodentate ligand with ^{99/99m}Tc gluconate (**1**) followed by addition of the tridentate chelator according to reaction scheme 1. The instable intermediates (**2**) formed in the initial step are converted into the "3+1" complexes **3a-d** after adding the tridentate ligand. They were identified on basis of their UV absorptions (445 nm for **3a,b**, 430 nm for **3c,d**). Besides the required mixed-ligand complexes the intermediate complexes **2** and a third component **4**, most likely species derived from the tridentate ligand, occurs. The maximum portion of **3** of about 60 % in the reaction mixture was observed after 30 - 45 min. A typical HPLC chromatogram of the product pattern formed is shown in Fig. 1. The required mixed-ligand complexes **3a-d** were separated from the mixture by HPLC (R_t values in Table 1). Analytical data and including log P values are summarized in Table 1. Preliminary log P values informs on the lipophilicity of the complexes. There is a considerable difference between **3a,b** and **3c,d** of about two orders of magnitude as function of the nature of the tridentate part in the molecules. These rather drastic differences are not so clear reflected in the biological properties. The distribution data of ^{99m/99}Tc ergoline complexes in rats at 10 and 60 minutes p. i. are presented in Table 2. All complexes showed considerable accumulation and retention in liver and

kidney of rats. The time course of the blood pool activity (Fig. 2) as well as the distribution results in Table 2 show a slow clearance for the Tc ergoline complexes with a (SSS)-chelate unit.

Scheme 1: Formation of Tc complexes **3a-d**

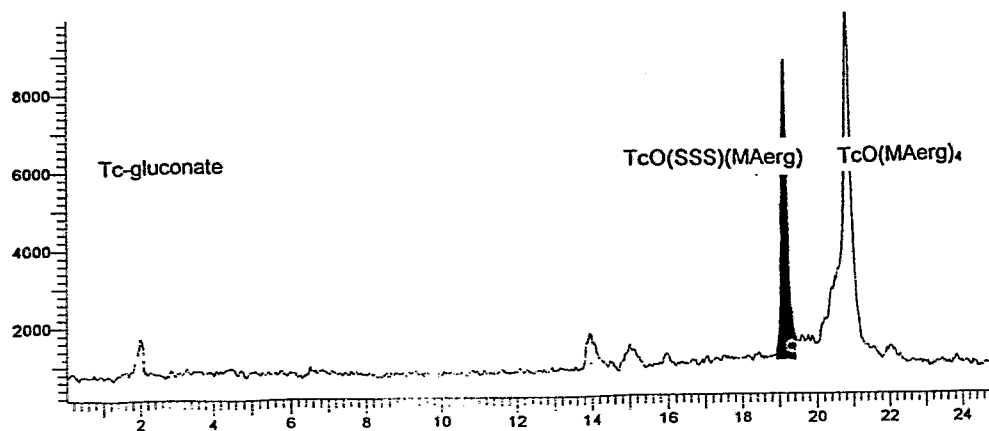
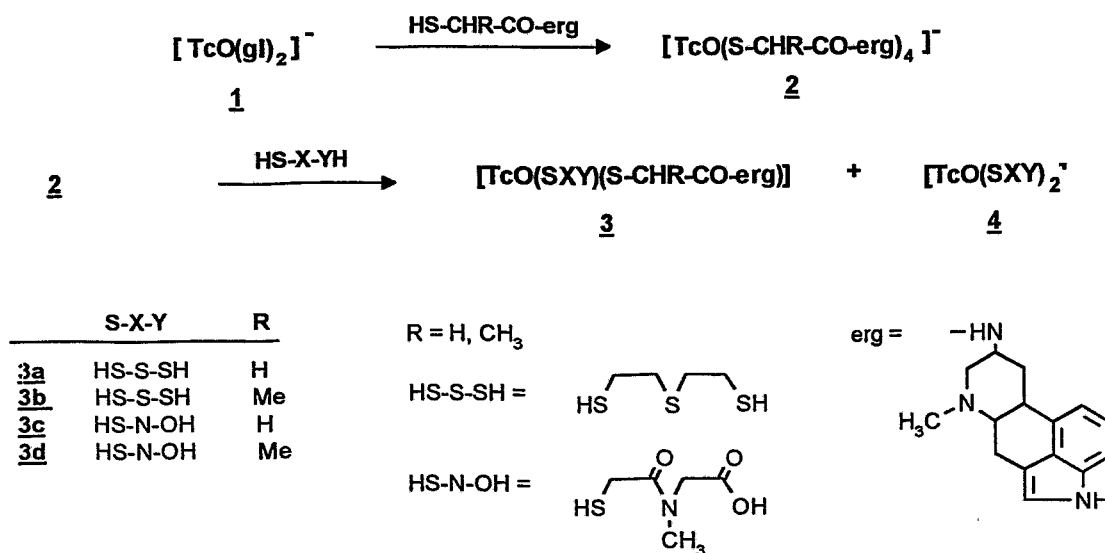


Fig. 1: HPLC-separation of [TcO(SSS)(MAerg)] (**3a**) from a reaction mixture on RP 18 column (Eurosphere, 250 x 4 mm) and 0.01 M phosphate buffer pH 5.8 (A) and acetonitrile (B) as eluents. Elution: 5 min 75 % A, 25 % B; 15 min from 75 % A / 25 % B to 10 % A / 90 % B; 5 min 10 % A / 90 % B. Flow rate: 1 ml / min

This result is comparable to the observed properties of blood elimination of amine-bearing [^{99m}Tc] oxotechnetium (V) complexes with a (SSS)-chelate unit (Syhre *et al.*, 1995). The brain uptake of the SSS-ergoline derivatives **3a,b** is low. 0.19 % of the injected dose was the maximum of initial brain uptake after the application. The slow brain clearance (Fig. 2) as well as the distribution of radioactivity in receptor containing brain regions shows, that the complex **3a** is able to cross the blood-brain-barrier and can be trapped in the brain. The accumulated dose in the receptor rich brain regions (caudate putamen and hippocampus) remains approximately constant within the investigation period of 10 to 120 minutes. The level of radioactivity which is calculated for the cerebellum is very low. All results were corrected with the radioactivity part contributing to the regional blood volume.

Table 1: Selected analytical data of complexes **3a-d**

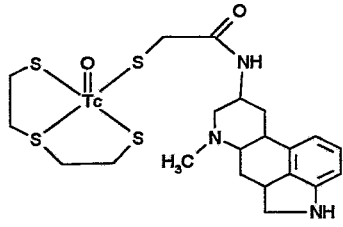
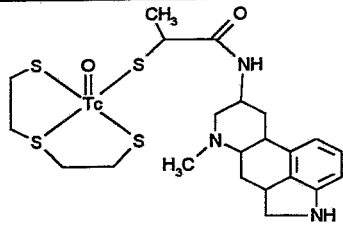
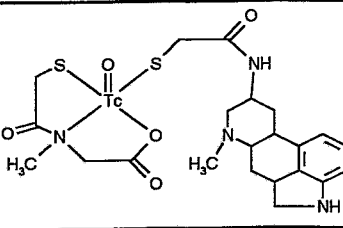
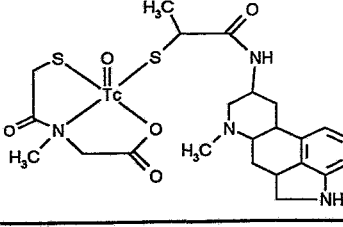
Complexes 3	Chemical structure	HPLC R _t [min]	lg P _{ow}
3a		19.1 method 1	2.9
3b		19.4 method 1	2.9
3c		17.0 method 2	0.9
3d		14.9 method 2	0.9

Table 2: Biodistribution of complexes **3a-d** in rats (means; n = 3)

Complex	min. p.i.	% Dose/organ				% Dose/g				
		heart	lung	kidney	liver	blood	heart	lung	kidney	liver
3a		0.6	2.5	7.7	24.9	4.3	0.8	2.1	4.2	3.0
	60	0.5	2.4	21.2	24.7	3.1	0.6	1.8	10.1	2.0
3b	10	0.5	1.8	10.1	23.2	2.8	0.7	1.5	7.0	2.5
	60	0.3	1.2	10.9	21.9	1.8	0.4	1.0	6.4	2.2
3c	10	0.7	1.2	15.9	15.8	1.6	0.8	1.0	13.2	2.5
	60	0.1	0.5	20.3	11.3	0.2	0.2	0.3	17.0	2.0
3d		0.2	0.6	12.1	20.5	0.8	0.3	0.5	7.8	2.4
	60	0.1	0.3	13.6	7.6	0.3	0.3	0.3	6.3	0.7

The ergoline derivatives with NMe-MAG₁ as tridentate ligand (**3c,d**) show within the investigation period of 2 to 60 minutes a rapid blood clearance as well as a rapid brain washout. As observed for **3a**, approximately 0.2 % initial brain uptake was observed for **3c** indicating that this complex might be able to cross the blood-brain barrier. A retention of radioactivity in the brain could, however, not be observed.

The initial brain uptake of the methylated compounds **3b** and **3d** were not found to be significant higher than the back ground activity. An influence of a methyl group on the biological behaviour, especially on the brain uptake, could not be noticed. Differences in the biologic behaviour of the studied Tc ergoline complexes are determined rather by the tridentate ligand than by the presence of an additional methyl group at the ergoline molecule.

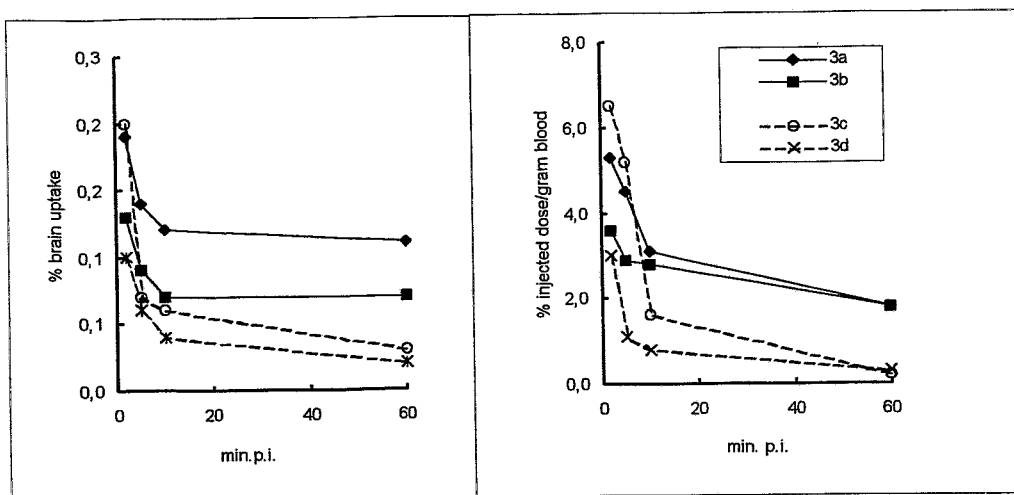


Fig. 2: Brain and blood clearance curves of Tc ergoline complexes **3a-d** in male Wistar rats

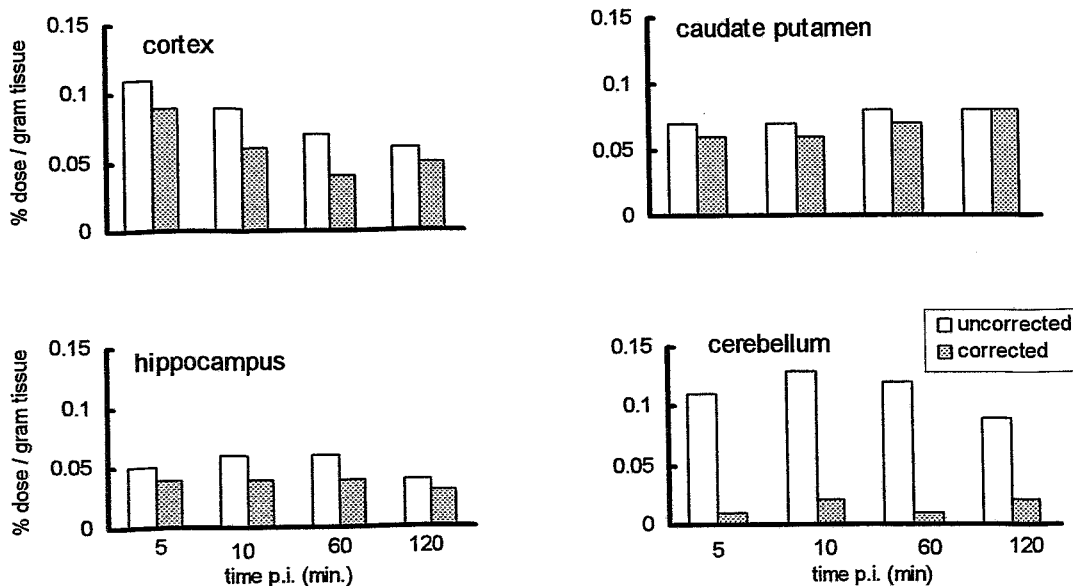


Fig. 3: Distribution of Tc ergoline complexes **3a,b** in receptor rich regions of the rat brain. Comparison of the data before as well as after correction of the radioactiv part of the regional blood volume.

References

- Schulze P.E., Noll St., Noll B., Spies H., Leibnitz P., Semmler W. and Johannsen B. (1995) Technetium and rhenium complexes derived from 6-methyl-8 α -aminoergoline. 1. Synthesis and molecular structure of [ReO(SSS)(MAerg)]. *This report*, pp. 82-84.
- Syhre R., Berger R., Pietzsch H.-J., Scheunemann M. and Spies H. (1995) Serotonin receptor-binding technetium and rhenium complexes. 6. Distribution and brain uptake in the rat of [^{99m/99}Tc] oxo-technetium(V) complexes with affinity to 5-HT₂ receptor. *This report*, pp. 51-58.

24. Preparation of 2,3-Dimercaptopropionic Acid Ethyl Ester

A. Hoeping, H. Spies

Introduction

Systematic studies on enzymatic cleavage of coordinate ester functionalities have been performed with Tc complexes of 2,3-dimercapto succinic acid derivatives (Johannsen *et al.*, 1995; Seifert *et al.*, 1995). To extend the series of ligands the ethyl ester of 2,3-dimercaptopropionic acid will be included. Unlike the methyl ester, this ethyl ester has not so far been described to our knowledge. The preparation of the methyl ester includes a multistep synthesis starting from 2-chloroprop-2-en acid methyl ester and proceeding via the dithioacylated precursor (Pavlic, 1946). Here we describe the synthesis of the ethyl ester.

Experimental

2,3-Dithioacylpropionic acid ethyl ester

29.2 ml 2,3-dibromopropionic acid ethyl ester (0.2 mol) were added drop by drop to a well stirred solution of 28.5 ml thioacetic acid (0.4 mol) and 55.6 ml triethylamine (0.4 mol) in 200 ml dry ethanol, within 1.5 h while cooling of the solution with ice/water. The reaction temperature had to be kept between 5 °C and 15 °C. Then the mixture was allowed to slowly warm to room temperature, and was stirred for another 5 h. Triethylammonium hydrobromide was filtered off and the solvent was removed in vacuo. The residue was dissolved in 100 ml dichloromethane and washed three times with 30 ml water. After drying and removing the solvent the dark yellow oil was fractionated in vacuo over a 20 cm Vigreux column.

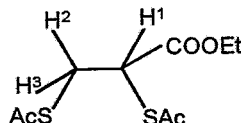
Yield: 32.1 g (71 %) yellow oil.

B. p.: 92 °C/ 0.015 Torr

R_f: 0.07 (Et₂O/n-hexane = 1:9)

Elemental analysis: (Found: C, 43.09; H, 5.71; S, 27.23; C₉H₁₄O₄S₂ requires C, 43.18; H, 5.64; S, 25.61 %)

¹H and ¹³C NMR data: (solvent CDCl₃; standard TMS)



δ_{H} (200 MHz): 1.27 (3 H, t, ³J(HH) 7.1 Hz, CH₃); 2.34 (3 H, s, CH₃, SAc), 2.38 (3 H, s, CH₃, SAc), 3.28 (1 H, dd, ²J(H²H³) 13.8 Hz, ³J(H¹H²) 6.35 Hz, H² (CH₂)), 3.42 (1 H, dd, ²J(H²H³) 13.8 Hz, ³J(H¹H³) 7.6 Hz, H³ (CH₂)), 4.19 (2 H, q, ³J(HH) 7.1 Hz, CH₂), 4.34 (1 H, dd, ³J(H¹H³) 7.6 Hz, ³J(H¹H²) 6.35 Hz, H¹ (CH))

δ_{C} (300 MHz): 13.93 CH₃ (Et), 29.98, 30.23 2 CH₃ (Ac), 45.62 CH, 61.2 CH₂ (Et), 169.66 CO (Et), 192.27, 193.67 2 CO (Ac)

2,3-Dimercaptopropionic acid ethyl ester

30 g of 2,3-dithioacylpropionic acid ethyl ester were dissolved in 150 ml of dry ethanol containing 2 % dry HCl. The mixture was allowed to stand at room temperature with occasional shaking. After 24 h the ethanol and ethyl acetate were removed and the same procedure was repeated for 48 h. The residue was distilled in vacuo over a 20 cm Vigreux column to yield 5.3 g (22.4 %) of a colourless oil.

R_f: 0.21 (Et₂O/n-hexane = 1:9)

Elemental analysis: (Found: C, 36.36; H, 5.42; S, 36.11; C₅H₁₀O₂S₂ requires C, 36.12; H, 6.06; S, 38.57 %)

¹H NMR data: δ_H (200 MHz; solvent CDCl₃; standard TMS) 1.25 (3 H, t, ³J(HH) 7 Hz, CH₃); 1.75 (1 H, m, SH), 2.18 (1 H, d, ³J(HH) 10Hz, SH), 2.85 (2 H, m, CH₂), 3.4 (1H, m, CH), 4.17 (2 H, q ³J(HH) 7 Hz, CH₂)

2,3-Dimercaptopropionic acid

1 g of 2,3-dimercaptopropionic acid ethyl ester was refluxed in 10 % aqueous HCl for 16 h. The mixture was extracted with trichloromethane (3 x 5 ml), dried over MgSO₄ and evaporated to dryness. The crude product was recrystallized from trichloromethane/n-hexane = 1:1.

Yield: 400 mg white crystals

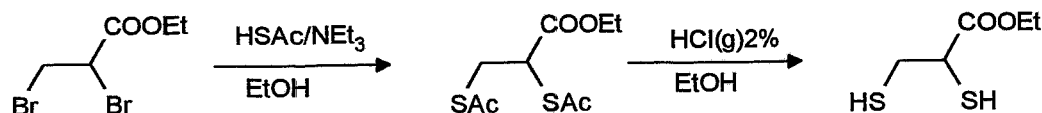
R_f: 0.51 (MeOH/CHCl₃ = 1:9).

M.p.: 71-73 °C; m.p.(Pavlic, 1946): 74-74.5 °C.

Remark: The elemental analyses were performed on a LECO CHNS 932 elemental analyser. The differences in the sulphur values are caused by apparatus problems.

Results

We found that the 2,3-dithioacylpropionic acid ethyl ester is readily available by reacting 2,3-dibromopropionic acid ethyl ester with thioacetic acid according to Scheme I.



The reaction has to be carried out at temperatures between 5 °C and 15 °C, because the yield is drastically decreased at higher temperatures.

The saponification of the dithioacyl compound proved to be crucial. Neither in aqueous nor in ethanolic alkaline solution did it yield the dithiol. However, in dry ethanol containing about 2 % of dry HCl the S-protected ester could be obtained, although in a low yield. Further attempts to optimize the reaction were not carried out.

Saponification in diluted aqueous HCl leads to 2,3-dimercaptopropionic acid.

References

- Johannsen B., Seifert S., Syhre R. and Spies H. (1995) Enzymatic hydrolysis of ester group bearing ligands in technetium complexes. *6th Europ. Symp. on Radiopharmacy and Radiopharmaceuticals*. March 5-8, 1995, Graz, Austria (abstr.).
- Seifert S., Syhre R., Hoepfing A., Klostermann K., Spies H. and Johannsen B. (1995) Preparation, characterization and enzymatic hydrolysis of Re/Tc complexes with dimercaptocarboxylic acids and ethyl esters. *This report*, pp. 91-97.
- Pavlic A.A. (1946) *U.S. 2,408,094* (1946)

25. Preparation, Characterization and Enzymatic Hydrolysis of Re/Tc Complexes with Dimercaptocarboxylic Acids and Ethyl Esters

S. Seifert, R. Syhre, A. Hoeping, K. Klostermann¹, H. Spies, B. Johannsen

¹Technische Universität Dresden

Introduction

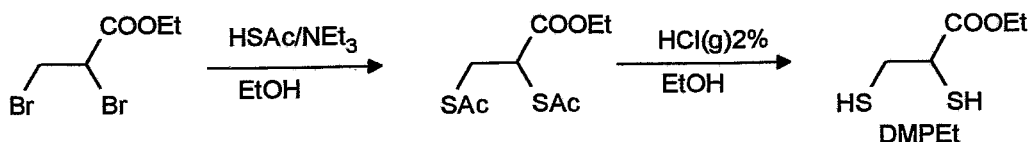
Complexes with ester functionality have now been recognized as valuable parts in the design of certain novel ^{99m}Tc radiopharmaceuticals. Coordinated ester groups should make the otherwise inert technetium complexes potentially susceptible to enzymatic cleavage and thus active *in vivo*.

To study the influence of the number and position of ester and free carboxylic groups in the ligands and the structure of ligand molecules on enzymatic hydrolysis of square-pyramidal oxocomplexes of rhenium(V) and technetium(V) with dithiolates systematic investigations have been performed. Initially the enzymatic hydrolysis of rhenium and technetium complexes containing more than two ester groups was studied with a series of mixed-ligand dimercaptosuccinic acid/ethyl ester complexes (Seifert *et al.*, 1994, 1995). Now the ligands 2,3-dimercapto-1-propionic acid (DMPA), 2,3-dimercapto-1-propionic acid ethylester (DMPEt) and 1,1-dicarboethoxy-2,2-dithioethene (CETE) are included in investigations. Complexes with these ligands and mixed complexes with these ligands and dimercaptosuccinic acid (DMSA) or its diethyl ester (DMSdiet) were prepared and analysed and the hydrolysis behaviour in solutions containing pig liver esterase (PLE), rat plasma (RP) or human plasma (HP) was studied *in vitro* and *in vivo*.

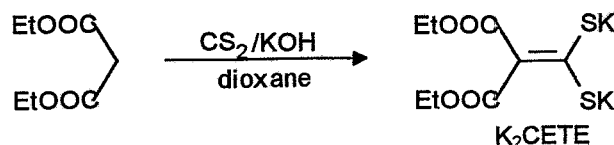
Experimental

Syntheses of ligands

2,3-dimercapto-1-propionic acid ethyl ester (DMPEt) was prepared via 2,3-dithioacylpropionic acid ethyl ester from 2,3-dibromopropionic acid ethyl ester according to the reaction scheme (Hoeping *et al.*, 1995).



1,1-dicarboethoxy-2,2-dithioethene (CETE) was prepared from diethylmalonate and carbon disulphide under aprotic conditions (Gompper *et al.* 1962; Jensen *et al.* 1968).



The reaction was carried out in dioxane with potassium hydroxide. The resulting yellow salt was washed with ether and dried in vacuum. Further purification was not necessary. The structure was established by IR spectroscopy.

Preparation of rhenium and technetium complexes

The [ReO(DMPEt)₂] complex was prepared by ligand exchange reaction of 100 mg of Ph₄As[ReOCl₄] dissolved in 3 ml acetone and 50 mg of the ligand DMPEt also dissolved in 2 ml acetone. After adding a drop of water and slow evaporation of the solvent, an orange microcrystalline residue was separated, washed with water and ether and dried in vacuum.

Yield: 56 mg = 44.4 %, m. p.: 193 - 195 °C.

Elemental analysis: (Found: C, 44.88; H, 3.99; S, 14.34, C₃₄H₃₆O₅S₄ReAs requires C, 44.68; H, 3.97; S, 14.03 %)

IR absorptions: $\nu_{\max}/\text{cm}^{-1}$ (KBr) 960 (Re=O), 1720 (CO)

UV/VIS absorptions: λ_{\max}/nm (acetone) 240 ($\log \epsilon / \text{dm}^3 \text{mol}^{-1} \text{cm}^{-1} = 4.04$); 268 (4.02); 305 (3.98)

Mass spectrum (FAB⁻MS): m/z 529, 531 (M⁺), 329, 331 (ReOS₄) and 297, 299 (ReOS₃)

The Re complex with CETE was formed by ligand exchange via Re gluconate because of the low solubility of the potassium salt of the ligand in acetone. Re gluconate (0.1 mmol) was prepared according to the literature (Noll *et al.*, 1993). A slight excess of K₂CETE (0.3 mmol) dissolved in water or 7 % NaHCO₃ solution was added while stirring. The resulting yellowish-brown precipitate was separated, washed with water and dried in vacuum.

Yield: 62.5 mg = 88 %, m. p.: > 350 °C (dec.)

BzEt₃N[ReO(CETE)₂] was prepared by stoichiometric addition of benzyltriethylammonium chloride to the ethanolic complex solution and precipitation at low temperatures.

M. p.: 63 °C

Elemental analysis: (Found: C, 40.49; H, 5.15; N, 1.76, S, 15.15, C₂₉H₄₂O₉NS₄Re requires C, 40.36; H, 4.90; N, 1.62, S, 14.86 %)

IR absorptions: $\nu_{\max}/\text{cm}^{-1}$ (KBr) 984 (Re=O), 1712 (CO), 1532 (C=C)

UV/VIS absorptions: λ_{\max}/nm (acetone) 241 ($\log \epsilon / \text{dm}^3 \text{mol}^{-1} \text{cm}^{-1} = 3.98$); 268 (3.96); 306 (3.93); 351 (3.87).

Mass spectrum (FAB⁻-MS): m/z 669, 671 (M);

The corresponding ^{99m}Tc complexes were obtained by stannous chloride reduction of pertechnetate in aqueous acetonetic ligand solutions. According to the general procedure 0.025 - 1.0 mg of the ligands, 0.1 mg ascorbic acid, and 7.0 mg NaHCO₃ were dissolved in saline and/or acetone and mixed with 1.0 - 2.0 ml pertechnetate eluate. 1 mg SnCl₂ · 2 H₂O dissolved in 100 μl ethanol was added and after 5 min the reaction solution was filtered through a millipore filter. Optimized ligand amounts are listed in Table 1.

Table 1: Optimized quantities of ligands [μg] for preparing the ^{99m}Tc complexes according to standard preparation conditions

Complex	DMSA	DMSset	DMSdiet	DMPet	DMPA	K ₂ CETE
<u>1</u> ([TcO(DMSdiet) ₂])			250			
<u>2</u> ([TcO(DMSset/DMSdiet)])		650	60			
<u>3</u> ([TcO(DMSA/DMSdiet)])	280		210			
<u>4</u> ([TcO(DMPet) ₂])				250		
<u>5</u> ([TcO(DMPA/DMPet)])				50	35	
<u>6</u> ([TcO(DMSA/DMPet)])	200			25		
<u>7</u> ([TcO(DMSdiet/DMPA)])			60		20	
<u>8</u> ([TcO(CETE) ₂])						1000
<u>9</u> ([TcO(DMSA/CETE)])	100					900

HPLC analyses of preparations and enzyme-incubated samples of complexes were carried out with a PRP-1 column (Hamilton, 250 · 4.1 mm, 10 μm , flow rate 2 ml/min) using a linear gradient system (t[min]/%B): (5/0), (10/50), (5/75) of either 0.1 % trifluoroacetic acid in water (A) and 0.1 % trifluoroacetic acid in acetonitrile (B) or 20 mM phosphate buffer of pH 7.4 (A) and acetonitrile (B). The effluent from the column was monitored by UV absorbance at 340 nm (Re) or γ -detection for the ^{99m}Tc labelled compounds.

For separation of 400 μl samples of ^{99m}Tc complexes a preparative PRP-1 column (305 · 7 mm, 10 μm , flow rate 4 ml/min) was used. After separation of the desired complex fraction, the acetonitrile was removed by vacuum evaporation and aliquots of the neutral phosphate buffer solution were used for incubation studies.

For *in vitro* studies 6 · 10⁻⁷ mol Re complex or 5 - 10 MBq ^{99m}Tc complex were incubated in a sample volume of 1 ml at 37 °C with 100 U pig liver esterase (PLE_{liqu.}, E.C. 3.1.1.1., or PLE immobilized on Eupergit C, Fluka) in phosphate buffer of pH 7.4 or blood plasma of rats (RP) or humans (HP) diluted 1:1 with phosphate buffer of pH 7.4. For reference the complexes alone were incubated in buffer solution.

For *in vivo* studies 0.5 ml complex solution (5 - 10 MBq ^{99m}Tc) was injected into the tail vein of Wistar rats (male, 5 - 6 weeks old). After the incubation time the rats were sacrificed by heart puncture under a light ether anaesthesia and the selected organs were isolated for weighing and counting. After precipitation of proteins with ethanol, centrifugation and filtration blood plasma and urine samples were analysed by HPLC using a PRP-3 column (150 · 4.1 mm) recommended for protein containing samples.

Octanol/water partition coefficients were determined by the shaking flask procedure in phosphate buffer solution of pH 7.4.

FAB⁻ mass spectra were recorded with a MAT 95 spectrometer (Finnigan) by mixing 1 μl sample solution with 5 μl glycerol and bombarding the mixture with caesium atoms of low energy of about 150 eV at room temperature.

Results and Discussion

Square-pyramidal rhenium and technetium complexes of the general formula $[\text{MO}(\text{L}_1\text{L}_2)]$ ($\text{M} = \text{Re}$ or Tc , $\text{L} =$ dimercapto ligand, $\text{L}_1 = \text{L}_2$ or $\text{L}_1 \neq \text{L}_2$) were prepared according to the procedure described above. In mixed-ligand preparations three complexes were formed, which had to be separated by chromatography.

Table 2 summarizes characteristic data for ^{99m}Tc complexes. As shown in the table, the R_f values of complexes containing free carboxylic groups shift to shorter times due to the dissociation of free carboxylic groups at pH 7.4. In these cases the analysis time can be shortened and the elution results in sharper peaks than in 0.1 % trifluoroacetic acid (pH 2.0).

Table 2: Chemical and biological characterization of ^{99m}Tc complexes 1 - 9

Comp. No.	log P (oct./wat.) pH 7.4	HPLC (PRP-1) R_t [min]		Enzymatic cleavage			
		pH 2.0	pH 7.4	in vitro PLE	in vitro RP	in vitro HP	in vivo rat
<u>1</u>	0.7	13.0	11.5	+	+	-	+
<u>2</u>	-1.5	11.0/11.6	7.5	+	+	-	+
<u>3</u>	< -2.0	9.2/9.7	5.2/5.9	-	-	-	-
<u>4</u>	0	12.1	10.0	+	+	+	+
<u>5</u>	< -2.0	9.9	5.4	+	+	+	+
<u>6</u>	< -2.0	8.7	3.9	+	+	+	+
<u>7</u>	< -2.0	10.4	6.1, 6.6	+	+	-	+
<u>8</u>	0.8	16.5	13.2	+	+	+	+
<u>9</u>	< -2.0	9.8	5.7, 6.0	+	+	+	+

The hydrolysis behaviour of complexes 1 - 3 is described in the above mentioned articles. The DMPEt complexes 4 - 6 are hydrolysed with PLE, RP and HP. Complex 4 shows a similar behaviour as known of Tc-ECD (Walovitch *et al.*, 1989). After a fast hydrolysis of the first ester group follows a slow second hydrolysis step with PLE (Fig. 1). With RP complex 4 hydrolyses faster to the diacid complex. Hydrolysis is completed after 60 minutes incubation time.

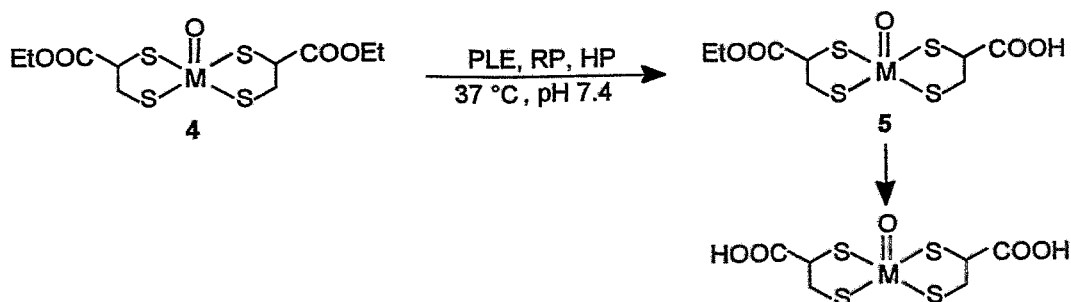


Fig. 1: Enzymatic cleavage of 4 with PLE, RP and HP

In contrast to the above observed result hydrolysis proceeds quickly and completely to the diacid complex if the monoacid complex **5** is incubated with PLE or RP.

Experiments with **5** and **6** show that neither DMPA nor DMSA in combination with DMPET in the complex molecule hinder hydrolysis of the single ester group. The results differ from those obtained with DMS ester complexes. As is known, no hydrolysis was observed with the ligand combination DMSA/DMSdiet in the complex molecule. On the other hand, a DMPA ligand does not prevent hydrolysis of the DMSdiet ligand in complex **7**. As expected from previous studies, only one of the two ester groups is hydrolysed with PLE and RP in this case.

The complexes with CETE (**8** and **9**), however, show quite a different hydrolysis behaviour.

After dissolution in a small quantity of DMSO/propylene glycol and dilution with phosphate buffer the rhenium complex **8** with CETE of the formula $[\text{ReO}(\text{CETE})_2]$ is hydrolysed with PLE to various hydrolysis products. Since it was impossible to prepare reference mixed ligand complexes with corresponding half-ester or diacid ligand molecules because of instability, FAB-mass spectra of these solutions were performed to analyse hydrolysis products. Moreover, hydrolysis products were separated by HPLC into several fractions and also analysed by FAB-MS.

After 2 h incubation with PLE, two hydrolysis steps were observed with both HPLC and FAB-MS. HPLC analysis results in products which are eluted at a PRP-3 column with R_t values of 4.8 and 2.8 min. and the mass spectra show m/z values of 641/643 and 613/615 indicating a first and second hydrolysis step (Fig. 2a-d). The $^{99\text{m}}\text{Tc}$ complex solution was hydrolysed to the same hydrolysis products, but the cleavage proceeded faster. The results obtained with Re and $^{99\text{m}}\text{Tc}$ complexes and PLE were confirmed by *in vivo* hydrolysis studies with the corresponding $^{99\text{m}}\text{Tc}$ complex solution. 10 min post injection of **8** in rat plasma, a dominant peak at about 5 min is found. 60 min p. i. products with R_t values of 2.8 and 1.0 min were observed in addition to that peak.

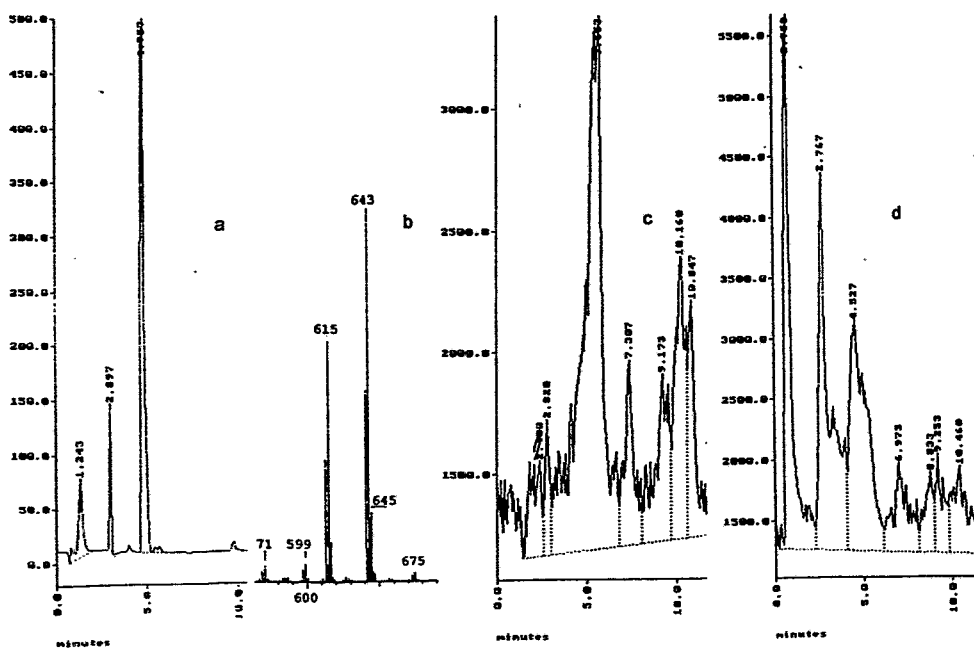


Fig. 2a-d: Enzymatic cleavage of Re and $^{99\text{m}}\text{Tc}$ CETE complexes with PLE; a: HPLC of Re complex solution after 2 h incubation with PLE at 37 °C; b: FAB mass spectrum of this solution; c: HPLC of a rat plasma sample of an *in vivo* hydrolysis study of $^{99\text{m}}\text{Tc}$ CETE complex 10 min p. i.; d: 60 min p. i.

The incubation with RP diluted 1:1 with buffer, however, resulted in only one hydrolysis step. The hydrolysis product increased clearly with time, but a second hydrolysis step was not observed (Fig. 3).

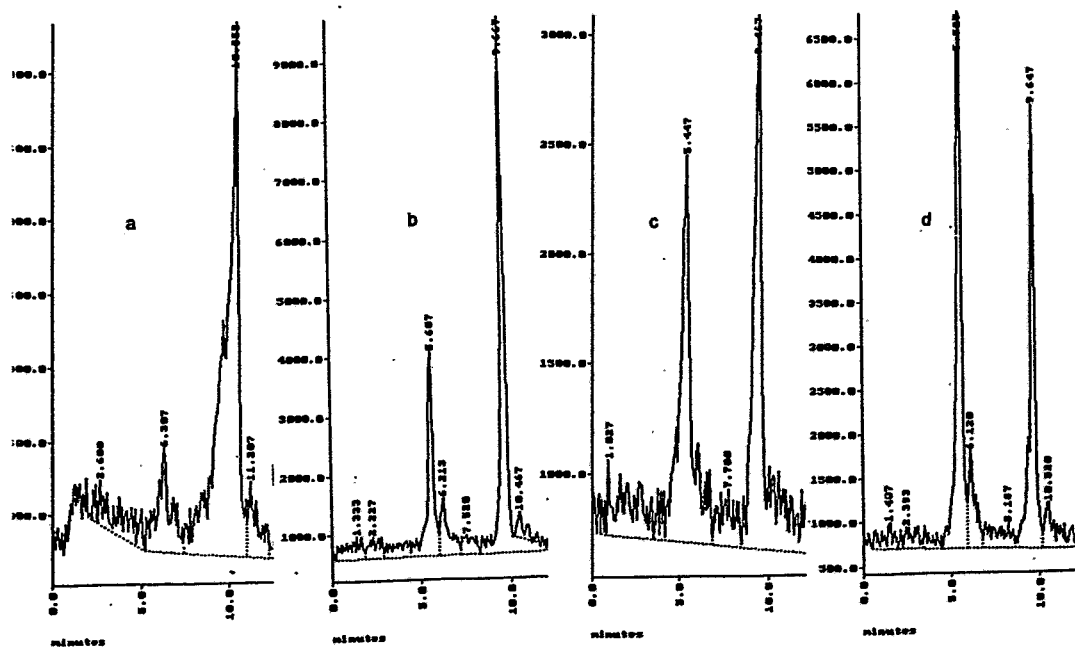


Fig. 3: Enzymatic hydrolysis of ^{99m}Tc -CETE complex **8** with 1:1 diluted RP at 37 °C as a function of time (a: 10 min, b: 1 h, c: 2 h, d: 3 h incubation time)

HPLC analyses of rhenium complex samples which were incubated with PLE for 3 days resulted in many peaks. In addition to real hydrolysis peaks, the mass spectra also contain other fragmentation products generated by cleavage of -COOEt (decarboxylation) and/or Et groups. The products found after long-time incubation with PLE are listed in Table 3.

Table 3: Products found after incubation of the rhenium CETE complex with liquid and immobilized PLE for 3 d at 25 °C

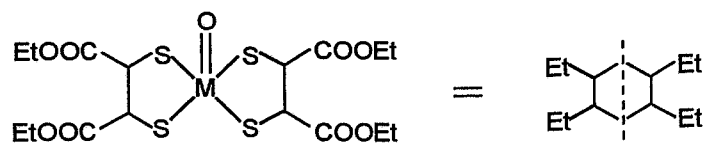
Solution	HPLC (R_t [min])	FAB-MS (m/z)
$[\text{ReO}(\text{CETE})_2]^-$	12.0	<u>669/671</u> (M), 467/469
$[\text{ReO}(\text{CETE})_2]^-$ + PLE _{liqu.}	12.0, 7.9, 7.1, 6.7, 6.2, 4.9, 4.3, 3.0	669/671 (M), 641/643 (M - Et), 613/615 (M - 2 Et), 497/499 (M - 2 COOEt - Et + 3 H or M - CH ₂ =C-(COOEt) ₂) 467/469 (M - 2 COOEt - 2 Et + H or M - S-CH=C-(COOEt) ₂) 439/441 (M - S-CH=C-(COOEt) ₂ - Et)
$[\text{ReO}(\text{CETE})_2]^-$ + PLE _{imm.}	11.0, 9.9, 9.1, 7.8, <u>6.9</u> ,	
1. fraction	9.0	497/499
2. fraction	7.8	641/643, 467/469
3. fraction	6.9, 7.2	671/673 (M + 2 H), 627/629, 581/583, <u>497/499</u>

Complex **9** is also hydrolysed with PLE, but cleavage proceeds slowly (about 50 % after 4 h) to a product with R_t 1.1 min. The composition of this compound is unknown but the low R_t value points to an acid complex, indicating hydrolysis of the CETE ligand molecule in addition to DMSA in the mixed-ligand complex.

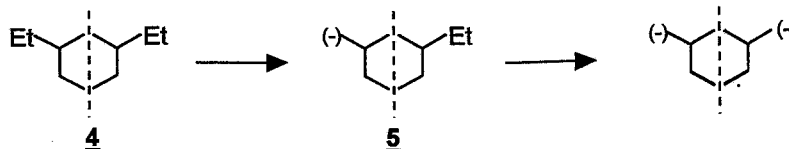
Complexes **8** as well as **9** are stable in phosphate buffer solution at 37 °C for more than 5 h. The cleavage of complexes, therefore, is really caused by enzymes.

To sum up, some hydrolysis rules can be established:

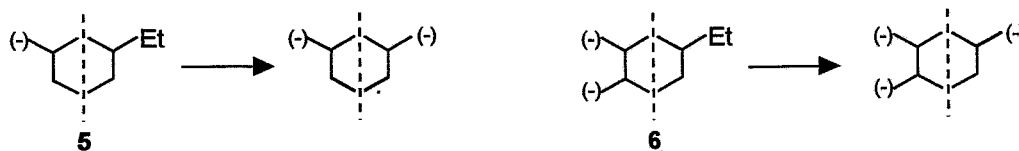
For better understanding symbols of individual complexes with different numbers of ester (Et) and free carboxylic groups (-) are introduced, e. g. for complex **1**: $[\text{MO}(\text{DMSdiet})_2]$ (M = Re, Tc):



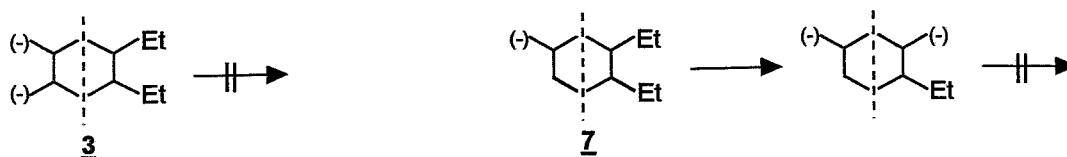
- Complexes like complex **4** with two ester functionalities (one at each of the bidentate ligands) show a hydrolysis behaviour similar to the neutral complex Tc-ECD. Hydrolysis proceeds successively at different rates despite the negative charge of the complex core and the absence of an ethylene bridge connecting both ligands as realized in the ECD ligand.



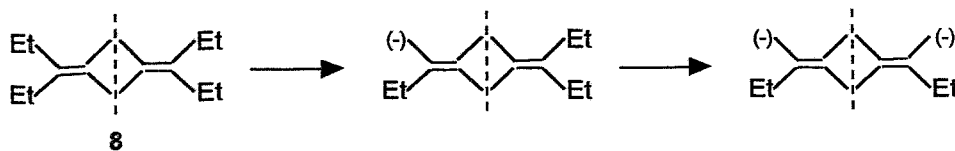
- In mixed-ligand complexes with both free carboxylic and ester groups in the bidentate ligands (**5** and **6**), hydrolysis of the single ester group is not prevented either by one (DMPA) or two (DMSA) free carboxylic groups in the complex.

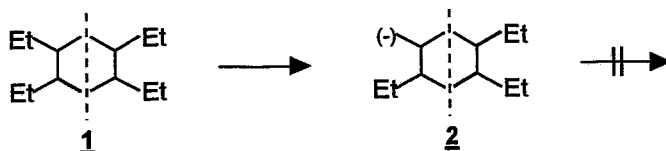


This is in contrast to the behaviour of complex **3**. As is known from previous studies, no hydrolysis was observed in this case for inexplicable reasons. In complex **7**, however, the DMPA ligand containing only one carboxylic group was unable to hinder hydrolysis of the DMSdiet ligand to the DMSset ligand. The second hydrolysis step (DMSset to DMSA) was not observed in accordance with the results obtained in previous studies.



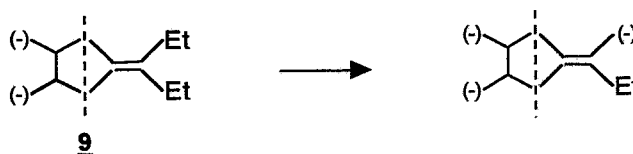
- Complexes containing geminal ester functionalities linked by a C=C double bond with the donor atoms of the ligand are hydrolysed up to a second step, but hydrolysis is stopped when one of the two ester groups of each ligand is hydrolysed.





Complex **8** shows significant differences in hydrolysis behaviour in comparison with the complex $[\text{Re}/\text{TcO}(\text{DMSdiEt})_2]$ (**1**), which also contains four ester groups. While only one ester group in this complex is directly hydrolysed with PLE or RP, the cleavage of complex **8** proceeds up to a second hydrolysis step. This is possibly caused by the geminal mercapto and carboxylic groups and/or the C=C double bond in the ligand molecules. Thus the two ligands form a "conjugated" four-ring chelate system with a different electron configuration than in normal five-ring chelates. This results in a shift of the $\text{Re}=\text{O}$ vibration to lower energies (984 cm^{-1}) caused by stabilizing the four rings by electron withdrawal from the $\text{Re}=\text{O}$ bond and the C=C bond. That could be the reason for the higher reactivity against enzymes and for further cleavage in PLE-containing solutions and also for decarboxylation.

- A bidentate ligand with two free carboxylic groups in the complex does not prevent hydrolysis of a ligand with geminal ester groups. The second ester functionality is not hydrolysed, as was observed also for other complexes.



Complex **9** is hydrolysed like complex **6**, but the cleavage proceeds slower than for complex **8**. Nevertheless, this behaviour also demonstrates a higher reactivity of the four ring chelate in comparison with a DMS diethyl ester ligand as in complex **3**.

In conclusion, we can postulate the following:

- Coordinated diesters are to a great extent hydrolysed as are diesters of organic compounds.
- The negative charge of the complex core does not influence hydrolysis.
- Enzymatic hydrolysis on one side of the complex is generally not influenced by the other side.
- In special cases (complex **3**) low structural differences are responsible for exceptional hydrolysis behaviour.

References

- Gompper R. and Töpfl W. (1962) Substituierte Dithiocarbonsäuren und Ketenmercaptale. *Chem. Ber.* **95**, 2861-2870.
- Hoepping A. and Spies H. (1995) Preparation of 2,3-dimercaptopropionic acid ethyl ester. *This report*, pp. 89-90.
- Jensen K.A. and Henriksen L. (1969) Studies of thioacids and their derivatives, XIV. Reactions of carbon disulfide with active methylene compounds. *Acta Chem. Scand.* **22**, 1107-1128.
- Noll B., Kolbe U., Noll St. and Spies H. (1992) Rhenium(V) gluconate as precursor for preparation of rhenium(V) complexes. *Annual Report 1992*, Institute of Bioinorganic and Radiopharmaceutical Chemistry, FZR 93-12, pp. 115-118.
- Seifert S., Syhre R., Spies H. and Johannsen B. (1994) Preparation, characterization and enzymatic hydrolysis of mixed ligand Re/Tc complexes with DMSA and DMS ethyl esters. *Annual Report 1994*, Institute of Bioinorganic and Radiopharmaceutical Chemistry, FZR-73, pp. 38-45.
- Seifert S., Syhre R., Spies H. and Johannsen B. (1995) Enzymatic cleavage of technetium and rhenium complexes with DMSA ester ligands. In: *Technetium and Rhenium in Chemistry and Nuclear Medicine 4* (M. Nicolini, G. Bandoli, U. Mazzi Eds.) Padova, pp. 437-440.
- Walovitch R.C., Hill T.C., Garrity S.T., Cheesman E.H., Burgess B.A., O'Leary D.A., Watson A.D., Ganey M.V., Morgan R.A. and Williams S.J. (1989) Characterization of technetium-99m L,L-ECD for brain perfusion imaging, part 1: pharmacology of technetium-99m ECD in nonhuman primates. *J. Nucl. Med.* **30** 1892-1901.

26. Preparation, Characterization and Enzymatic Hydrolysis of Re/Tc Complexes with Mercaptocarboxylic Acids and their Ethyl Esters

S. Seifert, R. Syhre, M. Friebe, K. Klostermann¹

¹Technische Universität Dresden

Oxorhenium(V) and oxotechnetium(V) complexes with ester bearing dimercapto compounds are enzymatically hydrolysed in a characteristic manner as described in preceding articles (Seifert *et al.*, 1994, 1995). Mixed-ligand "3+1" complexes containing an ester moiety at the monodentate ligand are generally hydrolysed (Seifert *et al.*, 1993). In order to extend the enzymatic cleavage to another kind of mixed ligand complexes, Re and Tc complexes with DMS esters and mercaptocarboxylic acid esters, it was necessary to prepare precursor complexes with monomercaptocarboxylic acids or its ethyl esters alone. Up to now the structure of such complexes is not sufficiently described (De Pamphilis *et al.*, 1978; Sundrehagen *et al.*, 1980). Because of difficulties at crystallization, the complexes were characterized in solution by chromatography and mass spectrometry, and their hydrolysis behaviour was studied.

Experimental

The following ligands were used for complexation reactions:

- mercaptoacetic acid and its ethyl ester (MAA and MAE)
- 2-mercaptopropionic acid and its ethyl ester (2-MPA and 2-MPE)
- 3-mercaptopropionic acid and its ethyl ester (3-MPA and 3-MPE)
- 2-mercaptosuccinic acid and its mono- and diethyl ester (MSA, MSet, MSdiet).

Both mercaptopropionic acid ethyl esters were prepared from the acids by esterification with ethanol in chloroform solution. 0.1 mol mercaptopropionic acid and 0.175 mol ethanol were dissolved in 40 ml chloroform and 5 g Dowex-H⁺ cation exchanger was added. After 15 h stirring and refluxing of the mixture and removing water using a water separator, the ion exchanger was filtered off and the solvent was evaporated. The crude products were purified by vacuum distillation (b. p.: 29 - 30 °C (2-MPE); 44 - 46 °C (3-MPE) at 4 - 5 mm Hg, yields 90 - 93 %).

2-mercaptosuccinic acid diethyl ester was prepared by refluxing 66.6 mmol MSA dissolved in 100 ml ethanol and passing dry HCl through the reaction solution for 4 h. After evaporation of ethanol the crude product was purified by vacuum distillation (b. p.: 100 - 105 °C at 34 mm Hg, yield 12.4 g = 90.7 %).

2-mercaptosuccinic acid β -monoethylester was obtained in three steps from MSA according to Friebe (dissertation 1995).

The rhenium complexes were prepared by dissolving 5 mg of Ph₄As[ReOCl₄] in 1 ml acetone and adding 5 mg (5 - 8 equivalents) of the ligands also dissolved in acetone and stirring the reaction solution. After some minutes 2 - 3 drops of water were added. The colour of the solution changed immediately from greyish-pink to intensive red when MA, MAE, 2-MP or 2-MPE and the mercaptosuccinic acid ester ligands were used and to green when 3-MP or 3-MPE complexes were formed. The prepared complexes were analysed by HPLC and FAB⁻MS and the enzymatic hydrolysis with pig liver esterase (PLE) was studied as described in the previous article.

For preparing the ^{99m}Tc complexes 1 - 2 ml pertechnetate eluate containing 7.0 mg sodium hydrogen carbonate, 0.1 mg ascorbic acid, 5 mg of the ligand and, when using ester ligands, 0.2 ml acetone were reduced with 1.0 mg stannous chloride dissolved in 100 μ l ethanol. After 5 min the reaction solution was filtered through a millipore filter and the organic solvents were evaporated in vacuum. If necessary, the residue was redissolved for hydrolysis studies by adding propylene glycol or DMSO.

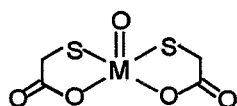
HPLC analysis of Re and Tc complexes with mercaptocarboxylic acids and their ethyl esters was performed using a PRP-1 column (250 x 4.1 mm, 10 μ m, flow rate 2 ml/min) in connection with a linear gradient system (t[μ min]/%B): (5/0), (10/50), (5/75) of 20 mmol phosphate buffer pH 7.4 (A) and acetonitrile (B).

FAB⁻ mass spectra were recorded with a MAT 95 spectrometer (Finnigan) by mixing 1 μ l sample solution with 5 μ l glycerol and bombardment with cesium atoms of low energy of about 150 eV at room temperature.

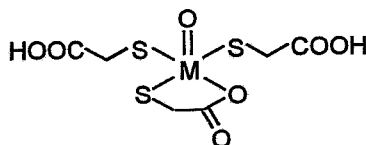
Results and Discussion

As expected from the significant differences in lipophilicity between acid and ester ligands, the R_t values of the complexes vary from 1 to 14 minutes as shown in Table 1. No differences in R_t values were found between rhenium and technetium complexes.

Generally the molecule ions and sometimes fragmentation products were found in FAB-MS. Moreover, the mass spectra show that several complexes are formed with individual ligands. With acid ligands containing one or two free carboxylic groups it was found that complexes with both monodentately and bidentately bound ligands are formed. Thus, with MAA, the complexes $[\text{ReO}(\text{MAA}_b)_2]^-$ (**6a**) as well as $[\text{ReO}(\text{MAA}_m)_2/\text{MAA}_b]^-$ (**6b**) were detected in the mass spectrum (Fig. 1).



$[\text{ReO}(\text{MAA}_b)_2]^-$ (**6a**), m/z 381, 383:



$[\text{ReO}(\text{MAA}_m)_2/\text{MAA}_b]^-$ (**6b**), m/z 473, 475

Fig. 1: Two forms of Re-MAA complexes found in FAB-MS. MAA_m : monodentately bound ligand (via mercapto group), MAA_b : bidentately bound ligand (via mercapto and carboxylic group)

As shown in Table 1, the same results could be found using MPA or MSA and also MSet for complexing rhenium.

Table 1: HPLC and FAB-MS data of Re complexes **1 - 9**

Complex	HPLC (R_t [min])	FAB-MS (m/z)
1 Re-MAE	10.9 9.6	529, 531 ($[\text{ReO}(\text{MAE})_2/\text{MAA}_b]^-$) 501, 503 ($[\text{ReO}(\text{MAE})/\text{MAA}_m/\text{MAA}_b]^-$) 473, 475 ($[\text{ReO}(\text{MAA}_m)_2/\text{MAA}_b]^-$) 381, 383 ($[\text{ReO}(\text{MAA}_b)_2]^-$)
2 Re-2-MPE	10.2	571, 573 ($[\text{ReO}(2\text{-MPE})_2/2\text{-MPA}_b]^-$) 543, 545 ($[\text{ReO}(2\text{-MPE})/\text{2-MPA}_m/2\text{-MPA}_b]^-$)
3 Re-3-MPE	11.8	571, 573 ($[\text{ReO}(3\text{-MPE})_2/3\text{-MPA}_b]^-$) 499, 501 ($\text{M}^- - \text{COOEt}$)
4 Re-MSdiet	14.3 11.7 9.5	787, 789 ($[\text{ReO}(\text{MSdiet})_2/\text{MSet}]^-$) 759, 761 ($[\text{ReO}(\text{MSdiet})/\text{MSet}_m/\text{MSet}_b]^-$) 553, 555 ($[\text{ReO}(\text{MSet})_2]^-$)
5 Re-MSet	9.5	731, 733 ($[\text{ReO}(\text{MSet}_m)_2/\text{MSet}_b]^-$) 553, 555 ($[\text{ReO}(\text{MSet})_2]^-$)
6 Re-MAA	1.6 5.4	473, 475 ($[\text{ReO}(\text{MAA}_m)_2/\text{MAA}_b]^-$) 381, 383 ($[\text{ReO}(\text{MAA}_b)_2]^-$)
7 Re-2-MPA	8.4	409, 411 ($[\text{ReO}(2\text{-MPA}_b)_2]^-$) 515, 517 ($[\text{ReO}(2\text{-MPA}_m)_2/2\text{-MPA}_b]^-$)
8 Re-3-MPA	1.2 3.7	515, 517 ($[\text{ReO}(3\text{-MPA}_m)_2/3\text{-MPA}_b]^-$) 409, 411 ($[\text{ReO}(3\text{-MPA}_b)_2]^-$)
9 Re-MSA	1.0	647, 649 ($[\text{ReO}(\text{MSA}_m)_2/\text{MSA}_b]^-$) 497, 499 ($[\text{ReO}(\text{MSA}_b)_2]^-$)

An unexpected reaction was observed at the ligand exchange reaction between $[\text{ReOCl}_4]^-$ and mercaptocarboxylic acid ethyl esters. With all ethyl ester ligands listed, complexes were formed containing one bidentately bound mercaptocarboxylic acid ligand as well as two monodentately bound ester ligands. The formation of rhenium or technetium complexes with four ester ligands was not found. The tendency towards hydrolysis of ester ligands during complex formation was confirmed by the existence of complex species containing one ester ligand and two acid ligands or only acid ligands which were detected in the reaction solution. Studies of the stability of mercaptocarboxylic acid ethyl esters in acidic ethanolic or acetonic solutions showed that the substances are stable over 24 h and more. The hydrolysis observed during complex formation is probably due to steric reasons or because of the influence of protons which become free during complex formation. To reduce the proton effect, the acidic acetonic complex solution formed during the ligand exchange reaction starting with $[\text{ReOCl}_4]^-$ was neutralized immediately after complex formation. The FAB mass spectrum of such a solution contains $[\text{ReO}(\text{MAE})_2/\text{MAA}_b]^-$ as the main product; that means that further hydrolysis was stopped but the formation of a complex with four ester ligands was not observed. The ligand-exchange reaction starting with rhenium gluconate in a neutral or weak alkaline solution results in nearly the same product distribution spectrum (Fig. 2).

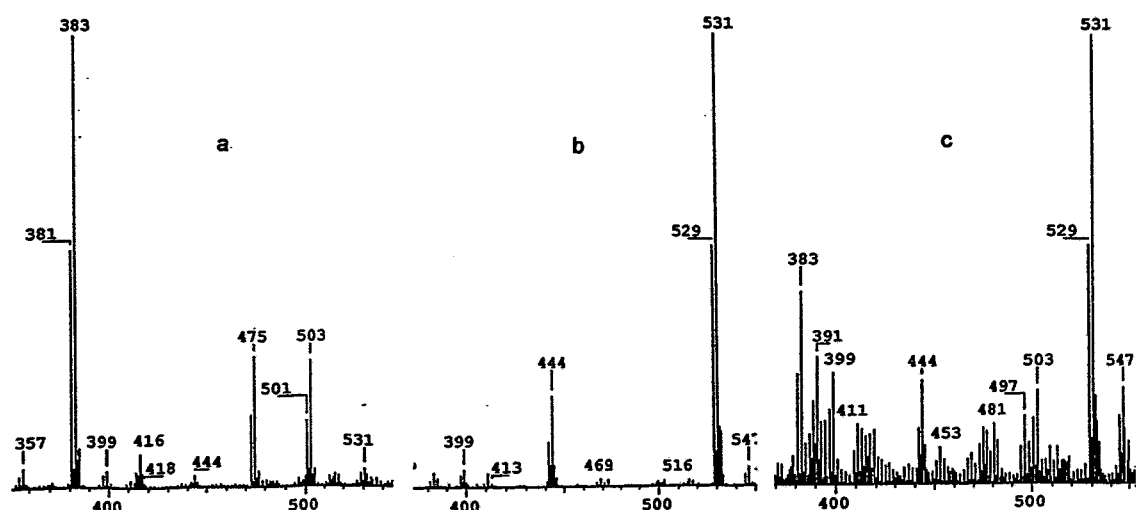


Fig. 2: FAB mass spectra of rhenium complex solutions formed by ligand exchange reaction (a): with $[\text{ReOCl}_4]^-$ and MAE in acidic acetonic solution, (b): the same as (a), immediately neutralized and (c): with Re gluconate and MAE in neutral solution

While the $[\text{ReO}(\text{MAE})_2/\text{MAA}_b]^-$ anion hydrolyses in acidic solution, the neutral complex solution is stable for several days. The R_t values of the corresponding $^{99\text{m}}\text{Tc}$ complexes prepared in neutral solution are in accordance with the values determined for Re complexes so that the same composition should be assumed.

Enzymatic hydrolysis of complexes with the monoester ligands MAE and MPE results in a complete cleavage of ester groups. Products obtained from the complexes **1** and **3** are eluted in HPLC at pH 7.4 with R_t values between 1.0 and 1.5 minutes indicating the presence of free carboxylic groups. In these cases the configuration of ester complexes remains. Thus, $[\text{ReO}(\text{MAE})_2/\text{MAA}_b]^-$ converts to $[\text{ReO}(\text{MAA}_m)_2/\text{MAA}_b]^-$. By contrast complex **2** is hydrolysed to a product which is eluted after 8.4 min. In this case the configuration is changed and a complex with two bidentately bound ligands is formed. This configuration seems to be favoured in solution and is also found in the mass spectrum as the dominant product.

Complexes **1** - **3** are completely hydrolysed with PLE to the acid complexes. Complex **4** by contrast is hydrolysed only to complex **5**. The rhenium complex **5** does not undergo hydrolysis with PLE. Fig. 3 summarizes the hydrolysis behaviour of rhenium and technetium thiomalic acid ethyl ester complexes with PLE.

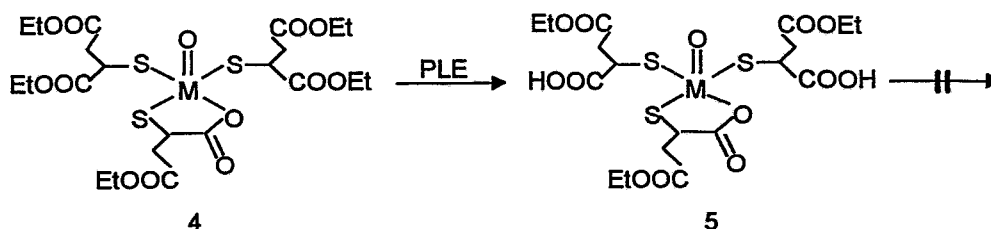


Fig. 3: Enzymatic hydrolysis of complex **4** with PLE in phosphate buffer of pH 7.4

The resulting complex **5** shows the same retention time at HPLC as the reference complex prepared with β -monoethyl ester ligand. Nevertheless, it is not clear which of the ethyl ester groups are hydrolysed and which not. While the rhenium complex **5** is very stable also in PLE solution, during preparation of the ^{99m}Tc complex a compound is formed which is eluted earlier than complex **5**. This compound is the main product after incubation with PLE and increases with time (Fig. 4). The low shift of the R_t value could point to a partial hydrolysis of the ester group of the bidentately bound ligand. Further long-time incubation studies using rhenium complex **5** and FAB-MS analysis will be performed to decide this question.

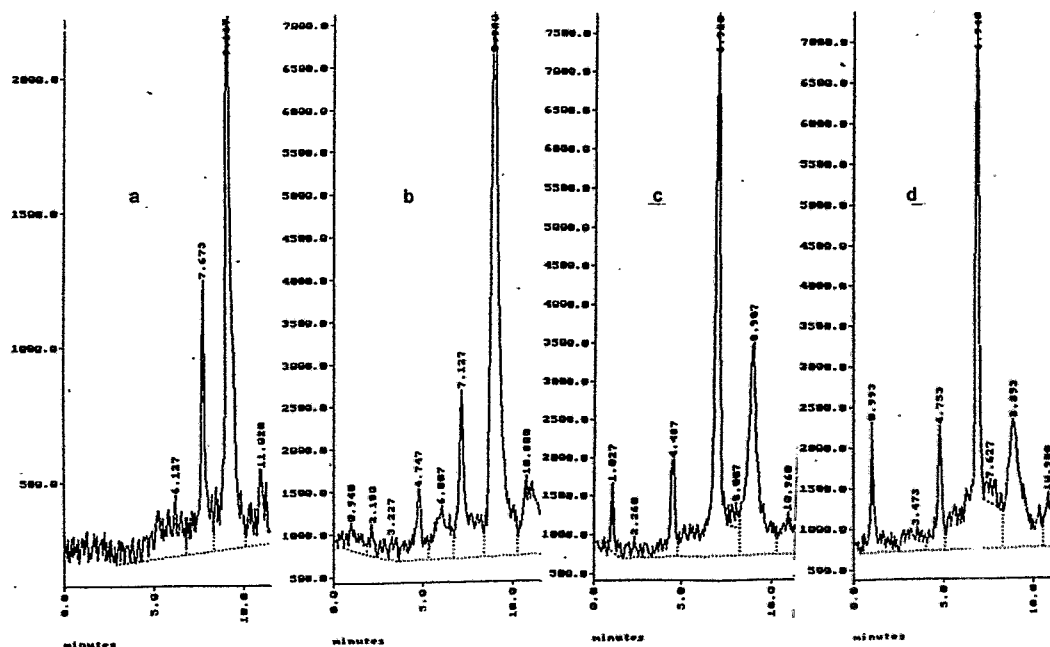


Fig. 4: HPLC patterns of the ^{99m}Tc complex **5** before and after incubation with PLE. a: after preparation, b: after 3 h without PLE, c: after 1 h, d: after 3 h with PLE in phosphate buffer pH 7.4 at 37 °C.

References

- DePamphilis B.V., Jones A.G., Davis M.A. and Davison A. (1978) Preparation and crystal structure of oxotechnetium-bis-(thiomercaptoacetate). *J. Am. Chem. Soc.* **100**, 5570-5571.
- Seifert, S., Syhre, R., Spies, H. and Johannsen, B. (1994) Preparation, characterization and enzymatic hydrolysis of mixed ligand Re/Tc complexes with DMSA and DMS ethyl esters. *Annual Report 1994*, Institute of Bioinorganic and Radiopharmaceutical Chemistry, FZR-73, pp. 38-45.
- Seifert S., Syhre, R., Hoepfing, A., Spies, H., Klostermann, K. and Johannsen, B. (1995) Preparation, characterization and enzymatic hydrolysis of Re/Tc complexes with dimercapto-carboxylic acids and ethyl esters. *This report*, pp. 91-97.

Seifert, S., Syhre, R., Fietz, Th. and Spies, H. (1993) Hydrolysis studies of ester substituted oxo-rhenium(V) complexes. *Annual Report 1993*, Institute of Bioinorganic and Radiopharmaceutical Chemistry, FZR-32, pp. 106-110.

Sundrehagen, E. and Nakken, K.F. (1980) The formation of technetium-99m complexes with 2-thio-carboxylic acid derivatives. *Int. J. Appl. Radiat. Isot.* **31** (10), 615-618.

27. Enzymatic Hydrolysis of Mixed Ligand Complexes of Rhenium and Technetium with DMS Ethyl Esters and Mercaptocarboxylic Acid Ethyl Esters and their Acids

S. Seifert, R. Syhre, K. Klostermann¹

¹ Technische Universität Dresden

Introduction

In preceding articles the enzymatic hydrolysis of ester complexes with dimercapto ligands and with mercapto ligands containing various numbers of ester groups was described (Seifert *et al.*, 1994 and in this report). The results have shown that complexes with DMS diethyl ester and DMS monoethyl ester or combinations of them and also combinations with DMSA react in a quite different way with PLE than complexes with mercaptocarboxylic acid ethyl esters like mercaptoacetic acid ethyl ester (MAE) or mercaptopropionic acid ethyl ester (MPE). It should be of interest to study the hydrolysis behaviour of mixed ligand complexes with both types of ligands to find out criteria responsible for the enzymatic cleavage of ester group bearing complex compounds. For this purpose rhenium complexes with MAE or MPE were prepared, analysed and transferred into mixed-ligand complexes with DMSdiet, DMSset or DMSA as co-ligands. Formation of the desired complexes was controlled by fast atom bombardment analysis. Moreover, a one-pot reaction for preparing the corresponding ^{99m}Tc complexes was worked out.

Experimental

The mixed ligand rhenium complexes were prepared by stoichiometric reaction of one equivalent of rhenium mercaptocarboxylic acid complexes or its ethyl ester complexes and one equivalent of DMS ethyl esters or DMSA. The rhenium complexes with the monodentate ligands were synthesized as described in the article above. The ligand exchange between mercaptocarboxylic acid and DMSA or its esters in acetonic/aqueous solution is detectable by a colour change from pink or green to orange. The reaction proceeds nearly quantitatively and is controlled by HPLC and mass spectrometry.

The corresponding ^{99m}Tc complexes were obtained by stannous chloride reduction of pertechnetate in aqueous acetonic ligand solutions. According to the general procedure 0.25 - 4.0 mg of the ligands, 0.1 mg ascorbic acid, and 7.0 mg NaHCO₃ are dissolved in saline and/or acetone and mixed with 1.0 - 2.0 ml pertechnetate eluate. 1 mg SnCl₂ · 2 H₂O dissolved in 10 µl ethanol is added and after 5 min the reaction solution is filtered through a millipore filter. The separation of mixed ligand complexes from the reaction mixture by HPLC is used as described in previous articles. The following ligand quantities needed for preparation (Table 1) were optimized empirically.

Table 1: Optimized quantities of ligands [µg] for preparing the ^{99m}Tc complexes

Complex	DMSA	DMS et*	DMS diet	MAE MPE	MAA[µg] MPA
<u>1</u> ([TcO(DMSdiet/(MAE) ₂])			120	2800	
<u>2</u> ([TcO(DMSset/(MAE) ₂])		1000		2000	
<u>3</u> ([TcO(DMSA/(MAE) ₂])	350			2000	
<u>4</u> ([TcO(DMSdiet/MAA])			120		2000
<u>5</u> ([TcO(DMSset/MAA)])		1000			2000
<u>6</u> ([TcO(DMSA/(2-MPE) ₂])	250			4000	
<u>7</u> ([TcO(DMSA/(3-MPE) ₂])	250			4000	

*DMS ethylester contains DMS diethylester

The HPLC analyses of preparations and incubated samples of complexes and FAB-MS analyses were carried out as described in previous articles. For *in vitro* and *in vivo* hydrolysis studies the same procedure is used as carried out above.

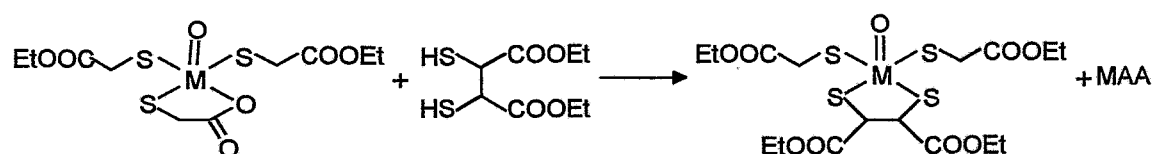
Results and Discussion

In Table 2 the results of FAB-MS analyses of rhenium complex solutions are summarized. Caused by the reaction of $[\text{ReOCl}_4]^-$ with MAE or MAA in acetonic solution, partially hydrolysed species of MAE complexes or MAA complexes are formed. The following ligand-exchange reactions to mixed-ligand complexes proceed with all these species and result in mixtures of complexes listed in Table 2.

Table 2: FAB mass spectrometry data of Re complexes **1**, **3** and **4** and their by-products contained in the reaction solution after ligand exchange of Re-MAE or Re-MAA with DMSA or DMS esters (main products are underlined)

Complex	m/z (found)	Formula
1	<u>675/677</u>	$[\text{ReODMSdiet}/(\text{MAE})_2]^-$
	<u>647/649</u>	$[\text{ReODMSdiet}/(\text{MAE}/\text{MAA})^-]$
	619/621	$[\text{ReODMSdiet}/(\text{MAA}_m)_2]^-$
	527/529	$[\text{ReODMSdiet}/\text{MAA}_b]^-$
3	<u>619/621</u>	$[\text{ReODMSA}/(\text{MAE})_2]^-$
	561/563	$[\text{ReO}(\text{DMSA})_2]^-$
4	<u>527/529</u>	$[\text{ReODMSdiet}/\text{MAA}_b]^-$
	619/621	$[\text{ReODMSdiet}/(\text{MAA}_m)_2]^-$

The preparation of rhenium complex **1** carried out with immediately neutralized Re-MAE solution shows the complex ion $[\text{ReODMSdiet}/(\text{MAE})_2]^-$ as the main product in FAB-MS. That means that the bidentately bound mercaptoacetic acid ligand in the complex $[\text{ReO}(\text{MAE})_2\text{MAA}]^-$ is substituted by the dimercaptosuccinate molecule according to the following reaction:



In the same way DMSA reacts with Re-MAE complex solution and complex **3** is formed. The formation of complex **4**, however, can take place by both kinds of exchange. The results obtained in the preparation of Re-MAA complexes described in the article above show that MAA bidentately bound to rhenium or technetium is favoured over monodentately bound ligands and is, in fact, the dominant complex $[\text{ReODMSdiet}/\text{MAA}_b]^-$ in complex **4** solutions.

The chromatographic behaviour of $^{99\text{m}}\text{Tc}$ complexes is in accordance with that of the rhenium complexes so that the same configuration of these complexes is assumed.

While the complexes **1** - **7** are stable in neutral solution, especially complexes **3**, **6** and **7** are hydrolysed in acidic solution. The rhenium complex solutions prepared in acidic acetonic solution have therefore to be immediately neutralized.

Enzymatic hydrolysis studies with the complexes listed in Table 3 demonstrate that monoester ligands like MAE or MPE are quantitatively hydrolysed, independently of the other coordinated ligand molecules. Thus, complex **1** is hydrolysed in a first fast step to complex **4** and then to complex **5**. As is known from previous studies, the DMSet ligand is not further hydrolysed.

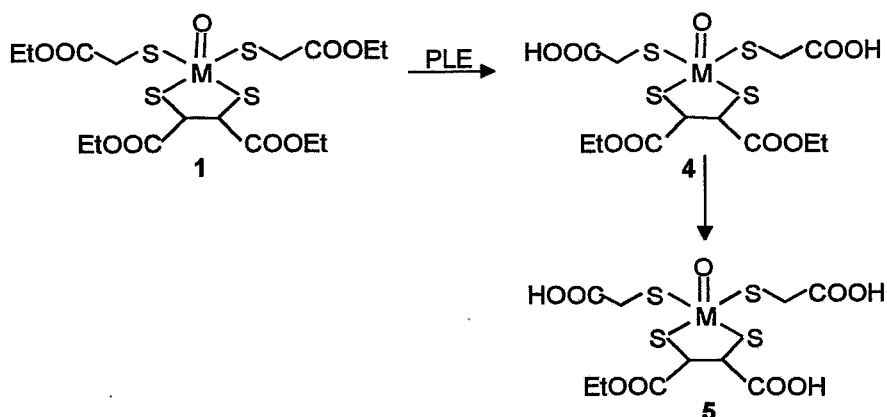


Table 3: Characterization of the $^{99\text{m}}\text{Tc}$ complexes

Complex	R_t [min]		Enzymatic cleavage	
	pH 2.0	pH 7.4	in vitro (PLE)	in vivo (rat)
<u>1</u>	13.5	11.2	+	+
<u>2</u>	11.0	7.2	+	+
<u>3</u>	9.3	5.6	+	+
<u>4</u>	10.3	9.5	+	+
<u>5</u>	8.6	2.0	-	-
<u>6</u>	-	5.5	+	+
<u>7</u>	-	5.7	+	+

Complexes 3, 6 and 7 are hydrolysed despite the presence of a DMSA ligand, but the reaction is slower than the cleavage of complex 1. It is also known, however, that a DMSdiet ligand is not hydrolysed if a DMSA ligand is involved in the complex molecule.

References

Seifert, S., Syhre, R., Spies, H. and Johannsen, B. (1994) Preparation, characterization and enzymatic hydrolysis of mixed ligand Re/Tc complexes with DMSA and DMS ethyl esters. *Annual Report 1994*, Institute of Bioinorganic and Radiopharmaceutical Chemistry, FZR-73, pp. 38-45.

28. Technetium and Rhenium Complexes of Mercaptoacetyl Glycine Ligands 6*. Preparation and X-ray Structure of $\text{Ph}_4\text{As}[\text{ReO}(\text{MAG}_1)\text{Cl}]$

B. Noll, St. Noll, P. Leibnitz, H. Spies and B. Johannsen

Introduction

Previous studies on oxotechnetium and oxorhenium complexes of mercaptoacetyl triglycine (MAG_3) (Noll *et al.*, 1992) and mercaptoacetyl diglycine (MAG_2) (Johannsen *et al.*, 1993) are extended to mercaptoacetyl glycine (MAG_1). This potential tridentate S,N,O ligand requires the presence of a co-ligand in order to stabilize the MO^{3+} core to a definite mononuclear species. MAG_1 being this co-ligand, either tridentate/monodentate (3+1) coordination, or alternatively, twofold bidentate coordination (2+2) to the MO^{3+} core are expected to occur. While these species are expected to be formed at an excess of the ligand over the metal, we found that using tetrachlorooxorhenate(V), $[\text{ReOCl}_4]^-$, as a precursor, the reaction with equimolar amounts of MAG_1 delivers $[\text{ReO}(\text{MAG}_1)\text{Cl}]^-$. Its synthesis and X-ray crystal structure determination are described in this report.

Experimental

Benzoylmercaptoacetyl glycine

Thiobenzoic acid (5.7 g, 40 mmol) was dissolved in 20 ml of methanol and neutralized with sodium methylate. This solution was dropped to chloroacetyl glycine (3.2 g, 21 mmol) in 750 ml of dry methanol while stirring under nitrogen. Stirring was continued for 12 h. Methanol was removed by rotary evaporation. 2 N hydrochloric acid was added to the residue, yielding a brown oil which was separated and dissolved in 80 ml of chloroform. While cooling and stirring vigorously, the product crystallized and after separation it was washed with water, chloroform and diethyl ether. Yield: 1.5 g (27 %). Melting point: 136 °C.

Elemental analysis: (Found: C, 51.69; H, 4.15; N, 5.34; S, 12.70, $\text{C}_{11}\text{H}_{11}\text{NO}_4\text{S}$ requires C, 52.17; H, 4.38; N, 5.53; S, 12.66 %).

IR absorptions: $\nu_{\text{max}}/\text{cm}^{-1}$ (KBr) 3380 (NH); 1740 (COOH); 1675 and 1620 (C=O); 1540 (NH).

Mercaptoacetyl glycine (MAG_1)

1.64 ml of sodium methylate were dropped to a solution of benzoylmercaptoacetyl glycine (1.1 g, 4 mmol) in 100 ml of methanol over a period of 30 min. The mixture was stirred for 1 h under nitrogen and then neutralized with methanolic ion exchange resin DOWEX 50WX8. After separation of the resin the solvent was removed by rotary evaporation. The residue was dissolved in 20 ml of water and extracted with 60 ml of benzene. The aqueous layer was filtered and the final product isolated by freeze drying.

Yield: 0.4 g (62 %); Melting point: 71 °C.

Elemental analysis: (Found: C, 31.97; H, 4.45; N, 9.17; S, 21.10, $\text{C}_4\text{H}_7\text{NO}_3\text{S}$ requires C, 32.21; H, 4.73; N, 9.39; S, 21.49 %).

IR absorptions: $\nu_{\text{max}}/\text{cm}^{-1}$ (KBr) 3350 (NH), 1725 (COOH), 1605 (C=O), 1550 (NH).

^1H NMR data: δ_{H} (250 Mhz; solvent $\text{DMSO}-d_6$; standard TMS) 3.8 (1H, -SH), 3,7 (2H, $-\text{CH}_2$), 3,2 (2H, $-\text{CH}_2\text{-SH}$), 8,3 (1H, CO-NH-)

$\text{Ph}_4\text{As}[\text{ReO}(\text{MAG}_1)\text{Cl}]$

270 mg (0.18 mmol) MAG_1 dissolved in 5 ml ethanol was dropped into a solution of 1.45 g (0.2 mmol) $\text{Ph}_4\text{As}[\text{ReOCl}_4]$ in 10 ml chloroform while stirring. The temperature was kept at 2 °C and nitrogen was passed through the solution. The colour changed from yellow to dark brown. After 30 min the solvents were evaporated in vacuo. The residue was washed with chloroform and ether and recrystallized from ethanol to give 72 mg (0.09 mmol = 52 %) dark brown crystals.

Elemental analysis: (Found: C, 43.60; H, 3.11; N, 1.85; S, 4.09; Cl, 4.10; $\text{C}_{28}\text{H}_{24}\text{NO}_4\text{SCl}$ requires C, 43.84; H, 3.15; N, 1,71; S, 4.18; Cl, 4.62 %).

IR absorptions: $\nu_{\text{max}}/\text{cm}^{-1}$ (KBr) 960 cm^{-1} (Re=O)

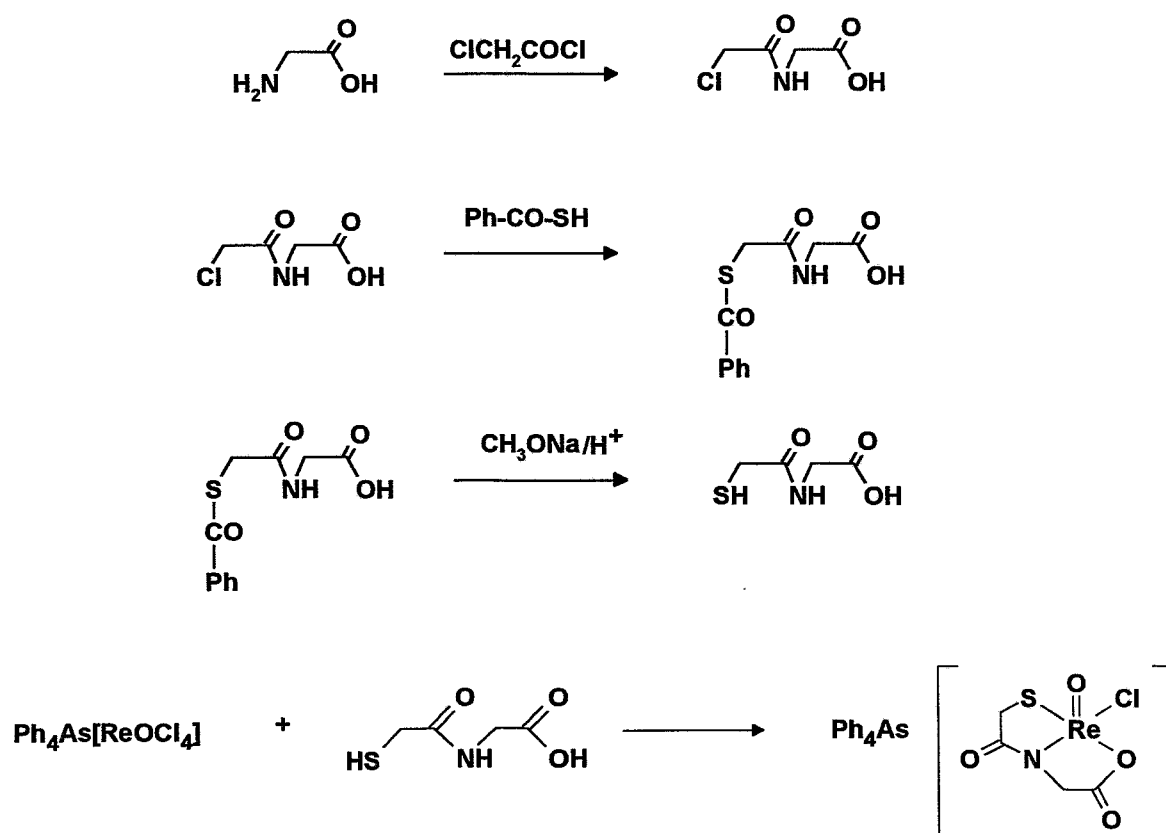
VIS absorption: $\lambda_{\text{max}}/\text{nm}$ (EtOH) 520 (1.62)

X-ray data were collected at room temperature (296 K) with an ENRAF-NONIUS CAD 4 diffractometer, graphite monochromatized Mo $\text{K}\alpha$ radiation ($\lambda = 0.71073 \text{ \AA}$).

Results and Discussion

The synthesis of mercaptoacetyl glycine (MAG₁) and its reaction with tetrachlorooxorhenate(V) (tetraphenylarsonium salt) is shown in reaction scheme 1. The exchange reaction of [ReOCl₄]⁻ with equimolar amounts of the ligand results in the complex [ReO(MAG₁)Cl]⁻, which was isolated in the form of the tetraphenylarsonium salt from ethanol as a crystalline material suitable for X-ray crystal analysis. Elemental analysis corresponds to the proposed formula and the IR spectrum confirms the presence of the Re=O group by an intensive band at 960 cm⁻¹. Support for the formulation is given by X-ray crystal structure determination. The structure consists of discrete anions and Ph₄As cations (crystal system: triclinic, space group: P1bar). A perspective view of [ReO(MAG₁)Cl]⁻ (Fig. 1) shows the square-pyramidal arrangement of the coordination sphere. The bond lengths of Re=O(1), Re-O(2) and Re-S in [ReO(MAG₁)Cl]⁻ (Table 1) are found in the region expected. It is remarkable, that these bond lengths are noticeably shorter than the corresponding distances in [ReOMAG₂]⁻, with the exception of the Re-N bond. A similar relation was observed when the neutral complexes [ReO(SSS)Cl] (Fietz *et al.* 1995) and [ReO(SSS)(tg)] ((Fietz 1996) (HSSH = SH-CH₂-CH₂-S-CH₂-CH₂-SH, HtgI = β-D-thioglucose)) were compared.

Scheme 1: Reaction pathway for preparation of MAG₁ and its reaction with [ReOCl₄]⁻



Formation of [ReO(MAG₁)Cl]⁻ recalls the reaction of 3-thiapentane-1,5-dithiol (HSSSH) as a tridentate ligand with [ReOCl₄]⁻, where a neutral chlorine-containing complex [ReO(SSS)Cl] was formed in a good yield (Fietz *et al.* 1995). Preliminary exchange experiments show that the chlorine at the Re core can be exchanged by monodentate thiols. It is therefore expected that [ReO(MAG₁)Cl] may be useful as a precursor for mixed-ligand "3+1" complexes in a similar manner as shown for [ReO(SSS)Cl] (Spies *et al.* 1995).

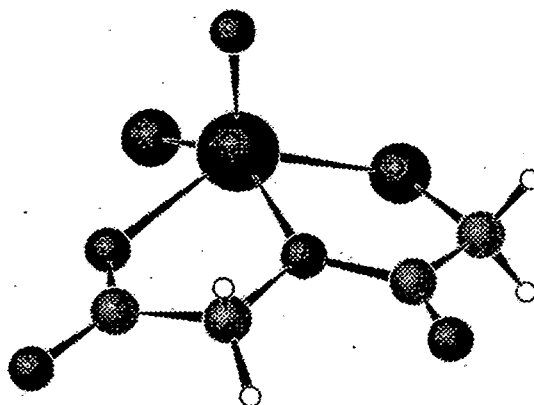


Fig. 1:CELLGRAPH drawing of the $[\text{ReO}(\text{MAG}_1)\text{Cl}]^-$ anion (the tetraphenylarsonium counterion has been omitted for clarity).

Table 1: Selected bond distances and angles for $[\text{ReOCIMAG}_1]^-$ (bond distances of $[\text{ReOMAG}_2]^-$ are in parentheses).

Bond	Distance [Å]	Bond	Angle [°]
Re=O(1)	1.649 (1.661)	S-Re-Cl	89.24
Re-O(2)	2.005 (2.013)	O(1)-Re-O(2)	114.5
Re-S	2.240 (2.267)	O(1)-Re-S	134.3
Re-Cl	2.343	O(1)-Re-Cl	106.8
Re-N	1.966 (1.964)	O(1)-Re-N	109.1
		S-Re-N	82.9
		O(2)-Re-Cl	82.7
		O(2)-Re-N	110.9
		N-Re-Cl	143.7

References

- Fietz T., Spies H., Pietzsch H.-J. and Leibnitz P. (1995) Synthesis and molecular structure of chloro(thiapentane-1.5-dithiolato)oxorhenium(V). *Inorg. Chim. Acta* **231**, 233-236.
- Fietz T. (1996) Rhenium-Komplexe mit 3+1-Koordination, *Thesis*, TU Dresden.
- Johannsen B., Noll B., Leibnitz P., Reck G., Noll St. and Spies H. (1993) Technetium and rhenium complexes of mercapto containing peptides. 1. Tc(V) and Re(V) complexes with mercaptoacetyl diglycine (MAG_2) and X-ray structure of $\text{AsPh}_4[\text{TcO}(\text{MAG}_2)]\cdot\text{C}_2\text{H}_5\text{OH}$. *Inorg. Chim. Acta*, **210**, 209-214.
- Noll B., Johannsen B., May K. and Spies H. (1992) Preparation of the renal function and imaging agent $^{99\text{m}}\text{Tc-MAG}_3$ starting from S-unprotected mercaptoacetyltriglycine. *Appl. Radiat. Isot.* **43**, 899-901.
- Spies H., Fietz T., Pietzsch H.-J., Johannsen B., Leibnitz P., Reck G., Scheller D. and Klostermann K. (1995) *J. Chem. Soc. Dalton Trans.* **1995**, 2277-2280.

*) Preceding reports are published in *Annual Reports 1992 and 1993*, Institute of Bioinorganic and Radiopharmaceutical Chemistry.

29. Technetium and Rhenium Complexes of Mercaptoacetyl Glycine Ligands. 7. Formation and Molecular Structure of a Re(V) Complex of Mercaptoacetyl Glycine Ethyl Ester with N,S,S,O-Coordination

B. Noll, St. Noll, P. Leibnitz, H. Spies, B. Johannsen, P.E. Schulze¹, W. Semmler¹
¹IDF Berlin

Introduction

Blocking of the carboxylic group in the potential tridentate S,N,O ligand mercaptoacetyl glycine (MAG₁) should lead to twofold bidentate coordination of the ligand to the metal when allowed to react with an appropriate oxorhenium(V) precursor. This report provides information on the reaction of MAG₁ with [ReOCl₄]⁻ in ethanol to give unexpectedly a neutral NSSO-coordinated oxorhenium(V) complex with an unsymmetrically coordinated mercaptoacetyl glycine ethyl ester (MAG₁-Et) as the ligand.

Experimental

[ReO(MAG₁Et-(S,N))(MAG₁Et-(S,O))] **1**:

MAG₁ (195 mg, 1.3 mmol) dissolved in 6 ml ethanol was added to a stirred solution of AsPh₄[ReOCl₄] (475 mg, 0.65 mmol) in 20 ml ethanol / 2 ml acetonitrile under a nitrogen atmosphere. The colour of the solution immediately turned a dark brown. The mixture was kept at about 40 °C for one hour and then allowed to stand at room temperature. After some days brown crystals were separated.

Yield 160 mg (0.29 mmol, 45 %); melting point 222 - 223 °C.

Elemental analysis: (Found: C, 26.42; H, 3.47; N, 4.94; S, 11.45. C₁₂H₁₉N₂O₇S₂Re requires C, 26.03; H, 3.46; N, 5.06; S, 11.58 %).

IR absorptions: $\nu_{\max}/\text{cm}^{-1}$ (KBr) 990 (Re=O), 1760 (CO ester)

Mass spectrum: m/z 554 (552) M+1

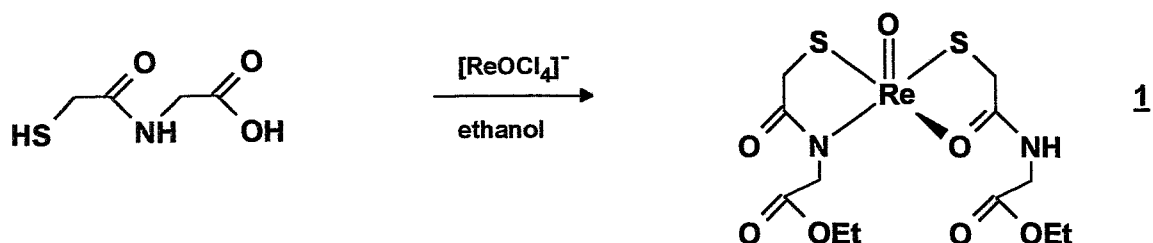
Results and Discussion

The synthesis of mercaptoacetyl glycine was described in the preceding report. When MAG₁ reacted with tetrachlorooxorhenate(V) in ethanolic solution, the formation of a neutral species was surprisingly observed (reaction scheme 1). Compound **1** was obtained as a crystalline material suitable for X-ray crystal analysis. Examination of the data (elemental analysis C₁₂H₁₉N₂O₇S₂Re, mass and IR spectra) suggests the coordination of two ligand molecules in the form of their ethyl esters to the Re=O core. A possible explanation of the ligand being an ethyl ester is the occurrence of esterification in ethanolic solution. Esterification is evidently favoured by the fact that the solution becomes acid due to the exchange of chloride with the incoming ligand.

A second discrepancy to expectations regards the neutrality of the complex. Formation of an anionic species was anticipated in view of the complexing properties of diamidedithiol (DADS) ligands (Brenner *et al.*, 1984; Schneider *et al.*, 1984) as well as our previous experience with mercapto/amide ligands from the MAG_n type. A possible explanation for neutrality of **1** is that one of the amide groups is not deprotonated and the ligand is coordinated as a monobasic one. In this case the carbonyl oxygen should coordinate because oxygen has a higher basicity than the nitrogen atom in neutral amide groups.

Support for one ligand being coordinated monobasically is given by X-ray crystal structure determination of **1** as shown in Fig. 1. The figure shows clearly the coordination of the amide oxygen.

Scheme 1: Reaction of MAG₁ with [ReOCl₄]⁻ in ethanol to give **1**



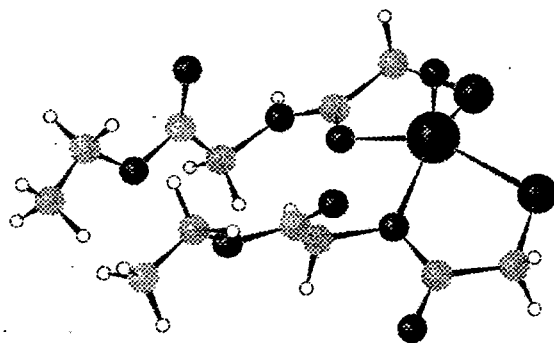


Fig. 1: Molecular structure of **1**, showing that one ligand molecule is bound to rhenium by the amide oxygen

If, as now appears, coordination of one amide group as a neutral donor is preferred, the question of the driving force arises. It is likely but remains to be proven that the tendency of the complex to become neutral may be responsible. With the ligand used - where besides the mercapto and amide group no additional donor groups are available - neutrality can be achieved by O-donation of the amide group without any steric restrictions. This is not the case with the MAG_2 or MAG_3 ligands where - when the N_1 amide is coordinated via the O atom - coordination of the neighbouring donor group in the peptide sequence would lead to the formation of an unfavourable seven-membered ring.

References

- Brenner D., Davison A., Lister-James J. and Jones A.G. (1984) Synthesis and characterization of a series of isomeric oxotechnetium(V) diamide dithiolates. *Inorg. Chem.* **23**, 3793-3797.
- Schneider R.F., Subramanian G., Feld T.A., McAfee J.G., Zapf-Longo C. Palladino E. and Thomas D. (1984) N,N'-bis(S-benzoylmercaptoacetamido) ethylenediamine and propylenediamine ligands as renal function imaging agents. I. Alternative synthetic methods. *J. Nucl. Med.* **25**, 223-229.

30. Preparation and Characterization of Rhenium(V) Complexes with Cysteine and its Derivatives Penicillamine and Cysteamine

S. Kirsch, B. Noll, D. Scheller¹, K. Klostermann¹, P. Leibnitz², H. Spies, B. Johannsen
¹TU Dresden, ²Bundesanstalt für Materialforschung, Berlin

Introduction

^{99m}Tc peptide complexes have aroused increasing interest in recent years. Direct labelling of peptides without a conjugated chelating moiety is possible, because of the variety of potential donor groups present in peptides. An outstanding role in ligating technetium or its surrogate rhenium plays the sulphur atom of cysteine (cys). The metals at the oxidation state +5 are expected to anchor on the S-donor and be able to induce proton dissociation from adjacent amide nitrogen, as well as interact with competitive donor atoms in the side-chain or the N- or C-terminus, leading to strong and specific metal-peptide complexes. However, labelling conditions and the peptide sequence may have a dramatic impact on the nature and stability of the complexes.

As an initial part of our studies on technetium(V) complexation with peptides we studied the coordination ability of the amino acid cysteine and its derivatives. Although the existence of 1:2 complexes of technetium with cysteine, cysteamine, cysteine ester, acetylcysteine and penicillamine has been shown already in the 70s (Johannsen *et al.*, 1978), their structures and the subtle interplay of donor groups under various conditions is not known until now, except for Tc(V) penicillamine (Franklin *et al.*, 1982).

The following work describes the preparation and characterization of Re complexes with cysteine, penicillamine and cysteamine as a model for its surrogate, technetium.

Experimental

Re cysteine complex [ReO(-S-CH₂-CH(COOH)-NH₂)-(-S-CH₂-CH(-COO-)-NH₂)]

4 ml (0.2 mmol) of a Re gluconate solution were added to a solution of 64 mg (0.4 mmol) of L-cysteine hydrochloride in 3 - 5 ml water while stirring under nitrogen. For neutralization the dark reddish brown solution was treated with a few drops of 1 M NaOH. The mixture was concentrated in vacuo and given on a column filled with DOWEX 50 WX 4 cation exchange resin (h = 5 cm, d = 1 cm, mesh size 100 - 200, counterion H⁺). The acid (pH 2 - 3), dark brown solution of the complex was allowed to stand at room temperature for crystallization. The resulting dark brown needles were washed twice with methanol and ether.

Yield: 33 mg (37 %), m.p.: >260 °C

Elemental analysis: (Found: C, 16.13; H, 2.47; N, 6.15; S, 14.22; ReO₅C₆H₁₁N₂S₂ requires C, 16.32; H, 2.29; N, 6.36; S, 14.56 %)

IR absorptions: $\nu_{\max}/\text{cm}^{-1}$ (KBr) 1700s (C=O); 976s (Re=O)

UV/VIS absorption: λ_{\max}/nm (water) 493

¹H NMR data: δ_{H} (90 MHz; solvent DMSO-D₆) 2.65 (1H, d), 3.1/3.6 (6H, m), 4.01 (1H, s), 6.08 (1H, d), 6.83 (1H, t), 7.57/7.83 (2H, dd), 13.33 (1H)

¹³C NMR data: δ_{C} (solvent DMSO-D₆) 40.95, 45.17, 64.11, 64.53, 171.47, 174.9

Mass spectrum: m/z 443 (M⁺, 85 %), 426 (10), 185 (100)

Re penicillamine complex [ReO(-S-C(CH₃)₂-CH(COOH)-NH₂)-(-S-C(CH₃)₂-CH(-COO-)-NH₂)]

30.0 mg (0.4 mmol) of D-penicillamine in 2 - 3 ml water were treated with 2 ml (0.2 mmol) of Re gluconate solution while stirring under nitrogen. After neutralization with 1 M NaOH, stirring was continued for 45 min. The mixture was concentrated in vacuo and given on a column filled with DOWEX 50 WX 4 cation exchange resin (h = 5 cm, d = 1 cm mesh size 100 - 200, counterion H⁺).

The eluted red solution was allowed to crystallize by slow evaporation at 25 °C.

Yield: 15.5 mg of dark red crystals (31 %), m.p.: >260 °C

Elemental analysis: (Found: C, 24.08; H, 3.78; N, 5.53; S, 12.91; ReC₁₀H₁₉O₅N₂S₂ requires C, 24.19; H, 3.65; N, 5.64; S, 12.91 %)

IR absorptions: $\nu_{\max}/\text{cm}^{-1}$ (KBr) 1656s (C=O), 968s (Re=O)

UV/VIS absorption: λ_{\max}/nm (water) 502

¹H NMR data: δ_{H} (90MHz, solvent DMSO-D₆) 1.31/1.49/1.65/1.91 (12H, 4s), 3.00 (1H,dd), 3.63 (1H, s), 5.75 (1H, d), 6.54 (1H, t), 7.67 (2H, t), 13.45 (1H)

Mass spectrum: m/z 498 (M⁺, 100 %), 480 (80), 382 (65)

Re cysteamine complex [ReO(-S-CH₂-CH₂-NH₂)₂-O-ReO(-S-CH₂-CH₂-NH₂)₂]

4 ml (0.4 mmol) of a Re gluconate solution were added to 45.2 mg (0.8 mmol) of cysteamine hydrochloride in 2 - 3 ml water while stirring under nitrogen. When the pH of the mixture had been adjusted to 10 with 0.1 M NaOH, a light red powder precipitated. The residue was filtered off and washed with methanol, acetone and ether.

Yield: 65 mg (92 %) of a red powder, only soluble in acidified water (pH < 3).

M.p.: >260 °C

Elemental analysis: (Found: C, 13.66; H, 3.30; N, 7.46; S, 17.37; (ReC₄H₁₂N₂S₂)₂O₃ requires C, 13.25; H, 3.34; N, 7.73; S, 17.69 %)

IR absorptions: $\nu_{\max}/\text{cm}^{-1}$ (KBr) 1632 (NH₂); 912 (Re=O); 680s (Re-O-Re)

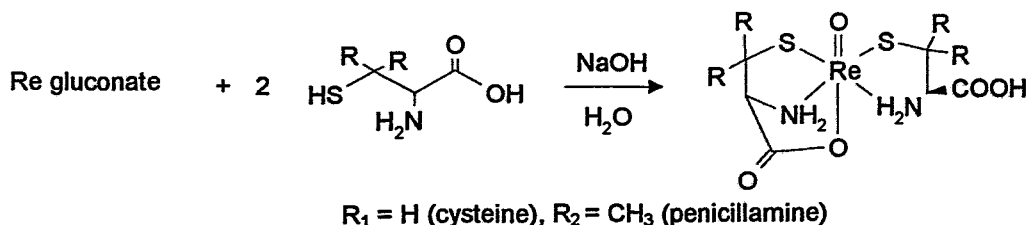
UV/VIS absorption: λ_{\max}/nm (water, pH 2) 512

Mass spectrum: m/z 354 (DCI neg. methane, 100 %), 310 (80)

Results and Discussion

Cysteine and penicillamine react with Re gluconate according to Scheme 1.

Scheme 1: Reaction of Re gluconate with cysteine (1) or penicillamine (2)



The molecular structure of Re penicillamine at low pH is expected to resemble that of Tc penicillamine at low pH as described by Franklin *et al.*, (1982). This is indeed the case as shown in Tables 1 and 2, which list selected bond angles and bond distances of Re penicillamine and Tc penicillamine found by Franklin *et al.*, (1982).

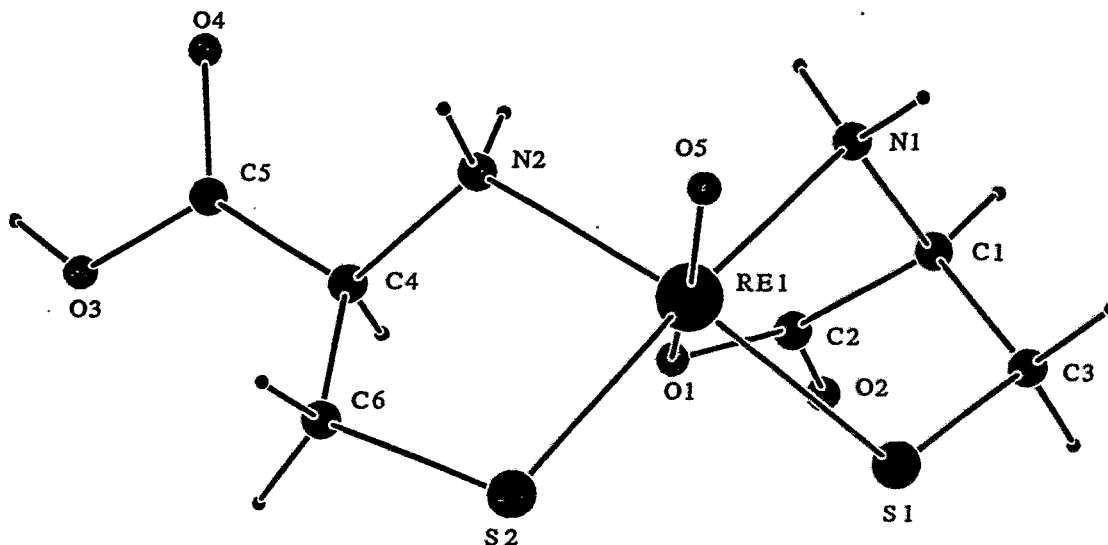


Fig 1: Crystal structure of Re cysteine

The structure comprises a distorted octahedron of ligand atoms about the Re atom (crystal group: orthorhombic, space group: P 2₁ 2₁ 2₁ (19)). There is a short Re-O (oxo) bond, which is a characteristic feature of many Re(V) complexes. The S and N atoms of the two ligating penicillamine

groups form a cis arrangement in the equatorial plane and are bent away from the oxo group in the usual manner. The smaller bond angle of O(1)-Re-N(1) compared to O(1)-Re-N(2) appears to be caused by the steric effects of the sixth coordinated oxygen atom of the ionized carboxylate group. The Re-O(2) distance is much longer than the Re-O(1) distance but is comparable to the Re-N distances and indicates a relatively strong bond.

Further analytical data also indicate this six-coordinated Re atom, i.e. the ^{13}C NMR spectrum shows six different carbon peaks for Re cysteine.

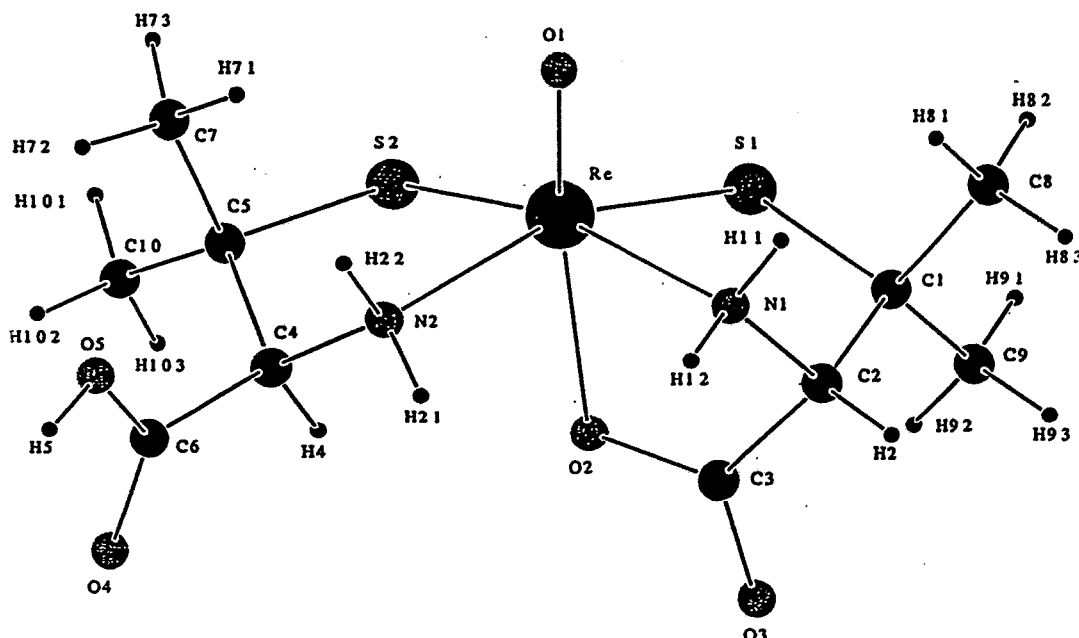


Fig. 2: Crystal structure of Re penicillamine

Table 1: Comparison of selected bond distances of Re penicillamine and Tc penicillamine, found by Franklin *et al.*, (1982)

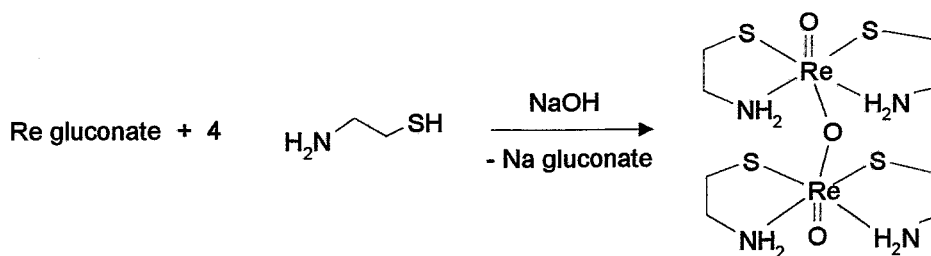
Me = Re, Tc	Bond distances for Re penicillamine	Bond distances for Tc penicillamine [\AA]
Me-O (1)	1.684 (6)	1.657 (4)
Me-N (2)	2.189 (6)	2.185 (6)
Me-O (2)	2.184 (6)	2.214 (4)
Me-N (1)	2.213 (7)	2.209 (6)
Me-S (2)	2.286 (2)	2.283 (2)
Me-S (1)	2.297 (2)	2.296 (2)

Table 2: Comparison of selected bond angles of Re penicillamine and Tc penicillamine, found by Franklin *et al.*, (1982)

Me = Re, Tc	Bond angles of Re penicillamine	Bond angles of Tc penicillamine [deg]
O (1)-Me-N (2)	98.3 (3)	99.1
O (1)-Me-O (2)	157.5 (3)	158.5
N (2)-Me-O (2)	73.4 (2)	72.9
O (1)-Me-N (1)	90.3 (3)	91.1
N (2)-Me-N (1)	93.6 (3)	93.7
O (2)-Me-N (1)	69.9 (2)	70.0
O (1)-Me-S (2)	106.7 (2)	107.0
N (2)-Me-S (2)	83.2 (2)	83.3
O (2)-Me-S (2)	93.3 (2)	92.1
N (1)-Me-S (2)	163.0 (2)	161.8
O (1)-Me-S (1)	105.7 (2)	106.2
N (2)-Me-S (1)	155.9 (2)	154.7
O (2)-Me-S (1)	83.3 (2)	82.9
N (1)-Me-S (1)	84.0 (2)	84.5
S (2)-Me-S (1)	92.13 (10)	90.55

For Re cysteamine we postulate a neutral dinuclear structure according Scheme 2.

Scheme 2: Reaction of Re gluconate with cysteamine



Contrary to cysteine and penicillamine cysteamine has no carboxyl groups to compensate the positive charge at low pH, which was proofed at pH 2 in electrophoresis. At higher pH stabilization of the original $[\text{ReO}(-\text{S}-\text{CH}_2-\text{CH}_2-\text{NH}_2)_2]^+$ is therefore accomplished by conversion to an oxo-bridged complex. This agrees with the IR spectrum, which shows an intensive peak at 680 cm^{-1} . The $\text{Re}=\text{O}$ signal is relatively small and with 912 cm^{-1} at a low wavelength, which are characteristic features of an oxygen-bridged Re complex (Pietzsch *et al.*, 1995). The elemental analysis fits with a Re : cysteamine molecular ratio of 1 : 2 in the complex.

The given results show that at low pH the amine groups in the cysteine moiety are unable to be deprotonated to compensate the positive charge. The carboxyl oxygen is therefore involved in the complex formation. As shown in the case of cysteamine, there is a strong tendency to occupy the transposition with a donating atom (carboxyl-O in the case of cysteine, oxygen-bridged complex in the case of cysteamine).

The complex structure apparently depends on the pH at which the cysteine complex was formed and the resulting structures are very different from each other (as it can be seen in the case of Re cysteamine). Marzilli and coworkers (Marzilli *et al.*, 1994), who studied the structure of Re and Tc ethylenedi-L-cysteine, also found that at low pH the carboxyl group is involved in the complex formation whereas at higher pH one of the amine groups is deprotonated.

As can be seen even for the simplest unit of peptides -amino acids- there are various possibilities of coordinating with technetium or rhenium, depending on pH or the donor system. Therefore it must be expected that in a peptide with varying sequences of amino acids, the binding of technetium at a

cysteine moiety is even more complicated. In order to obtain more information about these problems, further investigations must be made with other cysteine derivatives (acetylcysteine, cysteine esters) or di- or tripeptides containing a cysteine moiety.

References

- Franklin K.J., Howard-Lock H.G. and Lyne Lock C.J. (1982) Preparation, spectroscopic properties and structure of oxo-2,3,6-(D-penillaminato-N,S,O)-4,5-(D-penicillaminato-N,S) technetium(V). *Inorg. Chem.* **21**, 1941-1946.
- Johannsen B., Syhre R., Spies H. and Münze R. (1978) Chemical and biological characterization of different Tc complexes of cysteine and cysteine derivatives. *J. Nucl. Med.* **19**, 816-824.
- Marzilli L.G., Banaszcyk M.G., Hansen L., Kuklanyik Z., Cini R. and Taylor Jr.A. (1994) Deprotonation and denticity of chelate ligands. Rhenium(V) oxo analogues of technetium-99m radiopharmaceuticals containing N_2S_2 ligands. *Inorg. Chem.* **33**, 4850-4860.
- Pietzsch H.-J., Spies H., Leibnitz P. and Reck G. (1995) Technetium and rhenium complexes with thioether ligands IV. Synthesis and structural characterization of binuclear oxorhenium complexes with bidentate thioether coordination. *Polyhedron* **14**, 1849-1853.

31. Rhenium and Technetium Carbonyl Complexes for the Labelling of Bioactive Molecules or Small Peptides

1. Preliminary Investigations on the Complex Formation of the Tetradentate Thioether $HOOC-CH_2-S-CH_2CH_2-S-CH_2-COOH$ with $[ReBr_3(CO)_3]^+$

H.-J. Pietzsch, R. Alberto¹, R. Schibli¹, M. Reisgys, H. Spies, P.A. Schubiger¹
¹Paul-Scherrer-Institut Villigen (Switzerland)

We have started a collaboration with the Paul-Scherrer-Institut Villigen within the European collaboration COST action B3 programme which concerns "The development of novel radiotracers for nuclear medicine and their quality assurance".

Alberto *et al.* recently found a new pathway to the low valency carbonyl compound $[TcCl_3(CO)_3]^{2-}$ starting from TcO_4^- under normal pressure of CO and at moderate temperatures (Alberto *et al.*, 1995). The technetium (and rhenium) metal centre is in the oxidation state +1 which suggests coordination compounds of very high kinetic stability, particularly with π -acid ligands, such as thioethers.

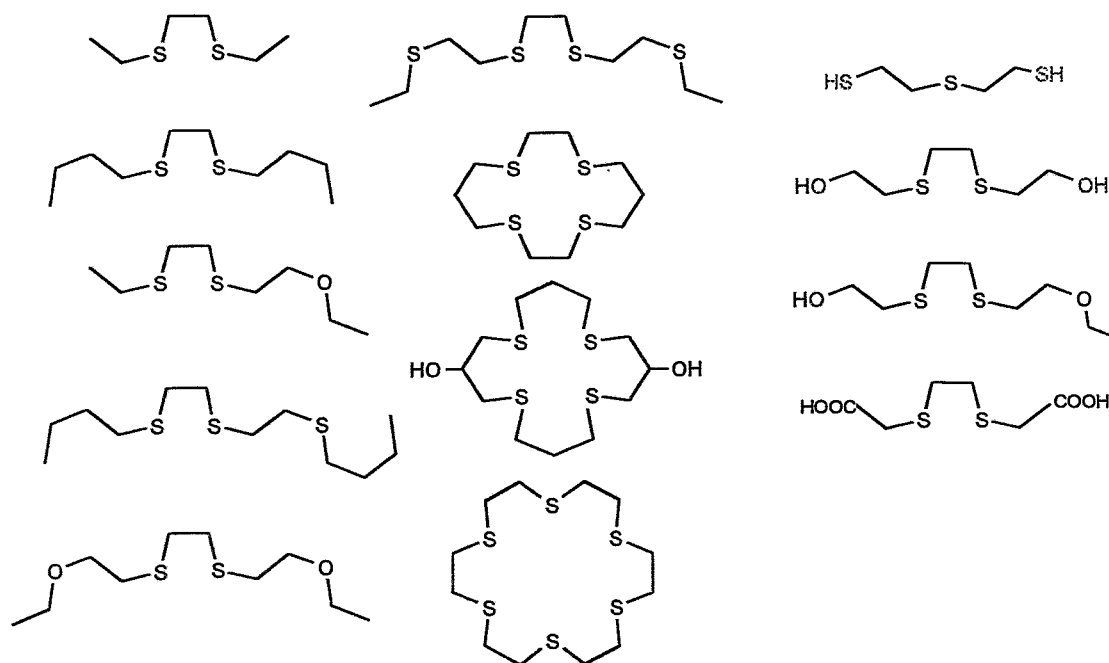


Fig. 1: Neutral and anionic thioether ligands to form technetium and rhenium carbonyl complexes

A variety of technetium and rhenium complexes on +3 and +5 valency have been synthesized and fully characterized with multidentate open-chain and cyclic thioethers such as compiled in Fig. 1. (Pietzsch *et al.*, 1993, 1995).

Preliminary investigations on complexation of $[\text{ReBr}_3(\text{CO})_3]^+$ with several ligands of these type have been performed during a short term scientific mission of one of us (H.-J. P.) at PSI.

As illustrated in Fig. 2a number of these chelates react readily with the $[\text{Re}(\text{OH})_2(\text{CO})_3]^+$ moiety in water or in organic solvents. Complexes 1 and 2 were characterized by mass- and IR spectroscopy, NMR and CHN analysis.

Since the fragment $[\text{M}(\text{OH})_2(\text{CO})_3]^+$ (M = Tc, Re) bears only a "+1" charge, thus neutral lipophilic complexes with $^{99\text{m}}\text{Tc}$ can be synthesized with ligands as presented in Fig. 1. Lipophilicity can be achieved and fine tuned with ligand systems of "-1" charge where a wide variety has been prepared at PSI and at FZR.

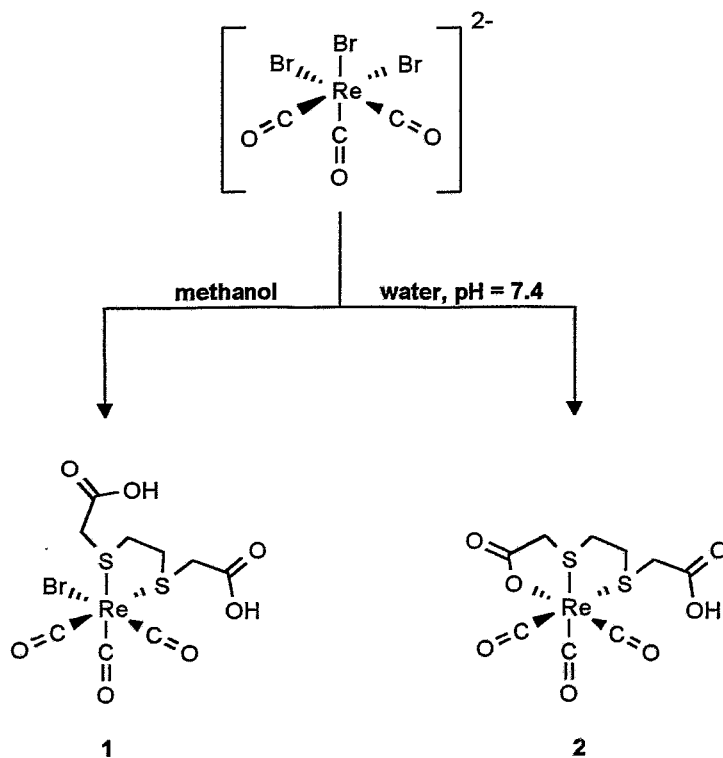
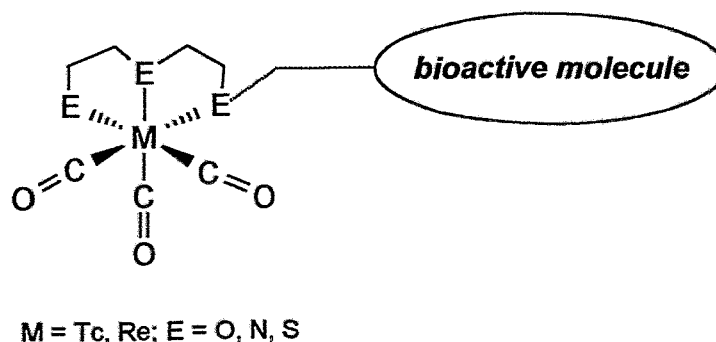


Fig. 2: Ligand exchange reaction of $[\text{ReBr}_3(\text{CO})_3]^+$ with $\text{HOOC-CH}_2\text{-S-CH}_2\text{CH}_2\text{-S-CH}_2\text{-COOH}$ in methanol and aqueous solution

It is planned to investigate the coordination chemistry part of the work at PSI while the *in vivo* and *in vitro* investigations will be done at FZR.

One of the final goal is the synthesis of lipophilic $^{99\text{m}}\text{Tc}$ compounds as potential tracers for organ imaging having the potential for convenient derivatization in order to provide series of candidates for structure-affinity studies:



References

- Alberto R., Schibli R., Egli A., Schubiger P.A., Herrmann W.A., Artus G., Abram U., and Kaden T.A. (1995) Metal carbonyl syntheses. XXII. Low pressure carbonylation of $[\text{MOCl}_4]^-$ and MO_4^{2-} : the technetium(I) and rhenium(I) complexes $[\text{NEt}_4]_2[\text{MCl}_3(\text{CO})_3]$, *J. Organomet. Chem.* **493**, 119-127.
- Pietzsch H.-J., Spies H., Leibnitz P., Reck G. and Johannsen B. (1993) Technetium complexes with thioether ligands. *Radiochimica Acta* **63**, 163-166.
- Pietzsch H.-J., Spies H., Leibnitz P. and Reck G. (1995) Technetium and rhenium complexes with thioether ligands. IV. Synthesis and characterization of binuclear oxorhenium(V) complexes with bidentate thioether coordination, *Polyhedron*, **14**, 1849-1853.

32. Technetium and Rhenium Complexes with Thioether Ligands

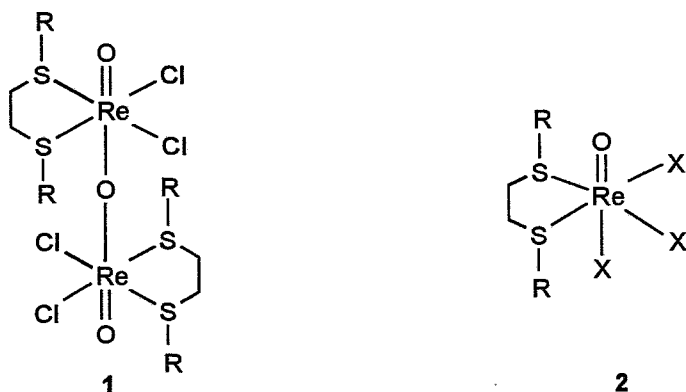
7. Mononuclear Trichlorooxorhenium(V) Complexes with Bi- and Tetradentate Thioethers

M. Reisgys, H.-J. Pietzsch, H. Spies, P. Leibnitz¹

¹Bundesanstalt für Materialforschung Berlin

Introduction

Neutral dirhenium complexes **1** with bidentate thioether ligands and a bridging oxo group were recently characterized (Pietzsch *et al.* 1995). Now we found a simple way of synthesizing their mononuclear relatives $[\text{ReO}(\text{S})\text{X}_3]$ (X = Cl, Br) **2**, which show great possibilities for substitution reactions on their halogen atoms.



Experimental

General procedure for the preparation of **2a-c** and **3a,b**

150 μmol NH_4ReO_4 (in 1.5 ml of HCl_{conc}) were added to a stirred solution of 200 μmol thioether in 1 ml glacial acetic acid. After stirring for 1 h at room temperature the green precipitate was filtered off and washed three times with glacial acetic acid and diethyl ether.

Yield: (50 - 80 %).

Preparation of tribromo(5,8-dithiadodecane)oxorhenium **2d**

150 μmol NH_4ReO_4 (in 1.5 ml of HBr 40 %) were added to a stirred solution of 200 μmol 5,8-dithiadodecane in 1 ml glacial acetic acid. After a reaction time of 1 h at 70 °C, the yellowish-green precipitate was filtered off and washed with glacial acetic acid and diethyl ether. Allowing the filtrate to stand overnight yielded green needles which were treated as previously described.

Yield: (29.2 mg, 30 %).

Reaction of **2b** with alcohols

Stirring the suspension of 51.4 mg **2b** in methanol for 30 min changed the colour from green to violet. The violet precipitate was filtered off and yielded 80 % of **4**. After a longer reaction time (> 1 h) the

colour of the precipitate turned to bluish-green, which indicated the formation of the binuclear oxo bridged complex **1b**.

Yield of **4**: (44.9 mg, 80 %).

M.p.: 137 °C conversion, 202 - 204 °C decomposition.

Elemental analysis: (Found: C, 25.64; H, 4.67; S, 12.73; Cl, 15.20, $C_{12}H_{25}O_2Cl_2S_2Re$ requires C, 25.88; H, 4.94; S, 12.56; Cl, 13.89 %)

Reaction of **2b** with thiophenol

At 5 °C 22.1 mg (200 μ mol) of thiophenol was added to a solution of 45.3 mg (88 μ mol) of **2** in dry acetone. The mixture was allowed to warm up to room temperature. The brown solution was allowed to stand overnight and yielded a brown solid, which was washed with diethyl ether to remove excess thiophenol. Recrystallization from acetone produced dark brown crystals.

Yield of **5**: (49.5 mg, 85 %).

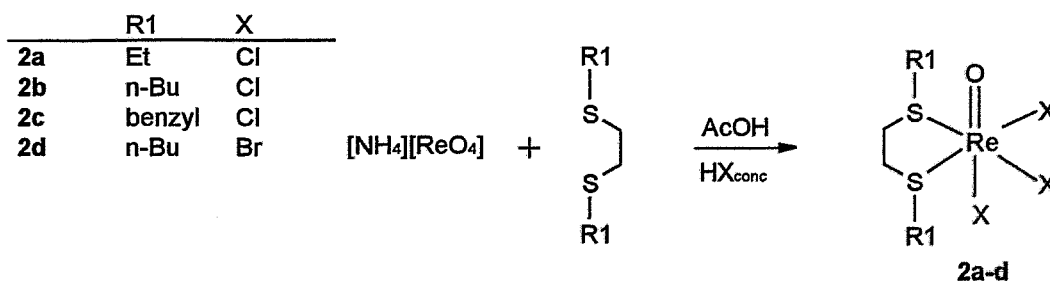
M.p.: 144 - 146 °C (from acetone).

Elemental analysis: (Found: C, 39.41; H, 4.74; S, 19.15; Cl, 8.04, $C_{22}H_{32}OCIS_4Re$ requires C, 39.89; H, 4.87; S, 19.36; Cl, 5.35 %)

Results and Discussion

The reaction of bidentate thioethers with $[NH_4][ReO_4]$ in glacial acetic acid and hydrohalic acid is a simple way of producing the trichloro(thioether)oxorhenium complexes **2** as green crystals (Scheme 1). Elemental analyses and melting points of **2a-d** are reported in Table 1. The absorption band of the stretching vibration at 976 cm^{-1} (**2a-d**) is characteristic of the $[ReO]^{3+}$ core (Kotegov *et al.*, 1974). The preliminary X-ray crystal structure of **2b** shows an octahedron. The sulphur atoms of the bidentate thioether ligand are *cis*-coordinated with respect to the oxygen.

Scheme 1:



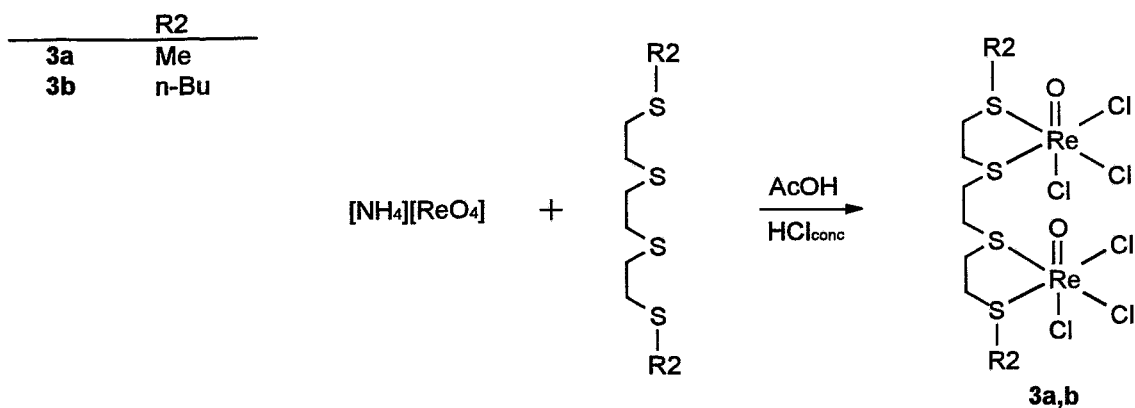
A binuclear rhenium complex **3** can be obtained by reaction with tetradentate thioethers in the same procedure as **2**. The metal atoms in complex **3** are not connected by an oxygen as in **1** but by an $S(CH_2)_2S$ bridge belonging to the thioether ligand (Scheme 2). The proposed structure is supported by the results of infrared spectroscopy (976 cm^{-1}), elemental analysis (see Table 1) and mass spectrometry (compound **3b**). The peak at $m/z = 944$ (4 %) is due to the molecular ion of **3b**. The fragments with $m/z = 457$ (20 %, $n\text{-BuS}(CH_2)_2SReOCl_3$), $m/z = 362$ (100 %, $n\text{-BuSReOCl}_3$) and $m/z = 308$ (5 %, $ReOCl_3$) confirm the postulated compound.

Table 1: Elemental analyses and melting points of **2a-d** and **3a,b**

	Elemental analysis				M.p. [°C]
	% C found (calc.)	% H found (calc.)	% S found (calc.)	% Hal found (calc.)	
2a	15.74 (15.71)	3.14 (3.08)	13.75 (13.98)	23.61 (23.18)	207-209*
2b	23.25 (23.32)	4.39 (4.31)	12.31 (12.45)	22.80 (20.65)	117-118
2c	32.65 (32.96)	2.94 (3.11)	11.17 (11.00)	18.52 (18.24)	120-121
2d	18.40 (18.53)	3.25 (3.39)	9.83 (9.89)	37.18 (36.97)	145-147
3a	11.44 (11.18)	2.20 (2.11)	15.50 (14.92)	24.41 (24.75)	170 *
3b	17.81 (17.82)	3.06 (3.20)	13.88 (13.59)	22.35 (22.54)	167 *

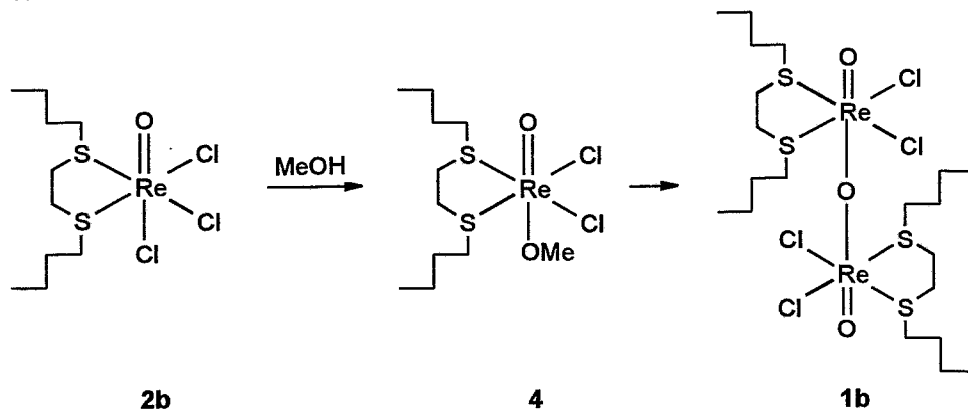
* decomposition

Scheme 2:

**Reactions:**

The relationship of the neutral, monomeric rhenium complex **2** with the oxo bridged dirhenium complex **1** is shown by the reaction of **2** with alcohols. In the alcoholic medium of methanol, a colour change of the solid complex from green to violet appears. The violet precipitate can be isolated and characterized as **4**.

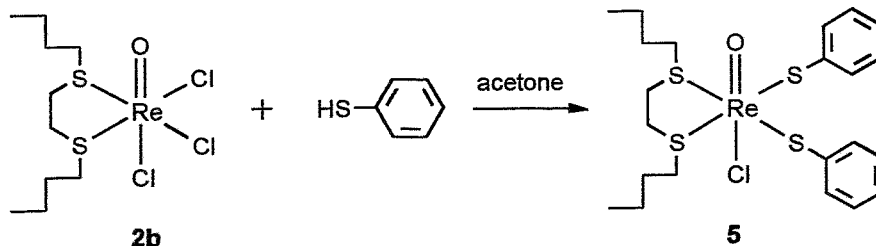
Scheme 3:



In the IR spectrum of **4** the absorption at 936 cm^{-1} indicates the stretching vibration of the $[\text{O}=\text{Re}-\text{O}]^{2+}$ core, which corresponds to the value of $[\text{ReO}(\text{HO}(\text{CH}_2)_2\text{S}(\text{CH}_2)_2\text{S}(\text{CH}_2)_2\text{O})\text{Cl}_2]$ at 940 cm^{-1} (Pietzsch *et al.* 1994). All attempts to dissolve the violet solid by organic solvents (acetone, chloroform, methanol) failed, because of a fast conversion into the binuclear complex **1b** (Scheme 3). The broad absorption band at 688 cm^{-1} in the infrared spectrum can be assigned to the $[\text{O}=\text{Re}-\text{O}-\text{Re}=\text{O}]$ moiety (Pietzsch *et al.* 1995).

Reaction of **2b** with an excess of thiophenol in dry acetone leads to substitution of two chlorine atoms by the thiophenol ligand (Scheme 4). All attempts to substitute the third chloride have so far been in vain.

Scheme 4:



The absorption band at 940 cm^{-1} indicates the $\text{Re}=\text{O}$ core of **5** and is similar to the result of the 4-methylphenol derivative, which is synthesized from **1b** with four equivalents of 4-methylthiophenol in chloroform. A preliminary X-ray structure analysis corresponds to the structure of **6** (Fig.1), which shows a distorted octahedron. The four sulphur atoms occupy the places equatorial to the $\text{O}=\text{Re}-\text{Cl}$ axis. Selected bond lengths and angles are summarized in Table 2.

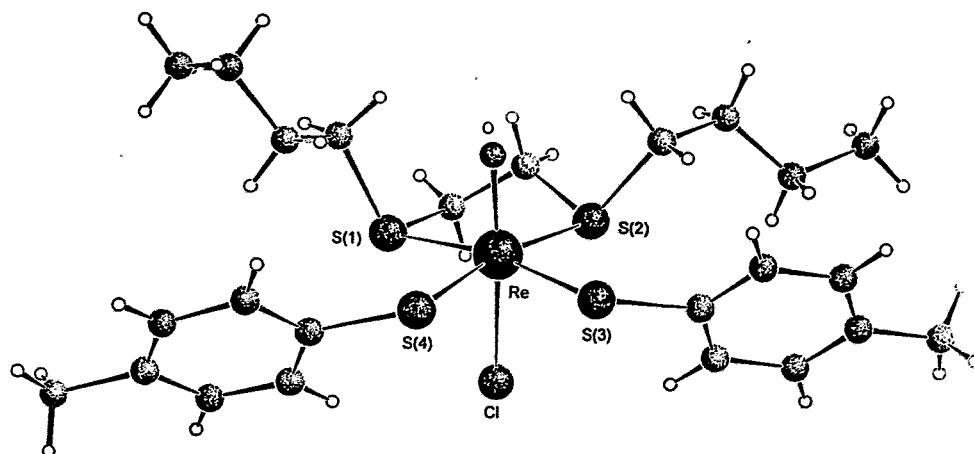


Fig. 1: Crystal structure of bis(4-methoxybenzenethiolato)chloro-(5,8-dithiadodecane) oxorhenium(V) (**6**)

Table 2: Selected bond distances (Å) and angles (deg) of bis(4-methoxybenzenethiolato)-chloro(5,8-dithiadodecane)oxorhenium(V) (**6**)

Re-O(1)	1.673(11)	Re-Cl	2.453(4)
Re-S(3)	2.292(5)	Re-S(2)	2.482(5)
Re-S(4)	2.318(5)	Re-S(1)	2.534(4)
O(1)-Re-S(3)	104.3(4)	S(4)-Re-S(2)	169.6(2)
O(1)-Re-S(4)	102.8(4)	Cl-Re-S(2)	78.5(2)
S(3)-Re-S(4)	78.8(2)	O(1)-Re-S(1)	86.8(4)
O(1)-Re-Cl	158.6(4)	S(3)-Re-S(1)	168.8(2)
S(3)-Re-Cl	93.4(2)	S(4)-Re-S(1)	98.4(2)
S(4)-Re-Cl	92.2(2)	Cl-Re-S(1)	75.8(2)
O(1)-Re-S(2)	87.4(4)	S(2)-Re-S(1)	83.9(2)
S(3)-Re-S(2)	96.9(2)		

References

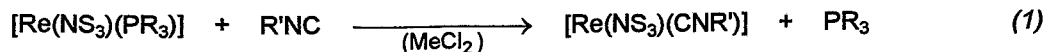
- Kotegov K.V., Khakimov F.Kh., Konovalov L.V. and Kukushkin Y.N. (1974) Rhenium compounds with diethyl ethylene disulphide. *Zh. Obshch. Khim.* **44**, 2237-2240.
- Pietzsch H.-J., Spies H., Leibnitz P. and Reck G. (1994) Technetium and rhenium complexes with thioether ligands. 6. Oxorhenium(V) complexes derived from the potentially tetradentate ligand 1,8-dihydroxy-3,6-dithiaoctane. *Annual Report 1994*, Institute of Bioinorganic and Radiopharmaceutical Chemistry, FZR-73, pp. 3-8.
- Pietzsch H.-J., Spies H., Leibnitz P. and Reck G. (1995) Technetium and rhenium complexes with thioether ligands. IV. Synthesis and structural characterization of binuclear oxorhenium(V) compounds with bidentate thioether coordination. *Polyhedron* **14**, 1849-1853.

33. Substitution Reaction on Trigonal Bipyramidal Coordinated Rhenium(III) Tripod Complexes. A Study of the Kinetics.

M. Glaser, H. Spies

Introduction

Recently we described the formation of isocyanide coordinated rhenium(III) complexes containing the tripodal ligand 2,2',2''-nitrilotris-(ethanethiol) by the reaction of an isocyanide with the phosphane complex $[\text{Re}(\text{NS}_3)(\text{PPh}_3)]$ according to (1), Spies *et al.*, (1994).



In this paper we are reporting on preliminary investigations regarding the kinetics of this reaction ($\text{PR}_3 = \text{PPh}_2\text{Me}$, PPhMe_2 ; $\text{R}' = \text{CH}_2\text{C}(\text{O})\text{OEt}$). Corresponding experiments concerning substitution by isocyanides were performed using complexes of nickel and platinum (Basolo *et al.*, 1971; Meier *et al.*, 1969).

Experimental

All reactions were carried out in a closed cuvet which was thermostated at 25 °C for at least 10 minutes. A solution of $\text{CNCH}_2\text{C}(\text{O})\text{OEt}$ in ethanol was added to a stirred solution of $[\text{Re}(\text{NS}_3)(\text{PR}_3)]$ in ethanol (including 200 μl of dichloromethane as an auxiliary solvent). UV-VIS spectra were recorded using Zeiss-Aspect 2.01 (100 times accumulation, integration time 50 - 60 ms).

The starting concentrations of $[\text{Re}(\text{NS}_3)(\text{PR}_3)]$ were determined by the photometric method (average value of absorption at 459 nm, 5 measurements).

The recorded spectra were analysed at $\lambda = 459 \text{ nm}$ using the following equations of rate laws:

$$\text{first order:} \quad \ln(A - A_e) = -kt \quad (a)$$

$$\text{second order:} \quad \frac{1}{[\text{Re}(\text{NS}_3)(\text{PR}_3)]_0} \frac{A - A_0}{A_e - A} = kt \quad (b)$$

A ... absorption during the reaction
 A_0 ... starting absorption
 A_e ... absorption of equilibrium

For determining k' , the value of A_e was obtained by nonlinear regression.

Results and Discussion

The reaction (1) was accompanied by a change of colour from green to olive brown. In Fig. 1 the UV-VIS spectra of the formation of $[\text{Re}(\text{NS}_3)\text{CNCH}_2\text{C}(\text{O})\text{OEt}]$ from $[\text{Re}(\text{NS}_3)(\text{PPhMe}_2)]$ are depicted. All bands except that at λ_{max} have a bathochromic shift. The overlay showed four isosbestic points, suggesting a clear reaction without formation of long-life intermediate states. This allowed us to evaluate the reaction and to compare the reactivity of the two precursor molecules in a more quantitative measure in terms of kinetic data.

In order to reduce the measurement error, all reactions were carried out in ethanol instead of dichloromethane. However, this excludes investigations on $[\text{Re}(\text{NS}_3)(\text{PPh}_3)]$ because of its low solubility.

Another problem arose under conditions of pseudo first-order in $[\text{Re}(\text{NS}_3)(\text{PR}_3)]$, because a side product was observed. The product is a light green compound of long retention time found by thin-layer chromatography (silica gel, chloroform). This effect became stronger with higher concentrations of isocyanide, so that the reaction could not be evaluated when an excess of isocyanide higher than twentyfold was used.

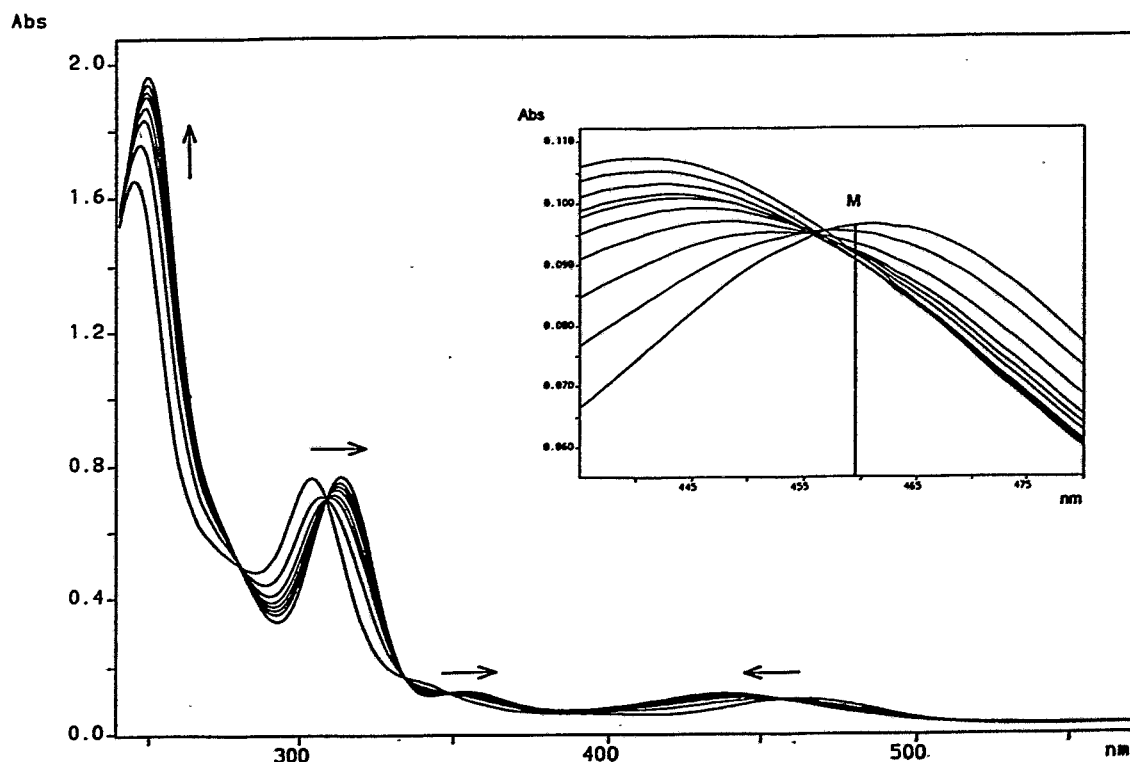


Fig. 1. UV-VIS spectra during the reaction of $[\text{Re}(\text{NS}_3)(\text{PPhMe}_2)]$ ($1.0 \cdot 10^{-4}$ M) with $\text{CNCH}_2\text{C}(\text{O})\text{OEt}$ ($2.6 \cdot 10^{-4}$ M) in dichloromethane (25 °C, integration time 22.9 ms, accumulation 10, scan intervals 1 s). Upper: M = wavelength chosen for photometric determinations ($\lambda = 459$ nm)

Evaluation of experimental data of pseudo first-order according to (a) produced the rate constants shown in Table 1. In all cases the plots of $\ln(A - A_\infty) = f(t)$ remained linear at least up to 70 % degree of conversion regarding $[\text{Re}(\text{NS}_3)(\text{PR}_3)]$.

Table 1: k' of substitution reactions of $[\text{Re}(\text{NS}_3)(\text{PR}_3)]$ and $\text{CNCH}_2\text{C}(\text{O})\text{OEt}$ ($c = 3 \cdot 10^{-3}$ M) in EtOH (25 °C) using conditions of pseudo first-order in the phosphane complex

Starting complex	$c_0, \text{Re}(\text{NS}_3)(\text{PR}_3)/10^{-4}$ M	$k'/10^{-3} \text{ s}^{-1}$	R
$\text{Re}(\text{NS}_3)(\text{PPh}_2\text{Me})$	1.5	31.1 ± 0.7	-0.9988
$\text{Re}(\text{NS}_3)(\text{PPh}_2\text{Me})$	2.4	14.2 ± 0.1	-0.9954
$\text{Re}(\text{NS}_3)(\text{PPh}_2\text{Me})$	2.8	16.3 ± 0.5	-0.9975
$\text{Re}(\text{NS}_3)(\text{PPhMe}_2)$	2.6	8.0 ± 0.1	-0.9997
$\text{Re}(\text{NS}_3)(\text{PPhMe}_2)$	4.0	7.3 ± 0.1	-0.9997
$\text{Re}(\text{NS}_3)(\text{PPhMe}_2)$	4.1	8.8 ± 0.3	-0.9977

In spite of the high error in determining k' , it should be noted that the substitution of PPhMe_2 by $\text{CNCH}_2\text{C}(\text{O})\text{OEt}$ occurs approximately one magnitude slower than in the case of PPh_2Me .

In another series of reactions equimolar quantities of reactants were used and the rate law was found to be second order in the phosphane complexes as shown in Fig. 2. Here k_{exp} of the compound con-

taining PPh_2Me was also significantly higher ($3.47 \pm 0.05 \text{ l}\cdot\text{mol}^{-1}\cdot\text{l}^{-1}$) than for the derivative of PPhMe_2 ($1.01 \pm 0.01 \text{ l}\cdot\text{mol}^{-1}\cdot\text{l}^{-1}$).

To explain the different rates of reaction the steric ligand parameter of TOLMAN can be used. This so-called cone angle θ , which is a measure of the shape of coordinated phosphanes, can be considered a popular tool in interpreting substitution reactions of phosphane-substituted transition metal complexes (Tolman, 1977; Ferguson, 1978; Brown, 1992). θ amounts to 136° for PPh_2Me and to 122° for PPhMe_2 , which indicates that steric rather than electronic effects seem to play an important role in the course of k_{exp} .

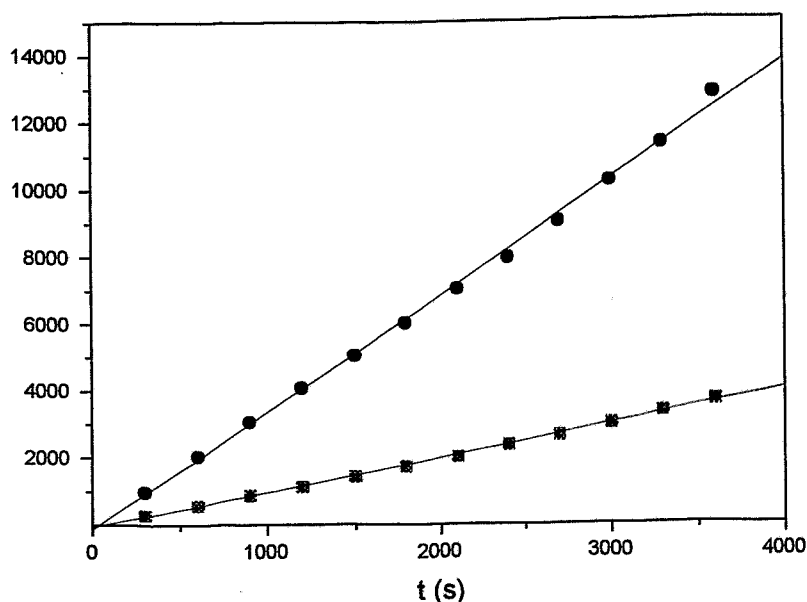


Fig. 2: Evaluation of substitution reaction (1) using equation (b) (ethanol, 25°C)
 ● $\text{PR}_3 = \text{PPh}_2\text{Me}$: $k_{\text{exp}} = 3.47 \pm 0.05 \text{ l}\cdot\text{mol}^{-1}\cdot\text{s}^{-1}$ ($c_0 = 3 \cdot 10^{-4} \text{ M}$, $R = 0.9989$)
 ■ $\text{PR}_3 = \text{PPhMe}_2$: $k_{\text{exp}} = 1.01 \pm 0.01 \text{ l}\cdot\text{mol}^{-1}\cdot\text{s}^{-1}$ ($c_0 = 5 \cdot 10^{-4} \text{ M}$, $R = 0.9994$)

References

- Basolo F., Johnston R.D. and Pearson R.G. (1971) Kinetics and mechanism of substitution reactions of the tetrakis(trifluorophosphine) complexes of nickel(0) and platinum(0). *Inorg. Chem.* **10**, 247-251.
- Brown T.L. (1992) A molecular mechanics model of ligand effects. 3. A new measure of ligand steric effects. *Inorg. Chem.* **31**, 1286-1294.
- Ferguson G., Roberts P.J., Alyea E.C. and Khan, M. (1978) Cone angle and ligand profile calculations for bulky phosphine ligands. *Inorg. Chem.* **17**, 2965.
- Meier M., Basolo F. and Pearson R.G. (1969) Rates of substitution reactions of tetrakis(triethylphosphite)metal(0) compounds of the nickel triad. *Inorg. Chem.* **8**, 795-801.
- Spies H., Glaser M., Pietzsch H.-J., Hahn F.E., Kintzel O. and Lügger T. (1994) Trigonal-bipyramidale Technetium- und Rhenium-Komplexe mit vierzähligen tripodalen NS_3 -Liganden. *Angew. Chem.* **106**, 1416-1418.
- Tolman C.A. (1977) Steric effects of phosphorus ligands in organometallic chemistry and homogeneous catalysis. *Chem. Rev.* **77**, 313-348.

34. Formation of $\{\text{Re}(\text{O})[(\text{SCH}_2\text{CH}_2)_2\text{NH}](\text{SPh})\}$ by Reaction of $\text{N}(\text{CH}_2\text{CH}_2\text{SH})_3$ with $[\text{Re}(\text{O})(\text{SPh})_4]^-$. A New Example of Metal Core Induced Transformation of a Ligand.

M. Glaser, H. Spies, K. Neubert, K. Klostermann¹
¹Institut für Analytische Chemie, TU Dresden

Introduction

Recently we reported the unexpected formation of the oxorhenium complex $\{\text{Re}(\text{O})[(\text{SCH}_2\text{CH}_2)_2\text{NH}](\text{SPh})\}$ **2**, including analysis of its molecular structure (Glaser *et al.*, 1994). This square-pyramidal coordinated compound was obtained by reaction of 2,2',2''-nitrilotris(ethanethiol) and $[\text{Re}(\text{O})(\text{SPh})_4]^-$. Further results of investigations regarding starting material and reaction conditions are now presented. It was likely and has to be proved, that the conversion of the tripodal ligand into the tridentate as present in the resulting complex, occurs during complex formation. The ligand cleavage was found to be induced by the influence of the rhenium core, which is also supported by the occurrence of a binuclear by-product **1** (Fig. 3).

Experimental

All reactions were carried out under a pure nitrogen atmosphere. The precursor $\{\text{BzEt}_3\text{N}\}[\text{ReO}(\text{SPh})_4]$ was prepared using $\{\text{BzEt}_3\text{N}\}[\text{ReOCl}_4]$ (McDonell *et al.*, 1985). $\{\text{BzEt}_3\text{N}\}[\text{ReOCl}_4]$ was synthesized as described (Fietz *et al.*, 1995). The ligands $\text{N}(\text{CH}_2\text{CH}_2\text{SH})_3$ and $\text{HN}(\text{CH}_2\text{CH}_2\text{SH})_2$ were obtained according to literature methods (Harley-Mason, 1947; Barbaro *et al.*, 1994). $\text{N}(\text{CH}_2\text{CH}_2\text{SH})_3$ was purified by column chromatography instead of preparing the corresponding hydrochloride. All the other chemicals were commercial products of reagent grade. For column chromatography the package material Merck Kieselgel 60 (40-63 μm) and a mixture of chloroform/acetone (12/1) were used as mobile phase. The MS spectra were obtained by a Finnigan MAT95 device. GC-MS spectra were performed using a GC 5890 (SERIES2) and a MS 5772 both from Hewlett Packard.

Common preparation of **2** using $\text{HN}(\text{CH}_2\text{CH}_2\text{SH})_2$

a) Reaction of $[\text{ReO}(\text{SPh})_4]^-$

50 mg (0.06 mmol) $\{\text{BzEt}_3\text{N}\}[\text{ReO}(\text{SPh})_4]$ and 0.017 ml (0.12 mmol) $\text{HN}(\text{CH}_2\text{CH}_2\text{SH})_2$ were dissolved in 5 ml of acetonitrile. This solution was stirred and refluxed for 4.5 h. The solvent was removed by a nitrogen stream and the product isolated by column chromatography. A second purification step was carried out by layering of cyclohexane over a concentrated dichloromethane solution of the product to give dark olive green crystals (15 mg, 56 %).

b) Reaction of $[\text{ReOCl}_4]^-$

A mixture of 0.026 ml (0.187 mmol) $\text{HN}(\text{CH}_2\text{CH}_2\text{SH})_2$ and 0.019 ml (0.187 mmol) PhSH in 1 ml acetonitrile was added to a stirred solution of 50 mg (0.094 mmol) $\{\text{BzEt}_3\text{N}\}[\text{ReOCl}_4]$ in 1 ml acetonitrile at 0 °C. A grey-greenish product precipitated immediately. After stirring for 3 h the reaction solution was heated up to 50 °C for 1 h forming a clear brownish solution. The product was worked up as described above (22 mg, 50 %).

Preparation of **2** with $[\text{ReO}(\text{SPh})_4]^-$ and $\text{N}(\text{CH}_2\text{CH}_2\text{SH})_3$

10 mg (0.012 mmol) $\{\text{BzEt}_3\text{N}\}[\text{ReO}(\text{SPh})_4]$ and 0.0034 ml (0.024 mmol) $\text{N}(\text{CH}_2\text{CH}_2\text{SH})_3$ were dissolved in 5 ml of acetonitrile. The mixture was stirred at 60 °C for 6 h. After evaporation of the solvent the product **2** was isolated by column chromatography (2.5 mg, 47 %). A trace of a light green fraction of a shorter retention time than **2** was obtained. The molecular formula corresponds to structure **1** suggested by its EI-MS spectrum (12 eV).

Results and Discussion

Both the tripodal tetradentate 2,2',2''-nitrilotris(ethanethiol) $[\text{N}(\text{SH})_3]$ and the tridentate bis(2-thiolatoethyl)amine $[\text{HN}(\text{SH})_2]$ react with $[\text{ReO}(\text{SPh})_4]^-$ to give **2**. While this product is the expected one for $\text{HN}(\text{SH})_2$ as the ligand, the formation of **2** from $\text{HN}(\text{SH})_2$ seems rather surprising. From the latter reaction, a five-coordinated structure **A** has to be expected.

The assumption that $\text{HN}(\text{SH})_2$ as a by-product of $\text{N}(\text{SH})_3$ reacts preferably with $[\text{ReO}(\text{SPh})_4]^-$ can be excluded: $\text{N}(\text{SH})_3$ was purified by column chromatography, using silica gel and trichloromethane/acetone. The resulting product did not contain $\text{HN}(\text{SH})_2$ as proved by its GC/MS spectrum (Fig. 1).

Another interpretation is based on the well-known fact that the trithiol utilized exhibits thermal lability in forming the bisthiol (Barbaro *et al.*, 1994). In a reference experiment to figure out the origin of the tridentate ligand the purified trithiol (see Fig. 1) was therefore treated under analogous conditions to the formation of **2** but without rhenium precursor. Investigation of this solution by MS-coupled gas chromatography did not show any trace of the supposed bisthiol. Thus the formation of **2** from $\{[\text{BzEt}_3\text{N}][\text{ReO}(\text{SPh})_4]\}$ must be due to an influence of the rhenium core. Fig. 3 illustrates two hypothetical pathways of a reaction leading to **2**.

Complex **A** should be formed initially by an exchange of all benzenethiolate ligands of the precursor. The metal has probably a Lewis-acid-like electron attracting influence supported by the oxygen to impart a positive partial charge on the bridge head nitrogen atom. Ionization enables C-N cleavage, followed by an attack of thiolate (i. e. R = Ph) at the terminal carbon atom, which gives the anionic species **B**.

Further reaction forms dimer **1** by elimination of $\text{RSCH}_2\text{CH}_2\text{S}^-$. **1** was identified using EI-MS (Fig. 2).

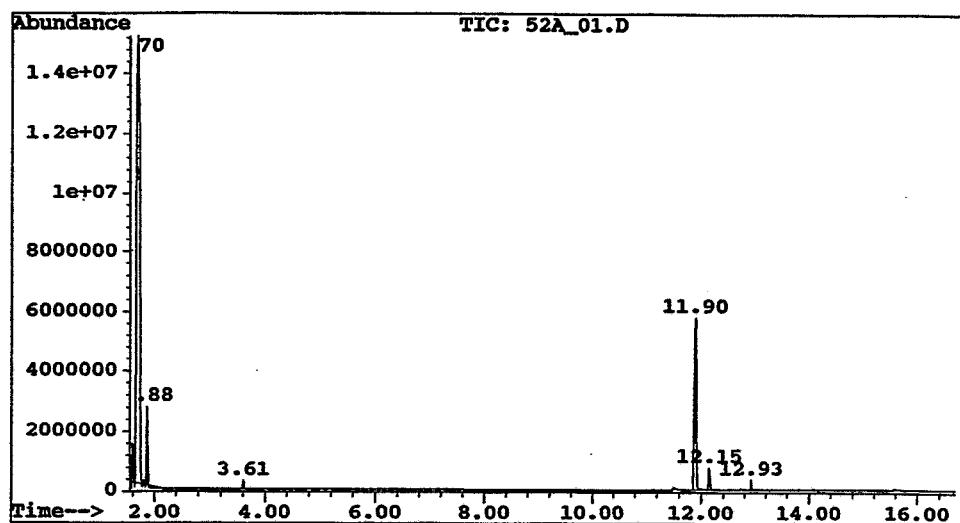


Fig. 1: GC-spectrum of purified 2,2',2''-nitriлотris(ethanethiol) ($R_f = 11.90$ min)

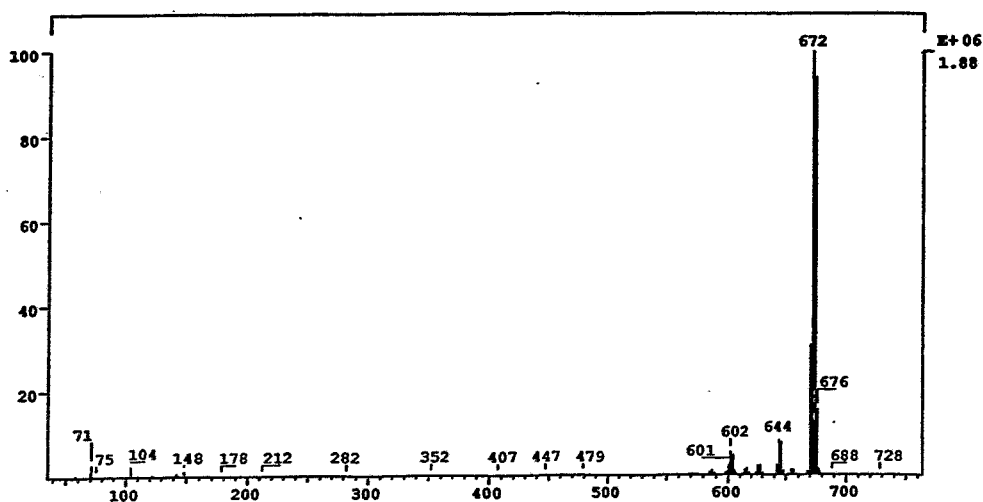


Fig. 2: EI mass spectrum of **1** ($M^+ = 672$ m/z, 12 eV)

1 could react with benzenethiol to give 2. Formation of 2 starting from B in reaction with benzenethiol should also be possible.

The reaction observed is another example of core-induced ligand conversion (Spies *et al.*, 1989). Cleavage of tertiary amines is also known to be catalysed by transition metals (Murahshi *et al.*, 1979). Complex 2 was also accessible by a typical mixed-ligand formation, using the precursors $[\text{BzEt}_3\text{N}][\text{ReOCl}_4]$ or $[\text{BzEt}_3\text{N}][\text{ReO}(\text{SC}_6\text{H}_5)_4]$ in a typical mixed-ligand reaction (Spies *et al.*, 1995) in the presence of bis(2-thiolatoethyl)amine (Fig. 3).

Preliminary investigations regarding the determination of pK_a revealed the partly acid character of the hydrogen atom bound at nitrogen (Berger *et al.*, 1995).

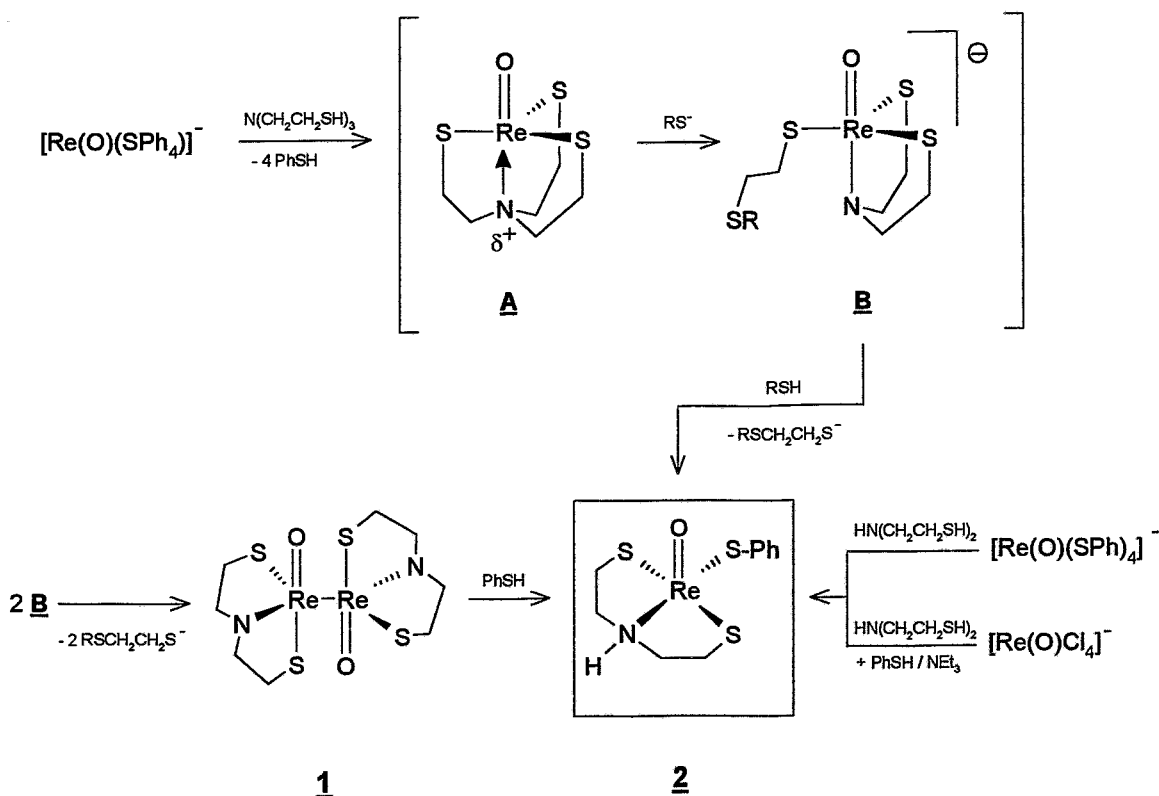


Fig. 3: Formation of 2 starting from $[\text{BzEt}_3\text{N}][\text{Re}(\text{O})(\text{SPh})_4]$ (proposed mechanism) and by a typical "3+1" reaction using $[\text{Re}(\text{O})(\text{SPh})_4]^-$ resp. $[\text{ReOCl}_4]^-$ precursors

References

- Barbaro P., Bianchini C., Scapacci G., Masi D. and Zanella P. (1994) Dioxomolybdenum(VI) complexes stabilized by polydentate ligands with NO_3 , N_2O_2 , and NS_2 donor-atom sets. *Inorg. Chem.* **33**, 3180-3186.
- Berger R. (1995) pK_a value determinations by HPLC of some Tc and Re complexes containing an ionizable group. *This report*, pp. 73-79.
- Fietz T., Spies H., Pietzsch H.-J. and Leibnitz P. (1995) Synthesis and molecular structure of chloro-(3-thiapentane-1,5-dithiolato)oxorhenium(V). *Inorg. Chim. Acta* **231**, 233-236.
- Glaser M., Spies H., Hahn F.E., Lügger T., Klostermann K. and Scheller D. (1994), *Annual Report 1994*, Institute of Bioinorganic and Radiopharmaceutical Chemistry, FZR-73, pp. 14-17.
- Harley-Mason J. (1947) Some aliphatic thiols and their derivatives. Part I. Aliphatic mercaptoamines. *J. Chem. Soc.* 320.
- McDonnell A.C., Hambley T.W., Snow M.R. and Wedd A.G. (1983) Synthesis and molecular structure of tetraphenylarsonium tetrakis(benzenethiolato)-oxorhenate(V)-acetonitrile. *Aust. J. Chem.* **36**, 253-258.

- Murahashi S.I. and Yano T. (1979) Novel palladium and ruthenium catalysed transformation of tertiary amines to secondary amines and sulphides with thiolate anions. *J. Chem. Soc., Chem. Comm.*, 270-271.
- Spies H. and Pietzsch H.-J. (1989) Cleavage of a ligand in a Tc/Schiff base system: An unusual reaction. *Inorg. Chim. Acta* **161**, 151-152.
- Spies H., Fietz T., Pietzsch H.-J., Johannsen B., Leibnitz P., Reck G., Scheller D. and Klostermann, K. (1995) Neutral oxorhenium(V) complexes with tridentate dithiolates and monodentate alkane- or arenethiolate co-ligands. *J. Chem. Soc., Dalton Trans.* 2277-2280.

35. Preparation of a Spiperone-like Isocyanide Ligand and its Complexation with Rhenium(III) Coordinated with 2,2',2''-Nitrilotris(ethanethiol) Using a New Access

M. Glaser, H. Spies

Introduction

This paper describes the preparation and characterization of a new oxo-free rhenium complex containing 2,2',2''-nitrilotris(ethanethiol) and a functionalized monodentate spiperone-like isocyanide co-ligand. The compound was synthesized in order to design technetium and rhenium coordination compounds as potential receptor binding tracers.

A convenient access for releasing the isocyanide ligand leading to the "4+1" complex (Spies *et al.*, 1994, 1995) in one step is described.

Experimental

Tables 1 and 2 contain all analytical and physical properties determined for compounds **2-6**.

*Preparation of 2-(p-fluorophenyl)-2-[3-(N-phtalimidpropyl)]-1,3-dioxolane **2***

20 g (81.6 mmol) of 2-(3-chloropropyl)-2-(4-fluorophenyl)-1,3-dioxolane (SIGMA) were added to 18 g (99.7 mmol) of potassium phthalimide suspended in 50 ml dimethylformamide. After stirring and refluxing for 20 h the reaction mixture was cooled down to room temperature and poured into 250 ml of ice water. White crystals were collected and washed with 50 ml of water and 3 x 50 ml of diethyl ether.

*Preparation of 2-(3-aminopropyl)-2-(p-fluorophenyl)-1,3-dioxolane-hydrate **3***

2.57 g (7.23 mmol) of **2** were covered with 5 ml of EtOH. 357 μ l (7.23 mmol) of hydrazine hydrate (95 %) were added slowly while stirring. After refluxing for 4 h the reaction mixture was cooled to 5 °C for 24 h. Filtrating and washing with 20 ml of diethylether gave 2.1 g of the adduct **A** (melting point: 160 - 165 °C). Suspending of **A** in 50 ml of a saturated NaCl solution and addition of 10 ml 5 N NaOH formed a clear mixture, which was extracted with 3 x 50 ml of diethylether. The unified extracts were dried over Na₂SO₄. After removal of the solvent, 5 ml of a yellow slowly solidifying oil were obtained. The product was purified by recrystallization from EtOH.

*Preparation of 2-(p-fluorophenyl)-2-[3-(N-formylamino)-propyl]-1,3-dioxolane **4***

0.5 g (2.06 mmol) **3** were dissolved in 10 ml of ethyl formiate and refluxed for 7 h. Standing over night at -20 °C and removal of the liquid phase by rotary evaporator gave the solid crude product, which was purified by column chromatography (MERCK Kieselgel 60, 40 - 63 μ m, column 100 x 15 mm, mobile phase trichlormethane/acetone = 6 : 1)

*Preparation of tris(2-thiolatoethyl)amine-[2-(p-fluorophenyl)-2-(3-isocyanpropyl)-1,3-dioxolane]-rhenium(III) **5***

To 100 mg (0.193 mmol) of {Re[(SCH₂CH₂)₃N](PPhMe₂)} (Spies *et al.*, 1995b) in 5 ml of dichloromethane a solution of 45 mg (0.965 mmol) of **4**, 300 mg (1.16 mmol) of triphenylphosphane, 90 μ l (0.965 mmol) of tetrachlormethane and 135 μ l (0.965 mmol) of triethylamine in 1 ml of dichloromethane was added under nitrogen. After stirring and heating for 5 h at 60 °C the solvent was removed by a stream of nitrogen. The crude product was purified using column chromatography analogously to **4**.

Table 1. Elemental analyses, melting points and yields of **2-6**

Complex	Formula	Elemental analysis ^a [%]				M. p. [°C]	Yield [%]
		C	H	N	S		
2	C ₂₀ H ₁₈ NO ₄ F	67.50 (67.60)	4.62 (5.11)	4.02 (3.94)		140-142 ^b	41
3	C ₁₂ H ₁₆ NO ₂ F·H ₂ O	59.47 (59.25)	6.12 (7.46)	5.55 (5.76)		85-95 ^b	28
4	C ₁₃ H ₁₆ NO ₃ F	61.39 (61.65)	6.59 (6.37)	5.33 (5.53)		35-42	26
5	C ₁₉ H ₂₆ N ₂ S ₃ O ₂ FRe	37.28 (37.06)	4.02 (4.26)	4.87 (4.55)	15.45 (15.62)	170-177	92
6	C ₁₇ H ₂₂ N ₂ S ₃ OFR _e	35.75 (35.71)	3.65 (3.88)	4.84 (4.90)	16.98 (16.82)	162-165 ^b	77

^a Calculated values are in parentheses, ^b from ethanol

Table 2. ¹H NMR, IR and UV/VIS data of compounds **2-6**

Complex	¹ H NMR (90 MHz, CDCl ₃)				IR (KBr) $\tilde{\nu}$ (cm ⁻¹)	UV/VIS λ (nm)
	δ (ppm)	mult.	int.	assign.		
2	1.74	m	2H	CH ₂ CH ₂ CH ₂ N	1708	
	1.92	m	2H	CH ₂ CH ₂ CH ₂ N		
	3.70	m	4H	OCH ₂ CH ₂ O		
	3.98	m	2H	CH ₂ CH ₂ CH ₂ N		
	6.97+7.37	m	4H	H-fluorophenyl		
	7.66+7.81	m	4H	H-phthalimide		
	1.22-1.98	m	4H	CH ₂ CH ₂ CH ₂ N		
4	3.03-3.39	m	2H	CH ₂ CH ₂ CH ₂ N	1680	
	3.86	m	4H	OCH ₂ CH ₂ O		
	5.68	m	1H	H-N		
	6.9-7.5	m	4H	H-Ar		
	7.92-8.13	m	1H	HC(O)		
5	2.13, 1.84	m	4H	CNCH ₂ CH ₂ CH ₂	2040	248.9 (4.38), 276 sh (3.66), 310.6 (4.02), 588 (2.38)
	2.96	m	12H	SCH ₂ CH ₂ N		
	3.90	m	4H	OCH ₂ CH ₂ O		
	4.77	t	2H	CNCH ₂		
	6.98	m	2H	<i>ortho</i> -H-Ar		
	7.47	m	2H	<i>meta</i> -H-Ar		
6	2.22	m	2H	NCH ₂ CH ₂ CH ₂ C(O)	1980, 1684	247 (4.60), 276 sh (3.78), 311 (4.14), 350 (3.08), 446 (3.23), 550 (2.3)
	2.98	m	12H	SCH ₂ CH ₂ N		
	3.34	t	2H	NCH ₂ CH ₂ CH ₂ C(O)		
	4.88	t	2H	NCH ₂ CH ₂ CH ₂ C(O)		
	7.09+8.08	m	4H	H-Ar		

Preparation of tris(2-thiolatoethyl)amine[4-(*p*-fluorophenyl)-4-oxo-butylisocyanide]-rhenium(III) **6**
 50 mg (81 μmol) of **5** were dissolved in 10 ml of acetone. After addition of 20 mg (105 μmol) of toluene-*p*-sulphonic acid the mixture was stirred for 1.5 h and stored for 12 h at room temperature. The solvent was removed using a stream of nitrogen and the crude product purified by column chromatography as described for **4**. Finally, the complex was recrystallized from ethanol to give olive-brown needles.

Results and Discussion

Regarding the affinity to D₂ receptors a phenyl group and a basic nitrogen atom 5-9 Å away from the centre of the phenyl ring are considered to be essential (Andersen *et al*, 1994). The *p*-fluoro-butyrophenone residue as an integrate part of several receptor-binding ligands, such as spiperone, haloperidol and ketanserin, was functionalized by an isocyanide group for binding to Re(III). Common action of the isocyanide and the tripodal ligand 2,2',2''-nitriлотris-(ethanethiol) yields [Re(NS₃)(CNR)] *in vitro*.

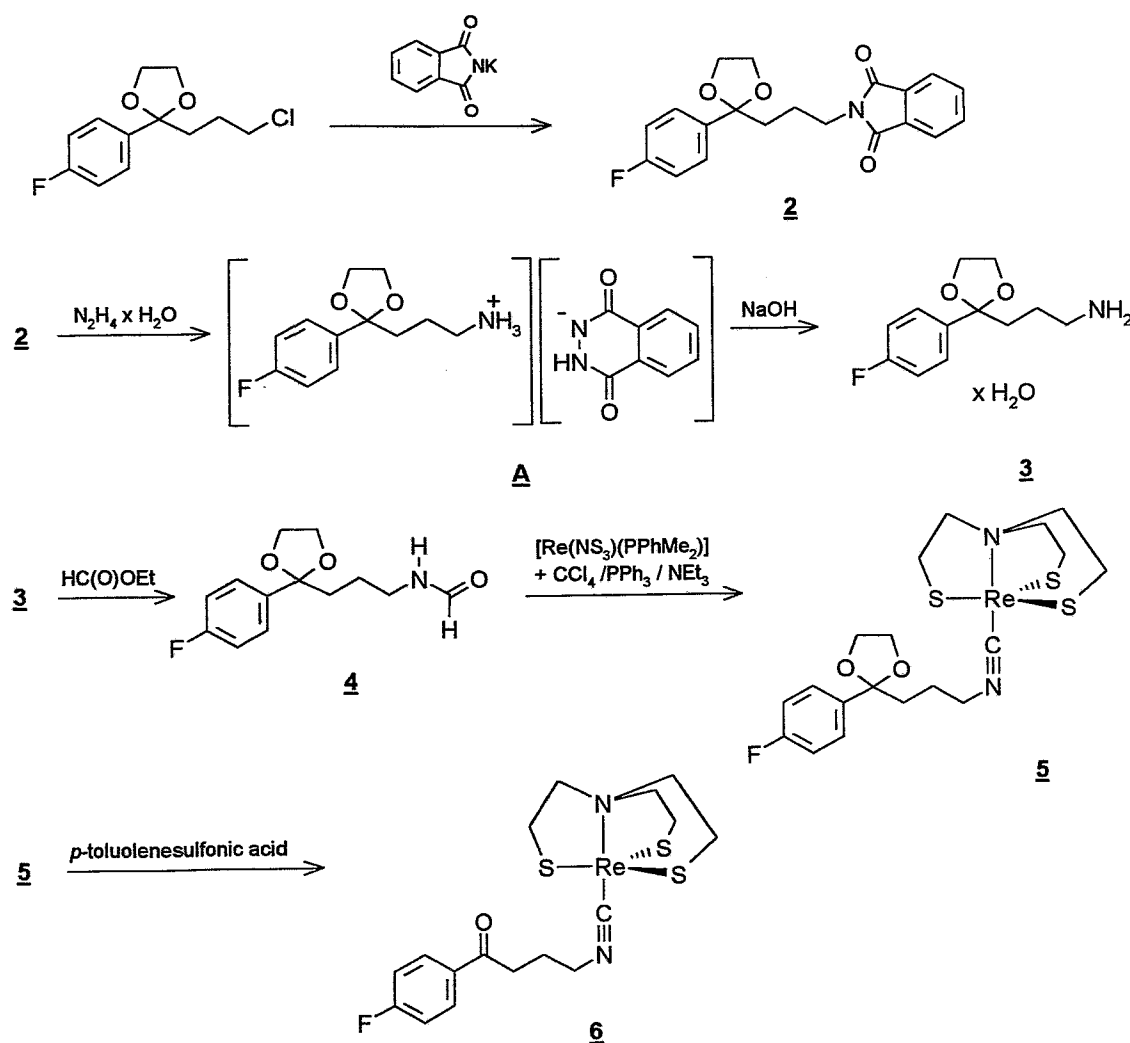


Fig. 1. Preparation of the rhenium complex **6** coordinated by tris(2-thiolatoethylamine) and bearing the *p*-fluorophenylbutyrophenone fragment

Fig. 1 shows all steps of the synthesis leading to **6** in detail. The CN-coupling to produce **3** was performed by a Gabriel synthesis (Ing and Manske, 1926). The system $\text{PPh}_3/\text{CCl}_4/\text{NEt}_3$ is known to mean as dehydrating agent for formamides (Appel, 1975). Combining this reaction with the substitution reaction of a phosphane-containing tripodal rhenium complex and the formamide **4** (Spies *et al.*, 1994) avoids isolation of the free isocyanide to give complex **5** in good yields. This convenient method also allows storing isocyanides, which are instable in the modification of formamide. Treatment of **5** with toluene-*p*-sulphonic acid in acetone removed the protecting group to give the spiperone derivative **6**. Preliminary *in vitro* investigations on the 5-HT₂ receptor, a congener of the D₂ type, to determine the inhibition of specific binding of [³H]ketanserin showed a significant effect for **5** (85 % inhibition of specific binding, 0.1 μM), while compound **6** did not show any effect under the same conditions (Johannsen *et al.*, 1995). The log P_{HPLC} data gained in correlation with the *n*-octanol/water partition coefficient (Berger *et al.*, 1995) suggest for both compounds high lipophilicity (**5**: log P_{HPLC} = 3.76, **6**: log P_{HPLC} = 3.52; mobile phase: acetonitrile/water = 3/1, pH = 7.4).

References

- Andersen K., Liljefors T., Gundertoft K., Perregaard J. and Boegesoe K.P. (1994) Development of a receptor-interaction model for serotonin 5-HT₂ receptor antagonists. Predicting selectivity with respect to dopamine D₂ receptors. *J. Med. Chem.* **37**, 950-962.
- Appel R. (1975) Tertiäres Phosphan/Tetrachlormethan, ein vielseitiges Reagenz zur Chlorierung, Dehydratisierung und PN-Verknüpfung. *Angew. Chem.* **87**, 863.
- Berger R., Fietz T., Glaser M., Spies H. and Johannsen B. (1995) Determination of partition coefficients for coordination compounds by using HPLC. *This report*, pp. 69-72.
- Ing H.R. and Manske R.H.F. (1926) A modification of the gabriel synthesis of amines. *J. Chem. Soc.* 2348-2351.
- Johannsen B., Scheunemann M., Spies H., Brust P., Wober J., Syhre R. and Pietzsch H.-J. (1995) Technetium(V) and rhenium(V) complexes for 5-HT_{2A} serotonin receptor binding: Structure-affinity considerations. *Nucl. Med. Biol.*, in press.
- Spies H., Glaser M., Pietzsch H.-J., Hahn F. E. and Lügger T. (1995) Synthesis and reaction of trigonal-bipyramidal rhenium and technetium complexes with a tripodal, tetradentate NS₃ ligand. *Inorg. Chim. Acta*, in press.
- Spies H., Glaser M., Pietzsch H.-J., Hahn F.E., Kintzel O. and Lügger T. (1994) Trigonal-bipyramidale Technetium- und Rhenium-Komplexe mit vierzähligen tripodalen NS₃-Liganden. *Angew. Chem.* **106**, 1416-1418.

36. Molecular Modelling on Technetium and Rhenium Complexes: Possibilities and Limitations

M. Glaser, H. Spies, B. Johannsen

Introduction

Molecular modelling is a summary term for all the computation tools delineated for the understanding of molecular phenomena and the design of new compounds. In the development of new radiotracers containing technetium or rhenium we wish to control the resulting properties of complexes to be synthesized in a better way. So we are for instance interested in predicting and interpreting affinity towards receptor sites.

Generally, there are two main groups of calculation methods. First, there are *ab initio* and semiempirical programmes (quantum mechanics), that provide i. e. the geometry of molecules (including transition states), the distribution of the density of electrons or the heat of formation. On the other hand, there are empirical programs called force field methods (molecular mechanics). Programmes of quantum mechanics are more sophisticated than the latter group, but they are restricted to only small molecules because of the computational expense which increases exponentially with the number of orbitals. The force field methods reduce the orbital interaction to constants of only some different spring forces and are therefore very quick. They are utilized for calculating geometries; in many cases they can give results of better quality than quantum mechanics, especially for large organic molecules i. e. biomolecules. However, these algorithms are only as good as their parameters. Common packages do not contain these parameters for technetium and rhenium.

In spite of this, it is possible to approximate model complexes containing these metals, using force field methods. The geometry of the core can be locked by artificially elevating the force constants of ligand bonds so that only the residue of the molecule remains to be considered.

Some reviews concerning molecular modelling have been published (basics: Kunz *et al.*, 1991; Lipkowitz *et al.*, 1990; coordination compounds: Hay, 1993; Hancock *et al.*, 1989; pharmaceutical applications: Hansch *et al.*, 1990).

In this paper we are reporting on some investigations regarding conformational analysis and RMS fittings of selected compounds bearing fragments of D₂ and 5-HT₂ antagonists.

Experimental

- CAChe Worksystem 3.5, CAChe Scientific, Inc. (1993), Macintosh Quadra 900 (mechanics using conjugate gradient, sequential search)
- SYBYL 6.1a, Tripos, Inc. (1994), Indigo 2 Extreme, R 4000, Silicon Graphics (mechanics using the Powell method, conformational analysis, RMS-fittings)

Results and Discussion

Conformational analyses

Minimizing the binding energy by optimizing the geometry of a given compound is the basic goal of modelling studies. One tool to perform this systematically can provide conformational analyses.

Recently we obtained an X-ray structural analysis of the potential receptor-binding rhenium complex (D₂ receptor) shown in Fig. 1 (Spies *et al.*, 1993). We intended to investigate the conformational space of **1**. The total number of possible conformers is determined by the equation $K = i^n$ (i = number of increments or steps of the dihedral angles, n = number of dihedral angles). Increments of 120 degrees correspond to with 243 conformers (5 dihedral angles of the coligand), but decreasing i to 15 degrees would lead to more than 7.9 million species!

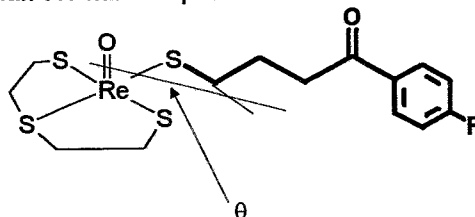
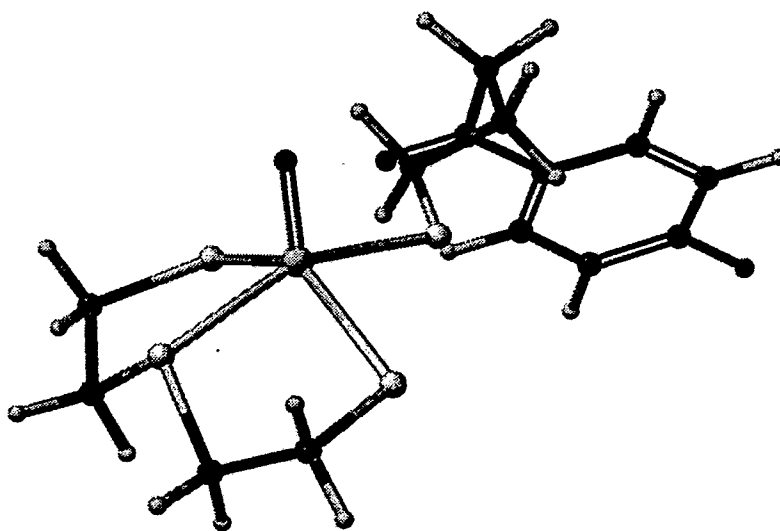
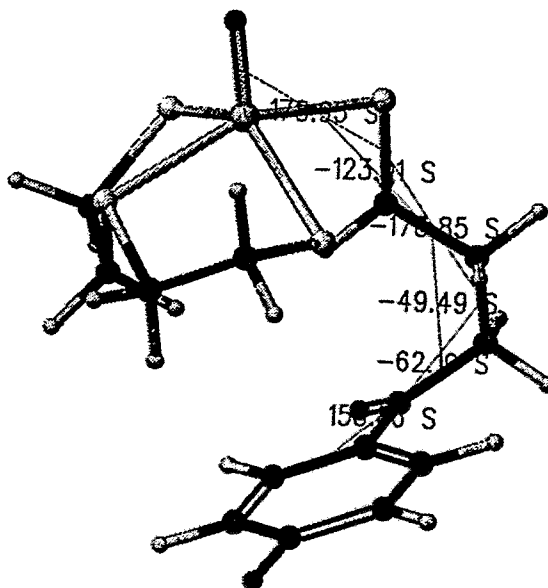


Fig. 1: Oxorhenium complex **1** containing the *p*-fluorobutyrophenone moiety of the D₂ antagonist spiperone (bold lines)

A sequential search was performed, starting with the dihedral angle O-Re-S-C where the geometry of the ligands was locked. The conformation of the lowest energy was used by this method as the starting point for the drive at the neighbouring dihedral angle etc. In contrast to the input the resulting conformation of all 6 angles suggested a position of the phenyl ring below the rhenium core. An one-point calculation with the coordinates from the crystal structure of **1** showed a significant higher binding energy than the resulting conformation of the sequential search (Fig. 2).



a)



b)

Fig. 2 a) X-ray structure of **1** [6], $E = 61.62$ kcal/mol, b) Result of a sequential search (increments 10 grd, input: X-ray structural data), $E = 28.08$ kcal/mol

The biggest change in potential energy is obviously determined by the first dihedral angle around the Re-S bond. Conformational analysis of this angle, starting with coordinates of the X-ray structural analysis, resulted in highest energies for conformations at -130° and 90° (equatorial positions) as shown in Fig. 3.

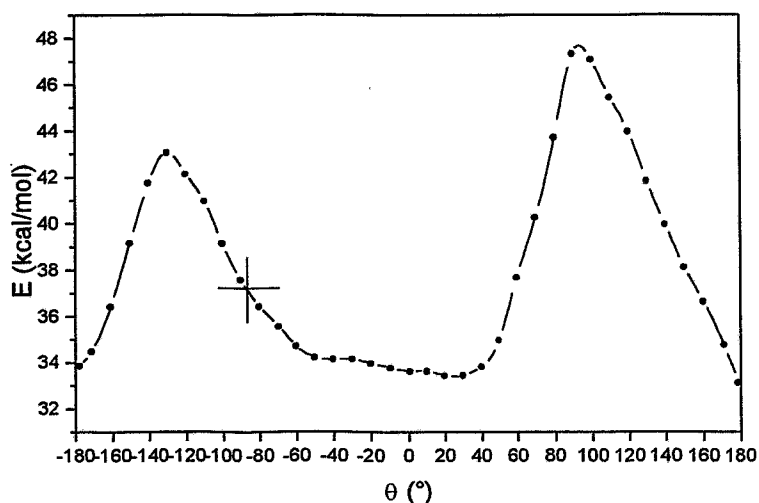


Fig. 3: Plot of the energy as function of the dihedral angle θ in **1**. The amount of the angle in the structural analysis (+) was not found to correspond with the calculated minimum.

RMS fittings

When the structure of the receptor is unknown, a common simple approach in assessing the binding properties of potential pharmaceuticals consists in building models by superimposing the structures of "active" molecules. Special programmes can create such pharmacophore-like models.

Some considerations refer to our work on potential receptor-binding technetium and rhenium complexes (Johannsen *et al.*, 1995).

Butaclamol, a typical D_2 antagonist, ketanserin and ritanserin as $5-HT_2$ antagonists are shown in Fig. 4.

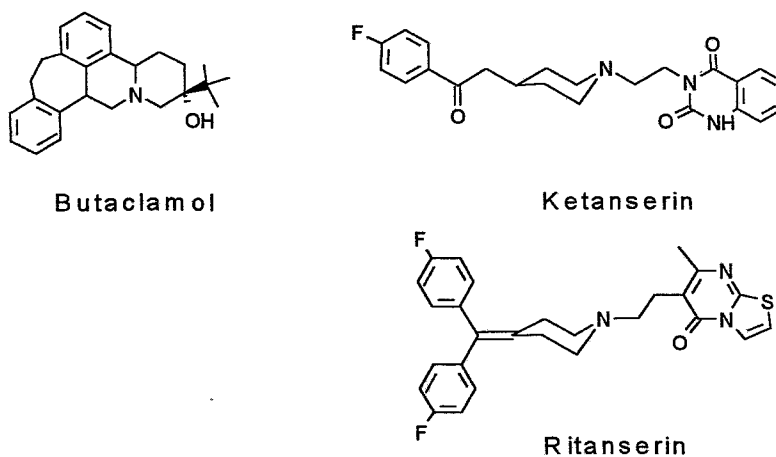


Fig. 4: Molecular formulas of D_2 and $5-HT_2$ receptor binding substances used as models for RMS fittings

In some studies the authors found a basic nitrogen at a distance of about 5 Å from the centre of a phenyl ring to be responsible for binding both on dopamine and ketanserin receptors (Andersen et al., 1994). Thus the compounds 2-4 containing an amine group should be of interest (Fig. 5).

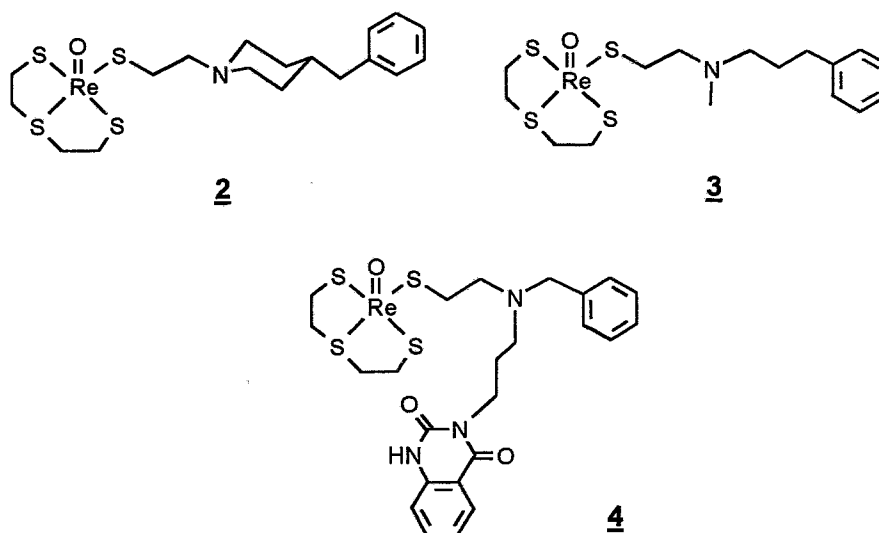


Fig. 5: Molecular formulas of the rhenium complexes used for RMS fittings, where 2 ($IC_{50} = 23$ nM) and 3 ($IC_{50} = 28$ nM) showed a significant affinity towards the 5-HT₂ receptor. Compounds of the type 4 remained "inactive" ($IC_{50} > 1000$ nM).

The structures 2-4 were optimized. The fitting with compounds in Fig. 4 according to the model of Fig. 6 was performed by calculating the root mean square distance (RMS) of selected points. The distance between nitrogen and the benzyl ring in 4 was too short compared with the model compounds (about 3.7 Å). This ring was therefore neglected in the following considerations. Furthermore, complex 4 was treated in three different optimized conformations 4a-b.

Butaclamol model

Butaclamol is a very rigid pentacyclic system which ought to correspond well to the pharmacophore of the dopamine receptor. We used three fitting points of the crystal structure: the nitrogen, the centre of the farthest phenyl ring and a point constructed 5 Å above this centre located on the normal (Tutorial, 1994).

The resulting RMS values are summarized in Table 1. We found only a slight decrease for 2 and 3.

Table 1: RMS values of the fittings using the model of butaclamol and lone-pair-model

	Butaclamol	Lone-pair-model		
		ketanserin	"left" phenyl ring	ritanserin "right" phenyl ring
<u>2</u>	0.992	0.785	0.601	0.645
<u>3</u>	0.885	0.929	0.753	0.796
<u>4a</u>	1.017	1.074	1.282	1.228
<u>4b</u>	1.232	0.611	0.791	0.499
<u>4c</u>	1.075	1.188	1.192	1.175

Lone-pair-model

A model we want to call "lone-pair-model" is depicted in Fig. 6 was described in the literature (Andersen et al., 1994). Fitting points for binding are the centres of the phenyl rings and a point in the direction of the lone pair 2.8 Å away from the basic nitrogen. This model was constructed using opti-

mized structures of ketanserin and ritanserin. Fig. 7 shows three selected superimpositions and Table 1 contains the calculated RMS values. These values are highest for the inactive **4**, with the exception of conformation **4b**. All in all, the results remain ambiguous.

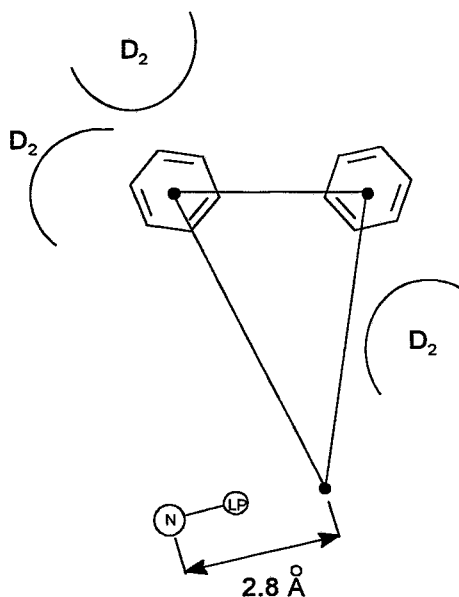


Fig. 6: Fitting model for the 5-HT₂ receptor including assumed binding sites of the D₂ receptor

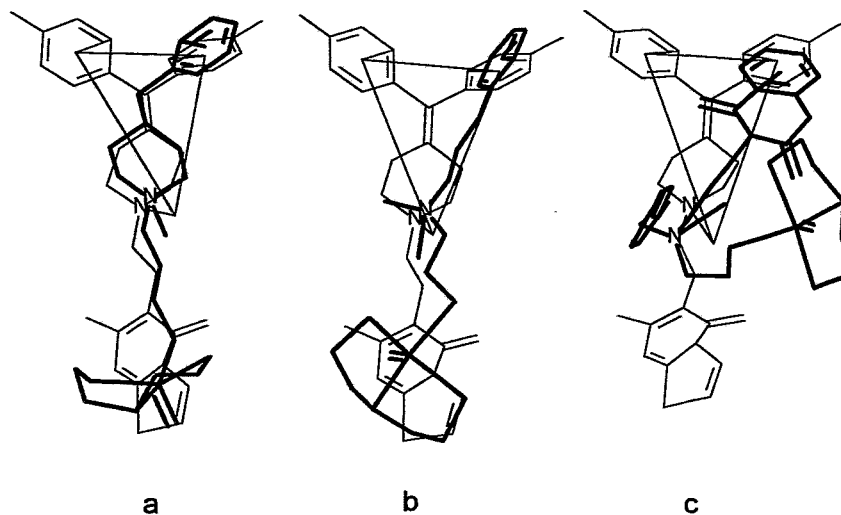


Fig. 7: Fittings on ritanserin: a) **2** (RMS = 0.645), b) **3** (RMS = 0.796) and c) **4a** (RMS = 1.228)

A comparison according to the lone-pair-model between **2** and some other conformations of **3** suggested, however, small RMS values (up to 0.075), which proves the results of the binding studies *in vitro* on 5-HT₂ receptors.

Some conclusions can be drawn:

- We found evidences, that the conformation of **1** does not correspond to the structure optimized by force field calculations (gas phase).
- RMS fittings with compounds of high receptor affinity lead to ambiguous results.
- The existence of a great number of conformers having quite similar energies is considered the main problem.
- Another point of view is the well-known fact that the active conformation must not be equal to a global minimum. Therefore, conformation analyses on rigid molecules should be more sophisticated.
- The main problem arises from the lack of force field parameters for technetium and rhenium. The semiempirical ZINDO/1 programme could be of help here. Although it is much slower, it provides in addition to geometries also heat of formation, dipol moments or answers for electron densities. Efforts in this field are in progress.

Acknowledgement

We wish to acknowledge the help of Prof. Michael J. Welch and Dr. David Reichard, St. Louis, who arranged an internship for M. G. to perform the modelling studies.

References

- Andersen K., Liljefors T., Gundertofte K., Perregaard J. and Boegesoe K.P. (1994) Development of a receptor-interaction model for serotonin 5-HT₂ receptor antagonists. Predicting selectivity with respect to dopamine D₂ receptors. *J. Med. Chem.* **37**, 950-962.
- Hancock R.D. and Martell A.E. (1989) Ligand design for selective complexation of metal ions in aqueous solution. *Chem. Rev.* **89**, 1875.
- Hansch C., Sammes P.G. and Taylor J.B. (1990) *Comprehensive Medical Chemistry 4*. Pergamon Press, Oxford
- Hay B.P. (1993) Methods for molecular mechanics modeling of coordination compounds. *Coord. Chem. Rev.* **126**, 177-236.
- Johannsen B., Scheunemann M., Spies H., Brust P., Wober J., Syhre R. and Pietzsch H.-J. (1995) Technetium(V) and rhenium(V) complexes for 5-HT_{2A} serotonin receptor binding: structure-affinity considerations. *J. Nucl. Med. Biol.*, in press.
- Kunz R.W. (1991) *Molecular Modeling für Anwender*. B. G. Teubner, Stuttgart.
- Lipkowitz K.B. and Boyd D.B. (1990) *Reviews in Computational Chemistry 1*. VCH Publishers Inc., New York.
- Spies H., Noll St., Noll B. and Klostermann K. (1993) Technetium and rhenium complexes derived from spiperone **1**. Synthesis of a 4-fluorobutyrophenone-containing neutral rhenium complex. *Annual Report 1993*, Institute of Bioanorganic and Radiopharmaceutical Chemistry, FZR-32, pp. 37-39.
- Tutorial (1994) SYBYL, Molecular Modeling Software 6.1a, Tripos Inc.

37. Cyclovoltammetric Investigations into Oxorhenium(V) Complexes of the "3+1" Type

T. Knieß, B. Noll, H. Spies

Introduction

Up to now a few studies exist into the electrochemical behaviour of oxorhenium(V) complexes. Complexes containing the Schiff-base ligand can be reduced and oxidized by electrochemical methods to species where rhenium is at the oxidation stage +4 and +6 (Tisato *et al.*, 1989; Seeber *et al.*, 1987). Anionic oxorhenium(V) complexes with Schiff-bases were investigated and it was found that oxidation to a neutral complex of the stage +6 is favoured (Seeber *et al.*, 1986). However, there are no clear statements concerning the reduction of such anionic complexes.

We wanted to study the redox behaviour of mixed ligand oxorhenium(V) complexes (Fig. 1) by cyclic voltammetry and to evaluate the influence of the substituent X and the ligand -SR in such complexes.

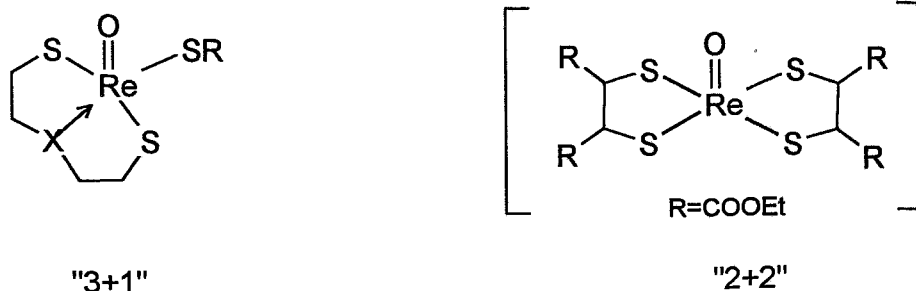


Fig.1: Mixed-ligand oxorhenium(V) complexes

Experimental

The oxorhenium(V) complexes were synthesized according to Spies *et al.*, (1995).

The electrochemical measurements were carried out with a Cyclic Voltammograph CV-27 (BAS) and a cell stand C-2 (BAS), supporting electrolyte: 0.1 M NBu_4PF_6 (Merck) in dry acetonitrile (Aldrich); inert gas: argon; working electrode: Pt-button electrode (diameter 1.6 mm); reference electrode: Ag/AgCl electrode; auxiliary electrode: Pt wire.

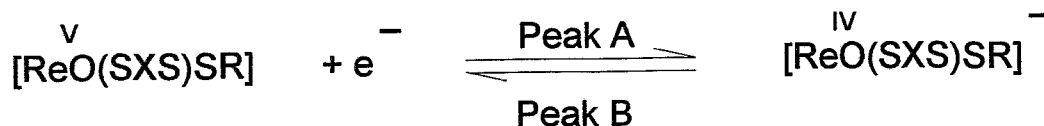
Results and Discussion

Various oxorhenium(V) complexes listed in Table 1 were investigated in the potential range from +1.00 V to -1.70 V. It turned out that the neutral "3+1" complexes show one reversible redox couple in the range from -1.61 V to -1.85 V.

This is in contrast to the anionic "2+2" complex $\text{NBu}_4[\text{ReO}(\text{dimercaptosuccinic aciddiethyl ester})_2]$, where only an indistinct cathodic step was observed.

Fig. 2 shows a cyclic voltammogram of the complex $[\text{ReO}(\text{SOS})\text{SCH}_2\text{CH}_3]$ **1**. There are two cathodic and two anodic steps, where the peaks C and D represent the redox couple of the added internal standard ferrocene/ferrocene⁺. The redox couple A, B explains a reversible one-electron process because the potential difference between the two peaks is about 60 mV.

The electron transition is expected to take place according to the following equation:



The comparable reduction was observed at oxotechnetium(V) complexes of the type $\text{TcOCl}(\text{L}_B)_2$ with L_B = Schiff-base ligand (Refosco *et al.* 1988).

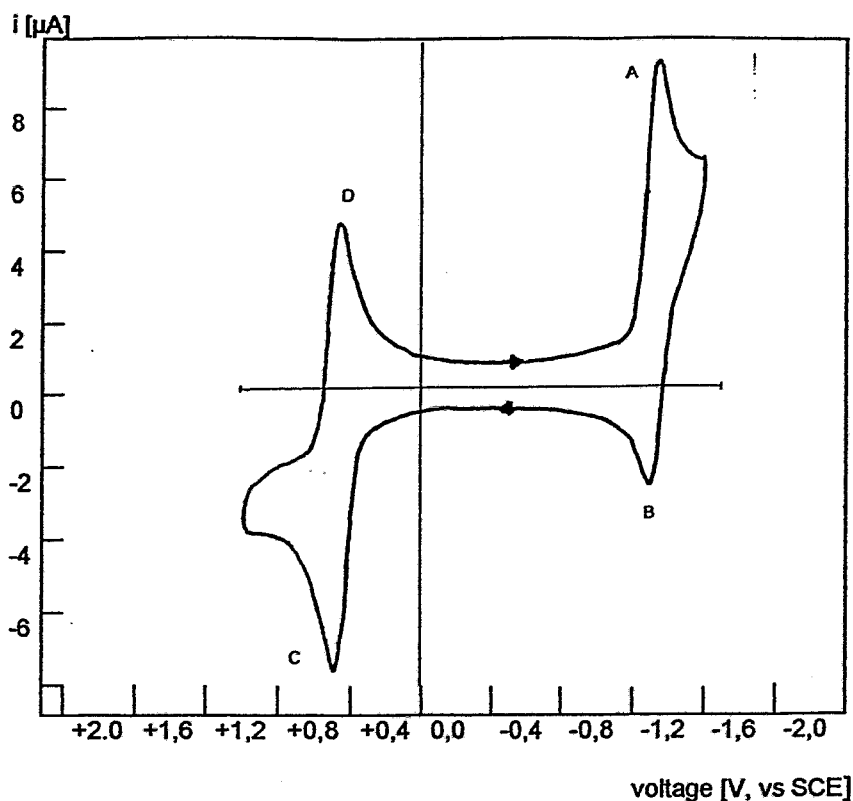


Fig. 2: Cyclic voltammogram of the complex $\text{ReO}(\text{SOS})\text{SCH}_2\text{CH}_3$ at 0,1 M $\text{Bu}_4\text{N}[\text{PF}_6]/\text{CH}_3\text{CN}$ (scan rate 200 mV/s)

Fig. 3 shows the cyclic voltammogram of the complex $[\text{ReO}(\text{SNCH}_3\text{S})\text{SCH}_2\text{CH}_3]$ **1** in the potential range from +1.50 V to -1.70 V after various repetitions of the cycle without ferrocene. In addition to the reversible peaks A and B one can see an anodic oxidation step F without wave in the cathodic direction. It does not change after several cycles. Such an anodic step was also observed by other authors at the above mentioned oxotechnetium(V) complexes (Refosco et.al. 1988). It is assumed that the intermediate anionic Tc(IV) complex is oxidized to unknown species in a slow irreversible competition reaction. The consumption of the postulated anion $[\text{ReO}(\text{SNCH}_3\text{S})\text{SCH}_2\text{CH}_3]$ could be the reason for the decrease in the anodic wave in Fig. 3.

In addition, new irreversible peaks G and E arise. More investigations are necessary for their identification.

The formal reduction potential E° was determined for all investigated complexes against the internal standard ferrocene (E° vs. $E^\circ \text{Fc}/\text{Fc}^+$). The results are documented in Table 1.

These preliminary results allow some conclusions concerning the influence of X in the tridentate ligand and the monodentate ligand -SR on the position of this redox step.

- Sulphur and oxygen as X do not show significant differences while $X = \text{NCH}_3$ causes a slight potential shift at about 50 mV in a negative direction.
- The negative shift from compound **1** to **9** in Table 1 may be caused by going from electron-donating to electron-drawing monodentate ligands.

We suppose that electron-donating groups increase the electron density at the rhenium atom and that is why an additional electron take-up (reduction) occurs at a higher potential. This is demonstrated by comparing compounds **2**, **3** with **8** and **9**, showing that quaternation of electron-donating amino groups shifts the redox potential at about 180 mV towards the positive range.

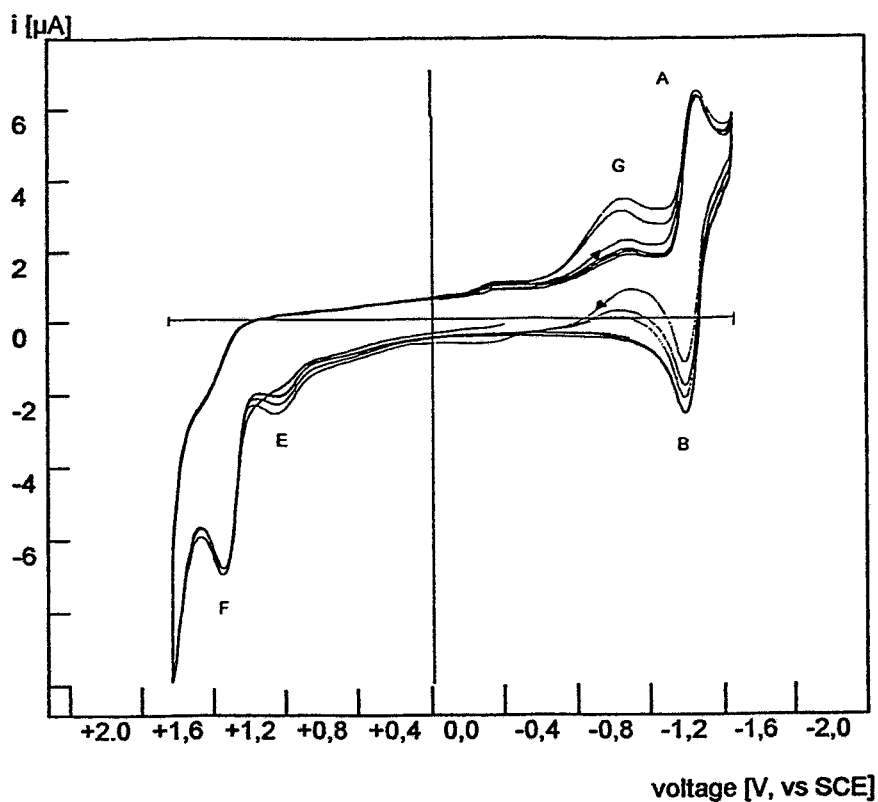


Fig. 3: Cyclic voltammogram of the complex $\text{ReO}(\text{SNCH}_3\text{S})\text{SCH}_2\text{CH}_3$ at 0,1 M $\text{Bu}_4\text{N}[\text{PF}_6]/\text{CH}_3\text{CN}$ (scan rate 220 mV/s)

Table 1: Redox potential E° of oxorhenium(V) complexes vs. $E^\circ \text{Fc}/\text{Fc}^+$

	R	X		
		S	O	NMe
1	$-\text{C}_2\text{H}_5$	-1,81 V	-1,80 V	-1,85 V
2	$-\text{CH}_2\text{-CH}_2\text{-NEt}_2$	-1,79 V		
3	$-\text{CH}_2\text{-CH}_2\text{-NMe}_2$	-1,77 V		
4	$-\text{CH}_2\text{-CH}_2\text{-OH}$	-1,71 V		
5	$-\text{CH}_2\text{-COOC}_2\text{H}_5$	-1,69 V	-1,69 V	-1,75 V
6	$-\text{CN}$	-1,68 V		
7	$-\text{C}_6\text{H}_5$	-1,65 V	-1,68 V	
8	$-\text{CH}_2\text{-CH}_2\text{-NEt}_2\text{Me}^+\text{I}$	-1,61 V		
9	$-(\text{CH}_2)_8\text{-NEt}_2\text{Me}^+\text{I}$	-1,60 V		

References

- Refosco F., Mazzi U., Deutsch E., Kirchoff J.R., Heinemann W.R. and Seeber R. (1988) Electrochemistry of oxo-technetium(V) complexes containing Schiff-base and quinolinol ligands *Inorg. Chem.* **27**, 4121-4127.
- Seeber R., Mazzocchin G. A., Refosco F., Mazzi U. and Tisato F. (1987) Electrochemistry of rhenium(V) complexes with N-(2-hydroxyphenyl)salicylideneimine as Schiff-base ligand *Polyhedron* **6**, 1647-1652.
- Seeber R., Mazzocchin G. A., Mazzi U., Refosco F. and Tisato F. (1986) Electrochemistry of rhenium(V) complexes with bidentate-bidentate and tridentate-bidentate Schiff-base ligands *Polyhedron* **5**, 1975-1982.
- Spies H., Fietz F., Pietzsch H.-J., Johannsen B., Leibnitz P., Reck G., Scheller D. and Klostermann K. (1995) Neutral oxo rhenium(V) complexes with tridentate dithiolates and monodentate alkane thiolate co-ligands. *J. Chem. Soc., Dalton Trans.*, 2277-2280.
- Tisato F., Refosco F., Mazzi U., Bandoli G. and Dolmella A. (1989) Synthesis, characterisation and electrochemical studies on technetium(V) and rhenium(V) oxo-complexes with N,N'-2-hydroxypropane-1,3-bis(salicylideneimine). *Inorg. Chem. Acta* **164**, 127-135.

38. Rhenium(V) Gluconate, a Suitable Precursor for the Preparation of Rhenium(V) Complexes

B. Noll, T. Knieß, M. Friebe, H. Spies, B. Johannsen

Introduction

Tc(V) gluconate has been used for a long time as a convenient substrate for ligand exchange reactions to obtain defined Tc(V) complexes (Johannsen *et al.*, 1978; Spies *et al.*, 1981). Initially the method was restricted to a 10^{-4} or higher molar level and was then successfully extended to n.c.a. ^{99m}Tc as present in $^{99}\text{Mo}/^{99m}\text{Tc}$ generator eluates (Noll *et al.*, 1990). With increasing involvement in rhenium chemistry relevant to nuclear medicine, we became interested in an analogous synthesis route starting from Re(V) gluconate. Taking the differences between Tc and Re chemistry into account, a procedure for the preparation of Re(V) gluconate has been developed. Whereas the preparation proved to be easily attainable at higher concentrations of rhenium (Noll *et al.*, 1992), downscaling to the concentration level of the $^{188}\text{W}/^{188}\text{Re}$ generator eluate appears to be difficult. This paper reports a successful attempt to study the formation of Re(V) gluconate in the μmol level based on polarographic investigations.

Experimental

UV/VIS spectra were recorded on a spectrophotometer Specord M40. Polarography was carried out with a DC/AC polarograph GWP 673 under the following conditions: direct fast polarography in 10 mV steps, droptime 1.6 s, reference electrode: saturated calomel electrode (SCE), supporting electrolyte: 0.5 M sodium gluconate, inert gas: argon.

Procedure for the preparation of rhenium(V) gluconate at the μmol level

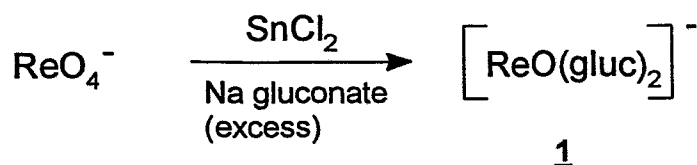
2.5 μmol ammonium perrhenate was dissolved in 5 ml 0.5 M sodium gluconate and the mixture was deoxygenated by argon. After ten minutes 25 μmol stannous chloride dissolved in 400 μl 1 M HCl was added. The preparation is ready for use after 90 minutes.

Polarographic measurements

Stannous chloride (10 μmol) dissolved in 400 μl 1 M HCl was added to 8 ml supporting electrolyte and the polarogram was recorded in a potential range from +100 to -1100 mV. The stannous concentration was determined by the cathodic wave at -800 mV. Equimolar amounts of ammonium perrhenate were added as a 0.3 M solution and the decrease in stannous concentration was registered.

Results and Discussion

Addition of stannous chloride to perrhenate in the presence of an excess of sodium gluconate causes a decrease of the UV absorption of perrhenate ions (230 nm), indicating a reduction of perrhenate, and a new low-intensity band ($\lg \epsilon = 1.5$) occurs at about 620 nm. It takes about one hour to reduce perrhenate completely with stannous ions:



A pure solid **1** product could not yet be isolated. As observed earlier for Tc(V) gluconate (Johannsen *et al.*, 1978), an excess of sodium gluconate is necessary to stabilize the complex. A concentration level of about 0.5 M sodium gluconate is used for preparation of **1** at the μmol level, and separation of the complex from an excess of ligand leads to decomposition of **1**.

While the formation of **1** can be monitored by UV spectrometry only to a concentration of about 10^{-2} mol/l because of the low extinction coefficient, further support for the formation of **1** at a concentration level of 10^{-2} mol/l and lower can be obtained by polarography. A typical polarogram is shown in Fig. 1. The perrhenate ion itself shows no half-wave under our experimental conditions. However, the consumption of stannous chloride by perrhenate, measured by the decrease of the stannous wave, reveals a 1:1 stoichiometry for the $\text{ReO}_4^-/\text{Sn}^{2+}$ reaction. Parallel to the decrease of the stannous wave (determined at -800 mV), an increase in an additional anodic wave ($e_{1/2} = -50$ mV) is observed, which we consider to be caused by rhenium(V) gluconate.

At concentrations lower than 10^{-2} mol/l of both perrhenate and stannous ions, the reaction rate becomes very low and perrhenate is incompletely reduced in acceptable times. This disadvantage can be overcome by using an excess of stannous ions. Polarographic experiments illustrate that e.g. a fourfold excess of stannous chloride over perrhenate leads to clean conversion of perrhenate into rhenium(V) gluconate within two hours without further reduction to lower oxidation states. Detailed results will be published in the literature (Noll *et al.*, 1996).

The ability of **1** to act as a precursor for the preparation of rhenium(V) complexes was demonstrated in its reaction with di- and tetradentate sulphur-containing ligands such as mercaptoacetyl diglycine (H_4MAG_2) (Johannsen *et al.*, 1993) and 2-aminobenzenethiol (Spies *et al.*, 1989).

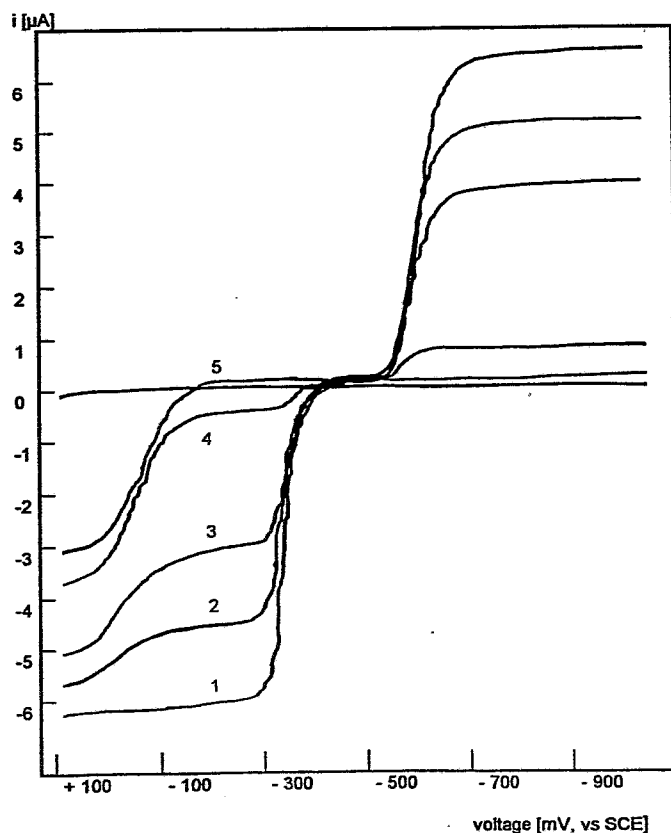


Fig. 1: DC-polarogramm of the reaction of $1 \cdot 10^{-5}$ mol ReO_4^- with $1 \cdot 10^{-5}$ mol Sn^{2+} ; decrease of the stannous step over the time. (1 = start, 2 = 20 min, 3 = 45 min, 4 = 105 min, 5 = complete reaction)

References

- Johannsen B. and Syhre R. (1978) Untersuchungen zur Komplexbildung von Tc-99 mit Gluconat. *Radiochem. Radioanal. Letters* **36**, 107-110.
- Johannsen B., Noll B., Leibnitz P., Reck G., Noll St. and Spies H. (1993) Technetium and rhenium complexes of mercapto containing peptides. *Inorg. Chim. Acta* **210**, 209-214.
- Noll B., Knieß T., Friebe M., Spies H. and Johannsen B. (1996) Rhenium(V) gluconate, a suitable precursor for the preparation of rhenium(V) complexes. *Isotopes Environ. Health Studies* **32**, in press.
- Noll B., Kolbe U., Noll St. and Spies H. (1992) Rhenium(V) gluconate as precursor for preparation of rhenium(V) complexes. *Annual Report 1992*, Institute of Bioinorganic and Radiopharmaceutical Chemistry, FZR 93-12, pp. 115-118.
- Noll B., Spies H., Scheibe O. and Pietzsch H.-J. (1990) ^{99m}Tc gluconate and ^{99m}Tc ethylene glycolate as starting complexes for ligand exchange relations. *Annual Report 1990*, Department of Radioactive Isotopes, ZfK-739, pp. 36-38.
- Spies H. and Johannsen B. (1981) Oxotechnetium(V) bis(dithiolato) complexes. *Inorg. Chim. Acta* **48**, 255-258.
- Spies H., Pietzsch H.-J. and Hoffmann I. (1989) Technetium complexes of 2-amino benzenethiol. *Inorg. Chim. Acta*, **161**, 17-19.

39. Structural Investigations of Technetium and Rhenium Complexes by EXAFS.

1. Studies on "n+1" Mixed-Ligand Rhenium Complexes.

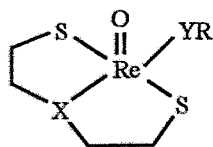
T. Reich¹, G. Bernhard¹, H. Nitsche¹, H. Spies, B. Johannsen

¹Institute of Radiochemistry, Research Center Rossendorf

Introduction

X-ray Absorption Spectroscopy (XAS) is a well established technique for the determination of element-specific information on oxidation states of an absorbing atom and on structural parameters of its nearest-neighbor environment (Koningsberger and Prins, 1988). XAS has become a valuable tool for studies of metal-based drugs and environmentally-relevant systems (Elder and Eidsness, 1987). This technique also extends the capability of studying radioactive technetium in small solid and liquid samples. This is crucial for the understanding of ^{99m}Tc radiopharmaceuticals as well as of the behaviour of the nuclear fission's by-product ^{99}Tc in the geosphere as a function of its oxidation state (Almahamid *et al.*, 1995; Martin *et al.*, 1989). As a result of the extremely small amount of technetium present in ^{99m}Tc radiopharmaceuticals (10^{-6} - 10^{-8} M), XAS studies employ the long-lived isotope ^{99}Tc (K edge at 21.044 keV) or rhenium (L_{III} edge at 10.535 keV) as surrogates.

As part of their joint research on radiotracers in biosystems, the Institute of Radiochemistry and the Institute of Bioinorganic and Radiopharmaceutical Chemistry at the Research Center Rossendorf studied novel rhenium complexes by Extended X-ray Absorption Fine Structure (EXAFS) spectroscopy. The aim of this study was the evaluation of the EXAFS method for the determination of structural parameters of the nearest-neighbor environment of Re(V) and Re(III) in "n+1" mixed-ligand complexes. To this end we report on a comparison of coordination numbers and inter-atomic distances obtained by EXAFS analysis with those known from recent single-crystal X-ray diffraction (XRD) studies for the following complexes (**1**, Leibnitz, 1994; **2**, Spies *et al.*, 1995a; **3**, Fietz *et al.*, 1995a; **4**, Spies *et al.*, 1994):



- 1** X = S, YR = SEt
2 X = O, YR = S-C₆H₄-OMe(p)
3 X = O, YR = Se-C₆H₅

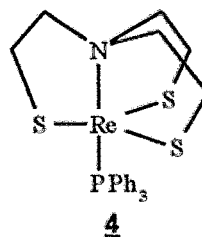


Fig. 1: Rhenium compounds used for EXAFS measurements

Experimental

Samples were prepared for measurements by mixing the rhenium complex with BN powder and pressing it into pellets. Rhenium L_{III} edge XAS spectra of samples 1 - 3 were measured at room temperature in transmission mode at the Stanford Synchrotron Radiation Laboratory (SSRL) on beamline 2-3 using a Si(220) double-crystal monochromator. Sample 4 was measured at the Hamburger Synchrotronstrahlungslabor (HASYLAB) on beamline RÖMO II equipped with a Si(311) double-crystal monochromator. For the EXAFS analysis we used the software package EXAFSPAK (George and Pickering, 1995). For energy calibration purposes, the first inflection point of the absorption edge was defined as 10535 eV. Theoretical scattering amplitudes and phases were calculated with the program FEFF6 (Mustre de Leon *et al.*, 1991). The program Atoms version 2.42g, which is part of FEFF6, was used to calculate inter-atomic distances in the complexes 1 - 4 from the atomic coordinates measured by XRD.

Results and Discussion

The EXAFS spectra and their corresponding Fourier transforms (FT's) of 1 - 4 are shown in Fig. 2. The fit results of the EXAFS spectra are given in Table 1. During the fit, the coordination numbers *N* of all shells were kept constant. As a result of the limited data range of the EXAFS spectra, differences in the distance from the central rhenium atom to sulfur or carbon atoms of less than 0.15 Å cannot be resolved. These atoms were fitted as single coordination shells, e.g., Re-S and Re-C. To compare the EXAFS results with those from XRD, we averaged the Re-S and Re-C inter-atomic distances measured by XRD over the corresponding coordination shells (see Table 1).

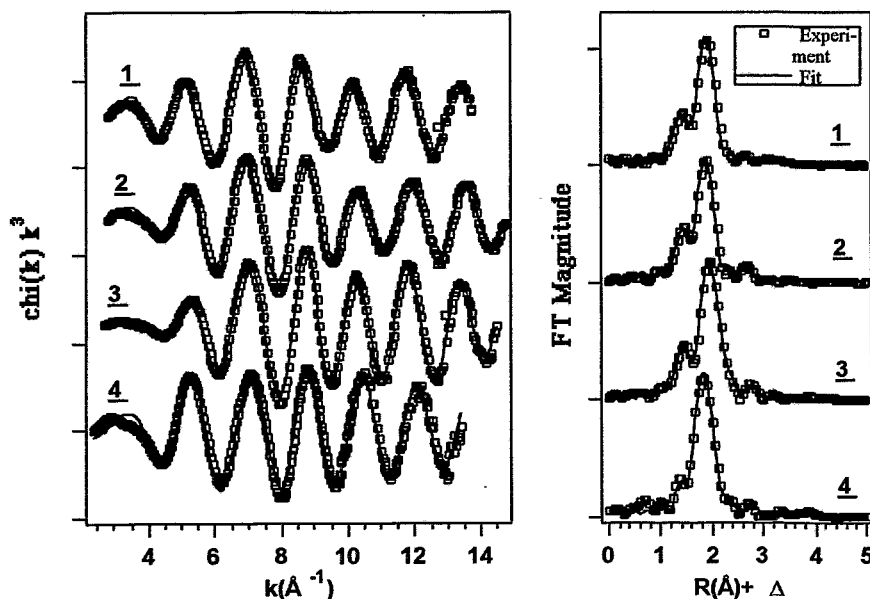


Fig. 2: Left panel: Experimental Re L_{III} edge EXAFS of complexes 1 - 4.
Right panel: Fourier-transformed EXAFS of samples 1 - 4

The coordination sphere of complexes 1 - 3 consists of a monodentate ligand YR and 3-thiapentane-1,5-dithiol or 3-oxapentane-1,5-dithiol ($\text{HS-CH}_2\text{CH}_2\text{-X-CH}_2\text{CH}_2\text{-SH}$, X = O, S) as chelate ligands with three donor atoms (Fietz *et al.*, 1995b; Spies *et al.*, 1995a; Fietz *et al.*, 1995a). These "3+1" oxorhenium(V) complexes possess a distorted tetragonal pyramidal coordination around the rhenium atom as shown for compound 3 in Fig. 3.

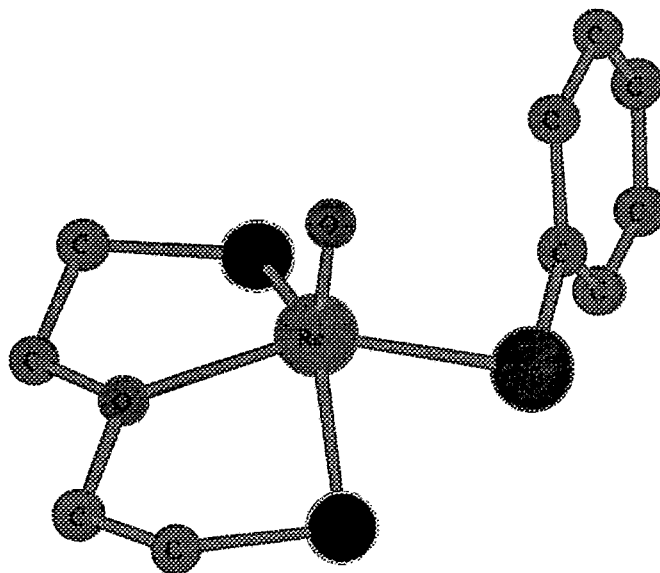


Fig. 3: A drawing illustrating the solid-state conformation of (3-oxapentane-1,5-dithiolato)(benzeneselenolato)oxorhenium(V) (**3**)

The EXAFS spectrum of complex **1** is dominated by the scattering of electrons originating from the absorbing rhenium atom off the four neighboring sulfur atoms. These give rise to the main peak in the FT centered around 2.0 Å (see Fig. 2). The shoulder at lower R is a result of the shorter Re=O bond. Note that a small feature above the noise level can be observed in the FT centered at 2.7 Å. This small peak can be explained as follows: the four carbon atoms of the tridentate dithiol ligand are located in the range of 3.26 - 3.40 Å from the rhenium. The distance to the nearest carbon atom of the monodentate SET ligand is with 3.39 Å within the same range. Thus, five carbon atoms with an average distance of 3.35 Å can be considered as a Re-C coordination shell giving rise to the small feature observed in the FT. The inter-atomic distances obtained by EXAFS are in good agreement with the XRD results. For the Re=O bond, the EXAFS gives a 0.03 Å longer distance than XRD, which is slightly more than the typical experimental uncertainty of the EXAFS analysis of ± 0.02 Å. A fit of the EXAFS with coordination numbers allowed to vary gives 0.9 and 4.0 for the Re=O and Re-S coordination shells, respectively. In the best fit for Re-C coordination shell, N equals 2.4 ± 0.7 . The similar situation has been observed for all fits with variable coordination numbers of the other complexes studied. Thus, reliable coordination numbers can be obtained by EXAFS for the first Re=O coordination shell and shells of neighboring atoms with higher atomic number like S or Se. For the light atoms at a longer distance such as Re-C, the error in N can be up to 50 %.

For complex **2**, the inter-atomic distances are in agreement with the XRD results. It should be noted that the Re-O shell at 2.08 Å contributes less than 5 % to the total EXAFS and partially overlaps with the dominating Re-S shell at 2.29 Å. Therefore it might be difficult to observe the presence of a single Re-O bond for this type of rhenium or technetium complexes by EXAFS if the presence of such a bond is not known *a priori*. The Re-C inter-atomic distance in complex **2** is 0.18 Å shorter than in **1**. This significant decrease is caused by the shorter Re-O bond of the tridentate dithiol ligand in **2** as compared to the corresponding Re-S bond in **1**. Although it might not be possible to obtain structural parameters for the Re-X (X = O, S) shell by EXAFS for the reasons mentioned before, a reduction of the Re-C distance will be indicative for a decrease of the Re-X bond.

The coordination of rhenium in complex **3** is similar to that of **2** except that the sulfur atom of the monodentate ligand is replaced by selenium. Electron scattering off the selenium atom contributes approximately 40 % to the EXAFS and is also the reason for a larger EXAFS amplitude of **3** in the k range of 3 - 10 Å⁻¹ as compared to the spectrum of **2** (see Fig. 2). It is known that high Z elements, e.g., selenium, are easier to detect by EXAFS than low Z elements, e.g., carbon and oxygen (Koningsberger and Prins, 1988). As in the case of complex **2**, electron scattering off the oxygen atom of the tridentate dithiol ligand contributes less than 5 % to the EXAFS amplitude. Therefore, the

Re-O shell could be included in the fit only because its presence was known *a priori*. The inter-atomic distances obtained of all four coordination shells are in agreement with the XRD results.

Table 1: Structural parameters of compounds **1** - **4**; comparison of EXAFS with XRD analysis

Sample	Re=O			Re-O				Re-S				
	EXAFS		XRD	EXAFS		XRD	EXAFS		XRD			
	N	s ² (Å ²)	R(Å)	N	s ² (Å ²)	R(Å)	R(Å)	N	s ² (Å ²)	R(Å)	R(Å)	
1	1	0.002	1.69	1.66				4	0.003	2.31	2.31 [*]	
2	1	0.002	1.69	1.68	1	0.004	2.08	2.11	3	0.002	2.29	2.29 [*]
3	1	0.002	1.68	1.65	1	0.001	2.07	2.10	2	0.002	2.29	2.28 [*]
4					1 [#]			2.18 [#]	4	0.002	2.27	2.25 [*]

Sample	Re-Se			Re-C				
	EXAFS		XRD	EXAFS		XRD		
	N	s ² (Å ²)	R(Å)	R(Å)	N	s ² (Å ²)	R(Å)	R(Å)
1					5	0.011	3.34	3.35 [*]
2					4	0.006	3.16	3.15 [*]
3	1	0.002	2.42	2.41	4	0.006	3.16	3.15 [*]
4					6	0.014	3.20	3.12 [*]

^{*}) averaged value of N inter-atomic distances

[#]) parameters for the Re-N bond

Complex **4** is a trigonal-bipyramidal mixed-ligand Re(III) complex (Spies *et al.*, 1994). Three sulfur atoms coordinate the rhenium atom in the equatorial plane. The nitrogen and phosphorus atoms are in *trans* position to each other. EXAFS analysis can not distinguish between neighboring elements like phosphorus and sulfur. Therefore, the phosphorus atom was treated in the fit as an additional sulfur atom in the Re-S coordination shell. The inter-atomic distance of the Re-S shell obtained is in agreement with XRD results. We like to emphasize that we do not report on parameters of the Re-N bond. An attempt to include a Re-N coordination shell gave a bond distance in agreement with the XRD result. But this might be an accidental coincidence. We believe that this shell should not be included in a fit because the separation in distance from the dominating Re-S shell is 0.10 Å, which is less than the expected resolution given by our data range in k-space.

In summary, the possibilities and limitations of the EXAFS analysis have been studied for several "n+1" mixed-ligand rhenium complexes. The inter-atomic distances obtained by EXAFS are in excellent agreement with the XRD results. The coordination numbers for the Re=O, Re-S, and Re-Se shells deviate less than 12 % from the expected values. It was possible to measure the distance between rhenium and carbon atoms which do not form bonds with the central atom. Although, the coordination number for the Re-C shell has a large uncertainty of approximately 50 %, the inter-atomic distance is accurate within ±0.02 Å. The reason for the somewhat larger deviation between EXAFS and XRD results for the Re-C bond length in **4** is not clear and will be investigated further. Observed changes of the Re-C distance can be used to estimate the Re-X (X = O,S) bond length of tridentate dithiol ligands. This is especially valuable because the direct measurement of the Re-X bond length by EXAFS may be difficult. In conclusion, analysis of the Re L_{III} or Tc K edge EXAFS is a valuable

tool for the accurate determination of structural parameters of "n+1" mixed ligand rhenium or technetium complexes. This is especially important for amorphous solid or liquid complexes where XRD can not be applied.

Acknowledgment

We thank R. Nicolai for her help during the sample preparation. We are grateful to P. G. Allen, M. A. Denecke, and D. K. Shuh for their help during the experiments. The majority of the EXAFS experiments were performed at SSRL, which is operated by the U.S. Department of Energy, Office of Basic Energy Sciences, Division of Chemical Sciences. We thank also HASYLAB for its support during the EXAFS experiment.

References

- Almahamid I., Bryan J.C., Bucher J.J., Burrell A.K., Edelstein N.M., Hudson E.A., Kaltsoyannis N., Lukens W.W., Shuh D.K., Nitsche H. and Reich T. (1995) Electronic and structural investigations of technetium compounds by X-ray absorption spectroscopy. *Inorg. Chem.* **34**, 193-198.
- Elder R. C. and Eidsness M. K. (1987) Synchrotron X-ray studies of metal based drugs and metabolites. *Chem. Rev.* **87**, 1027-1046.
- Fietz T., Spies H., Leibnitz P. and Scheller D. (1995a) Mixed-ligand oxorhenium(V) complexes with rhenium-selenium bonds. Molecular structure of (3-oxapentane-1,5-dithiolato)(benzeneselenolato)oxorhenium(V). *J. Coord. Chem.*, accepted for publication.
- Fietz T. (1995b) Rhenium-Komplexe mit 3+1-Koordination. *Thesis*, TU Dresden.
- George G.N. and Pickering I.J. (1995) EXAFSPAK, a suite of computer programs for analysis of X-ray absorption spectra. Stanford Synchrotron Radiation Laboratory, Stanford, CA.
- Koningsberger D.C. and Prins R. (1988) *X-ray absorption. Principles, application, techniques of EXAFS, SEXAFS and XANES*, 1st ed., John Wiley and Sons, Inc., New York.
- Leibnitz P. (1994) private communication.
- Martin J.L., Yuan J., Lunte C.E., Elder R.C., Heineman W.R. and Deutsch E. (1989) Technetium-diphosphonate skeletal imaging agents: EXAFS structural studies in aqueous solution. *Inorg. Chem.* **28**, 2899-2901.
- Mustre de Leon J., Rehr J.J., Zabinsky S.I. and Albers R.C. (1991) Ab initio curved-wave X-ray absorption fine structure. *Phys. Rev. B* **44**, 4146-4156.
- Spies H., Fietz T., Pietzsch H.-J., Johannsen B., Leibnitz P., Reck G. and Klostermann K. (1995a) Neutral oxorhenium(V) complexes with tridentate dithiolates and monodentate alkane- or arene-thiolate co-ligands. *J. Chem. Soc., Dalton Trans.* 2277-2280.
- Spies H., Fietz T., Glaser M., Pietzsch H.-J. and Johannsen B. (1995b) The "n+1" concept in the synthesis strategy of novel technetium and rhenium tracers. In: *Technetium and Rhenium in Chemistry and Nuclear Medicine* (Edited by Nicolini M., Bandolini G. and Mazzi U.) SGEDITORIALI Padova, 4, pp. 243-246.
- Spies H., Glaser M., Pietzsch H.-J., Hahn F.E., Kintzel O. and Lügger T. (1994) Trigonal-bipyramidale Technetium- und Rhenium-Komplexe mit vierzähligen tripodalen NS_3 -Liganden. *Angew. Chem.* **106**, 1416-1419.

40. The Permeability of Several Lipophilic ^{99/99m}Tc Complexes through Cerebral Endothelial Cell Monolayers of Low Electrical Resistance

B. Ahlemeyer, P. Brust, S. Matys, J. Wober, H.J. Pietzsch, M. Scheunemann, B. Johannsen

Introduction

The blood-brain barrier (BBB) controls the transport of drugs and solutes from the blood into the brain by membrane permeability of the endothelial cells of brain capillaries. Recently a number of investigators studied the transport of drugs across the blood-brain barrier with primary cultures of cerebral endothelial cells (de Boer *et al.*, 1994). However, one of the main disadvantages of endothelial cell cultures is the low electrical resistance compared to *in vivo* suggesting a large amount of transport through intercellular spaces of the endothelial monolayer. Therefore, the paracellular permeability was determined with [¹⁴C] sucrose (van Bree *et al.*, 1988; Pardridge, 1990; Saheki *et al.*, 1994; Mizuguchi *et al.*, 1994; Pirro *et al.*, 1994; Fischer *et al.*, 1995), with fluorescein sodium (Jaehde *et al.*, 1993) or by electrical resistance as well as microscopic control of the integrity of the monolayer (Jaehde *et al.*, 1994; Masereeuw *et al.*, 1994). The ratio of total permeability to paracellular permeability (permeability index, PI) is used as a parameter for the ability of a drug to be transported or to diffuse through endothelial cell membranes (Pirro *et al.*, 1994). In transport studies, some authors compared only the results of filters with the same resistance values (Jaehde *et al.*, 1994; Masereeuw *et al.*, 1994), with the same paracellular permeabilities or they corrected total transport by transport at 4 °C (Audus and Borchardt, 1986), but filters at 4 °C may not have the same leakiness as the filters measured for total transport. In the case of high electrical resistance of the cell monolayer (>100 Ohm/cm²), total transport reflects transendothelial transport because of the very low paracellular permeability. However, in the case of low electrical resistance (<100 Ohm/cm²), total transport has to be corrected by paracellular transport. We therefore decided to correct total transport by paracellular transport of the same filter.

In the present study we examined whether the permeability coefficient of fluorescein sodium can be used as a parameter for paracellular permeability by comparing the results with the permeability coefficient of drugs at 4 °C, which also reflects temperature-independent transport through intercellular spaces.

In addition, we measured the transendothelial permeability coefficient of several ^{99/99m}Tc complexes with high affinity to 5-HT₂ receptors and compared the results with *in vivo* findings (Johannsen *et al.*, 1995). Similar studies with several ^{99/99m}Tc complexes were already carried out by Pirro *et al.* (1994).

Experimental

Materials

Fluorescein sodium was purchased from Sigma Chemicals, Deisenhofen, Germany and [³H]-L-leucine (2 TBq/mmol) was from Amersham Life Science, Braunschweig, Germany. The ^{99/99m}Tc complexes 15-19 (specific activity between 32 and 127 TBq/mol) were synthesized in our laboratory, and the purity and stability was controlled directly after synthesis by chromatographic methods. All other chemicals were derived as previously described in this report.

Measurement of transendothelial resistance

The transendothelial resistance (TEER) was measured 1 h before the transport studies using the EVOM-system with the 12-well endohm (WPI, Berlin, Germany). The TEER values were expressed as the difference of TEER measured across the endothelial cell layer and a background resistance measured across cell-free filters all coated with collagen.

Measurement of permeability coefficients

The transport studies were performed with endothelial cells grown on 12-well Costar filters after 4 and 6 days in culture. Cell monolayers on Transwell filters were washed two times with 0.1 M phosphate buffered saline (with 0.9 mM Ca²⁺ and 0.5 mM Mg²⁺, PBS⁺⁺, pH = 7.4). We used PBS⁺⁺ instead of a HEPES-buffered saline, because Douglas *et al.* (1993) have recently shown that 12 mM HEPES increased the permeability of macromolecules like albumin 4fold without changing the electrical resistance. Luminal to basolateral transport was initiated by adding 0.5 ml of the drug in PBS⁺⁺ to the upper chamber (the lower chamber contained 1.5 ml PBS⁺⁺). An aliquot was immediately sampled from the upper chamber to calculate the initial concentration. At designated times aliquots were sampled from the lower chamber. Basolateral to luminal transport was initiated by adding 1.5 ml of

the drug in PBS⁺⁺ to the lower chamber (the upper chamber contained 0.5 ml PBS⁺⁺) and an aliquot was sampled from the lower chamber to calculate the initial concentration. At designated times, aliquots were sampled from the lower chamber. The amounts of fluorescein sodium, [³H]-L-leucine and ^{99m/99}Tc complexes that had permeated through the filter were quantified by a fluorescence spectrophotometer (model Hitachi F-4500, Colora Messtechnik, Germany), a β-counter (model LSC600, Beckmann Instruments, Germany) and a COBRA II Auto-gamma (Packard, Germany).

The total amount of substrate that had permeated through the endothelial cell monolayer (p_{tot}) was calculated by dividing it by the initial substrate concentrations in the donor chamber. The permeability coefficients (clearance/area) were obtained from the slope of the permeated amounts vs time by linear regression.

The total permeability coefficients of the drug and of fluorescein sodium (p_{tot}) were corrected by the permeability coefficient through cell-free filter (p_{fil}) to obtain the paracellular (p_m) and the endothelial permeability coefficients (p_e) by the following equation:

$$1/p_m \text{ or } 1/p_e = 1/p_{tot} - 1/p_{fil}$$

The transendothelial permeability coefficient of the drug (μl/min/cm²) was determined by:

$$p_{trans} = p_e - p_m$$

Results and Discussion

The relationship between the electrical resistance and the permeability coefficient of fluorescein is shown in Fig. 1. The electrical resistance was higher after 4 days and concomitantly the paracellular permeability coefficient was lower compared to the results after 6 days. At low resistance values of 20 Ohm/cm² we found here a wide range of paracellular permeability coefficients between 0.58 and 3.28 μl/cm² min. In addition, we found approximately paracellular permeability coefficients of 0.59 and 0.51 μl/min/cm² in filters of 20 and 55 Ohm/cm² (Fig. 1). The results suggest that the passage of small ions as measured by electrical resistance does not provide the best information on the passage of greater molecules with molecular weights in the range of 150 - 400. The leakiness for these substrates is better evaluated by measurement of the permeability coefficient of fluorescein derivatives in the same range of molecular weight.

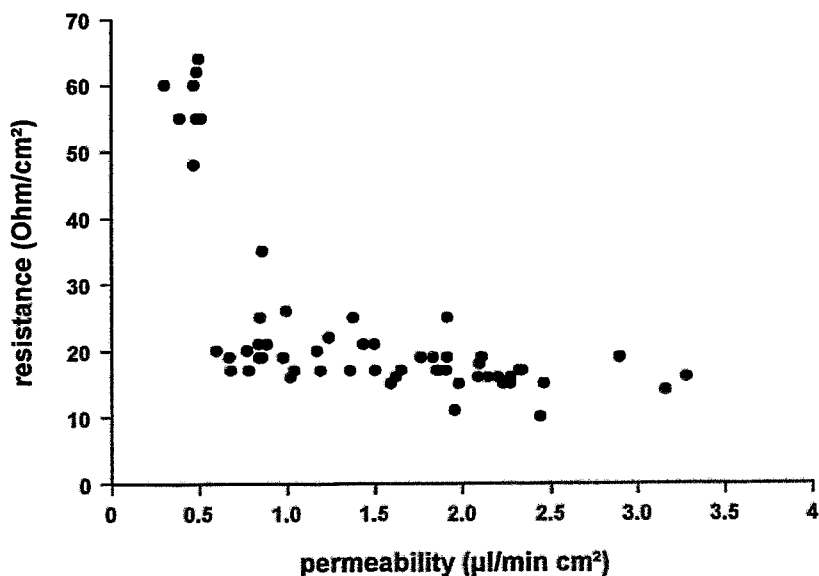


Fig. 1: The relationship between the electrical resistance [Ohm/cm²] and the permeability coefficient [μl/min cm²] of fluorescein sodium through endothelial cell monolayers on polycarbonate filters

Other authors found the same (Dehouck *et al.*, 1993; Mizuguchi *et al.*, 1994; Saheki *et al.*, 1994; Fischer *et al.*, 1995) or 2 - 10 times lower paracellular permeability coefficients as revealed with [¹⁴C]-sucrose (p_{sucrose}) (van Bree *et al.* 1988, Pardridge *et al.* 1990). However, the electrical resistance of the endothelial monolayers was much higher. For example, the authors found a p_{sucrose} of 1.8 $\mu\text{l}/\text{cm}^2$ min at 100 Ohm/cm² (Fischer *et al.*, 1995) and a p_{sucrose} of 0.6 $\mu\text{l}/\text{cm}^2$ min at 660 Ohm/cm² (Dehouck *et al.*, 1993). This again shows that even at 5-100 times higher electrical resistance values, the authors found paracellular permeability coefficients in the same range as found in cultures of low electrical resistance of 20 Ohm/cm². As shown in Fig. 1, the paracellular permeability coefficient may vary even at the same resistance values, which therefore shows the necessity of measuring the paracellular permeability coefficient for each filter during the study of transendothelial transport.

The total endothelial permeability coefficient of a drug at 4 °C in approximately the same molecular range as fluorescein sodium also reflects temperature-independent transport through intercellular spaces. In the same monolayers we measured the permeability coefficients of fluorescein sodium and [³H]-L-leucine at 4 °C (Fig. 2).

The paracellular permeability coefficients of fluorescein sodium and [³H]-L-leucine at 4 °C were the same from the luminal to the basolateral and from the basolateral to the luminal chamber. Similar experiments were mentioned by Audus and Borchart (1986). In their study the [¹⁴C]-sucrose permeability coefficient is qualitatively in the range of transport of [³H]-L-leucine - unfortunately, no data were shown in their report.

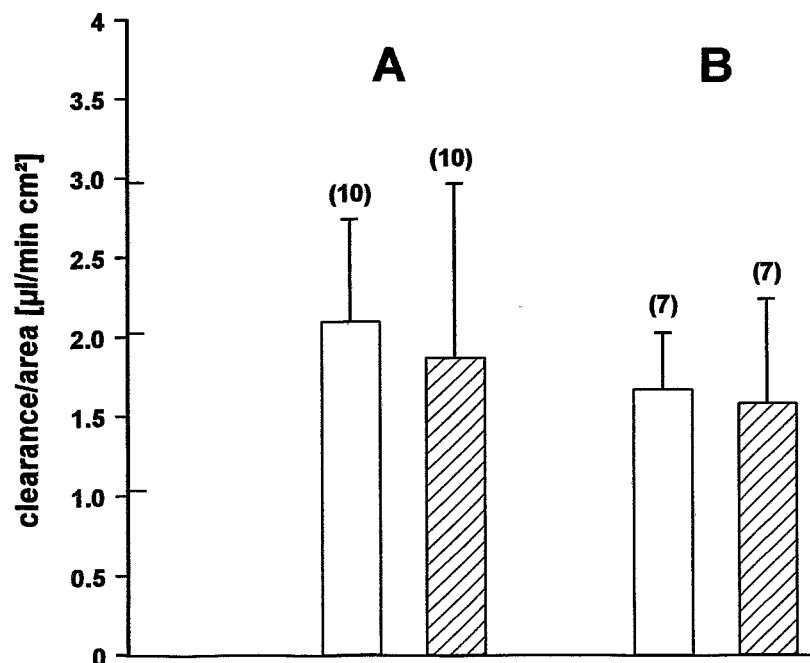


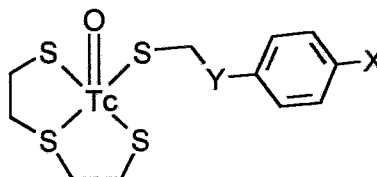
Fig. 2: The permeability coefficients of fluorescein sodium (empty columns) and [³H]-L-leucine at 4 °C (filled columns) in the same monolayers of endothelial cells after 6 days in culture for the luminal to basolateral (A) and basolateral to luminal (B) transport. Mean values \pm SD of n filters are shown.

Our results show that measurement of the permeability coefficient of fluorescein sodium is suitable for evaluating paracellular permeability with the advantage of being able to correct the total transport by paracellular transport of the same filter and to reduce the number of filters used in an experiment. We examined the transendothelial permeability coefficients of several ^{99/99m}Tc complexes with moderate to high affinity to 5-HT₂ receptors (Fig. 3).

We found different permeability coefficients for the luminal to basolateral and basolateral to luminal transport directions. The transendothelial flux rates (in % of the initial amount in the donor chamber) in the range from 0.36 - 1.44 % for the ^{99/99m}Tc complexes 15 - 18 are comparable to the *in vivo* brain uptake rates in the range from 0.4 - 0.8 %. In addition, the transendothelial flux rates of the ^{99/99m}Tc-

complexes 15 - 18 and of [^3H]-L-leucine at 37 °C (0.8 - 1.6 %) are approximately the same, showing a high passage of these complexes comparable to neutral amino acid brain uptake. However, the $^{99/99\text{m}}\text{Tc}$ complex 19 showed different *in vivo* and *in vitro* results with a high rat brain uptake of 2 % *in vivo* and no detectable *in vitro* transport through endothelial monolayers of porcine brain microvessels. It may be hypothesized that species differences caused the discrepant results.

Although the log P and therefore the lipophilicity of all the $^{99/99\text{m}}\text{Tc}$ complexes in our study varied only between 3.25 and 3.8, we found different transendothelial permeability coefficients (factor 3). Pirro *et al.*, (1994) have also examined several $^{99/99\text{m}}\text{Tc}$ complexes with varying lipophilicity (log P values from 1.76 - 4.56) to find *in vitro* extraction rates (% clearance vs time) from 48 - 85 %. It may therefore be suggested that high lipophilicity does not necessarily imply high transendothelial or blood-brain barrier permeability.



complex 19: Y=CH₂, X=H

complex 16: Y=(CH₂)-N(CH₃)-(CH₂)₃, X=F

complex 15: Y=(CH₂)-N(CH₃)-(CH₂)₃, X=H

complex 18: Y=(CH₂)-piperidyl-(CH₂); X=H

complex 17: Y=(CH₂)₂-N(CH₃)-(CH₂)₃; X=H

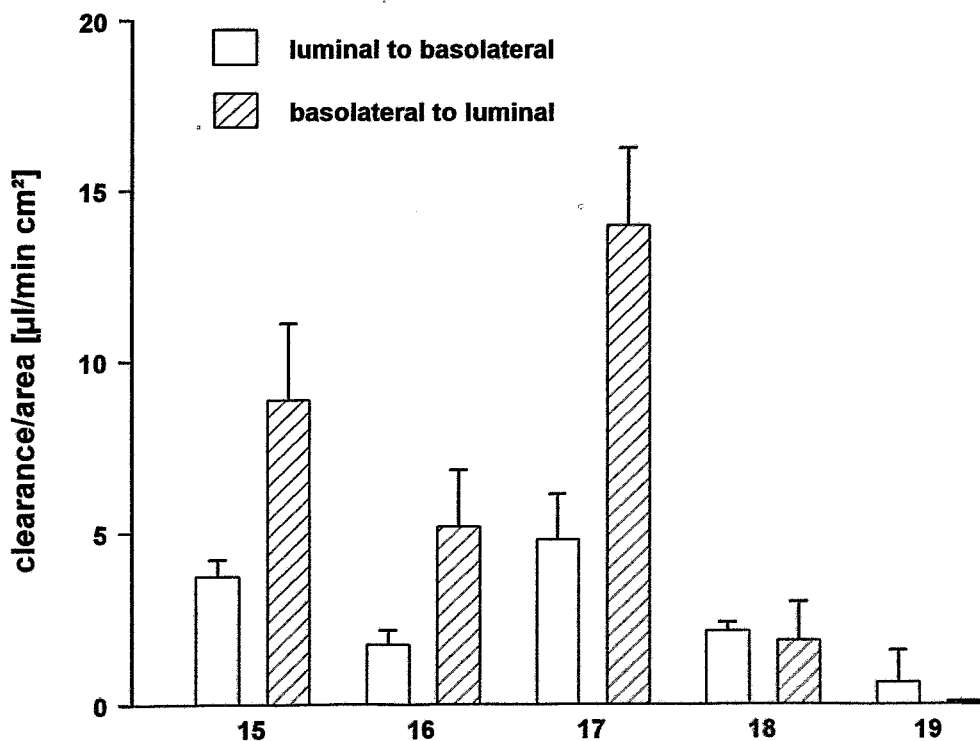


Fig. 3: The permeability coefficients of several $^{99/99\text{m}}\text{Tc}$ complexes for the luminal to basolateral (empty columns) and basolateral to luminal (filled columns) transport direction. Mean values \pm SD of 5 filters are shown.

It was the aim of our present examination to find an easy and sophisticated way of studying drug transport through endothelial cell monolayers even at a low electrical resistance of the monolayers. We have shown that fluorescein sodium is suitable for evaluating the paracellular permeability coefficient, which makes it possible to determine the transendothelial permeability of a drug. In addition, we measured the transendothelial permeability of several lipophilic ^{99m}Tc complexes to find comparable *in vivo* and *in vitro* results.

Acknowledgment

This work was supported by a research grant of the Saxon Ministry of Science and Art (7541.82-FZR/309).

References

- Audus K.L. and Borchardt R.T. (1986) Characteristics of the large neutral amino acid transport system of bovine brain microvessel endothelial cell monolayers. *J. Neurochem.* **47**, 484-488.
- de Boer A.G., de Vries H.E., de Lange E.C.M., Danhof M., Kuiper J.J. and Breimer D.D. (1994) Drug transport to the brain: *in vitro* versus *in vivo* approaches. *J. Control. Release* **28**, 259-263.
- Dehouck M.P., Dehouck B., Fruchart J.C. and Cecchelli R. (1993) An *in vitro* model of blood-brain barrier based on co-culture of brain capillary endothelial cells and astrocytes. *Proc. Int. Symposium on Blood Binding and Drug Transfer* p. 243-255.
- Douglas G.C., Swanson J.A. and Kern D.F. (1993) HEPES buffer perfusate alters rabbit lung endothelial permeability. *Am. J. Physiol.* **75**, 1423-1425.
- Fischer S., Renz D., Schaper W. and Karliczek G.F. (1995) *In vitro* effects of fentanyl, methohexital and thiopental on brain endothelial permeability. *Anaesthesiology* **82**, 451-458.
- Jaehde U., Goto T., de Boer A.G. and Breimer D.D. (1993) Blood-brain barrier transport rate of quinolone antibacterials evaluated in cerebrovascular endothelial cell cultures. *Eur. J. Pharmaceut. Sci.* **1**, 49-55.
- Jaehde U., Masereeuw R., de Boer A.G., Fricker G., Nagelkerke J.F., Vonderscher J. and Breimer D.D. (1994) Quantification and visualization of the transport of octreotide, a somatostatin analogue, across monolayers of cerebrovascular endothelial cells. *Pharm. Res.* **11**, 442-448.
- Johannsen B., Pietzsch H.-J., Scheunemann M., Spies H. and Brust P. (1995) Oxotechnetium (V) and oxorhenium (V) complexes as potential imaging agents for the serotonin receptors. *J. Nucl. Med.* **36**, 27P.
- Masereeuw R., Jaehde U., Langemeijer M.W.E., de Boer A.G. and Breimer D.D. (1994) *In vitro* and *in vivo* transport of zidovudine (AZT) across the blood-brain barrier and the effect of transport inhibitors. *Pharm. Res.* **11**, 324-330.
- Mischek U., Meyer J. and Galla H.J. (1989) Characterization of g-glutamyltranspeptidase activity of cultured endothelial cells from porcine brain capillaries. *Cell Tiss. Res.* **256**, 221-225.
- Mizuguchi H., Hashioka Y., Utoguchi N., Kubo K., Nakagawa S. and Mayumi T. (1994) A comparison of drug transport through cultured monolayers of bovine brain capillary and bovine aortic endothelial cells. *Biol. Pharm. Bull.* **17**, 1385-1390.
- Pardridge W.M., Triguero D., Yang J. and Cancilla P.A. (1990) Comparison of *in vitro* and *in vivo* models of drug transcytosis through the blood-brain barrier. *J. Pharmacol. Exp. Ther.* **253**, 884-891.
- Pirro J.P., Di Rocco R.J., Narra R.K. and Nunn A.D. (1994) Relationship between *in vitro* trans-endothelial permeability and *in vivo* single-pass brain extraction. *J. Nucl. Med.* **35**, 1514-1519.
- Saheki A., Terasaki T., Tamai I. and Tsuji, A. (1994) *In vivo* and *in vitro* blood-brain barrier transport of 3-hydroxy-3-methylglutaryl coenzyme A (HMG-CoA) reductase inhibitors. *Pharm. Res.* **11**, 305-311.
- van Bree J.B.M.M., de Boer A.G., Danhof M., Ginsel L.A. and Breimer D.D. (1988) Characterization of an *in vitro* blood-brain barrier: effects of molecular size and lipophilicity on cerebrovascular endothelial transport rates of drugs. *J. Pharmacol. Exp. Ther.* **247**, 1233-1239.

41. Conditioned Media of Astrocytes and Other Proliferating Cells Increase the Activity of Alkaline Phosphatase and γ -Glutamyltranspeptidase in Cultured Cerebral Endothelial Cells

B. Ahlemeyer, S. Matys, and P. Brust

Introduction

The passage between the blood and the extracellular fluid of the brain is controlled by endothelial cells of brain capillaries which are the main constituents to form the blood-brain barrier (BBB). Since Panula *et al.* (1978) isolated and cultured cerebral endothelial cells, they have been successfully used as an *in vitro* model for the BBB (Jóo, 1992). However, the activities of the two marker enzymes γ -glutamyltranspeptidase (γ -GT) and alkaline phosphatase (ALP) decreased as a function of culture time (Fukushima *et al.*, 1990; Meyer *et al.*, 1992), leading to the debate whether the differentiated function of the endothelium is preserved in culture.

Previous studies revealed that astrocytes are able to induce BBB functions in cultured endothelial cells. It is controversially discussed whether membrane interactions between astrocytes and endothelial cells are necessary for increased integrity and activity of BBB-related enzymes (De Bault and Cancilla, 1980; Tao-Cheng *et al.*, 1987; Lathera *et al.*, 1990; Meyer *et al.*, 1991; Tontsch and Bauer, 1991; Hurwitz *et al.*, 1993) or whether soluble factors released from astrocytes as well as membrane bound structures are sufficient (Arthur *et al.*, 1987; Maxwell *et al.*, 1987; Rubin *et al.*, 1991; Raub *et al.*, 1992; Mizuguchi *et al.*, 1994; Takemoto, *et al.*, 1994; Wolburg *et al.*, 1994). In addition, there are some discrepancies between the *in vivo* and *in vitro* results. For example, C6 glioma cells and C6 glioma conditioned medium decreased permeability (Raub *et al.*, 1992) and upregulated γ -GT activity *in vitro* (De Bault and Cancilla, 1980; Lathera *et al.*, 1990; Maxwell *et al.*, 1987; Takemoto *et al.*, 1994) even though implanted C6 glioma tumours *in vivo* increased permeability of the BBB (Stewart *et al.*, 1985). Holash and Stewart (1993) demonstrated that retinal vessels *in vivo* did not express detectable γ -GT activity although astrocytes ensheat the capillaries. In addition, in most studies a heterologous model was used, i.e. neonatal rat astrocytes induced BBB features in adult bovine or porcine brain endothelial cells. Taking all things together, it is not clear at all which BBB features correlate with the presence of astrocytes or astrocytelike cells or factors.

We therefore examined the effect of conditioned medium of adult porcine astrocytes and other proliferating cells on the activity of ALP and γ -GT in adult porcine brain endothelial cells. We used an autologous model, i.e. the astrocytes were of the same developmental stage and from the same species as the endothelial cells.

Experimental

Materials

Fetal calf serum, collagen type I/III, Percoll, dextran, glycylglycine, forskolin and protein assay kit were purchased from Sigma Chemicals, Deisenhofen, Germany. Collagenase/dispase, dispase, L-glutamic acid α -(4-methoxy- β -naphthylamide), p-nitrophenylphosphate, Ig G fractions of mouse anti-human factor VIII, mouse anti-gliial fibrillary acidic protein (GFAP), mouse anti-smooth muscle actin, mouse anti-neurofilament, and sheep anti-mouse Ig-G-fluorescein antibodies were from Boehringer, Mannheim, Germany. Medium 199 and antibiotics were obtained from Gibco BRL, Eggenstein, Germany. All other chemicals were derived from Merck, Darmstadt, Germany.

Cell cultures

Primary cultures of porcine brain microvessel endothelial cells were obtained according to Mischek *et al.* (1989). Briefly, pig brains, cleaned of meninges and white matter, were minced and incubated for 3 h at 37 °C in medium 199 containing 0.8 % dispase. After centrifugation with 15 % dextran at 6800 x g for 10 min, isolated capillaries were digested with 0.1 % collagenase/dispase for 3 h. Endothelial cells were separated from erythrocytes and cell debris by a Percoll gradient. Cells were seeded on collagen type I/III coated petri dishes (35 mm diameter, Becton Dickinson, Heidelberg, Germany) with a density of $1 - 2 \times 10^4$ cells/cm². The cells were cultured in medium 199 with 10 % fetal calf serum, 100 U/ml penicillin, 100 μ g/ml streptomycin and 2.5 μ g/ml amphotericin at 37 °C with 5 % CO₂ and 95 % air. The medium was changed every second day. These primary cultures were confirmed to be endothelial cells >95 % by an immunostaining method using factor VIII related antigen after 6 days in culture.

Porcine astrocytes were derived from the white matter of adult porcine brain. After 1 h of digestion with 0.1 % dispase, the cell homogenate was dissociated successively through nylon meshes of 300, 125 and 45 μm pore size and was seeded in petri dishes. The medium was changed 3 h after seeding, thereafter every second day. The astrocytes were cultured in the same medium as the endothelial cells to avoid effects of medium components by the use of astrocyte-conditioned medium. Astrocytes were identified to be 99 % pure cultures by immunostaining using GFAP antigen.

Rat astrocytes were prepared according to McCarthy and de Vellis (1980). Briefly, brains of neonatal rats were freed of meninges and cerebral cortices and were homogenized mechanically and enzymatically. The resulting cell suspension was seeded into culture flasks. After reaching confluence the cultures were shaken overnight to remove microglial cells and treated with 10 μM cytosine arabinoside for 48 h which eliminates the progenitor cells.

The cell lines CHO (Chinese hamster ovary fibroblasts), Sp.LOE (mouse osteochondroma) and KTCTL-2 (human adenocarcinoma) were from the Deutsches Krebsforschungszentrum Heidelberg, Germany (provided by Dr. Gudrun Kampf). All cell lines were cultured in medium 199, supplemented with 10 % fetal calf serum and antibiotics. Conditioned medium was used from confluent and subconfluent cultures of astrocytes (ACM-K and ACM-SK), CHO cells (CHOCM-K and CHOCM-SK), KTCTL-2-cells (NCM-K and NCM-SK) and Sp.LOE cells (SCM-K and SCM-SK).

The conditioned medium was collected 72 h after adding the fresh media to subconfluent and confluent cultures. Thereafter, it was sterile filtrated to remove cell debris and stored at $-20\text{ }^{\circ}\text{C}$ before use. Endothelial cells were incubated with a mixture of conditioned medium and fresh medium (1:2) 24 h after seeding.

The extracellular matrix of astrocytes, chondrocytes and CHO cells was obtained from confluent cultures washed with 0.1 M phosphate buffered saline (with 0.9 mM Ca^{2+} and 0.5 mM Mg^{2+} , PBS^{++} , pH 7.4) and lysed by incubation at room temperature with sterile water. The petri dishes were controlled to be cell-free by microscope. The endothelial cells were seeded and cultured on this matrix until the day of the experiment.

Alkaline phosphatase (ALP) and γ -glutamyltranspeptidase (γ -GT) assay

For the biochemical assay, the cells were washed three times with 0.9 % saline, then scraped from the petri dish and were homogenized by short sonification. Cell suspension was used for both enzyme activity and protein determination.

ALP activity was determined by incubating the cell suspension with substrate solution containing 4 mM p-nitrophenylphosphate, pH 10.37. Formation of p-nitrophenol was measured kinetically at 420 nm and compared with the saline/substrate solution. Specificity of the test was demonstrated with levamisol (5 mM) which inhibited ALP activity completely. One unit of enzyme activity was defined by the formation of 1 μmol p-nitrophenol per min at $25\text{ }^{\circ}\text{C}$, using an extinction coefficient of $17300\text{ M}^{-1}\text{ cm}^{-1}$. The γ -GT activity was determined by incubating the cell suspension with substrate solution containing 2.7 mM L- γ -glutamyl-3-carboxy-4-nitroanilide and 20 mM glycylglycine in tris-buffer pH 9. Formation of carboxy-4-nitroanilide was measured kinetically at 410 nm and compared with the saline/substrate solution. One unit of enzyme activity was defined by the formation of 1 nmol carboxynitroanilide per min at $25\text{ }^{\circ}\text{C}$, using an extinction coefficient of $9500\text{ M}^{-1}\text{ cm}^{-1}$.

Immunostaining

Cells were washed three times with PBS^{++} and fixed with 99 % ethanol (mouse anti-factor VIII) at room temperature and methanol at $-20\text{ }^{\circ}\text{C}$ for 20 min. In order to reduce nonspecific binding, the monolayer was preincubated with 0.5 % bovine serum albumin (BSA) in PBS^{++} for 30 min before addition of the first antibody. After 1 h, the cells were washed several times and fluorescein conjugated sheep anti-mouse-Ig G was added for 30 min. Thereafter, the cells were washed and observed in an inverted microscope (Olympus IMT 2) equipped for epifluorescence and for photography. Control experiments were performed without the first antibody. Contaminating cells were determined using mouse anti-GFAP, mouse anti-neurofilament and mouse anti-smooth muscle actin antibodies to identify astrocytes, neurons and pericytes/smooth muscle cells.

Protein determination

Cell protein was determined by a modified Lowry test, using the assay kit from Sigma.

Statistics

Significant differences were evaluated by the Bartlett-test to test homogeneity of variances and by the ANOVA-1 and Duncan-Test with * $p < 0.05$, ** $p < 0.01$ and *** $p < 0.001$.

Results and Discussion

The effect of conditioned media of astrocytes and different cell lines on ALP and γ -GT activity after 4 and 7 days in culture in cerebral endothelial cells is shown in Table 1 and 2. In addition, we measured both enzyme activities after 7 days in cells grown on the matrices of astrocytes, chondrocytes and CHO fibroblasts (Table 3). Taking all things together, we found various effects on endothelial cells, i.e. after 4 days an increase in ALP and after 7 days an increase in ALP and γ -GT activities.

Table 1: The effect of conditioned medium on the activities of ALP [U/mg protein] and γ -GT [U/mg protein] in cultured cerebral endothelial cells after 4 days in culture. The endothelial cells were incubated with conditioned medium of subconfluent and confluent cultures of adult porcine astrocytes (PACM-SC and PACM-C), of neonatal rat astrocytes (RACM-C), of Chinese hamster ovary fibroblasts (CHO-SC and CHO-C), of the osteochondroma cell line (SCM-SC and SCM-C), adenocarcinoma cells (NCM-SC and NCM-C) and forskolin (50 μ M). All values are given as mean values \pm standard deviation (SD) of n experiments.

Incubation	ALP [U/mg protein]	γ -GT [U/mg protein]	n
Control	0.36 \pm 0.06	2.35 \pm 1.08	20
PACM-SC	0.50 \pm 0.11**	2.59 \pm 0.49	8
PACM-C	0.44 \pm 0.09*	2.00 \pm 0.94	8
RACM-C	0.30 \pm 0.03	2.06 \pm 0.82	8
forskolin (50 μ M)	0.67 \pm 0.12 ***	2.11 \pm 0.74	8
CHO-CM-SC	0.40 \pm 0.05	2.97 \pm 0.40	8
CHO-CM-C	0.35 \pm 0.03	2.79 \pm 1.30	8
SCM-SC	0.28 \pm 0.1	1.55 \pm 0.60	8
SCM-C	0.36 \pm 0.11	2.19 \pm 0.51	8
NCM-SC	0.34 \pm 0.07	2.42 \pm 0.67	8
NCM-C	0.39 \pm 0.06	2.08 \pm 0.89	8

Table 2: The effect of conditioned medium on the activities of ALP [U/mg protein] and γ -GT [U/mg protein] in cultured cerebral endothelial cells after 7 days in culture. The endothelial cells were incubated as described in Table 1. All values are given as mean values \pm SD of n experiments.

Incubation	ALP [U/mg protein]	γ -GT [U/mg protein]	n
Control	0.28 \pm 0.06	0.98 \pm 0.52	24
PACM-SC	0.43 \pm 0.17	1.91 \pm 0.65 ***	16
PACM-C	0.51 \pm 0.29 *	1.94 \pm 1.06 **	16
RACM-C	0.28 \pm 0.06	2.49 \pm 0.33 ***	6
Forskolin (50 μ M)	0.20 \pm 0.02	0.63 \pm 0.17	8
CHOCM-SC	0.48 \pm 0.33	1.09 \pm 0.81	12
CHOCM-C	0.65 \pm 0.37 *	1.64 \pm 0.43 *	12
SCM-SC	0.33 \pm 0.18	1.53 \pm 0.55	12
SCM-C	0.32 \pm 0.20	2.02 \pm 0.65 ***	12
NCM-SC	0.27 \pm 0.03	2.02 \pm 0.65 ***	8
NCM-C	0.30 \pm 0.05	1.97 \pm 0.43 ***	8

The effect of several conditioned media and forskolin on the ALP activity

After 4 days we found a 1.4- and 1.2fold increase in ALP by conditioned medium of subconfluent and confluent adult porcine astrocytes and a 1.8fold increase in ALP by forskolin (50 μ M), which increases the c-AMP content and therefore stimulates cell differentiation in endothelial cells (Rubin *et al.*, 1991). We used conditioned media of subconfluent and confluent monolayers to find out whether induction of ALP or γ -GT depends on the concentration of soluble factors released by the cells (in subconfluent cultures a lower enrichment of soluble factors is suspected). However, after 4 days a significant increase in ALP was found using only conditioned medium of subconfluent adult porcine astrocytes (Table 1). As shown by Sivron *et al.* (1993), confluent astrocytes are able to secrete factors which stimulate proliferation of cells (neurons), whereas subconfluent astrocytes stimulate differentiation. Our results suggest that stimulation of cell differentiation by forskolin and factors released by proliferating astrocytes are the reasons for the increase in ALP.

The effect on ALP was also observed after 7 days in culture. However, only the conditioned media of confluent astrocytes and CHO-cells had a significant inductive effect. Forskolin as well as the conditioned medium of chondrocytes and adenocarcinoma cells failed to increase ALP, suggesting that an increase in the intracellular c-AMP and stimulation of cell differentiation is not effective here to induce ALP. In addition, after 7 days we measured the ALP activity in cells which were incubated with conditioned media of confluent porcine astrocytes only from day 1-4. We did not find any increase in ALP with 0.24 \pm 0.11 U/mg protein (controls see Table 2). The results suggest that the presence of factors released by astrocytes in the phase of cell proliferation (stimulation of cell differentiation) did not affect ALP after 7 days in culture.

In conclusion, our results suggest that stimulation of cell differentiation is only effective in subconfluent cell cultures (after 4 days), whereas other mechanisms are responsible for induction of the marker enzyme ALP in confluent cultures (after 7 days).

While most studies to evaluate inductive factors for BBB features measured the γ -GT activity, only very few authors were interested in the increase in ALP. Meyer *et al.* (1991) found that ALP was strongly increased by astroglial coculture with cell-to-cell contact, but not by incubation with neonatal rat astrocyte-conditioned medium after 9 days. Because their results were obtained by histochemistry (coculture of different cell types did not permit the biochemical quantification of enzyme activity), it may be suggested that a 50 % increase in ALP as biochemically measured by us is too low to be de-

tected by histochemistry. Consistent with our results, Takemoto *et al.* (1994) found that glioma conditioned medium induces ALP in calf pulmonary artery endothelial cells. They identified interleukin-6 as the inductive factor. Beck *et al.* (1986) also found an increase in ALP after 7 days by factors released by C6 glioma cells.

Similar to our suggestion that stimulation of cell differentiation is effective only in cell culture up to 4 days, Wolburg *et al.* (1994) found that the inductive effect on the tight junction complexity of forskolin and astrocyte-conditioned medium is stronger in 36-h-old than in 11-day-old endothelial cell cultures. After 4 days they also measured after 4 days a stronger effect of forskolin than of astrocyte-conditioned medium, i.e. a decrease in permeability by 50 and 20 %. Recent studies by Beuckmann *et al.* (1995) also showed that a membrane-permeable analogue of c-AMP increased the activity of ALP sixfold compared with the controls.

The effect of several conditioned media and forskolin on γ -GT activity

We did not find any increase in γ -GT after 4 days in culture. However, after 7 days, there was an increase in γ -GT compared with the control cultures of 70-100 %, using conditioned media of subconfluent and confluent adult porcine and neonatal rat astrocytes, of confluent CHO fibroblasts, chondrocytes and adenocarcinoma cells. The increase in γ -GT was higher with conditioned media of confluent than of subconfluent cultures. Forskolin had no effect. After 7 days the γ -GT activity in cells, which were incubated with conditioned media of confluent porcine astrocytes from day 1-4 was also significantly increased to 2.08 ± 0.95 U/mg protein (controls see Table 2). Furthermore, we observed that conditioned media increase the number of cells on top of the monolayer with γ -GT activities as high or higher than revealed by histochemistry.

Several authors have already described an increase in γ -GT by astrocyte-conditioned media or astrocyte-like structures or by coculture with astrocytes. Consistent with our results, Maxwell *et al.* (1987) measured an increase in the γ -GT activity after 6 days in culture by incubating endothelial cells for the first 3 days with conditioned medium of rat C6 glioma cells. By contrast, Tontsch & Bauer (1991) found that only coculture with glioma cells or incubation with plasma membranes is sufficient to induce γ -GT in a passaged, cloned endothelial cell line, while the C6 glioma conditioned medium had no effect. However, Meyer *et al.* (1991) found that a C6 glioma coculture has only a weak effect while neonatal rat astrocytes strongly induce γ -GT in porcine endothelial cells.

It is important to note that we found an increased number of cells on top of the monolayer with as high or higher γ -GT activities. The phenomenon that endothelial subpopulations with high activities of γ -GT were found on top of the monolayer forming capillarylike structures has already been described by others (Lattera *et al.*, 1990; Roux *et al.*, 1994). Lattera *et al.* (1990) observed that only coculture conditions with cell-to-cell contact generate this endothelial cell change, whereas Roux *et al.* (1994) reported the induction of three-dimensional structures with high γ -GT and ALP activities also by incubation with C6 glioma and neonatal astrocyte-conditioned media. Hurwitz *et al.* (1994) used an autologous coculture model with human endothelial cells and astrocytes to find an inductive effect on γ -GT by coculture as revealed by histochemistry. In their studies the endothelial cells grew on polycarbonate filters with astrocytes on the upper side of the filters and high γ -GT activities were found exclusively in the tube-forming endothelial cells. However, in our studies we found that these γ -GT positive cells were associated with cell clusters. Wang *et al.* (1993) used a clone of a cerebral resistance vessel and also found γ -GT positive cells, especially in cell clusters. He reported a distinct population of endothelial cells with properties of a long-term survival culture.

The cells on top of the monolayer were identified to be 60 % factor VIII-positive and of endothelial origin. All these cells were smooth-muscle actin-positive (and could therefore be identified as endothelial cells, smooth muscle cells and/or pericytes). Because conditioned media of various confluent cell cultures (neonatal rat and adult porcine astrocytes, chondrocytes, CHO cells and adenocarcinoma cells) are able to increase γ -GT, this effect does not seem to be astrocyte specific. It may be suggested that factors released by these cells a) increase the number of cells on top of the monolayer with activities of high γ -GT or b) increase the γ -GT activities in all the cells or c) increase the number of cells on top of the monolayer, which increases the γ -GT activities in all the cells. The increase in γ -GT seems to be the result of an increase in the number of cells on top of the monolayer with high γ -GT activities. In studying the effect of conditioned media on the activity of marker enzymes, attention has therefore to be paid as to whether the composition of the cell culture is the same as in the control cultures.

The effect of matrices of astrocytes, chondrocytes and CHO cells on endothelial enzyme activities
 After 7 days in culture the cell growth on all three matrices was reduced with 64 ± 12 , 60 ± 5 and 58 ± 16 μg protein/petri dish on astrocyte, chondrocyte and CHO fibroblast-derived matrix (controls 100 ± 29 μg protein/petri dish). We found a significant decrease in γ -GT with chondrocyte and CHO cell derived matrix (Table 3).

Table 3: The effect of astrocyte- (AX), CHO cell- (CHOX) and chondrocyte- (SX) derived matrix on the activities of ALP [U/mg protein] and γ -GT [U/mg protein] in cultured cerebral endothelial cells after 7 days in culture. All values are given as mean values \pm SD of n experiments.

	ALP [U/mg protein]	γ -GT [U/mg protein]	n
Control	0.28 ± 0.06	0.98 ± 0.52	24
AX	0.21 ± 0.04	1.51 ± 0.40	8
CHO-X	0.23 ± 0.09	0.36 ± 0.18 ***	8
S-X	0.26 ± 0.08	0.27 ± 0.34 **	8

For comparison, Mizuguchi *et al.* (1994) found a 0.5fold increase in γ -GT by culturing endothelial cells on glia matrix after 4 days. They further increased γ -GT by using glia matrix and endothelial-cell-conditioned medium. However, we measured γ -GT after 7 days in culture.

Taking all things together our results showed a) that stimulation of cell differentiation is only effective to induce ALP in subconfluent endothelial cell cultures, b) that other mechanisms are responsible for the increase in ALP after 7 days in culture, and c) that conditioned media of confluent astrocytes and other proliferating cells increased the activity of γ -GT after 7 days in culture as a result of an increased number of cells on top of the endothelial cell monolayer with high γ -GT activities. The mechanism of this phenomenon has to be clarified. In addition, we found no correlation between the induction of ALP and γ -GT, which indicates that expression of the two enzymes may be differently regulated. Our results indicate that conditioned media from astrocytes and various cell lines contain soluble factors which can change enzyme activities and cell culture composition and that some BBB features may not require an intimate cell-to-cell contact.

Acknowledgment

This work was supported by a research grant of the Saxon Ministry of Science and Art (7541.82-FZR/309).

References

- Arthur F.E., Shivers R.R. and Bowman P.D. (1987) Astrocyte-mediated induction of tight junctions in brain capillary endothelium: an efficient *in vitro* model. *Dev. Brain Res.* **36**, 155-159.
- Beck D.W., Roberts R.L. and Olson J. (1986) Glial cells influence membrane associated enzyme activity at the blood-brain barrier. *Brain Res.* **381**, 131-137.
- Beuckmann C., Hellwig S. and Galla H.J. (1995) Induction of blood/brain-barrier associated enzymes alkaline phosphatase in endothelial cells from cerebral capillaries is mediated via c-AMP. *Eur. J. Biochem.* **229**, 641-644.
- DeBault L.E. and Cancilla P.A. (1980) γ -Glutamyltranspeptidase in isolated brain endothelial cells: induction by glial cells *in vitro*. *Science* **207**, 653-655.
- Fukushima H., Fujimoto M. and Ide M. (1990) Quantitative detection of blood-brain barrier-associated enzymes in cultured endothelial cells of porcine brain microvessels. *In Vitro Cell. Dev. Biol.* **26**, 612-620.
- Holash J.A. and Stewart P.A. (1993) The relationship of astrocyte-like cells to the vessels that contribute to the blood-ocular barriers. *Brain Res.* **629**, 218-224.
- Hurwitz A.A., Berman J.W., Rashbaum W.K. and Lyman W.D. (1993) Human fetal astrocytes induce the expression of blood brain barrier specific proteins by autologous endothelial cells. *Brain Res.* **625**, 238-243.

- Joó F. (1992) The cerebral microvessels in culture, an update. *J. Neurochem.* **58**, 1-17.
- Lattera J., Guerin C. and Goldstein G.W. (1990) Astrocytes induce neural microvascular endothelial cells to form capillary-like structures *in vitro*. *J. Cell. Physiol.* **144**, 204-215.
- Maxwell K., Berliner J.A. and Cancilla P.A. (1987) Induction of γ -glutamyltranspeptidase in cultured cerebral endothelial cells by a product released by astrocytes. *Brain Res.* **410**, 309-314.
- McCarthy D. and deVellis J. (1980) Preparation of separate astroglial and oligodendroglial cell cultures from rat cerebral tissue. *J. Cell Biol.* **85**, 890-902.
- Meyer J., Mischek U., Veyhl M., Henzel K. and Galla H.J. (1990) Blood-brain barrier characteristic enzymatic properties in cultured brain capillary endothelial cells. *Brain Res.* **514**, 305-309.
- Meyer J., Rauh J. and Galla H.J. (1991) The susceptibility of cerebral endothelial cells to astroglial induction of blood-brain barrier enzymes depends on their proliferative state. *J. Neurochem.* **57**, 1971-1977.
- Mischek U., Meyer, J. and Galla, H.J. (1989) Characterization of γ -glutamyl transpeptidase activity of cultured endothelial cells from porcine brain capillaries. *Cell. Tiss. Res.* **256**, 221-226.
- Mizuguchi H., Hashioka Y., Fujii A., Utoguchi N., Kubo K., Nakagawa S., Baba, A. and Mayumi T. (1994) Glial extracellular matrix modulates γ -glutamyltranspeptidase activity in cultured bovine brain capillary and bovine aortic endothelial cells. *Brain Res.* **651**, 155-159.
- Panula P., Joó F. and Rechart L. (1978) Evidence for the presence of viable endothelial cells in cultures derived from dissociated rat brain. *Experientia* **34**, 95-97.
- Raub T.J., Kuentzel S.L. and Sawada G.A. (1992) Permeability of bovine brain microvessel endothelial cells *in vitro*: barrier tightening by a factor released from astrogloma cells. *Exper. Cell. Res.* **199**, 330-340.
- Roux F., Durieu-Trautmann O., Chaverot N., Claire M., Maily P., Bourre J.M., Strosberg A.D. and Couraud P.O. (1994) Regulation of gamma-glutamyltranspeptidase and alkaline phosphatase activities in immortalized rat brain microvessel endothelial cells. *J. Cell. Physiol.* **159**, 101-113.
- Rubin L.L., Hall D.E., Porter S., Barbu K., Cannon C., Horner H.C., Janatpour M., Liaw C.W., Manning K., Morales J., Tanner L.I., Tomaselli K.J. and Bard F. (1991) A culture model of the blood-brain barrier. *J. Cell Biol.* **115**, 1725-1735.
- Sivron T., Eitan S., Schreyer D.J. and Schwartz M. (1993) Astrocytes play a major role in the control of neuronal proliferation *in vitro*. *Brain Res.* **629**, 199-208.
- Stewart P.A., Hayakawa K., Hayakawa E., Farrell C.L. and Del Maestro R.F. (1985) A quantitative study of the blood-brain barrier permeability ultrastructure in a new rat glioma model. *Acta Neuropathol.* **67**, 96-102.
- Takemoto H., Kaneda K., Hosokawa M., Ide M. and Fukushima H. (1994) Conditioned media of glial cell lines induce alkaline phosphatase activity in cultured artery endothelial cells. *FEBS Lett.* **350**, 99-103.
- Tao-Cheng J.H., Nagy Z. and Brightman M.W. (1987) Tight junctions of brain endothelium *in vitro* are enhanced by astroglia. *J. Neurosci.* **7**, 3293-3299.
- Tontsch U. and Bauer H.C. (1991) Glial cells and neurons induce blood-brain barrier related enzymes in cultured cerebral endothelial cells. *Brain Res.* **539**, 247-253.
- Wang B-L., Grammas P. and DeBault L. (1993) Characterization of a γ -glutamyltranspeptidase positive subpopulation of endothelial cells in a spontaneous tube-forming clone of rat cerebral resistance-vessel endothelium. *J. Cell. Physiol.* **156**, 531-540.
- Wolburg H., Neuhaus J., Kniesel U., Krauß B., Schmid E.M., Öcalan M., Farrell C. and Risau W. (1994) Modulation of tight junction structure in blood-brain barrier endothelial cells. *J. Cell Sci.* **107**, 1347-1357.

42. Chronic Fluoxetine Treatment did not Change Monoamine Oxidase Activity in Cerebral Endothelial Cells

B. Ahlemeyer, P. Brust, A. Friedrich, J. Wober, S. Matys

Introduction

Endothelial cells of brain capillaries are the main constituents of the blood-brain barrier (BBB) which regulates the transfer of water, electrolytes and nutrients between the blood and the extracellular fluid of the brain. Circulating catecholamines and their precursors are known to be extracted from the blood and to enter the endothelial cells, but were metabolized by three enzymes: monoamine oxidase, catechol-O-methyltransferase and phenol sulphotransferase (Hardebo *et al.*, 1980). Monoamine oxidase (MAO, EC 1.4.3.4) is found in isolated brain microvessels with great variations between different species (Kalaria and Harik, 1987) and between different developmental states (Tsang *et al.*, 1986). In cultured endothelial cells of brain microvessels the total MAO activity and the ratio MAO A/MAO B varied as a function of culture time with controversial results by different authors (Baranczyk-Kuzma *et al.*, 1986; Méresse *et al.*, 1989).

Preliminary results have shown a specific serotonin transporter in endothelial cells of porcine brain microvessels (Brust and Bergmann, 1994). Serotonin (5-HT) is the main substrate of MAO A. Adaptive mechanisms during inhibition of serotonin uptake by chronic treatment with fluoxetine upregulate 5-HT uptake sites as well as 5-HT₂ receptors in rat brain (Hrdina and Vu, 1993).

Therefore, we tried to find out 1) whether the activities of total MAO and MAO A vary in freshly isolated cells and during cell culture and 2) whether the inhibition of cellular 5-HT uptake by fluoxetine changes the activities of the MAO isoenzymes.

Experimental

Materials

Fluoxetine hydrochloride was obtained from Eli Lilly, Indianapolis, USA and deprenyl from RBI, Cologne, Germany. Collagenase/dispase and sodium dodecylsulfate were from Boehringer, Mannheim, Germany. All other chemicals were derived as previously described in this report.

MAO assay

Endothelial cell monolayers were cultured for up to 8 days in the absence or presence of 1 μ M fluoxetine. Fluoxetine was added 1 day after seeding. After 4, 6, and 8 days in culture the endothelial cell monolayers were washed three times with 0.1 M phosphate buffered saline (with 0.9 mM Ca²⁺ and 0.5 mM Mg²⁺, PBS⁺⁺, pH 7.4) scraped from the petri dish and were homogenized by short sonification.

The determination of MAO activity was based on a colorimetric quantification of the H₂O₂ formed (Kalaria *et al.*, 1987). The reaction mixture (0.7 ml) contained: 3 mM Na acid, 500 μ g cell protein and 1 mM tryptamine as substrate in PBS⁺⁺. Blanks consisted of parallel incubations without substrate. Incubations were performed for 30 min at 37 °C and the reaction was stopped by adding 0.5 ml of the H₂O₂ measuring solution with: 0.5 M phosphate-citrate buffer, pH 7.4, 1.8 mM ABTS and 5 U of horseradish peroxidase. After 15 sec 0.25 ml of 0.75 M HCl containing 15 % SDS was added and the coloured product was measured photometrically at 414 nm. MAO A activity was determined by preincubation with 0.6 μ M deprenyl, which is known to inhibit MAO B (Kalaria *et al.*, 1987). Data were compared with the H₂O₂ standards and were expressed as nmol H₂O₂/mg protein min.

Results and Discussion

In freshly isolated endothelial cells of porcine brain microvessels we found 4 times higher activities of total MAO than after 4 days in culture. In addition, the total MAO activity significantly decreased from 0.36 ± 0.08 after 4 days to 0.27 ± 0.04 nmol H₂O₂/mg protein min after 8 days in culture and MAO A was predominant. MAO B activity slightly increased from 4 % to 17 % of the total MAO activity in the cells after 4 to 8 days in culture (Table 1).

In porcine brain microvessels, about two times higher values of the total MAO activity (2.9 nmol H₂O₂/mg protein min with tryptamine as substrate) were reported compared with our results in freshly isolated endothelial cells (Kalaria *et al.*, 1987). In this study MAO B activity is predominant as revealed by [³H]-pargyline binding.

In endothelial cells of bovine brain microvessels Méresse *et al.* (1989) found - in contrast to our data - an increase in the total MAO activity during culture with 0.05, 0.1 and 0.35 nmol H₂O₂/ mg protein min after 4, 8, and 12 days in culture. However, the activity of the total MAO in isolated brain capillaries was 0.25 nmol H₂O₂/mg protein min and therefore considerably lower than our values in freshly isolated endothelial cells. In endothelial cells of bovine brain microvessels others measured 0.12, 0.6, and 0.5 nmol H₂O₂/mg protein min of the total MAO activity after 7, 10 and 14 days (Baranczyk-Kuzma *et al.*, 1986). The ratio MAO A/ MAO B varied during culture, with MAO A being 80 %, 66 % and 80 % of the total MAO after 7, 10, and 14 days. The reasons for the discrepant results are probably differences in species, but variations in the methods to quantitate MAO should also be considered.

Table 1: The activity of the total MAO and MAO A activity in endothelial cells of porcine brain microvessels grown in the absence or presence of 1 µM fluoxetine after various days in vitro (DIV). Mean values ± SD of n experiments are shown. Significant differences between groups (connected by a line) were tested using the Bartlett test, ANOVA1 and DUNCAN-Test with *** p < 0.001.

DIV	incubation with	Total MAO activity [nmol H ₂ O ₂ / mg protein min]	MAO A activity [nmol H ₂ O ₂ / mg protein min]
0	-	1.31 ± 0.52	1.30 ± 0.51 (n=7)
4	-	0.36 ± 0.08 ***	0.35 ± 0.06 (n=8) **
4	1 µM fluoxetine	0.37 ± 0.06 ***	0.37 ± 0.07 (n=9) ***
6	-	0.32 ± 0.08	0.28 ± 0.05 (n=7)
6	1 µM fluoxetine	0.36 ± 0.05	0.32 ± 0.05 (n=7)
8	-	0.27 ± 0.05	0.23 ± 0.02 (n=12)
8	1 µM fluoxetine	0.23 ± 0.02	0.25 ± 0.02 (n=7)

Tricyclic antidepressants such as imipramine or amitriptyline are not only inhibitors of the 5-HT transporter but also weak and reversible MAO inhibitors (Strolin Benedetti and Dostert, 1992). It has been shown that 10 µM amitriptyline binds on MAO B and inhibits the isoenzyme by 25 % (Roth, 1976). Similar results were found by Donnelly and Murphy (1977) showing that 63 µM amitriptyline inhibits the total MAO activity by 50 %. Although the chemical structure of fluoxetine does not comply with that of the tricyclic antidepressants, we had to exclude the possibility that even low concentrations of fluoxetine (which would still bind on the endothelial cells after washing the cell monolayer) disturb the assay of MAO activity. We therefore measured the activities of the total MAO and MAO B preincubated with various concentrations of fluoxetine. Fluoxetine (1 µM) did not affect the total MAO, but we found an inhibition of MAO B by 20 ± 8 % and 47 ± 11 % (mean value ± standard deviation of 8 experiments) using 10 and 100 µM fluoxetine. Imipramine (10 and 100 µM) inhibited MAO B by 5 ± 3 % and 33 ± 6 % (mean value ± SD of 8 experiments), respectively. Therefore, 1 µM fluoxetine can be used to study the effect of the chronic inhibition of 5-HT uptake on MAO activity without disturbing the assay of MAO. Our results are also important in relation to the clinical use of fluoxetine, because the inhibition of MAO is undesirable in some cases of depression.

In preliminary studies we showed the existence of a specific 5-HT transporter in porcine brain microvessels with high affinity binding of ³H-imipramine in nanomolar concentrations, which was inhib-

ited by fluoxetine (Brust and Bergmann, 1994). Fluoxetine (1 μ M) was therefore sufficient to bind on the 5-HT transporter and is expected to inhibit the cellular uptake of 5-HT, a main substrate of MAO A (Wong *et al.*, 1983). Although adaptive mechanisms in rat brain by chronic fluoxetine treatment were demonstrated (Hrdina and Vu, 1993), in our experiments fluoxetine (1 μ M) changed neither the total MAO activity nor the ratio MAO B/ MAO A.

In endothelial cells of gerbil brain microvessels, 0.3 mM imipramine blocked the uptake and metabolism of 5-HT (Spatz *et al.*, 1981). However, specific inhibition of MAO activity did not change the uptake of 5-HT, suggesting that transport rather than metabolism is the rate-limiting step in the 5-HT uptake. Other findings indicate that endothelial cells are able to newly synthesize 5-HT (Maruki *et al.*, 1984). Consistent with our results, both studies suggest that the 5-HT metabolism and 5-HT transport may be differentially regulated.

Taking all things together our results show that MAO A is predominant in cerebral endothelial cells and that serotonin uptake does not play an important role in regulating cellular MAO activity.

Acknowledgment

This work was supported by a research grant of the Saxon Ministry of Science and Art (7541.82-FZR/309).

References

- Baranczyk-Kuzma A., Audus K.L. and Borchardt R.T. (1986) Catecholamine-metabolizing enzymes of bovine brain microvessel endothelial cell monolayers. *J. Neurochem.* **46**, 1956-1960.
- Brust P. and Bergmann R. (1994) Characterization of serotonin uptake sites on the blood-brain barrier. *J. Neurochem.* **63**, S13C.
- Donnelly C.H. and Murphy D.L. (1977) Substrate- and inhibitor-related characteristics of human platelet monoamine oxidase. *Biochem. Pharmacol.* **26**, 853-858.
- Hardebo J.E., Emson P.C., Falck B., Owman C. and Rosengren E. (1980) Enzymes related to monoamine transmitter metabolism in brain microvessels. *J. Neurochem.* **42**, 826-832.
- Hrdina P.D. and Vu T.B. (1993) Chronic fluoxetine treatment upregulates 5-HT uptake sites and 5-HT₂ receptors in rat brain: an autoradiographic study. *Synapse* **14**, 324-331.
- Kalaria R.N. and Harik S.I. (1987) Blood-brain barrier monoamine oxidase: enzyme characterization in cerebral microvessels and other tissues from six mammalian species, including human. *J. Neurochem.* **49**, 856-867.
- Maruki C., Spatz M., Ueki Y., Nagatsu I. and Bembry J. (1984) Cerebrovascular endothelial cell culture: metabolism and synthesis of 5-hydroxytryptamine. *J. Neurochem.* **43**, 316-319.
- Méresse S., Dehouck M.P., Delorme P., Bensaid M., Tauber J.P., Delbart C., Fruchart J.C. and Cecchelli R. (1989) Bovine brain endothelial cells express tight junctions and monoamine oxidase activity in long-term culture. *J. Neurochem.* **53**, 1363-1371.
- Mischek U., Meyer J. and Galla H.J. (1989) Characterization of γ -glutamyl transpeptidase activity of cultured endothelial cells from porcine brain capillaries. *Cell Tiss. Res.* **256**, 221-226.
- Roth J.A. (1976) Evidence for a single catalytic binding site on human brain type B monoamine oxidase. *J. Neurochem.* **27**, 1107-1110.
- Spatz M., Maruki C., Abe T., Rausch W.D., Abe K. and Merkel N. (1981) The uptake and fate of radiolabelled 5-hydroxytryptamine in isolated cerebral microvessels. *Brain Res.* **220**, 214-219.
- Strolin Benedetti M. and Dostert P. (1992) Monoamine oxidase: from physiology to the design and clinical application of reversible inhibitors. in: *Advances in Drug Research* Vol. 23 ed. B. Testa 23 (Academic Press, New York), pp. 67-74.
- Tsang D., Ho K.P. and Wen H.L. (1986) Ontogenesis of multiple forms of monoamine oxidase in rat brain regions and liver. *Dev. Neurosci.* **8**, 243-250.
- Wong D.T., Bymaster F.P., Reid L.R. and Threkeld P.D. (1983) Fluoxetine and two other serotonin uptake inhibitors without affinity for neuronal receptors. *Biochem. Pharmacol.* **32**, 1287-1293.

43. PCR Analysis of Blood-Brain Barrier Specific Transporters in RBE4 Cells

R. Bergmann, F. Roux¹, L. R. Drewes², P. Brust

¹INSERM U26, Paris, ²University of Minnesota, School of Medicine, USA

Introduction

Immortalized brain endothelial cell lines are now being investigated as an alternative for studying drug transport through the blood-brain barrier (BBB). In order to realize their potential utility as *in vitro* models, such immortalized cells must exhibit transport systems characteristic of endothelial cells *in vivo*. Studies of the molecular regulation of low-abundance BBB-specific gene transcript thus require isolation of poly(A)⁺mRNA (Boado and Pardridge, 1991). The polymerase chain reaction (PCR) was used to examine the recently established cell line (Roux *et al.*, 1994) for expression of transport systems that may be important as conduits for drug delivery to the brain. Messenger RNA encoding several membrane transport systems including the glucose transporters (Glut-1 and Glut-3), amino acid transporter for cationic amino acids (system y⁺) and multidrug resistance transporters (mdr1a, mdr1b, and mdr2), working as ATP-dependent drug efflux pumps, were examined. Their expression in the RBE4 cells was compared to mRNA from rat brain microvessels, rat choroid plexus, and rat brain cortex.

Experimental

mRNA isolation

Rats were decapitated, brains were immediately removed and cleared of meninges and superficial large blood vessels. The choroid plexus were collected and frozen in liquid nitrogen. The brains were homogenized with a Potter-homogenizator. Rat brain capillaries were isolated in α MEM with 1 % dextran by a combination of centrifugation with dextran (15 %), filtration (125 μ m and 50 μ m screens) and washing. Immediately after the isolation of the microvessels, the Poly(A)⁺RNA from microvessels (MV), brain homogenate (Br), choroid plexus (Cp) and from RBE4 cells were isolated using the MicroFastTrack[®] (Invitrogen). Qualitative and quantitative analyses of the extracted mRNA were assessed by measuring the absorbance at 260, 280, 320 nm. All preparations had an A₂₆₀/A₂₈₀ ratio of 1.6 or higher.

mRNA-PCR

The synthesis of cDNA was performed in final volumes of 20 μ l consisting of 7 μ l 10xPCR buffer (Promega), 6 mM MgCl₂, 1.25 mM in each dNTP (dATP, dCTP, dGTP, dTTP), 20 pmoles of the right primer and 20 U of ribonuclease inhibitor (Boehringer Mannheim). The reactions were started by addition of 100 units of Moloney murine leukaemia virus reverse transcriptase (GIBCO-BRL). The mixture was incubated at 37 °C for 25 min and at 42 °C for 35 min for the synthesis of single-stranded cDNA. Prior to the end of incubation in each tube one AmpliWax[™] PCR Gem (Perkin-Elmer Cetus) was added. Then the tubes were heated for 5 min at 100 °C. After this denaturing step the temperature was set to 4 °C and 80 μ l of the PCR master mix were added. The 80 μ l master mix consisted of 20 μ moles of the second primer, 8 μ l 10xPCR buffer (Promega), 6 mM MgCl₂, 2 U of Taq polymerase and deionized water. Thirty five cycles (94 °C, 1 min; 55 °C, 1min; 72 °C, 1 min) followed by 15 min of final extension at 72 °C were performed with a programmable thermocycler (model 9600, Perkin-Elmer Cetus).

Alternatively the EZ rTth RNA PCR Kit (Perkin Elmer) was used for reverse transcription to cDNA. The subsequent amplification of the DNA was carried out by the thermocycler GeneAmp PCR System 2400 (Perkin Elmer), using the PCR process. 15 μ l of the amplification reaction was assayed in parallel with a known amount of molecular weight marker on 3 % Nu-Sieve agarose 3:1 (FMC Bioproducts, Rockland, ME) gels and viewed under UV light after ethidium bromide staining (negative pictures are presented) and photographed with a Polaroid system. The PCR products were alternatively analysed by polyacrylamide gel electrophoresis with the DNA Fragment Analysis Kit (Pharmacia Biotech) and stained with the Silver Staining Kit, DNA (Pharmacia Biotech). The AmpliSize[™] DNA Size Standard (BIO-RAD) with a molecular weight range from 50 to 2,000 bp was used as standard to estimate the molecular weights of DNA fragments. The used primers are presented in Table 1.

Table 1. Oligonucleotide sequences of PCR primers

Primer	Type	Sequence	Mol. weight (bp)
Glut-1	upper	5' - CTG CTA CAG TGT ATC CTG-3'	502
Glut-1	lower	5' - GAC ATC CAG GGC AGC TC-3'	502
Glut-3	upper	5' - CCT ACA GAG CGC AGC CC -3'	300
Glut-3	lower	5' - CGC ATC CTG GAA GAT TCC -3'	300
mdr-1a	upper	5' - AGA GGG GTG TTT CCA TCA-3'	176
mdr-1a	lower	5' - TGC CGT GCT CCT TGA C-3'	176
mdr-1b	upper	5' - GAA GCG CTG GAC AAA GCC-3'	247
mdr-1b	lower	5' - GTG CCA TGT TTG AAC ACC -3'	247
System y ⁺	upper	5' - CCG TGA GAA TGC TGG TCC-3'	239
System y ⁺	lower	5' - TCG TCA AAA GTT GCA CTC C-3'	239

Two methods were used for semiquantitative estimation of the band intensities. The Polaroid photographs of the gels or the silver stained gels were scanned with an HP ScanJet IIc (resolution 600 dpi). The relative intensities of the bands were determined in the appropriate regions of the gel with the TINA 2.07c (Raytest) programme and presented by the Corel Draw 4.0. The amounts of resulting DNA fragments were compared in experiments with samples of equal amounts of mRNA from the different sources. The cDNA were produced in the same PCR process and analysed in one gel.

Results and Discussion

The present study describes a procedure for isolation of poly(A)⁺ mRNA and their semiquantitative determination using the PCR. The mRNA was isolated from an immortalized endothelial cell line (RBE4 cells), from isolated rat brain microvessels, from rat choroid plexus and subsequent transcription to cDNA, using specific primers for the glucose and system y⁺ transporters and for the mdr genes. The results are presented in Table 2.

Table 2. Semiquantitative characterization of the transporter mRNA expression

Primer	Amount mRNA [ng]	mRNA source			
		Microvessel	Choroid Plexus	Brain	RBE4 cells
Water	0				
Glut-1	0,05	0	0	0	n.d.
	0,50	++	0	0	n.d.
	1,00	n.d.	n.d.	n.d.	+
	5,00	+++	++	++	n.d.
	10,00	++++	+++	++	n.d.
Glut-3	1,00	0	0	0	+
	5,00	0	0	+	++
mdr1a	5,00	+	+	+	+
	10,00	++++	++	++	++
	25,00	n.d.	n.d.	n.d.	+++
mdr1b	5,00	+	+	+	+++
	10,00	++	+	++	+++
	25,00	n.d.	n.d.	n.d.	++++
mdr2	10,00	0	0	0	0
System y ⁺	5,00	++	+	+	+++
	10,00	+++	+	+	++++
	25,00	n.d.	n.d.	n.d.	++++

(n.d.) - not determined; (0) - not detected; (+) - 1 - 25 %, (++) - 26 - 50 %, (+++) - 51 - 75 %, (++++) - 76 - 100 % of the heaviest band of the corresponding PCR product in the electrophoresis gel.

The electrophoretic analysis of Glut-3 PCR products is shown in Fig. 1. Comparisons with mRNA isolated from rat brain microvessels indicated a substantial decrease in Glut-1 transporter expression in RBE4 cells, and an unexpected expression of Glut-3 transporter (Fig. 1).

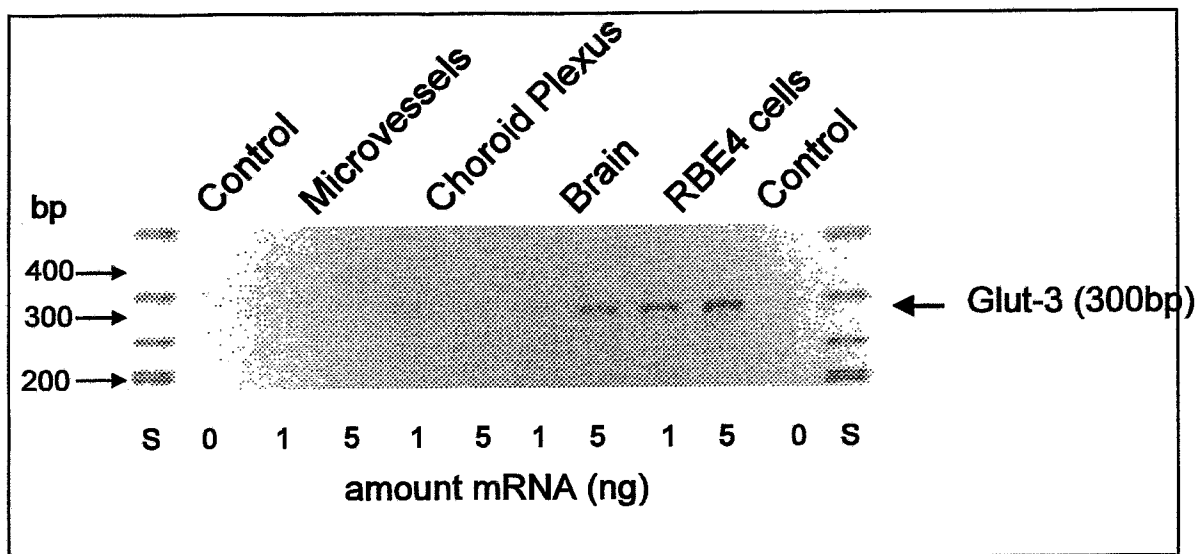


Fig. 1: Electrophoretic pattern of Glut-3 RT-PCR products of isolated mRNA from microvessels, choroid plexus, brain cortex and RBE4 cells

Wadhvani *et al.* (1993) found a 10 times higher level of Glut-1 in rat brain microvessels than in the PC12 cell line. This result is consistent with our finding that the level of Glut-1 in the microvessels is higher than in the RBE4 cells. Glut-3 is variably expressed in the brain vasculature of different brain regions. Additionally neuroepithelial cells of the rat switch from Glut-1 to Glut-3 gene expression during the final stage of neural differentiation. Glut-3 is an extremely abundant transporter associated with neuronal cell membranes and processes (Gerhardt *et al.*, 1994). The expression of system γ^+ transporter mRNA in the RBE4 cells, the brain capillaries, the choroid plexus and the brain samples was comparable. The analysis of expression of the mdr mRNA's showed the increased expression of mdr1b in relation to the mdr1a mRNA. Mdr2 was not found in the rat brain. The three P-glycoprotein isoforms of the rat (Silverman *et al.*, 1991) appear functionally distinct. Only mdr1a and mdr1b can confer multi drug resistance (Deuchars *et al.*, 1992) and may play a physiological role in regulating the access of certain molecules to the central nervous system, or in the secretory functions of the BBB.

These results indicate that the application of the PCR is a useful approach for screening and defining the membrane transport systems expressed by brain endothelial cell lines. Furthermore, it is suggested that RBE4 cells may be a valuable *in vitro* BBB model for studies of drug transport into the brain via the carrier-mediated system γ^+ basic amino acid transporter and for studies of drug extraction from the brain via P-glycoprotein (mdr1). So it seems useful to carry out transport studies with RBE4 cells and radioligands targeted at the multidrug resistance P-glycoprotein (Herman *et al.*, 1995). The differences between RBE4 cells and brain microvessels in the pattern of Glut-1 and Glut-3 glucose transporter expression indicate that progress must be made for RBE4 cells to exist in a more differentiated or *in vivo*-like state.

Acknowledgment

Supported in part by NIH grant NS 27229 and the Saxon Ministry of Science and Art (Grant 7541.82-FZR/309). The authors thank Dr. L.R. Drewes of the University of Minnesota, Duluth, for the opportunity to work in his laboratory and for extensive technical support and Dr. N. Borson for technological help and discussions.

References

- Boado R.J. and Pardridge W.M. (1991) A one-step procedure for isolation of poly(A)⁺ mRNA from isolated brain capillaries and endothelial cells in culture. *J. Neurochem.* **57**, 2136-2139.
- Deuchars K.L., Duthie M. and Ling V. (1992) Identification of distinct P-glycoprotein gene sequences in rat. *Biochem. Biophys. Acta* **1130**, 157-165.
- Gerhardt D.Z., Leino R.L., Borson D., Taylor W.E., Gronlund K.M., McCall A.L. and Drewes L.R. (1994) Localization of glucose transporter Glut 3 in brain: Comparison of rodent and dog using species-specific carboxyl-terminal antisera. *Neuroscience* **66**, 237-246.
- Herman L.W., Sharma V., Kronauge J.F., Barbarics E., Herman L.A. and Piwnica-Worms D. (1995) Novel Hexakis(areneisonitrile)technetium(I) complexes as radioligands targeted to the multidrug resistance P-glycoprotein. *J. Med. Chem.* **38**, 2955-2963.
- Roux F., Durieutrautmann O., Chaverot N., Claire M., Maily P., Bourre J.M., Strosberg A.D. and Couraud P.O. (1994) Regulation of gamma-glutamyl transpeptidase and alkaline phosphatase activities in immortalized rat brain microvessel endothelial cells. *J. Cell. Physiol.* **159**, 101-113.
- Silverman J.A., Raunio H., Gant T.W. and Thorgeisson S.S. (1991) Cloning and characterization of a member of the rat multidrug resistance (mdr) gene family. *Gene* **106**, 229-236.
- Wadhvani K.C., Fukuyama R., Giordano T., Rapoport S.I. and Chandrasekaran (1993) Quantitative reverse transcriptase-polymerase chain reaction of glucose transporter 1 mRNA levels in rat brain microvessels. *Analytical Biochem.* **215**, 134-141.

44. Is the Serotonin Transporter on the Blood-Brain Barrier Involved in the Regulation of Cerebral Blood Volume and Cerebral Blood Flow in the Rat?

Ch. Schenker, P. Brust

Introduction

The neurotransmitter serotonin is involved in the regulation of the cerebral blood flow (CBF) and the permeability of the blood-brain barrier (BBB) via receptor-mediated mechanisms. Recently we obtained evidence of the presence of a specific serotonin transporter on the BBB (Brust *et al.* 1995). The possible physiological function of the serotonin transporter seems to be to limit the action of this neurotransmitter on the cerebral vasculature. Thereby the transporter may contribute to the regulation of the cerebral microcirculation. The aim of this study was to examine the influence of fluoxetine, an inhibitor of serotonin transport, on the cerebral blood volume (CBV) and cerebral blood flow (CBF) of the anesthetized rat.

Experimental

Materials

The following reagents were employed: fluoxetine hydrochloride (M.W. 345.8) was a generous gift from Eli Lilly & Co. (Indianapolis, IN). High specific activity from [³H]diazepam was purchased from Amersham-Searle (Arlington Heights, IL, U.S.A.). ^{99m}TcO₄⁻ was obtained as eluent from a ^{99m}Tc generator. Soluene 350 and Instagel were obtained from Packard (Groningen, Netherlands).

Method

Male Wistar rats were anaesthetized with 2 ml (1.3 g/5ml H₂O) of urethane. The femoral vein was catheterized for tracer injection with PE-50 tubing which contained heparinized saline. A second catheter was inserted into the femoral artery and connected to a syringe fitted to a withdrawal pump calibrated at 1 ml/min. The tracer (total volume: 0.3 ml) was rapidly injected into the femoral vein. Fluoxetine (1 μM) was administered along with ^{99m}TcO₄⁻ (3 MBq) or [³H]diazepam (0.37 MBq). Ten seconds before tracer injection the withdrawal pump was started. Twenty seconds after bolus injection, the pump was stopped and the animal was killed immediately by injection of saturated KCl and then decapitated. The withdrawn blood was transferred to scintillation vials and measured for its radioisotope content. The last 10 μl of the withdrawn blood and aliquots of the injectate were also measured. The brain was rapidly removed and bilateral samples taken from the frontal cortex, striatum, hippocampus, hypothalamus, thalamus, visual cortex, colliculi and cerebellum were weighed, dissolved (2 ml soluene/isopropanol mixture of 1:1, 56 °C, 10 h) and their radioisotope content determined by β-scintillation spectroscopy, using 20 ml of a mixture of 0.1 M HCl and Instagel

(1:10). The blood samples were decolorized by addition of hydrogen peroxide. The technetium-99m counts in the samples were measured in a gamma counter.

Computations

The cerebral blood flow (F) was determined according to the equation (Gjedde *et al.* 1980):

$$F = C_{br}(T) / \int C(t) \cdot dt$$

where F is the blood flow, $C_{br}(T)$ is the content of [3H]diazepam per unit weight of the brain sample at the termination of the experiment, and $C(t)$ is the concentration of labelled [3H]diazepam in the blood. The cerebral vascular ("blood") volume (V) was calculated as follows:

$$V = C_{br}(T) / C(T)$$

where $C_{br}(T)$ is the content of $^{99m}TcO_4^-$ per unit weight of the brain sample at the termination of the experiment. $C(T)$ is the arterial blood concentration of $^{99m}TcO_4^-$ at the end of the study. The student's t-test was used to assess the statistical significance.

Table 1: Physiological parameters, values are averages \pm SD for the number of animals shown.

Parameter	Control (n =10)	Fluoxetine (n = 13)
Weight (g)	306 \pm 114	343 \pm 58
Arterial pH	7.368 \pm 0.032	7.366 \pm 0.049
Arterial PCO ₂	39.9 \pm 9.1	33.2 \pm 12.7
Arterial PO ₂	78.0 \pm 14.7	87.1 \pm 12.0
Haematocrit (%)	45 \pm 00	45 \pm 00

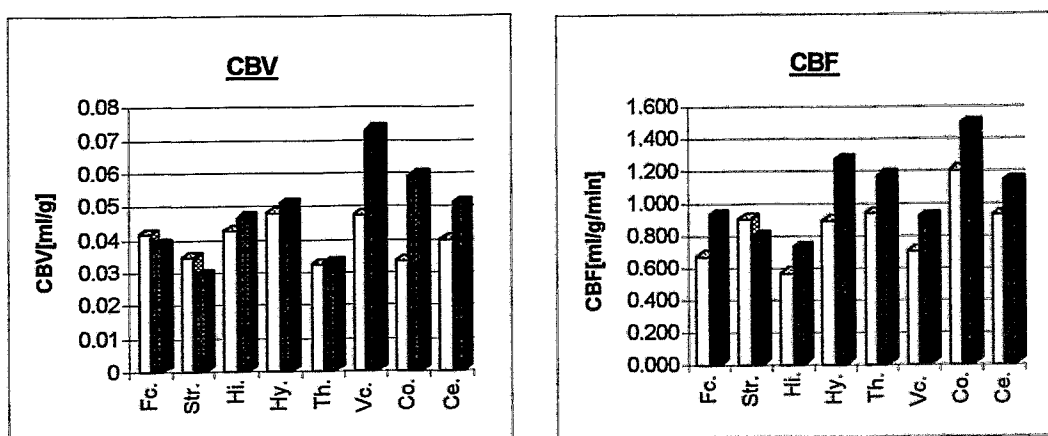


Fig. 1: The cerebral blood volume (left) and cerebral blood flow (right) of male Wistar rats determined using [3H]diazepam and $^{99m}TcO_4^-$, respectively, with and without coinjection of 1 μ M fluoxetine (controls: open columns, fluoxetine: filled columns)

Results and Discussion

The general physiological variables (P_{aO_2} , P_{aCO_2} , pH and haematocrit reading) of the rats were within the normal range and did not differ between the groups (Table 1). Fig. 1A shows the cerebral blood volume measured by intravenous injection of $^{99m}TcO_4^-$. In control animals the values of the blood volume ranged from 0.032 ± 0.012 ml·g $^{-1}$ in the thalamus to 0.048 ± 0.014 ml·g $^{-1}$ in the hypothalamus. After intravenous injection of fluoxetine no significant change of the blood volume was observed in most brain regions. However, in the visual cortex and colliculi fluoxetine induced a significant increase in blood volume from 0.047 ± 0.012 ml·g $^{-1}$ to 0.073 ± 0.028 ml·g $^{-1}$ and 0.033 ± 0.004 ml·g $^{-1}$ to 0.059 ± 0.021 ml·g $^{-1}$. The underlying mechanisms of this selective increase are unclear.

Fig. 1B shows the cerebral blood flow measured by intravenous injection of [3H]diazepam. In control animals the CBF values ranged from 0.57 ± 0.20 ml·g $^{-1}$ ·min $^{-1}$ in the hippocampus to 1.20 ± 0.05 ml·g $^{-1}$ ·min $^{-1}$ in the colliculi. Intravenous injection of fluoxetine did not elicit significant changes of the CBF. The CBF values were only ~10% higher than those of the controls.

In conclusion, these findings suggest that the serotonin transporter is not involved in the regulation of CBF and CBV at the blood-brain barrier. Knowledge of these data is important to us since we intend to investigate the possible involvement of the serotonin transporter in the blood-brain transfer of receptor-binding ^{99m}Tc tracers in the near future.

Table 2: The cerebral blood volume (CBV) and cerebral blood flow (CBF) of rat brain using [3H]diazepam and $^{99m}TcO_4^-$ as control and after coinjection of fluoxetine (1 μ M, i.v.)

Region	CBV[ml/g]		CBF[ml/g/min]	
	Control	+ Fluoxetine	Control	+ Fluoxetine
Fc.	0.042 ± 0.011	0.039 ± 0.015	0.670 ± 0.128	0.925 ± 0.178
Str.	0.035 ± 0.012	0.029 ± 0.012	0.895 ± 0.399	0.789 ± 0.242
Hi.	0.043 ± 0.017	0.046 ± 0.020	0.566 ± 0.199	0.721 ± 0.221
Hy.	0.048 ± 0.014	0.051 ± 0.015	0.885 ± 0.506	1.261 ± 0.343
Th.	0.032 ± 0.012	0.032 ± 0.010	0.931 ± 0.083	1.165 ± 0.269
Vc.	0.047 ± 0.012	$0.073 \pm 0.028^*$	0.700 ± 0.137	0.909 ± 0.225
Co.	0.033 ± 0.003	$0.059 \pm 0.021^*$	1.199 ± 0.046	1.484 ± 0.399
Ce.	0.040 ± 0.016	0.051 ± 0.017	0.925 ± 0.308	1.138 ± 0.394

Abbreviations: Fc.=Frontal cortex, Str.= Striatum, Hi.=Hippocampus, Hy.=Hypothalamus, Th.=Thalamus, Vc.=Visual cortex, Co.=Colliculis, Ce.=Cerebellum

*differs significantly from control ($p < 0.05$).

References

- Brust P., Bergmann R. and Johannsen B. (1995) Specific binding of [3H]diazepam indicates the presence of a specific serotonin transport system on endothelial cells of potcine brain. *Neuroscience letters* **194**, 21-24.
- Brust P., Baethmann A., Gjedde A. and Ermisch A. (1991) Artrial natriuretic peptide augments the blood-brain transfer of water but not leucine and glucose. *Brain Research* **564**, 91-96.
- Cumming P. and Gjedde A. (1993) Kinetics of the uptake of [3H]paroxetine in the rat brain. *Synapse* **15**, 124-129.
- Gjedde A., Hansen A.J. and Siemkowicz E. (1980) Rapid simultaneous determination of regional blood flow and blood-brain glucose transfer in brain of rat. *Acta Physiol. Scand.* **108**, 321-330.
- Pirro J.P., Di Rocco R.J., Narra R.K. and Nunn A.D. (1994) Relationship between *in vitro* transendothelial permeability and *in vivo* single-pass brain extraction. *J. Nucl. Med.* **35**, 1514-1519.
- Sakurada O., Kennedy C., Jehle J., Brown J.D., Carbin G.L. and Sokoloff L. (1977) Measurement of local cerebral blood flow with iodo[^{14}C]antipyrine. *Sakurada et al.* H59-H66.
- Scheffel U., Kim S., Cline E.J. and Kuhar M.J. (1994) Occupancy of the serotonin transporter by fluoxetine, paroxetine, and sertraline: *in vivo* studies with [^{125}I]RTI-55. *Synapse* **16**, 263-268.
- Tinguely D., Baumann P., Conti M., Jonzier-Perey M. and Schöpf J. (1985) Interindividual differences in the binding of antidepressives to plasma proteins: the role of the variants of alpha 1-acid glycoproteine. *J. Clin. Pharmacol.* **27** 661-666.

45. Tumour Cell-Targeting with the Radiometals Yb-169 and In-111

G. Kampf¹, G. Knop¹, W.-G. Franke¹, G. Wunderlich¹, P. Brust, B. Johannsen

¹Klinik und Poliklinik für Nuklearmedizin, Universitätsklinikum „Carl Gustav Carus“,
Technische Universität Dresden

Introduction

Our previous investigations into the uptake of various ¹⁶⁹Yb complexes by cultured cells (Kampf *et al.* 1994, 1995) were extended to include the analogous complexes with In-111 in order to elucidate the influence of the metal species on their protein-binding and its consequences for cellular uptake.

Further the principal possibilities of targeting tumour cells with radiometals were to be studied with both nuclides as models for radiolanthanides or other trivalent metals. Such knowledge is especially important for evaluation of a potential therapeutic approach.

Experimental

The compounds tested were complexes of Yb-169 and In-111 with the chelators citrate and the aminopolycarbonic acids nitrilotriacetic acid (NTA), ethylenediamine tetraacetic acid (EDTA), and diethylenetriaminepentaacetic acid (DTPA). The labelling procedures of the ¹⁶⁹Yb complexes were described by Kampf *et al.* (1994), the sources were ¹⁶⁹YbCl₃ (Swierk, Poland, spec.act. 15 GBq/mg Yb) and carrier-free ¹¹¹InCl₃ (Mallinckrodt).

The procedure of the protein-binding assay by ultrafiltration through Centricon-30 tubes (Amicon) was described by Kampf *et al.* (1995). As proteins those of the fetal calf serum (FCS) used normally for cell growth were added.

For the cell-targeting experiments non-radioactive YbCl₃ or InCl₃ was added as a carrier for achieving defined metal concentrations with the citrate and NTA complexes in the incubation medium. The amount of the radioactive metal complex was not changed, but the carrier concentration was varied. Checking by TLC showed that complex formation was not influenced by the carriers.

The methods for growing, incubating, and preparing cells for radioactivity measurement were described by Kampf *et al.* (1994). For these studies the malignant cell line KTCTL-2 (human adenocarcinoma of the kidney, from Heidelberg) was used after it had been seen (Kampf *et al.* 1995) that the normal cell line V79/4 behaves basically in the same way.

Results and Discussion

Formation of metal colloids in protein-free RPMI 1640 medium

When the metal complexes are added to the protein-free incubation medium (RPMI 1640) in normal air atmosphere and mixed by shaking or pipetting, carbon dioxide evaporates from the medium and the pH moves towards 8.0 or higher.

Under these conditions metal colloids are formed from the citrate complexes in the absence of proteins, with Yb already at very low metal concentrations (3.5×10^{-8} mmol/ml), but with In only at higher ones (3.5×10^{-7} mmol/ml). The colloids were detected by prefiltration of the solution intended for ultrafiltration in the protein-binding assay through a Dynagard (Microgon) sterile filter (0.2 µm). The size of the colloids is larger with high metal concentrations; with the small ones only very little radioactivity is retained by the sterile filter. The whole portion of the colloids results from the radioactivity of the Dynagard filter (bigger colloids), of the ultrafilter after removal of the concentrate by reverse centrifugation (smaller colloids), and of the empty retentate tube (very small colloids adhering to the plastic wall). Evaluation by thin-layer chromatography (TLC) shows the different positions of the metal complexes and the metal colloids (Fig. 1).

Protein-binding of Yb and In complexes and their cellular uptake

In protein-containing medium the ultrafiltration studies show greater affinity of the In than the Yb complexes to the serum proteins, and the citrates are bound to a greater extent than the aminocarbonic acid complexes. With citrate and NTA this effect is demonstrated in Fig. 2. As revealed by TLC, the complexes as a whole are bound to the proteins, the metals are not dissociated from the complex ligand. The metal-protein complex (as formed with with ¹⁶⁹YbCl₃) would be retained at the start; however, the metal-ligand complex separates from the protein and moves forward, but does not reach the position of the original complex (not shown).

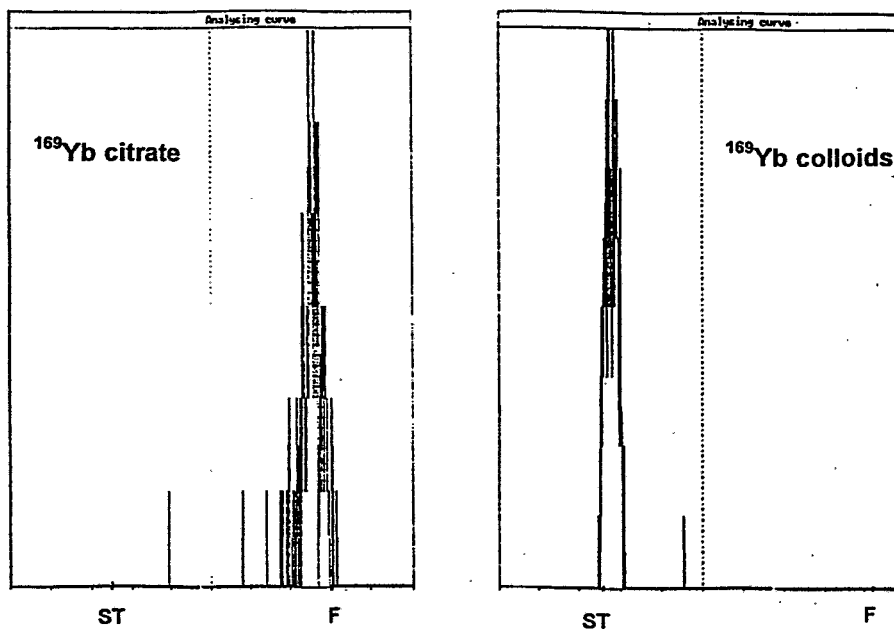


Fig. 1: TLC profiles of ^{169}Yb citrate and ^{169}Yb colloids (aluminium-cellulose, methanol/water 30:70), ST = start, F = front

The complexes of both metals with EDTA and DTPA are not associated with proteins, and the colloids, once formed, are not bound by the serum proteins.

Fig. 2 demonstrates the relation between protein-binding, colloid formation, and cellular uptake of the metals. As shown by the example of Yb citrate, the metal colloids formed in the protein-free medium are largely taken up by or bound to the cells; in the presence of proteins, however, colloid formation is inhibited. With increasing serum content of the medium, protein-binding of the citrate complexes prevents colloid formation, and already a small serum content (3 - 5%) leads to a drastic drop in metal uptake. The protein-bound portion is no longer available for cellular uptake.

With Yb and In complexes basically the same dependence of cellular uptake on protein-binding is observed. However, with In citrate colloid formation occurs only at higher concentrations (3.5×10^{-7} mmol/ml). In Fig. 2 the results with 3.5×10^{-8} mmol/ml are depicted. As In citrate shows higher affinity to proteins than Yb citrate, with 3 % serum content already 90 % of the complex in the low concentration are protein-bound.

By contrast, uptake of the aminocarbonic acid complexes of both metals is stimulated by small doses of proteins. From the picture of InNTA with its moderate protein-binding an enhancement of In uptake by protein-binding might be suggested; however, since with Yb-NTA and with the EDTA and DTPA complexes the same uptake behaviour but no protein-binding can be seen, this increase cannot be caused by metal uptake in protein-bound form. The stimulation must result from a simple matrix effect of the proteins on the cells, and is also observed with the albumin fraction alone (Kampf *et al.*, 1995). In control experiments with ^{125}I -labelled human serum albumin no uptake of the protein was observed (Fig. 3), there was only some adsorption to the cells.

Though protein-binding up to 90 % is observed with In-NTA, there is still unbound complex in the medium for cellular uptake.

In undiluted serum, when colloids cannot be formed, uptake of all complexes studied is at the level of the Yb-NTA uptake (see Fig. 5).

These results show that protein-binding of the metal complexes is influenced both by the chelating ligand and the metal species. By contrast, uptake of the metals by the cells is not influenced by the nuclide except via concentration, but it is decisively influenced by the ligand coordinated to the metal.

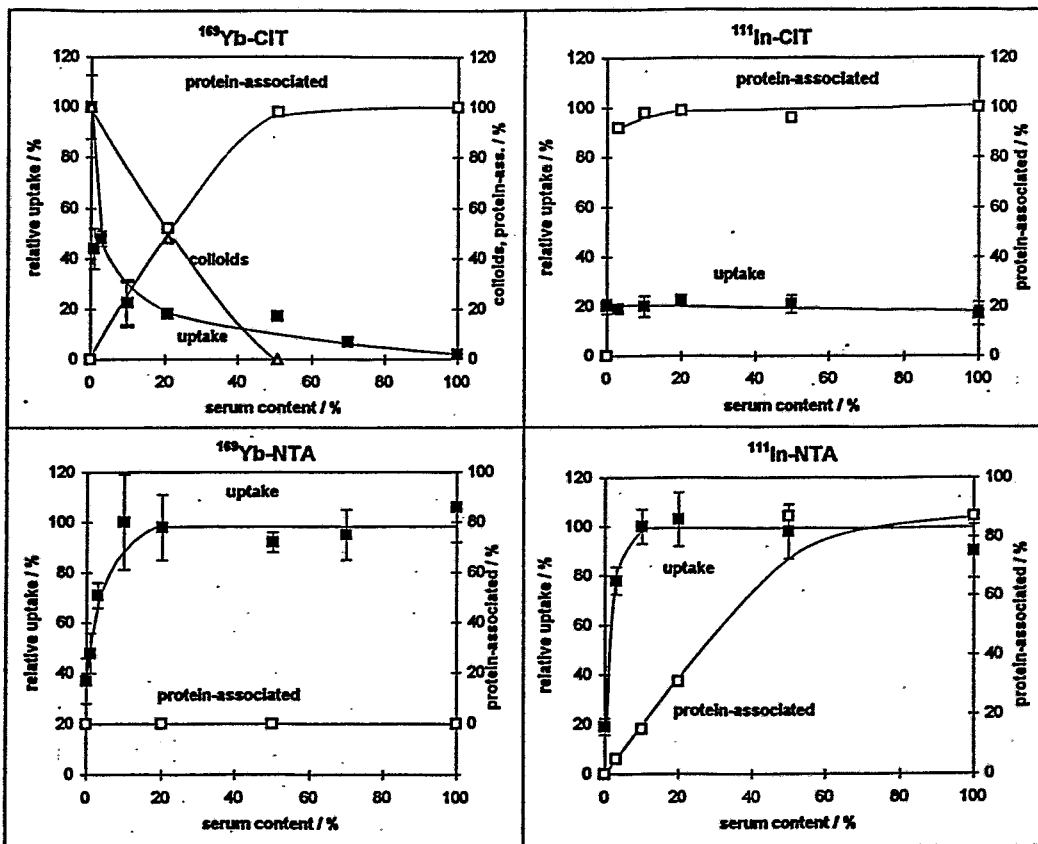


Fig. 2: Protein-binding, colloid formation, and cellular uptake of ^{169}Yb and ^{111}In complexes with citrate (CIT) and NTA in dependence on the serum content of the incubation medium. For the citrate complexes the highest Yb uptake without protein (colloids) was taken as 100%. $n = 8 - 12$.

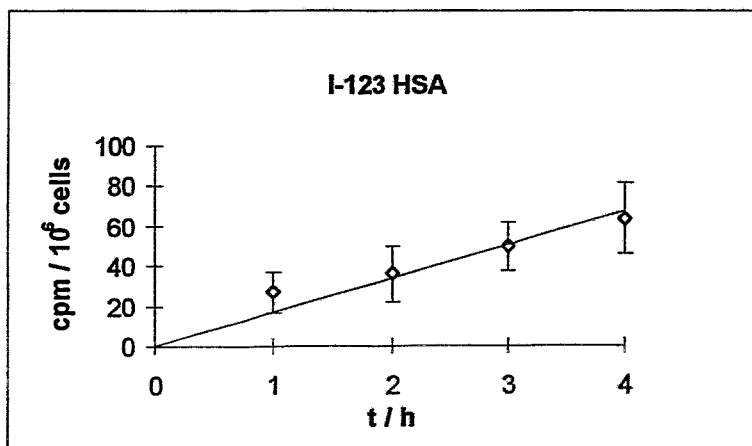
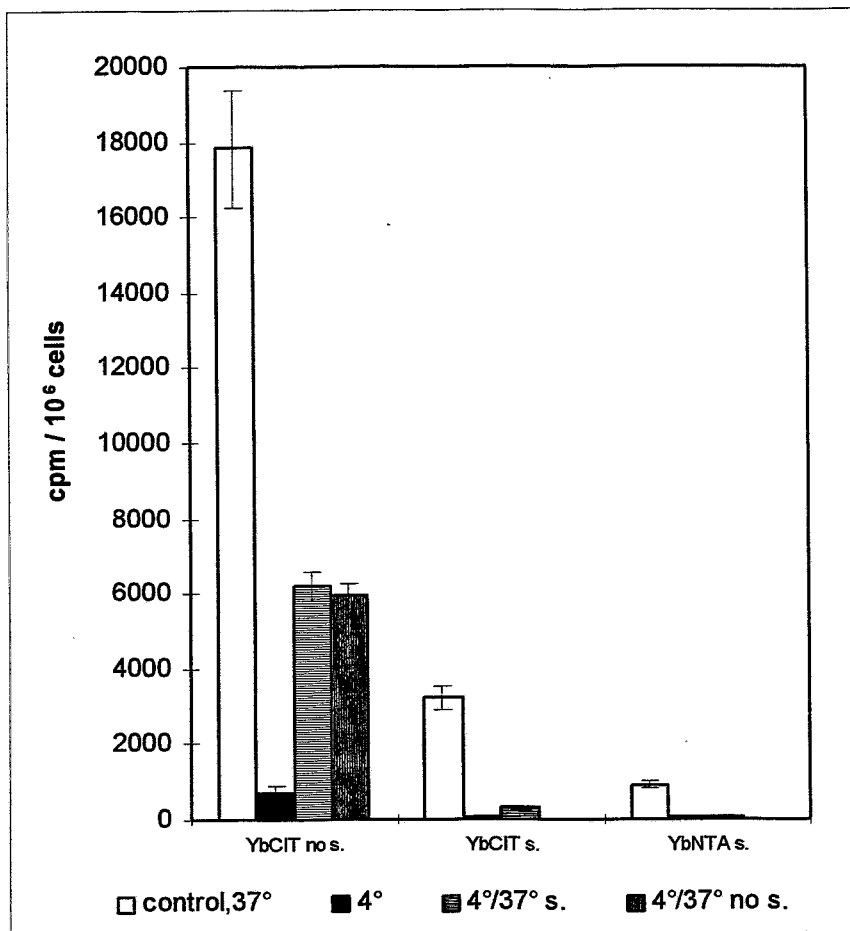


Fig. 3: Association of ^{123}I -labelled HSA with V79 and KTCTL-2 cells. $n = 4$.

Binding / adsorption of the metal colloids to the cell surface

In order to gain some information on the uptake mechanism, experiments of metal adsorption to the cellular membrane in the cold followed by postincubation at 37 °C were performed with Yb complexes. Fig. 4 shows that during incubation at 4 °C the cells take up neither the colloids nor the complexes.



However, it is known from earlier experiments (Kampf *et al.* 1995) that the metal from the Yb citrate complex adsorbs or binds to the cell surface as revealed by radioactivity measurement of the trypsin-EDTA solution used for cell dissociation after incubation.

Fig. 4: Effect of post-incubation (4 °C / 37 °C) after first incubation with ¹⁶⁹Yb citrate (Yb colloids) or ¹⁶⁹Yb-NTA at 4 °C., n = 4. Left group: first incubation without serum (no s.), s = in the presence of 10 % serum.

After careful rinsing with buffer (PBS, 12 times) of the monolayers incubated at 4 °C, with very low radioactivity removed by the last rinsings, the cells were postincubated at 37 °C. During this postincubation the cells internalize at least part of the metal colloids bound to the cell surface. This is excellently visible with Yb citrate in the absence of serum (left panel). After the adsorption of the colloid particles, the serum content of the postincubation medium is irrelevant for internalization, the M(III) level in the cells is as high with 10 % serum as in the absence of serum. However, the uptake level of the controls is not reached. In the presence of 10 % serum less colloids are formed which can be bound to the cell surface, and the effect is not so clear (central panel). With Yb-NTA no adsorption of the complex molecules occurs, and the effect of postincubation is absent (right panel).

From these and our previous results there is no indication of an uptake pathway for the aminocarbonic acid complexes. Since these complexes are not dissociated in the incubation medium, it may be a simple or facilitated diffusion of the whole complex.

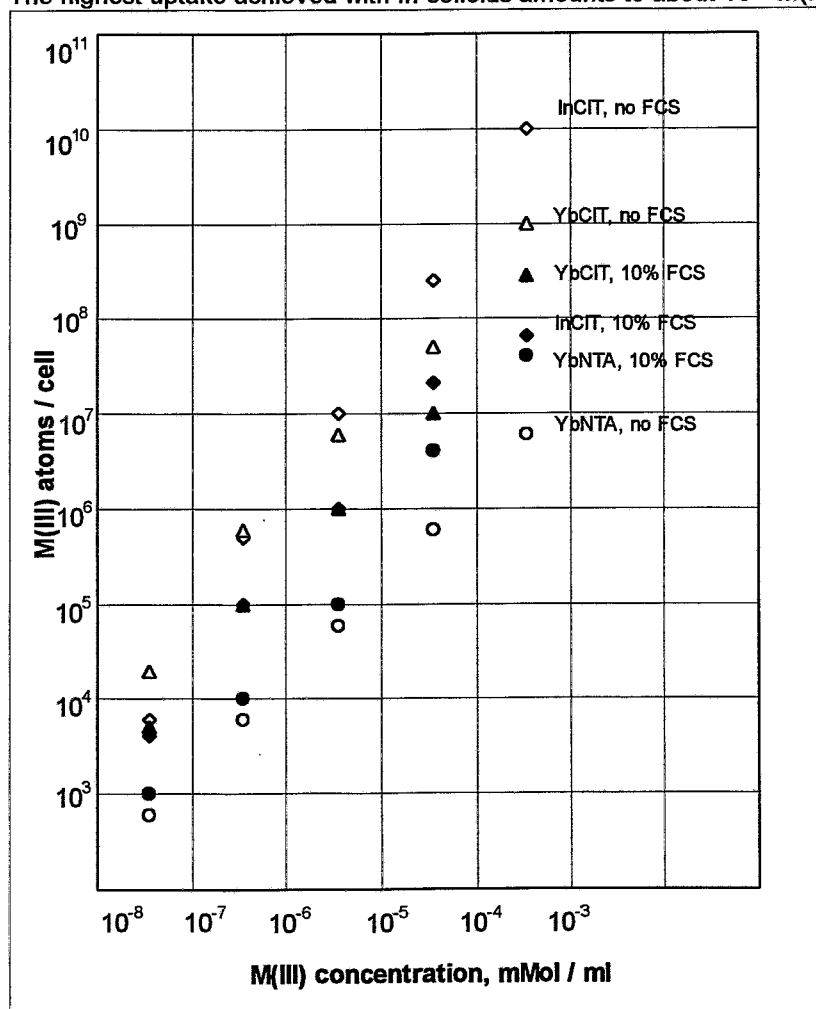
However, our results described here and the knowledge that from the citrate complexes the M(III) are taken up by the cells via an energy-consuming process (Kampf *et al.*, 1994, 1995; Planas-Bohne and Duffield, 1988) suggest that internalization of the colloid particles proceeds by a kind of endocytosis, by pinocytosis. The adsorption or binding of the colloids to the cell membrane even at the low temperature and the following internalization resemble the process of binding and incorporation of a

receptor-ligand complex by ATP-dependent endocytosis. In this context it is very interesting that coated colloidal nanoparticles (av. diameter 230 nm) loaded with peptides are taken up by brain blood vessel endothelial cells *in vitro* and are transported through the blood-brain barrier *in vivo*. The authors (Kreuter *et al.* 1995) also suggest an internalization pathway via phagocytosis or endocytosis.

Loading of the cells with M(III) atoms

The results of the carrier experiments are exhibited in Fig. 5. The amount of radioactivity taken up by the cells is nearly constant with all complex concentrations offered to the cells, i.e. metal uptake is exactly proportional to the concentration. This is the case with all complexes and colloids studied. The uptake of In and Yb from the citrate complexes is comparable.

The highest uptake achieved with In colloids amounts to about 10^{10} M(III) atoms / cell, and there is no indication of saturation yet.



Even with Yb-NTA, the complex from which no colloids are formed, an uptake of more than 10^7 Yb atoms / cell can be reached in the presence of serum.

As regards radiation biophysical aspects, about 3×10^4 β^- -emitting nuclide particles per cell are necessary for a cellular survival rate of 10^{-12} . The cellular metal concentrations reached with the colloids and also with the complexes thus lie far above the level necessary for such cell inactivation and should be therapeutically effective also with inhomogeneous distribution in the tumour, using the clinically applied nuclides with energies causing crossfire.

Fig. 5: Approximate number of cell-associated M(III) atoms in dependence on complex concentration, $n = 6$.

Conclusions

The protein affinity of the citrate complexes causes their predominant scavenging by the plasma proteins. Hence only the non-bound rest can be accumulated in cells and tumours, and the amounts are comparable to those of the NTA complexes. This means that the uptake of the metal ligand complexes themselves is low. Several years' experience with the metal ligand complexes suggest that the cellular uptake of the complexes can only be increased via the concentration offered, but - as these studies show - a substantial enhancement of metal accumulation can be achieved by offering them to the cells as metal colloids.

With both ^{169}Yb and ^{111}In , the normal as well as the tumour cells studied prefer metal uptake as colloids rather than metal ligand complexes (factor 10 - 20).

In this way a cell can be loaded *in vitro* with about 10^{10} metal atoms, which according to radiation biophysical knowledge should be sufficient for therapeutic irradiation with an appropriate β^- -emitter. The principal possibility of a high targeting of cells with M(III) atoms could be revealed in these *in vitro* studies. The problem which remains is the exploitation of such results for clinical purpose, the selective transport into tumour cells or tumour-accompanying tissue *in vivo*.

These studies were partly supported by Mallinckrodt Pharma.

References

- Kampf G., Knop G., Matys S., Kunz G., Wenzel U., Bergmann R. and Franke W.-G. (1993) Relations between the uptake of the radiometal ^{169}Yb into normal and tumour cells and their metabolic activity depending on the ligand species. *Annual Report 1993*, Institute of Bioinorganic and Radiopharmaceutical Chemistry, FZR-32, pp.146-150.
- Kampf G., Knop G., Wenzel U., Franke W.-G., Brust P. and Johannsen B. (1994) Evidence of active uptake of ^{169}Yb complexes into tumour cells *in vitro*, stability of their cellular fixation, and the role of their protein-binding. *Annual Report 1994*, Institute of Bioinorganic and Radiopharmaceutical Chemistry, FZR-73, pp. 143-151.
- Kreuter J. et al. (1995) Passage of peptides through the blood-brain barrier with colloidal polymer particles (nanoparticles). *Brain Research* 674, 171.
- Planas-Bohne F. and Duffield J. (1988) Factors influencing the uptake of iron and plutonium into cells. *Int. J. Radiat. Biol. Relat. Stud. Phys. Chem. Med.* 53, 489.

II. PUBLICATIONS, LECTURES, POSTERS AND PATENTS

PUBLICATIONS

Ahlemeyer B., Matys S., Brust P., Johannsen B. (1995)

Hirndothelzellen als *In-vitro*-Modell für die Blut-Hirn-Schranke: Anwendung zur Untersuchung des Transportes von Radiotraceren.

Nucl.-Med. **34**, A140.

Bergmann R., Brust P., Kampf G., Coenen H.H., Stöcklin G. (1995)

Evaluation of radiolabelled selenomethionine as a tracer for measurement brain protein synthesis by PET.

Nucl. Med. Biol. **22**, 475-481.

Brust P., Bergmann R., Johannsen B. (1995)

Specific binding of [³H]imipramine indicates the presence of a specific serotonin transport system on porcine brain endothelial cells.

Neurosci. Lett. **194**, 21-24.

Brust P., Matys S., Ahlemeyer B., Wober J., Bergmann R., Johannsen B. (1995)

A specific transport system for serotonin is present on endothelial cells of the porcine brain.

J. Cereb. Blood Flow Metab. (Suppl. 2), S21.

Brust P., Pietzsch H.-J., Scheunemann M., Wober J., Syhre R., Spies H., Johannsen B. (1995)

Biological characterization of oxorhenium(V) and oxotechnetium(V) complexes with binding affinity to the serotonin 5-HT₂ receptor.

Eur. J. Nucl. Med. **22**, 781.

Brust P., Spies H., Noll B., Noll St., Berger R., Syhre R., Wober J., Kretzschmar M., Johannsen B.

(1995) Synthese, Charakterisierung und Rezeptorbindungseigenschaften von p-Fluoro-Butyrophenon-substituierten Rheniumkomplexen.

Nucl.-Med. **34**, A120.

Droescher P., Römer J. (1995)

Synthesis of high specific activity 17-cyanomethyl-17β-hydroxy-[14, 15, -³H]estra-4,9-dien-3-one.

J. Labelled Comp. Radiopharm. **36**, 111.

Fietz T., Spies H., Pietzsch H.-J., Leibnitz P. (1995)

Synthesis and molecular structure of chloro(3-thia-pentane-1.5-dithiolato)-oxorhenium(V)

Inorg. Chim. Acta **231**, 233-236.

Füchtner F., Steinbach J., Mäding P., Johannsen B. (1996)

Basic hydrolysis of 2-[¹⁸F]fluoro-1,3,4,6-tetra-O-acetyl-D-glucose in the preparation of 2-[¹⁸F]fluoro-2-deoxy-D-glucose.

Appl. Radiat. Isot. **47**, 61-66.

Glaser M., Spies H., Lügger T., Hahn F.E. (1995)

Formation of Rhenium(III) Carbonyl Complex by Electrophilic Attack on Rhenium Isocyanides:

Synthesis and Molecular Structure of {Re[N(CH₂CH₂S)₃][CNC(CH₃)₃]} and {Re[N(CH₂CH₂S)₃](CO)}

J. Organomet. Chem. **503**, C32-C35.

Johannsen B., Spies H.

Chemistry of technetium(V) as relevant for nuclear medicine

Topics Curr.Chem. **176**, 77-121.

Johannsen B., Pietzsch H.-J., Scheunemann M., Spies H., Brust P (1995)

Oxotechnetium(V) and oxorhenium(V) complexes as potential imaging agents for the serotonin receptor. J. Nucl. Med. **36**, 27P.

- Kampf G., Franke W.-G., Knop G., Wenzel U., Wunderlich G., Seifert S., Brust P., Johannsen B. (1995) Zum Einfluß der Struktur von ^{169}Yb - und $^{99\text{m}}\text{Tc}$ -Komplexen auf ihre Aufnahme in Normal- und Tumorzellen. Nucl.-Med. **34**, A121.
- Kampf G., Knop G., Franke W.-G., Wunderlich G., Brust P., Johannsen B. (1995) Protein-binding and uptake of Yb-169 and In-111 complexes by cultured tumour cells: influence of the complex structure and the metal ion. Eur. J. Nucl. Med. **22**, 903 .
- Malin R., Steinbrecher R., Janssen J., Semmler W., Noll B., Johannsen B., Frömmel C., Höhne W., Schneider-Mergener J. (1995) Identification of technetium-99m binding peptides using combinatorial cellulose-bound peptide libraries. J. Am. Chem. Soc. **117**, 11821-11822.
- Mihail J.D., Obert M., Bruhn J.N., Taylor S.J. (1995) Fractal geometry of diffuse mycelia and rhizomorphs of *Armillaria* species. Mycol. Research **99**, 81-88.
- Noll B., Noll St., Spies H., Johannsen B., Dinkelborg L., Semmler W. (1995) Tc complexes of N-alkylated mercaptoacetyl glycines as potential tracers for imaging atherosclerotic lesions. In: Technetium and Rhenium in Chemistry and Nuclear Medicine (Edited by Nicolini M., Bandoli G. and Mazzi U.) SGEDITORIALI Padova **4**, pp. 433-436.
- Noll B., Johannsen B., Spies H. (1995) Sources of radiochemical impurities in the $^{99\text{m}}\text{Tc}/\text{S}$ -unprotected MAG_3 system. Nucl. Med. Biol. **22**, 1057-1062.
- Obert M., Bergmann R., Linemann H., Brust P. (1995) Analyses of an image of the human brain obtained by positron emission tomography in terms of fractal geometry. In: Fractal Reviews in the Natural and Applied Sciences (M. Novak, ed.) Chapman and Hall, London, pp. 145 - 152.
- Obert M., Brust P., Linemann H., Bergmann R., Jestszemski F., Johannsen B. (1995) Investigation of the distribution of a radiotracer in a human brain - A multifractal analysis of a positron emission tomography image. Nucl.-Med. **34**, A138.
- Pietzsch H.-J., Spies H., Leibnitz P., Reck G., Johannsen B. (1995) Technetium and rhenium complexes with multidentate thioether ligands. In: Technetium and Rhenium in Chemistry and Nuclear Medicine (Edited by Nicolini M., Bandoli G. and Mazzi U.) SGEDITORIALI Padova, **4**, 231-234.
- Pietzsch H.-J., Spies H., Leibnitz P., Reck G. (1995) Technetium and rhenium complexes with thioether ligands. IV. Synthesis and structural characterization of binuclear oxorhenium(V) complexes with bidentate thioether coordination. Polyhedron **14**, 1849-1853.
- Seifert S., Syhre R., Spies H., Johannsen B. (1995) Enzymatic cleavage of technetium and rhenium complexes with DMSA ester ligands. In: Technetium and Rhenium in Chemistry and Nuclear Medicine (Edited by Nicolini M., Bandoli G. and Mazzi U.) SGEDITORIALI Padova, **4**, 437-440.
- Seifert S., Muth O., Jantsch K., Johannsen B. (1995) Radiochemical purity of $^{99\text{m}}\text{Tc}$ -HM-PAO: Critical parameters during kit preparation. Nucl. Med. Biol. **22**, 1063-1066.

Spies H., Fietz T., Glaser M., Pietzsch H.-J., Johannsen B. (1995)
The "n+1" concept in the synthesis strategy of novel technetium and rhenium tracers.
In: Technetium and Rhenium in Chemistry and Nuclear Medicine (Edited by Nicolini M., Bandoli G. and Mazzi U.) SGEDITORIALI Padova, 4, 243-246.

Spies H., Glaser M., Hahn F.E., Lügger T., Scheller D. (1995)
Synthesis and characterization of isocyanide-containing rhenium(III) complexes
trans-[ReCl₃(CNR)(PPh₃)₂] and crystal structure of *trans*-[ReCl₃(CN-*t*-C₄H₉)(PPh₃)₂].
Inorg. Chim. Acta 232, 235-239.

Spies H., Fietz T., Pietzsch H.-J., Johannsen B., Leibnitz P., Reck G., Scheller D., Klostermann K.
(1995) Neutral oxorhenium(V) complexes with tridentate dithiole ligands and monodentate alkyl/aryl
thioles as co-ligands.
J. Chem. Soc., Dalton Trans., 2277-2280.

Spies H., Johannsen B. (1995)
Functionalization of technetium complexes to make them active *in vivo*.
The Analyst 120, 775-777.

Steinbach J., Mäding P., Füchtner F., Johannsen B. (1995)
N.c.a. ¹¹C-labelling of benzenoid compounds in ring positions: synthesis of nitro-[1-¹¹C]benzene and
[1-¹¹C]aniline.
J. Labelled Comp. Radiopharm. 1, 33-41.

Syhre R., Seifert S., Spies H., Johannsen B. (1995)
Beziehungen zwischen *in vitro* Hydrolyseeigenschaften und *in vivo* Verhalten von ^{99m}Tc-DMSA-
Ethyylester mit unterschiedlichem Veresterungsgrad.
Nucl.-Med. 34, A121.

LECTURES

Ahlemeyer B.
Endothelzellkulturen von Schweinehirnkapillaren als *in vitro* Modell für die Blut-Hirn-Schranke.
Institut für Pharmakologie und Toxikologie der Philipps-Universität Marburg, 10.1.1995.

Brust P., Spies H., Noll B., Noll St., Berger R., Syhre R., Wober J., Kretzschmar M., Johannsen B.
Synthese, Charakterisierung und Rezeptorbindungseigenschaften von p-Fluor-butyrophenon-substitu-
ierten Rheniumkomplexen.
DGN Jahrestagung, Dresden, 29.3.-1.4.1995.

Brust P.
Regulation von Transportprozessen am cerebralen Endothel durch endogene Peptide.
Workshop der Gesellschaft für Zell- und Gewebezüchtung e.V. „Endothelzellen: Differenzierung und
Vermittlung pharmakologischer Reaktionen“. Münster, 27.-28.9.1995.

Brust P., Matys S., Ahlemeyer B., Wober J., Bergmann R., Johannsen B.
A specific transport system for serotonin is present on endothelial cells of the porcine brain.
XVIIth Int. Symp. Cereb. Blood Flow Metab., Cologne, Germany, 2.-6.7.1995.

Brust P., Pietzsch H.-J., Scheunemann M., Wober J., Syhre R., Spies H., Johannsen B.
Biological characterization of oxorhenium(V) and oxotechnetium(V) complexes with binding affinity to
the serotonin 5-HT₂ receptor.
European Nuclear Medicine Congress, Brussels, Belgium, 26.-30.8.1995.

Brust P., Matys S., Wober J., Friedrich A., Bergmann R., Ahlemeyer B.
Blood-brain barrier properties *in vitro* as related to the neurotransmitter serotonin.
Cerebral Vascular Biology Conference, Paris, France, 10.-12.7.1995.

Füchtner F., Steinbach J., Mäding P., Johannsen B.
Alkaline hydrolysis of 2-[¹⁸F]fluoro-1,3,4,6-tetra-O-acetyl-D-glucose in the preparation of 2-[¹⁸F]fluoro-2-deoxy-D-glucose.
11th International Symposium on Radiopharmaceutical Chemistry, Vancouver, Canada; 13.-17.8.1995.

Füchtner F., Steinbach J., Mäding P., Johannsen B.
Basische Hydrolyse von Tetraacetyl-[¹⁸F]FDG zur Herstellung von [¹⁸F]FDG.
3. Arbeitstagung der AG Radiochemie/Radiopharmazie der Deutschen Gesellschaft für Nuklearmedizin, Ladenburg, 28.-30.9.1995.

Johannsen B.
Technetiumkomplexe von N-Alkyl-MAG-Verbindungen.
Institut für Diagnostikforschung an der FU Berlin, 20.1.1995.

Johannsen, B.*
Möglichkeiten und Grenzen von Technetium in der Medizin.
Institut für Kernchemie, Johannes Gutenberg Universität Mainz, 10.5.1995

Johannsen, B.*
Recent radiopharmaceutical research at the FZR.
Brookhaven National Laboratory, Medical Department, Brookhaven, USA, 16.6.1995.

Johannsen, B.*
Recent trends in radiopharmaceutical research for diagnostic and therapeutic nuclear medicine.
2. IAEA-Coordinator meeting of ARCAL XV on Production and Quality control of radiopharmaceuticals. Salvador, Brazil, 2.-6.10.1995.

Johannsen, B.*
Technetium chemistry applied to the development of radiopharmaceuticals.
2. IAEA-Coordinator meeting of ARCAL XV on Production and Quality control of radiopharmaceuticals. Salvador, Brazil, 2.-6.10.1995.

Johannsen, B.*
T-99m radiopharmaceuticals - recent and future trends.
2. IAEA-Coordinator meeting of ARCAL XV on Production and Quality control of radiopharmaceuticals. Salvador, Brazil, 2.-6.10.1995.

Johannsen B., Seifert S., Syhre R., Spies H.
Enzymatic hydrolysis of ester group-bearing ligands in technetium complexes.
6th Eur. Symp. on Radiopharmacy and Radiopharmaceuticals, Graz, Austria, 5.-8.3.1995.

Johannsen B., Pietzsch H.-J., Scheunemann M., Spies H., Brust P.
Oxotechnetium(V) and oxorhenium(V) complexes as potential imaging agents for the serotonin receptor. 42nd Annual Meeting Amer. Soc. Nucl. Med., Minneapolis, USA, 12.-15.6.1995.

Kampf G., Franke W.-G., Knop G., Wenzel U., Wunderlich G., Seifert S., Brust P., Johannsen B.
Zum Einfluß der Struktur von ¹⁶⁹Yb- und ^{99m}Tc-Komplexen auf ihre Aufnahme in Normal- und Tumorzellen.
Deutsche Gesellschaft für Nuklearmedizin e.V., Jahrestagung, Dresden, 31.3.1995.

Linemann H.
POSITOME IIIp, Sampling und Schwächungskorrektur.
TU Dresden, Klinik für Nuklearmedizin, 31.1.1995.

Mäding P., Steinbach J.
Neue Ergebnisse zur ¹¹C-Kernmarkierung substituierter Aromaten.
4. Arbeitstagung der Regionalgruppe Zentraleuropa der International Isotope Society (IIS), Bad Soden, Taunus, 11.-12.5.1995.

Mäding P., Steinbach J., Füchtner F.

Ergebnisse zur n.c.a. ^{11}C -Markierung von Benzenderivaten im aromatischen Ring.

3. Arbeitstagung der AG Radiochemie/Radiopharmazie der Deutschen Gesellschaft für Nuklearmedizin, Ladenburg, 28.-30.9.1995.

Obert M., Bergmann R., Linemann H., Brust P.

Analyses of an image of the human brain obtained by positron emission tomography in terms of fractal geometry.

Int. Symp. on Fractals, Marseille, Frankreich, 7.-14.2.1995.

Obert M.

Fraktale und PET.

Justus-Liebig-Universität Gießen, Inst. f. Biochemie u. Endokrinologie, Gießen, 12.5.1995.

Römer J., Steinbach J.

Schnelle Synthese von 16α - ^{18}F Fluorestradiol.

4. Arbeitstagung der Regionalgruppe Zentraleuropa der International Isotope Society (IIS), Bad Soden, Taunus; 11.-12.5.1995.

Römer J., Steinbach J., Kasch H., Johannsen B.

Untersuchungen zur schnellen Herstellung von 16α - ^{18}F Fluorestradiol.

3. Arbeitstagung der AG Radiochemie/Radiopharmazie der Deutschen Gesellschaft für Nuklearmedizin, Ladenburg; 28.-30.9.1995.

Spies H., Pietzsch H.-J., Noll B., Johannsen B.

New ways to functionalized technetium and rhenium tracers.

European Nuclear Medicine Congress., Brussels, Belgium, 27.8.1995.

Steinbach J., Mäding P., Füchtner F.

Synthesis of n.c.a. ^{11}C -ring labelled benzenoid compounds.

7th Symposium on the medical application of cyclotrons, Turku, Finland, 22.-25.5.1995.

Steinbach J.

PET-Centre Rossendorf.

Interregional Training Course on Nuclear Medicine for Developing Countries, Berlin; 24.9.-20.10.1995.

Steinbach J., Chebani K., Zessin J., Mäding P., Johannsen B.

Untersuchungen zur Synthese von ^{11}C -markierten Pyridinkörpern durch Pyrolyse.

3. Arbeitstagung der AG Radiochemie/Radiopharmazie der Deutschen Gesellschaft für Nuklearmedizin, Ladenburg; 28.-30.9.1995.

Steinbach J.*

Radiopharmazeutische Chemie - Besonderheiten und Zielstellung für PET (Positronen-Emissions-Tomographie).

Institutskolloquium, Hans-Knöll-Institut Jena, 14.11.1995

Sybre R., Seifert S., Spies H., Johannsen B.

Beziehungen zwischen *in vitro* Hydrolyseeigenschaften und *in vivo* Verhalten von $^{99\text{m}}\text{Tc}$ -DMSA-Ethylester mit unterschiedlichem Veresterungsgrad.

Deutsche Gesellschaft für Nuklearmedizin e.V., Jahrestagung, Dresden, 31.3.1995.

* invited lecture

POSTERS

- Ahlemeyer B., Matys S., Brust P., Johannsen B.
Hirndothelzellen als *In-vitro*-Modell für die Blut-Hirn-Schranke: Anwendung zur Untersuchung des Transportes von Radiotracer.
Deutsche Gesellschaft für Nuklearmedizin e.V., Jahrestagung, Dresden, 29.3.-1.4.1995.
- Ahlemeyer B., Matys S., Brust P.
Evidence for cell populations with different activities of alkaline phosphatase in endothelial cell cultures of porcine brain microvessels.
2nd Int. Symp. on Drug Transport to the Brain, Amsterdam, Netherlands, 2.-4.2.1995.
- Ahlemeyer B., Matys S., Brust P.
No evidence for inductive factors released by porcine astrocytes to increase the activity of the marker enzymes ALP and γ -GT in cerebral endothelial cells of porcine microvessels.
Cerebral Vascular Biology Conference, Paris, France, 10.-12.7.1995.
- Ahlemeyer B., Matys S., Brust P.
Charakterisierung des Transports für große neutrale Aminosäuren in kultivierten Hirndothelzellen: Hinweis auf unterschiedliche Permeabilitäten für die basolateral-luminale und luminal-basolaterale Transportrichtung.
Workshop der Gesellschaft für Zell- und Gewebezüchtung e.V. „Endothelzellen: Differenzierung und Vermittlung pharmakologischer Reaktionen“. Münster, 27.-28.9.1995.
- Ahlemeyer B., Brust P., Syhre R., Matys S., Pietzsch H.-J., Johannsen B.
Transportuntersuchung von ^{99m}Tc -Derivaten über die Blut-Hirn-Schranke: Anwendung eines *In-vitro*-Modells und Vergleich mit *In-vivo*-Befunden.
Workshop der Gesellschaft für Zell- und Gewebezüchtung e.V. „Endothelzellen: Differenzierung und Vermittlung pharmakologischer Reaktionen“. Münster, 27.-28.9.1995.
- Bergmann R., Roux F., Borson N., Drewes L.R.
PCR analysis of blood-brain barrier specific transporters in RBE4 cells.
2nd Int. Symp. on Drug Transport to the Brain, Amsterdam, Netherlands, 2.-4.2.1995.
- Füchtner F., Steinbach J., Mäding P., Johannsen B.
Alkaline hydrolysis of 2-[^{18}F]fluoro-1,3,4,6-tetra-O-acetyl-D-glucose in the preparation of 2-[^{18}F]fluoro-2-deoxy-D-glucose
6th Workshop on targetry and target chemistry, Vancouver, Canada; 17.-19.9.1995.
- Kampf G., Knop G., Franke W.-G., Wunderlich G., Brust P., Johannsen B.
Protein-binding and uptake of Yb-169 and In-111 complexes by cultured tumour cells: influence of the complex structure and the metal ion.
European Nuclear Medicine Congress, Brussels, Belgium, 26.-30.8.1995.
- Obert M., Brust P., Linemann H., Bergmann R., Jestczemski F., Johannsen B.
Investigation of the distribution of a radiotracer in a human brain - A multifractal analysis of a positron emission tomography image.
Deutsche Gesellschaft für Nuklearmedizin e.V., Jahrestagung, Dresden, 29.3.-1.4.1995.
- Pietzsch H.-J., Scheunemann M., Spies H., Fietz T., Brust P., Seifert S., Syhre R., Johannsen B.
Tc(V) and Re(V) complexes for serotonin receptor binding: structure affinity considerations.
7th International Conference on Bioinorganic Chemistry, Lübeck, 3.-8.9.1995.
- Preusche St., Steinbach J., Füchtner F., Krug H., De Leenheer M., Ghyoot M.
The new cyclotron of the Rossendorf PET-Center.
14th Intern. Conference on Cyclotrons and their Applications, Capetown, South Africa, 8.-13.10.1995.
- Spies H., Berger R., Syhre R., Johannsen B.
The role of lipophilicity in the design of technetium and rhenium radiotracers.
Intern.Symp. on Lipophilicity in Drug Res. and Toxicology, Lausanne, Switzerland, 21.-24.3.1995.

Spies H., Johannsen B., Pietzsch H.-J., Noll B., Noll St., Scheunemann M., Fietz T., Berger R., Brust P., Leibnitz P.

Technetium and rhenium complexes as potential receptor-binding ligands.

XIth Intern. Symp. on Radiopharmaceutical Chemistry, Vancouver, Canada, 13.-17.8.1995.

Steinbach J., Mäding P., Chebani K., Zessin J., Füchtner F., Johannsen B.

Aspects of the synthesis of ^{11}C -labelled aromatic compounds.

11th Intern. Symp. on Radiopharmaceutical Chemistry, Vancouver, Canada; 13.-17.8.1995.

Uhlirova H., Matucha M., Kretzschmar M., Bubner M.

Uptake and distribution of trichloroacetic acid in Norway Spruce (*Picea abies*/L. Karst.) shoot.

6th Int. Bioindicator Symp. Ceske Budejovice, Czech, 22.-28.5.1995.

PATENTS

Spies H., Schulze P.E., Noll B., Noll St., Dinkelborg L. (1995)

N-Alkyl-Peptidchelatorbildner, deren Metallkomplexe mit Radionuklidern, Verfahren zu ihrer Herstellung und diese Verbindungen enthaltende radiopharmazeutische Zusammensetzungen.

DE 43 37 600 A 1.

Spies H., Schulze P.E., Noll B., Noll St., Dinkelborg L. (1995)

N-alkyl-peptide chelate formers, their metal complexes with radionuclides, processes for producing them and radiopharmaceutical compositions containing these compounds.

WO 95/12610.

Johannsen B., Pietzsch H.-J., Scheunemann M., Brust P., Spies H. (1995)

Tc-99m labelled serotonin receptor-binding substances. Nr. 95200771.4.

III. TEACHING AND TRAINING ACTIVITIES

TEACHING ACTIVITIES

Summer term 1995

B. Johannsen:

One-term course on **Metals in Biosystems**.

Introduction into Bioinorganic Chemistry, including aspects of medicine, nutrition and ecology.

Winter Term 1995/1996

B. Johannsen, J. Steinbach, H. Spies, P. Brust, W.-G. Franke

One-term course on **Radiopharmaceutical Chemistry**.

Topics covered in the course include: radiotracer principle, introduction into nuclear medicine, production of radionuclides, generators and kits, ^{99m}Tc radiopharmaceuticals, radioiodination, PET radiopharmaceuticals, cell labelling, quality control, pharmacokinetics, rational tracer design, radiation safety, GMP and legal aspects.

B. Johannsen, H. Spies, G. Wagner, G. Wunderlich

One-term laboratory course on Radiopharmacy.

INTERNATIONAL TRAINING ACTIVITIES

IAEA Study Tour to Rossendorf, 5.-6.11.1995

as part of the Interregional training course on nuclear medicine for developing countries
(course director: H. Deckart, Berlin-Buch)

Training in radiopharmaceutical preparation

Jose David Moreira Saldarreaga, Ecuador, IAEA sholarship, 6.1.-8.7.1995

Laboratory course on radioluminography and cryocut technique

Dr. M. Matucha (Institut für Experimentelle Botanik, Prag) 22.-29.9.1995.

IV. SCIENTIFIC COOPERATION

In multidisciplinary research such as carried out by this Institute, collaboration, the sharing of advanced equipment, and above all, exchanges of ideas and information obviously play an important role. Effective collaboration has been established with colleagues at universities, in research centres and hospitals.

Cooperative relations and joint projects

The *Technische Universität Dresden* (Dr. Scheller, Dr. Klostermann, Inst. of Analytical Chemistry) plays an essential part in SPECT tracer research by performing analytical characterization of new tracers and providing support with the synthesis of organic compounds (Dr. Habicher, Inst. of Organic Chemistry), as well as in biochemical research (Dr. Fischer, Dr. Kaspar, Institute of Pathology).

Common objects of radiopharmacological and medical research link the Institute with the *Universitätsklinikum "Carl Gustav Carus"*, above all with its Departments of Nuclear Medicine (Prof. Franke). A joint team of staff members from both the Institute and the Clinic of Nuclear Medicine are currently working at the Rossendorf PET centre.

Very effective cooperation also exists with the *Bundesanstalt für Materialforschung Berlin* (Dr. Reck, Mr. Leibnitz) who have carried out X-ray crystal structure analysis of new technetium and rhenium complexes.

Our long-standing cooperation with the *University of Padua* (Prof. Mazzi) and the "*Demokritos*" *National Research Centre for Physical Sciences* in Athens (Dr. Chiotellis) has been continued. The fruitful contacts to the *Paul Scherrer Institut*, Villigen, Switzerland, are very appreciated. A new joint research project was started in 1995. The cooperation is part of the EU research programme COST-B3 with the working group on "New chelating systems for Tc and Re for medical application" (chaired by Dr. Spies, Rossendorf).

Joint work on technetium complexes with tripodal ligands has been carried out with the *Freie Universität Berlin* (Prof. Hahn, Inst. of Inorganic and Analytical Chemistry).

Cooperation on a special topic concerning bioinorganic chemistry is in progress with the *Arzneimittelwerk Dresden* (Dr. Unverferth).

Identification of common objects in PET radiopharmacy has led to collaborative research with the *Humboldt-Universität Berlin* and the *Universität Leipzig*.

In the field of PET tracers, cooperation exists with the *Montreal Neurological Institute* (Prof. Gjedde, Prof. Thompson), the *Turku Medical PET Centre* (Prof. Wegelius, Dr. Solin), the CO₂-Group of the *Max-Planck-Gesellschaft an der Universität Jena* (Prof. Dinjus) and the *Hans-Knöll-Institut Jena* (Dr. Kasch).

Cooperation on the biochemical aspects of radiotracer research exists with the *Universität Münster* (Prof. H.-J. Galla, Inst. of Biochemistry), the *University of Minnesota* in Duluth (Prof. L.R. Drewes, Department of Biochemistry and Molecular Biology) and the *Friedrich-Schiller Universität Jena* (Dr. Bauer, Inst. of Pathophysiology).

In helpful discussions both abroad and at Rossendorf numerous colleagues have contributed to defining areas of cooperation and shaping projects.

Special thanks go to Dr. E. Chiotellis, National Research Centre, Athens, Greece, Dr. G. Ensing, Malinckrodt Medical B. V., Petten, Netherlands, Dr. P.A. Schubiger, Paul-Scherrer-Institut, Villigen, Switzerland, Dr. W. Semmler, IDF Berlin and Prof. M.J. Welch, Mallinckrodt Institute of Radiology, Washington University, St. Louis, USA.

V. SEMINARS

TALKS OF VISITORS

Prof. U. Weser, Universität Tübingen
Molekulare Aspekte des Cu-Transports im biologischen Geschehen
24. 03. 1995

Dipl. Chem. R. Ruloff, Universität Leipzig
Gadoliniumkomplexe als Kontrastmittel für die Kernspintomografie
28. 04. 1995

Dr. J. van den Hoff, Medizinische Hochschule Hannover
Kinetische Modelle zur Quantifizierung physiologischer und biochemischer Prozesse mittels PET
19. 05. 1995

Prof. P. Riederer, Universität Würzburg
Neurodegeneration und Neuroprotektion
23. 06. 1995

Prof. L.R. Drewes, Universität Duluth, USA
Nutrient Delivery to the Neuron: The Role of Glucose Transporters
30. 06. 1995

Dr. R. Bauer, Institut für Pathologische Physiologie der Universität Jena
Pathogenese des frühkindlichen Hirnschadens, Rolle der Hirndurchblutungsregulation und des
Energistoffwechsels
08. 09. 1995

Priv. Doz. Dr. P.A. Schubiger, Paul-Scherrer-Institut Villigen, Schweiz
Fortschritte in der Markierungstechnik
15. 09. 1995

Dr. Pietrzyk, Max-Planck-Institut für Neurologische Forschung, Köln*
Bildüberlagerung in der nuklearmedizinischen Diagnostik
22. 09. 1995

Dr. K.P. Bogeso, Firma H. Lundbeck A/S, Dänemark
Pharmacophore Models for Dopamine D₂ and Serotonin 5-HT₂ Receptors
06. 10. 1995

Dr. W. Burchert, Medizinische Hochschule Hannover, Abt. für Nuklearmedizin und Spezielle
Biophysik, PET-Zentrum*
Flußmessungen mit PET-Radiotracern, dargestellt an Beispielen
11. 10. 1995

Dr. M. Kasper, Institut für Pathologie, Universitätsklinikum Dresden
Phänotypische Veränderungen der Zellen des Lungenparenchyms nach Bestrahlung
27. 10. 1995

Dr. U. Pleiß, Bayer AG Wuppertal
Die Rolle der Isotopenchemie bei der Entwicklung von Wirkstoffen
08. 12. 1995

Dr. T. Bonasera, Universität Uppsala, Schweden
Synthesis and evaluation of fluorine-18 labeled androgen, estrogen and progesterone receptor ligands
for PET
14. 12. 1995

* held at the Dresden University Hospital as a seminar of the PET Center Rossendorf

VI. ACKNOWLEDGEMENTS

ACKNOWLEDGEMENTS FOR FINANCIAL AND MATERIAL SUPPORT

The Institute is part of the Research Center Rossendorf Inc., which is financed by the Federal Republic of Germany and the Free State of Saxony on a fifty-fifty basis.

Three research projects concerning technetium tracer design and PET radiochemistry were supported by the Deutsche Forschungsgemeinschaft (DFG):

- Development and characterization of mixed-ligand complexes of technetium and rhenium with multidentate chelating agents
Sp 401/2-3 (H. Spies)
- Technetium complexes with thioether ligands
Pi 255/1-1 (H.-J. Pietzsch)
- PET with steroids
Ste 601/3-1 (J. Steinbach)

One project was supported by commission of the European Communities:

- New chelating systems for technetium and rhenium for nuclear medical application
COST B3, working group 5
In collaboration with Greece, Italy and Switzerland

In addition, the Free State of Saxony provided support for a project covering the establishment of cell cultures:

- Characterization of transport of radiopharmaceuticals through the blood-brain barrier using a cultured cell model
7541.82-FZR/309

Two projects were supported by cooperation with the pharmaceutical industry:

- Receptor-binding technetium tracers
Mallinckrodt Medical B.V.
- Cooperation in basic radiochemical research
Institut für Diagnostikforschung Berlin GmbH

The project:

- Data processing
was supported by Siemens AG.